

**The link between healthy speech perception and
pathological voice hearing – a pivotal role for
Broca’s region**

Inaugural-Dissertation

zur Erlangung des Doktorgrades
der Mathematisch-Naturwissenschaftlichen Fakultät
der Heinrich-Heine-Universität Düsseldorf

vorgelegt von

Mareike Clos
aus Henstedt-Ulzburg

Düsseldorf, Dezember 2013

aus dem Institut für Neurowissenschaften und Medizin (INM-1)
des Forschungszentrums Jülich

Gedruckt mit der Genehmigung der
Mathematisch-Naturwissenschaftlichen Fakultät der
Heinrich-Heine-Universität Düsseldorf

Referent: Univ. Prof. Dr. Simon Eickhoff
Korreferent: Univ. Prof. Dr. Tobias Kalenscher

Tag der mündlichen Prüfung: 19.11.2013

TABLE OF CONTENTS

ABSTRACT	5
ZUSAMMENFASSUNG	7
GENERAL INTRODUCTION	11
STUDY 1	
Effects of prior information on decoding degraded speech: An fMRI study	23
STUDY 2	
Tackling the multifunctional nature of Broca’s region meta-analytically: Connectivity- based parcellation of area 44	43
STUDY 3	
Aberrant connectivity of areas for decoding degraded speech in patients with auditory verbal hallucinations	91
STUDY 4	
Resting state functional connectivity in patients with chronic hallucinations	110
STUDY 5	
Aberrant resting-state connectivity in non-psychotic individuals with auditory hallucinations	121
STUDY 6	
Model-based analyses of resting state fMRI reveal hyperconnectivity in an introspective socio-affective network in major depression	135
SUMMARY & GENERAL DISCUSSION	163
ACKNOWLEDGMENTS	175

ABSTRACT

The six neuroimaging studies presented in this dissertation investigate the mechanisms and brain networks underlying top-down processes in normal speech perception on the one hand and pathological speech perception by auditory verbal hallucinations (AVH, “voice hearing”) on the other hand. The first fMRI study shows that, physiologically, speech perception is influenced by prior expectations in such a manner that unintelligible degraded speech sounds can suddenly be decoded when prior lexical-semantic information is available. This perceptual effect is presumably based on lexical-semantic expectations provided by higher order areas such as the left angular gyrus which may affect the semantic processing in the left middle temporal gyrus and modulate expected auditory signals in the thalamus. Broca’s region (area 44/45) could contribute to this process by searching for meaningful content in impoverished speech-like sequences. However, as study 2 demonstrates, in area 44 of Broca’s region merely the anterior-ventral part seems to be devoted to this task as this region is functionally heterogeneous. In particular, meta-analytic parcellation based on the whole-brain co-activation pattern across a wide range of neuroimaging experiments revealed that left area 44 contains five subunits primarily involved in rhythmic sequencing (posterior-ventral cluster), phonological processes in speech articulation (posterior-dorsal-cluster), working memory (anterior-dorsal cluster), detection of meaning in language and social contexts (anterior-ventral cluster) and cognitive control (inferior frontal junction cluster), respectively.

Furthermore, the fMRI resting state functional connectivity analysis reported in study 3 emphasizes the importance of Broca’s region in AVH in psychotic patients. In particular, the results of this analysis suggest that imbalances in the functional connectivity pattern of the speech-relevant part of Broca’s region might lead to the misattribution of self-produced

verbal imagery to an external source. Specifically, the perception of alien voices in the absence of sensory stimulation might arise from a decoupling between Broca's region and the verbal monitoring system in combination with increased interactions within the speech articulation network. In addition, study 3 also provides evidence for abnormal top-down influences on speech processing in AVH reflected in disturbed connectivity of the left middle temporal gyrus and the left angular gyrus with other regions involved in speech perception. Moreover, the fMRI resting state analysis presented in study 4 suggests that Broca's right-sided homotope might equally contribute to the pathology of AVH. Furthermore, abnormal coupling with medial temporal lobe memory structures might reflect intrusions of verbal memory fragments that are subsequently perceived as alien voices. Evidence for disturbed connectivity between areas involved in language and memory processes was also found in non-psychotic individuals with AVH in study 5. Finally, study 6 demonstrates an important negative finding that strengthens the specificity of the aforementioned results on disturbed functional connectivity of Broca's region in AVH. In particular, it could be shown that major depression is specifically associated with hyperconnectivity of regions involved in affective and introspective processes but not with any abnormal connectivity within the speech perception network from study 1. Therefore, abnormal connectivity between Broca's region and other regions implicated in speech perception seems to be specific to the symptom of AVH, as they are found in psychotic and non-psychotic patients showing this clinical phenotype but not in patients with affective psychosis (i.e., major depression). Together, these studies thus demonstrate that Broca's region is multifunctional and forms an important hub in top-down driven speech perception where degraded bottom-up speech signals are restored to meaningful sentences based on lexical-semantic expectations as well as in the pathology of AVH where speech is perceived in the absence of bottom-up sensory signals.

ZUSAMMENFASSUNG

Die sechs bildgebenden Studien, die in dieser Dissertation dargestellt werden, untersuchen die Mechanismen und Gehirn-Netzwerke, welche die Grundlage für „top-down“ Prozesse in sowohl normaler Sprachwahrnehmung als auch pathologischer Sprachwahrnehmung im Fall von verbal-akustischen Halluzinationen (VAH, „Stimmen hören“) bilden. Die erste fMRT-Studie zeigt, dass Sprachwahrnehmung auf physiologischer Ebene durch vorherige Erwartungen derart beeinflusst wird, dass zur Unverständlichkeit degradierte Sprachklänge plötzlich decodiert werden können, wenn zuvor lexikalisch-semantiche Informationen präsentiert wurden. Dieser Wahrnehmungseffekt beruht vermutlich auf lexikalisch-semantiche Erwartungen, die von hierarchisch höheren Arealen wie dem linken Gyrus angularis bereitgestellt werden und welche die semantiche Verarbeitung im linken mittleren temporalen Gyrus beeinflussen und die erwarteten akustischen Signale im Thalamus modulieren. Die Broca-Region (Areal 44/45) könnte zu diesem Prozess beitragen, indem sie nach bedeutungsvollen Inhalten in sprachähnlichen Sequenzen sucht. Wie Studie 2 jedoch zeigt, ist es lediglich der anterior-ventrale Teil von Areal 44 der Broca-Region, der dieser Aufgabe gewidmet ist. Eine meta-analytische Parzellierung, die auf dem Ko-Aktivierungsmuster des gesamten Gehirns über eine Vielzahl an bildgebenden Experimenten beruht, offenbarte, dass das linke Areal 44 in fünf heterogene Untereinheiten unterteilt werden kann. Diese sind vornehmlich jeweils in rhythmische Sequenzierung (posterior-ventrales Cluster), phonologische Artikulationsprozesse (posterior-dorsales Cluster), Arbeitsgedächtnis (anterior-dorsales Cluster), Erkennung von Bedeutung im sprachlichen und sozialen Kontext (anterior-ventrales Cluster) und kognitive Kontrolle (inferior frontale Junktion Cluster) involviert.

Weiterhin unterstreicht die fMRT-Analyse der funktionellen Konnektivität im Ruhezustand in Studie 3 die Bedeutung der Broca-Region für VAH bei psychotischen Patienten. Insbesondere weisen die Ergebnisse dieser Analyse darauf hin, dass ein Ungleichgewicht im funktionellen Verbindungsmuster mit dem sprach-relevanten Teil der Broca-Region zu einer Fehlattribution von selbstgenerierten verbalen Vorstellungen, welche als externe Stimmen wahrgenommen werden, führen könnte. Konkret könnte die Wahrnehmung von fremden Stimmen in Abwesenheit von sensorischer Stimulation durch eine Entkopplung zwischen der Broca-Region und dem verbalen Kontrollsystem in Kombination mit erhöhten Wechselwirkungen innerhalb des verbalen Artikulationsnetzwerks entstehen. Zusätzlich bietet Studie 3 auch Hinweise auf anormale „top-down“ Einflüsse auf die Sprachverarbeitung bei VAH, die sich in gestörten Verbindungen des linken mittleren temporalen Gyrus und des linken Gyrus angularis mit anderen Sprachwahrnehmungs-Regionen widerspiegeln. Darüber hinaus lässt die fMRT-Analyse der funktionellen Konnektivität im Ruhezustand in Studie 4 vermuten, dass das rechtsseitige Broca-Homotop ebenfalls zur VAH-Pathologie beiträgt. Außerdem könnte eine anormale Kopplung mit Gedächtnisregionen des medialen Temporallappens das unkontrollierte Eindringen von verbalen Erinnerungsfragmenten verursachen, die anschließend als fremde Stimmen wahrgenommen werden. Weiterhin gibt auch Studie 5 Hinweise auf gestörte Konnektivität zwischen Sprach- und Gedächtnisregionen bei nicht-psychotischen Individuen mit VAH. Studie 6 demonstriert schließlich einen wichtigen Negativbefund, der die Spezifität der zuvor genannten veränderten funktionellen Konnektivität von der Broca-Region bei VAH unterstreicht. Insbesondere zeigt diese Studie, dass die Symptomatik depressiver Patienten spezifisch mit Hyperkonnektivität von affektiven und introspektiven Hirnregionen assoziiert ist, aber nicht mit anormaler Konnektivität innerhalb des Sprachwahrnehmungsnetzwerks aus Studie 1. Da die anormale Konnektivität

zwischen der Broca-Region und anderen Sprachwahrnehmungsregionen nur bei psychotischen Patienten sowie nicht-psychotischen Individuen mit VAH aber nicht bei Patienten mit affektiver Psychose (d.h. Depressionen) vorhanden ist, scheint dieses gestörte Konnektivitätsmuster spezifisch für die Symptomatik von VAH zu sein. Insgesamt zeigen diese Studien, dass die multifunktionelle Broca-Region eine wichtige Schaltstelle darstellt sowohl für „top-down“ getriebenes Sprachverständnis, bei dem degradierte Sprachsignale basierend auf lexikalisch-semanticen Erwartungen als bedeutungsvolle Sätze wahrgenommen werden, als auch für VAH, bei denen Sprache wahrgenommen wird obwohl keine „bottom-up“ sensorischen Signale vorhanden sind.

GENERAL INTRODUCTION

“Broca’s region” as one of the language centers in the human brain has long ago been mapped to the posterior part of the left inferior frontal gyrus (IFG) corresponding to the cytoarchitectonic areas 44 and 45 (Brodmann, 1909). More recently, the borders of these areas 44 and 45 have been redefined cytoarchitectonically using observer-independent techniques in multiple brains (Amunts et al., 1999). The region’s name goes back to the neurologist Paul Broca who reported in 1861 that the severe loss of speech production capabilities in a patient was due to a lesion in this left-sided region (Broca, 2011). Later studies confirmed the importance of Broca’s region for the production of speech (Richardson et al., 2012) but showed that Broca’s region is also involved in the perception of speech (Fitch et al., 1997; Watkins and Paus, 2004; Grodzinsky and Friederici, 2006), in particular when speech is difficult to understand (Caplan et al., 2000; Giraud et al., 2004). Furthermore, it has been demonstrated that Broca’s region contributes to non-language functions such as working memory (Rogalsky and Hickok, 2011), action observation and execution (Heiser et al., 2003) and music (Koelsch, 2011). The region’s multifunctional character constitutes a strong argument against the original simplistic conception of Broca’s region being “the seat of the faculty of language” (Broca, 2011).

Network interactions and mechanisms of predictive coding in normal speech perception

In contrast to the functional localization approach to mental capacities, the functional integration account (Friston, 2002) proposes that specific functions are orchestrated in a network of specialized regions rather than being localized in a specific region. Thus, the specific contribution of Broca’s region to language is determined by its interactions within the network of connected regions (Eickhoff et al., 2009). Hence, although Broca’s region

might contribute to both speech production and speech perception, these different functions are accomplished in concert with distinct networks. Furthermore, these interactions and the associated specific functional response patterns of brain regions should be influenced in a dynamic fashion by contextual factors and task requirements (Friston, 2002; Stephan, 2004). In particular, such interactions in functional networks which give rise to mental capacities like language have been suggested to depend on inter-regional connectivity which can be distinguished into “driving” forward connections from lower to hierarchically higher brain regions (bottom-up) and “modulating” backward connections (top-down) that can modulate brain activity and define the specialization of a given region in a certain context (Friston, 2002).

According to this framework of predictive coding (Friston, 2005), these backward connections convey predictions of the possible causes of sensory events based on the integration of neural activity at lower levels with prior knowledge. In particular, these predictions are compared to the actual sensory input and differences between the predicted and the observed information are fed back to the hierarchically higher node as the prediction error. The prediction error, in turn, is used to optimize subsequent predictions, as it indicates the fit of the current priors (Rao and Ballard, 1999). Importantly, the incorporation of prior knowledge and context information into predictions might resolve potential ambiguities in perceptual processes and thus should help to decode noisy stimuli. This facilitation is most likely due to a sharpening of sensory representations at lower levels (Kok et al., 2012) and should be particularly relevant in the domain of speech perception because spoken language comprehension requires a fast and reliable decoding of a stream of often-ambiguous sounds into a meaningful statement (Arnal and Giraud, 2012).

Based on these considerations, the first study reported here investigates how the perception of degraded speech is influenced by prior information and what neural effects are associated with these perceptual processes. This was achieved by conducting an event-related functional magnetic resonance imaging (fMRI) experiment with 29 healthy participants. The stimulus material consisted of pairs of spoken sentences in spectrally degraded and nondegraded (original) format. Importantly, the degraded sentences were incomprehensible when heard in isolation, however, they suddenly became intelligible when preceded by the nondegraded (original) sentence version. We used this phenomenon to probe brain activation evoked by the successful decoding of degraded speech when prior information was provided by the preceding nondegraded sentence.

One region, multiple functions

Next, if the function of a certain structurally defined brain area, such as Broca's region, is largely determined by the network it is connected to and interacts with (Friston, 2002), it should be possible to identify specific functional subunits within such region based on the connectivity pattern. This principle forms the foundation of connectivity-based parcellation (CBP), a method which aims at subdividing a region of interest into distinct subunits or modules with an internally homogeneous connectivity pattern that is at the same time maximally distinct from the connectivity pattern of the other subunits (Knösche and Tittgemeyer, 2011). Connectivity measures that are frequently used for such a parcellation include diffusion imaging which can infer axonal connections based on the diffusion direction of water molecules (Johansen-Berg et al., 2004) and resting state functional connectivity, which is based on the correlation of fMRI time-series between regions in absence of an experimental task (Zhang and Li, 2012). Another measure of functional

connectivity can be attained with meta-analytic connectivity modeling (MACM; Laird et al., 2009; Eickhoff et al., 2011). The core idea behind MACM is that regions that are consistently co-activated with each other demonstrate functional connectivity and should therefore be considered to be part of the same functional network. This method is thus a measure of task-dependent connectivity based on the likelihood of co-activation of regions across many experiments. The co-activation likelihood can be computed using the BrainMap database (www.brainmap.org; Fox and Lancaster, 2002) in which a large number of neuroimaging studies are recorded. Moreover, for all included studies this database contains not only the coordinates of all foci activated in each reported contrast but moreover provides elaborate meta-data for coding the experiment in question in terms of behavioral domains (e.g. cognition, perception, action) and paradigm classes (e.g. overt speech, n-back task, stroop task). This information can then be used to not only infer connectivity in terms of co-activation of brain regions but also to characterize the ensuing subunits functionally.

In the second study, we used the MACM-CBP approach to parcellate area 44 in order to better understand the organization and the functional role of this posterior part of Broca's region. Given its multifunctional character, this parcellation might provide an answer to the longstanding quest whether this region contains several specialized functional subunits or whether its multifunctional character can be reduced to a single core function of a relatively homogeneous area (Grodzinsky and Santi, 2008; Fedorenko et al., 2012). In support of the former view, a previous multi-receptor mapping study has indicated that area 44 is structurally heterogeneous as it contains two distinguishable subareas (Amunts et al., 2010). In study 2 we thus examined whether distinct functional subunits within area 44 can be detected based on the co-activation pattern of the individual voxels within histologically defined area 44 voxels across a wide range of neuroimaging experiments.

Disturbed interactions at rest in pathological voice hearing

In order to understand how a complex function such as speech perception evolves from brain processes, it can also be illuminating to consider brain dysfunction. For normal speech perception, study 1 examines the importance of top-down expectations for decoding ambiguous speech sounds. This phenomenon of perceiving more than physically present in the bottom-up signal might be related to auditory verbal hallucinations (AVH), that is, hearing voices in the absence of actual sensory stimulation. AVH are a common symptom of various psychotic disorders, particularly of schizophrenia, and are usually experienced as very distressing. Although several neurocognitive models of AVH have been proposed, no unequivocal pathomechanism has been identified yet (Seal et al., 2004; Jones, 2010). Firstly, AVH have been suggested to result from the misattribution of inner speech to external sources. According to this account, self-produced verbal thoughts are experienced as alien voices because a dysfunctional self-monitoring prevents the recognition of the verbal thoughts as being self-generated (Allen et al., 2007). Secondly, an imbalance between top-down verbal imagery and bottom-up sensory processing of speech might lead to perception of voices in absence of actual sensory stimulation. That is, excessive dominance of verbal expectations might overrule signals conveyed by bottom-up processing (Grossberg, 2000; Aleman et al., 2003). Thirdly, a failure to appropriately inhibit stored memory representations might lead to spontaneous intrusions of verbal memory fragments which are then experienced as AVH (Badcock et al., 2005; Waters et al., 2006).

However, given the very complex and heterogeneous nature of hallucinations, it seems very likely that several such cognitive and perceptual mechanisms are involved in AVH (Seal et al., 2004). Furthermore, according to the functional integration account (Friston, 2002) these cognitive and perceptual mechanisms should arise from network interactions between

several brain regions and the regions' specific functions should be reflected in their connectivity patterns. Consequently, the investigation of network connectivity has been proposed as being more beneficial for understanding the pathology of AVH than examining the contribution of single regions (Allen et al., 2012). A promising approach to better understand the network interactions underlying AVH might be the examination of resting state functional connectivity in patients experiencing AVH (Northoff and Qin, 2011). Since hallucinations arise from internal sources in the absence of external stimulation, resting state fluctuations reflecting purely intrinsic interactions between brain regions might be particularly sensitive to reveal the network mechanisms involved in AVH. Furthermore, resting state measurements might be less challenging for psychiatric patients, as they only need to lie still in the scanner and "rest" with their eyes closed rather than participate actively in cognitive tasks.

In order to shed more light on disturbed network interactions implicated in AVH, we thus conducted two resting state analyses involving 49 psychotic patients with frequent AVH and 49 matched healthy control participants in study 3 and 4. We employed a seed-based approach in both studies in which we evaluated the correlations between the time-series of the seeds and all other voxels in the rest of the brain. We tested these correlations for increased and decreased connectivity in the patient group compared with the healthy controls. In study 3, we aimed to test whether an imbalance between top-down expectations and bottom-up auditory processing is part of the pathophysiology of AVH. Consequently, we used those four regions that were primarily involved in expectation-based decoding of degraded speech in study 1 as seed regions. These regions were Broca's region in the left IFG, the left middle temporal gyrus (MTG), the left angular gyrus (AG), and the left thalamus.

In study 4, the resting state analysis was seeded from the left superior temporal gyrus and the right inferior frontal gyrus based on their association with the experience of acute hallucinations in psychotic patients reported in an earlier study (Diederer et al., 2010). These two regions therefore formed a good starting point to evaluate differences in network connectivity that might underlie the predisposition to experience AVH in psychotic patients. However, potential confounds in resting state connectivity studies comparing psychotic patients with healthy controls can arise from the differences between these two groups with regard to other psychopathological characteristics than just the presence of AVH as well as from the fact that most patients are (and need to be) on psychoactive medication. Accordingly, observations of aberrant connectivity of brain regions in these patients might reflect general psychopathology or medication effects rather than the neurobiological causes of the specific symptom AVH. Therefore, the examination of “healthy” subjects with AVH should represent an important complementary strategy. Indeed, AVH are surprisingly common in the general population, with lifetime prevalence reported to be between 10 to 15% (Tien, 1991). Analyzing non-psychotic subjects with AVH should thus allow to specifically investigate this particular symptom without interference from medication effects or other aspects of psychopathology (Sommer et al., 2010; Daalman et al., 2011). Accordingly, resting state functional connectivity in a group of 25 non-psychotic individuals with AVH (but no other psychiatric symptoms) and 25 healthy control participants without AVH were compared for study 5. In contrast to psychotic patients, the hallucinations were not experienced as distressing and the non-psychotic individuals were functioning normally in their daily lives. Resting state scans were acquired for all participants and analyzed using a seed-based approach by computing the correlations of the time-series from five seed regions with the rest of the brain. Building on previous findings, the seeds comprised one

region previously reported to be activated prior to the onset of AVH in psychotic patients (left parahippocampal gyrus; Diederer et al., 2010) and two bilateral regions associated with acute AVH in non-psychotic individuals (inferior frontal and superior temporal gyri; Diederer et al., 2012).

Finally, a frequently voiced concern in the context of functional imaging and connectivity studies assessing clinical populations is the question regarding the specificity of the findings. As hypothesized, studies 3, 4 and 5 revealed differences in resting state functional connectivity of areas relevant for top-down modulation in the context of language comprehension in psychotic patients with AVH as well as in non-psychotic subjects with a similar phenotype. But may these findings merely reflect more general aspects of psychopathology expressing themselves in abnormal connectivity? Study 6 sheds some light on the question by reporting an analysis of functional resting state connectivity in 57 patients with major depression and 57 matched healthy control participants. The main analysis was based on the “introspective socio-affective” network (ISA) derived from two earlier meta-analyses (Schilbach et al., 2012). This ISA network included the anterior and subgenual cingulate cortices, the dorsomedial prefrontal cortex, the precuneus and the left amygdala. Importantly, we additionally also analyzed the speech perception network delineated in study 1 comprising Broca’s region, left MTG, left AG and left thalamus in this sample of depressed patients. If aberrations in this network would be related to general psychopathological mechanisms, we would expect differences between patients with “affective psychosis”, i.e., major depression, and healthy controls. Should no such differences be found, this would strongly argue towards a symptom-specific neuronal endophenotype, as depression is not commonly associated with impairments in speech processing or AVH (Hammar and Ardal, 2009; Marazziti et al., 2010).

REFERENCES

- Aleman, A., Bocker, K.B., Hijman, R., de Haan, E.H., Kahn, R.S. 2003. Cognitive basis of hallucinations in schizophrenia: role of top-down information processing. *Schizophr.Res.* 64: 175-185.
- Allen, P., Aleman, A., McGuire, P.K. 2007. Inner speech models of auditory verbal hallucinations: evidence from behavioural and neuroimaging studies. *Int.Rev.Psychiatry.* 19: 407-415.
- Allen, P., Modinos, G., Hubl, D., Shields, G., Cuchia, A., Jardri, R., Thomas, P., Woodward, T., Shotbolt, P., Plaze, M., Hoffman, R. 2012. Neuroimaging auditory hallucinations in schizophrenia: from neuroanatomy to neurochemistry and beyond. *Schizophr.Bull.* 38: 695-703.
- Amunts, K., Lenzen, M., Friederici, A.D., Schleicher, A., Morosan, P., Palomero-Gallagher, N., Zilles, K. 2010. Broca's region: novel organizational principles and multiple receptor mapping. *PLoS.Biol.* 8.
- Amunts, K., Schleicher, A., Burgel, U., Mohlberg, H., Uylings, H.B., Zilles, K. 1999. Broca's region revisited: cytoarchitecture and intersubject variability. *J.Comp Neurol.* 412: 319-341.
- Arnal, L.H., Giraud, A.L. 2012. Cortical oscillations and sensory predictions. *Trends Cogn Sci.* 16: 390-398.
- Badcock, J.C., Waters, F.A., Maybery, M.T., Michie, P.T. 2005. Auditory hallucinations: failure to inhibit irrelevant memories. *Cogn Neuropsychiatry.* 10: 125-136.
- Broca, P. 2011. Remarks on the seat of spoken language, followed by a case of aphasia (1861). *Neuropsychol Rev.* 21:227-229.
- Brodmann K. (1909) *Vergleichende Lokalisationslehre der Grobhirnrinde in ihren Prinzipien dargestellt auf Grund des Zellenbaues.* Leipzig: Barth JA.
- Caplan, D., Alpert, N., Waters, G., Olivieri, A. 2000. Activation of Broca's area by syntactic processing under conditions of concurrent articulation. *Hum.Brain Mapp.* 9: 65-71.
- Daalman, K., van, Z.M., Bootsman, F., Boks, M., Kahn, R., Sommer, I. 2011. Auditory verbal hallucinations and cognitive functioning in healthy individuals. *Schizophr.Res.* 132: 203-207.
- Diederer, K.M., Daalman, K., de Weijer, A.D., Neggers, S.F., van, G.W., Blom, J.D., Kahn, R.S., Sommer, I.E. 2012. Auditory hallucinations elicit similar brain activation in psychotic and nonpsychotic individuals. *Schizophr.Bull.* 38: 1074-1082.
- Diederer, K.M., Neggers, S.F., Daalman, K., Blom, J.D., Goekoop, R., Kahn, R.S., Sommer, I.E. 2010. Deactivation of the parahippocampal gyrus preceding auditory hallucinations in schizophrenia. *Am.J.Psychiatry.* 167: 427-435.
- Eickhoff, S.B., Bzdok, D., Laird, A.R., Roski, C., Caspers, S., Zilles, K., Fox, P.T. 2011. Co-activation patterns distinguish cortical modules, their connectivity and functional differentiation. *Neuroimage.* 57: 938-949.
- Eickhoff, S.B., Heim, S., Zilles, K., Amunts, K. 2009. A systems perspective on the effective connectivity of overt speech production. *Philos.Transact.A Math.Phys.Eng Sci.* 367: 2399-2421.

- Fedorenko, E., Duncan, J., Kanwisher, N. 2012. Language-selective and domain-general regions lie side by side within Broca's area. *Curr.Biol.* 22: 2059-2062.
- Fitch, R.H., Miller, S., Tallal, P. 1997. Neurobiology of speech perception. *Annu.Rev.Neurosci.* 20: 331-353.
- Fox, P.T., Lancaster, J.L. 2002. Opinion: Mapping context and content: the BrainMap model. *Nat.Rev.Neurosci.* 3: 319-321.
- Friston, K. 2002. Functional integration and inference in the brain. *Prog.Neurobiol.* 68: 113-143.
- Friston, K. 2005. A theory of cortical responses. *Philos.Trans.R.Soc.Lond B Biol.Sci.* 360: 815-836.
- Giraud, A.L., Kell, C., Thierfelder, C., Sterzer, P., Russ, M.O., Preibisch, C., Kleinschmidt, A. 2004. Contributions of sensory input, auditory search and verbal comprehension to cortical activity during speech processing. *Cereb.Cortex.* 14: 247-255.
- Grodzinsky, Y., Friederici, A.D. 2006. Neuroimaging of syntax and syntactic processing. *Curr.Opin.Neurobiol.* 16: 240-246.
- Grodzinsky, Y., Santi, A. 2008. The battle for Broca's region. *Trends Cogn Sci.* 12: 474-480.
- Grossberg, S. 2000. How hallucinations may arise from brain mechanisms of learning, attention, and volition. *J.Int.Neuropsychol.Soc.* 6: 583-592.
- Hammar, A., Ardal, G. 2009. Cognitive functioning in major depression--a summary. *Front Hum.Neurosci.* 3: 26.
- Heiser, M., Iacoboni, M., Maeda, F., Marcus, J., Mazziotta, J.C. 2003. The essential role of Broca's area in imitation. *Eur.J.Neurosci.* 17: 1123-1128.
- Johansen-Berg, H., Behrens, T.E., Robson, M.D., Drobnyak, I., Rushworth, M.F., Brady, J.M., Smith, S.M., Higham, D.J., Matthews, P.M. 2004. Changes in connectivity profiles define functionally distinct regions in human medial frontal cortex. *Proc.Natl.Acad.Sci.U.S.A.* 101: 13335-13340.
- Jones, S.R. 2010. Do we need multiple models of auditory verbal hallucinations? Examining the phenomenological fit of cognitive and neurological models. *Schizophr.Bull.* 36: 566-575.
- Knösche, T.R., Tittgemeyer, M. 2011. The role of long-range connectivity for the characterization of the functional-anatomical organization of the cortex. *Front Syst.Neurosci.* 5: 58.
- Koelsch, S. 2011. Toward a neural basis of music perception - a review and updated model. *Front Psychol.* 2: 110.
- Kok, P., Jehee, J.F., de Lange, F.P. 2012. Less is more: expectation sharpens representations in the primary visual cortex. *Neuron.* 75: 265-270.
- Laird, A.R., Eickhoff, S.B., Kurth, F., Fox, P.M., Uecker, A.M., Turner, J.A., Robinson, J.L., Lancaster, J.L., Fox, P.T. 2009. ALE Meta-Analysis Workflows Via the Brainmap Database: Progress Towards A Probabilistic Functional Brain Atlas. *Front Neuroinform.* 3: 23.
- Marazziti, D., Consoli, G., Picchetti, M., Carlini, M., Faravelli, L. 2010. Cognitive impairment in major depression. *Eur.J.Pharmacol.* 626: 83-86.

- Northoff, G., Qin, P. 2011. How can the brain's resting state activity generate hallucinations? A 'resting state hypothesis' of auditory verbal hallucinations. *Schizophr.Res.* 127: 202-214.
- Rao, R.P., Ballard, D.H. 1999. Predictive coding in the visual cortex: a functional interpretation of some extra-classical receptive-field effects. *Nat.Neurosci.* 2: 79-87.
- Richardson, J.D., Fillmore, P., Rorden, C., Lapointe, L.L., Fridriksson, J. 2012. Re-establishing Broca's initial findings. *Brain Lang.* 123: 125-130.
- Schilbach, L., Bzdok, D., Timmermans, B., Fox, P.T., Laird, A.R., Vogeley, K., Eickhoff, S.B. 2012. Introspective minds: using ALE meta-analyses to study commonalities in the neural correlates of emotional processing, social & unconstrained cognition. *PLoS.One.* 7: e30920.
- Seal, M.L., Aleman, A., McGuire, P.K. 2004. Compelling imagery, unanticipated speech and deceptive memory: neurocognitive models of auditory verbal hallucinations in schizophrenia. *Cogn Neuropsychiatry.* 9: 43-72.
- Sommer, I.E., Daalman, K., Rietkerk, T., Diederens, K.M., Bakker, S., Wijkstra, J., Boks, M.P. 2010. Healthy individuals with auditory verbal hallucinations; who are they? Psychiatric assessments of a selected sample of 103 subjects. *Schizophr.Bull.* 36: 633-641.
- Stephan, K.E. 2004. On the role of general system theory for functional neuroimaging. *J.Anat.* 205: 443-470.
- Tien, A.Y. 1991. Distributions of hallucinations in the population. *Soc.Psychiatry Psychiatr.Epidemiol.* 26: 287-292.
- Waters, F.A., Badcock, J.C., Michie, P.T., Maybery, M.T. 2006. Auditory hallucinations in schizophrenia: intrusive thoughts and forgotten memories. *Cogn Neuropsychiatry.* 11: 65-83.
- Watkins, K., Paus, T. 2004. Modulation of motor excitability during speech perception: the role of Broca's area. *J.Cogn Neurosci.* 16: 978-987.
- Zhang, S., Li, C.S. 2012. Functional connectivity mapping of the human precuneus by resting state fMRI. *Neuroimage.* 59: 3548-3562.

STUDY 1

Effects of prior information on decoding degraded speech: An fMRI study

Mareike Clos¹, Robert Langner^{1,2}, Martin Meyer³, Mathias S. Oechslin⁴, Karl Zilles^{1,5,6}, Simon B. Eickhoff^{1,2}

¹Institute of Neuroscience and Medicine (INM-1; INM-2), Research Center Jülich, Germany

²Institute of Clinical Neuroscience and Medical Psychology, Heinrich Heine University, Düsseldorf, Germany

³Neuroplasticity and Learning in the Normal Aging Brain (HAB LAB), University of Zurich, Switzerland

⁴Faculty of Psychology and Educational Sciences, Geneva Neuroscience Center, University of Geneva, Switzerland

⁵C. and O. Vogt Brain Research Institute, University of Düsseldorf, Germany

⁶JARA-Translational Brain Medicine, Germany

Human Brain Mapping (2012) Advance online publication

doi:10.1002/hbm.22151

Impact factor (2011): 5.880

Own contributions

Conception and design of experiment

Programming of stimuli presentation

Measurements and statistical analysis

Interpretation of results

Preparing figures

Writing the paper

Total contribution: 80%

Effects of Prior Information on Decoding Degraded Speech: An fMRI Study

Mareike Clos,^{1*} Robert Langner,^{1,2} Martin Meyer,³ Mathias S. Oechlin,⁴
Karl Zilles,^{1,5,6} and Simon B. Eickhoff^{1,2}

¹*Institute of Neuroscience and Medicine (INM-1, INM-2), Research Center Jülich, Germany*

²*Institute of Clinical Neuroscience and Medical Psychology, Heinrich Heine University, Düsseldorf, Germany*

³*Neuroplasticity and Learning in the Normal Aging Brain (HAB LAB), University of Zurich, Switzerland*

⁴*Faculty of Psychology and Educational Sciences, Geneva Neuroscience Center, University of Geneva, Switzerland*

⁵*C. and O. Vogt Brain Research Institute, University of Düsseldorf, Germany*

⁶*JARA-Translational Brain Medicine, Germany*

Abstract: Expectations and prior knowledge are thought to support the perceptual analysis of incoming sensory stimuli, as proposed by the predictive-coding framework. The current fMRI study investigated the effect of prior information on brain activity during the decoding of degraded speech stimuli. When prior information enabled the comprehension of the degraded sentences, the left middle temporal gyrus and the left angular gyrus were activated, highlighting a role of these areas in meaning extraction. In contrast, the activation of the left inferior frontal gyrus (area 44/45) appeared to reflect the search for meaningful information in degraded speech material that could not be decoded because of mismatches with the prior information. Our results show that degraded sentences evoke instantaneously different percepts and activation patterns depending on the type of prior information, in line with prediction-based accounts of perception. *Hum Brain Mapp* 00:000–000, 2012. © 2012 Wiley Periodicals, Inc.

Key words: auditory expectations; Broca's region; middle temporal gyrus; predictive coding; speech perception

INTRODUCTION

The comprehension of spoken utterances is a highly challenging task due to the transient nature of auditory speech stimuli and its vulnerability to ambiguity. The

success of our sensory system to convey most stimuli with reasonable precision despite the regular disturbance of noise has been attributed to its constant anticipation of upcoming events [Bar, 2007; Enns and Lleras, 2008; Friston, 2005]. That is, perception is not simply a passive

Additional Supporting Information may be found in the online version of this article.

Contract grant sponsor: Human Brain Project; Contract grant number: R01-MH074457-01A1; Contract grant sponsor: DFG; Contract grant number: IRTG 1328; Contract grant sponsor: The Initiative and Networking Fund of the Helmholtz Association within the Helmholtz Alliance on Systems Biology; Contract grant sponsor: the Förderung des akademischen Nachwuchses (FAN) of the Zürcher Universitätsvereins (ZUNIV); Contract grant

sponsor: Swiss National Foundation; Contract grant number: 320030-120661.

*Correspondence to: Mareike Clos, Forschungszentrum Jülich, INM-2, 52425 Jülich, Germany. E-mail: m.clos@fz-juelich.de

Received for publication 18 March 2012; Revised 2 June 2012; Accepted 5 June 2012

DOI: 10.1002/hbm.22151

Published online in Wiley Online Library (wileyonlinelibrary.com).

reflection of sensory input but arises from an active integration of sensory data and prior expectations. According to the framework of predictive coding [Friston, 2005; Rao and Ballard, 1999], such expectations can resolve perceptual ambiguities because prior knowledge and context information incorporated in the predictions might help to decode noisy stimuli. Predictive coding is conceptually related to, e.g., semantic or contextual priming but refers to the use of any kind of prior information. In fact, priming may thus be regarded as a special instance of predictive coding in which a single piece of prior information (the prime) influences the processing of the subsequent stimulus.

Evidence for predictive coding has been observed in visual processing [e.g., Hosoya et al., 2005; Sharma et al., 2003; Summerfield et al., 2006], in tactilo-motor interactions [Blakemore et al., 1998], in motor preparation [Jakobs et al., 2009] and in audiovisual perception [Arnal et al., 2011; den Ouden et al., 2009, 2010]. However, rather little is known about the role of predictive coding in auditory speech perception despite the fact that comparable expectation-generating mechanisms involving interactions between bottom-up and top-down processing have often been deemed crucial for speech perception [e.g., Davis and Johnsrude, 2007; Grossberg, 2003]. Furthermore, auditory processing is thought to be hierarchically organized such that higher processing levels respond to increasingly more complex and abstract sound properties. In accordance with this hierarchical organization, research has identified at least three distinct levels of auditory processing in non-human primates. Specifically, with increasing complexity, sound information proceeds from the core region of the auditory cortex to the belt and the more lateral parabelt area [Kaas and Hackett, 2000; Rauschecker et al., 1995]. Neuroimaging studies have found a comparable hierarchical processing pattern in humans in response to complex sounds [Hall et al., 2002] and to spoken language [Scott et al., 2000]. Whereas the core and belt areas of the auditory cortex in the superior temporal gyrus are responsive to the amplitude and frequency modulations of speech, left lateralized cortical regions including the posterior inferior parietal lobe, middle temporal gyrus, fusiform and parahippocampal gyrus, dorsomedial prefrontal cortex, inferior frontal gyrus, ventromedial prefrontal cortex, and posterior cingulate gyrus seem to be involved in speech-specific semantic processing [Binder et al., 2009].

Previously, indications for effects of prior knowledge on speech perception have been demonstrated in studies showing that speech can be decoded even when extremely distorted [Remez et al., 1994; Saberi and Perrott, 1999; Shannon et al., 1995] and that perception of degraded speech can improve through training [Davis et al., 2005; Giraud et al., 2004; Hannemann et al., 2007]. Moreover, comprehension of degraded speech stimuli after training was associated with increased blood-oxygen-level-dependent (BOLD) activity in the right superior temporal sulcus and bilateral middle and inferior temporal gyri [Giraud

et al., 2004] and with increased gamma band activity in left temporal regions [Hannemann et al., 2007] when compared to exposure to the degraded stimuli prior to the training. As noted above, however, experiments in the visual domain have demonstrated analogous perceptual and/or neural effects of prior information also without requiring a training phase. That is, degraded images could be recognized instantaneously once the original (nondegraded) image had been shown [e.g., Ludmer et al., 2011; Porter, 1954]. However, the neural mechanisms of corresponding phenomena in the auditory domain (i.e., speech perception) are yet unknown.

To shed light on this question, we used functional magnetic resonance imaging (fMRI) to measure brain activity during the perception of spectrally degraded sentences following exposure to an equally degraded or, which is the critical condition, following exposure to a nondegraded sentence. Importantly, the employed spectral degradation (see Methods for details) produced sentences that were incomprehensible when heard in isolation but which became comprehensible (i.e., their meaning could be extracted) when having been preceded by their original (nondegraded) version. In light of the predictive-coding framework, the comprehension of degraded speech can be explained by the formation of a template based on the processing of the preceding nondegraded sentence. This template consists of predictive codes that, if matching with subsequent input, carry enough information for the successful decoding of degraded speech. Subsequently, we refer to this prediction-based understanding of speech as “meaning extraction,” although we do not claim that this process can be mechanistically equated with a direct decoding of the degraded sentence. Alternatively, understanding might stem from an indirect meaning reactivation that is triggered after the degraded sentence is “recognized” based on structural commonalities (e.g., prosody) with the template. Most probably, however, both processes—direct meaning decoding based on lexical-semantic predictions and meaning retrieval based on a structural match with previous language input—run in parallel. In any case, the prediction-dependent understanding of degraded language offers an excellent opportunity to investigate the neural mechanisms of integrating sensory data and prior knowledge in speech processing.

METHODS

Participants

Twenty-nine healthy participants took part in this study (14 females, mean age = 34.5 years, SD = 12.2 years). All participants were right-handed, native speakers of German, had no history of neurological or psychiatric diseases, and gave written informed consent prior to participation. The study was approved by the local ethics committee of the RWTH Aachen University.

TABLE I. Overview of conditions

Reference	Target	Condition
<i>Structural prior</i>		
Degraded sentence A	Degraded sentence A	Structural match
Degraded sentence A	Degraded sentence B	Structural mismatch
<i>Propositional prior</i>		
Nondegraded sentence A	Degraded sentence A	Propositional match
Nondegraded sentence A	Degraded sentence B	Propositional mismatch

Paradigm and Stimuli

The participants performed a delayed-matching-to-sample task in which a target sentence had to be compared with a preceding reference sentence. The stimuli comprised 25 sentences, each in a nondegraded and a degraded version. All stimuli had been developed for a previous fMRI experiment and are described in detail in Meyer et al. [2004]. In brief, the sentences were recordings of short declarative infinitival statements of similar length (mean duration = 3.8 s, SD = 0.3 s), spoken by the same female speaker. A transcription of these sentences can be found in the Supporting Information. Degraded versions of these sentences (see the Supporting Information for a sound example) were created by low-pass filtering and an additional removal of aperiodic signals. This procedure included a reduction of spectral information to frequencies containing the F_0 as well as the 2nd and 3rd harmonic (see Supporting Information Fig. S1 for spectrograms of a nondegraded sentence and its degraded version). Thus, the resulting degraded stimuli merely retained the prosodic parameters of the original version (i.e., intonation, duration, and suprasegmental acoustic modulations) but lack any segmental and lexical information. Unlike purely low-pass filtered sentences, the degraded sentences employed in the present study sound like a humming voice heard from behind a door and are virtually impossible to understand without prior presentation of the nondegraded version as a reference [Meyer et al., 2002].

The experiment consisted of five blocks, each containing two subblocks of 10 events. For each event, the stimuli were presented in pairs consisting of a reference sentence followed by a target sentence for comparison. While the target sentence always was a degraded sentence, the type of the preceding reference sentence alternated between sub-blocks: it was degraded in the first sub-block and nondegraded in the second sub-block. The reason for keeping the order of sub-blocks constant (rather than randomizing them) was twofold. First, we wanted to minimize task-switching demands. Second, we wanted to ensure that the target sentences preceded by degraded reference sentences (structural match and mismatch conditions, cf., Table I) were processed as spectrally degraded, incomprehensible sentences. Therefore, we decided to present them always in the first sub-block before the template based on the intact sentence could be formed (i.e., before encountering

the nondegraded version in the second sub-block). Each sub-block consisted of five matching and five nonmatching pairs presented in randomized order. Within each block, the pairs in either sub-block were based on combinations of the same five sentences to ensure equivalent stimulus material and hence sensory input for both sub-blocks. The order of sentence presentation within each sub-block and the order of blocks were pseudo-randomized across participants. In sum, the type of reference sentence (degraded vs. nondegraded) varied between sub-blocks to minimize trial-to-trial task-switching effects, while the type of reference–target match (match vs. mismatch) varied between trials (i.e., within sub-blocks) to allow for an event-related analysis of hemodynamic activity (see below). The current experiment thus uses an event- (epoch-) related design for modeling and analysis, which was embedded in an overarching block-structure of event-presentation to reduce confounding effects of task-switching.

Our pairing scheme yielded four conditions (Table I): (1) a structural match condition when two identical degraded sentences were presented; (2) a structural mismatch condition when two different degraded sentences were presented; (3) a propositional match condition when a nondegraded reference sentence was identical to the degraded target (i.e., the target sentence was the degraded version of the reference sentence); and (4) a propositional mismatch condition when a nondegraded reference was different from the degraded target (i.e., the target sentence was not the degraded version of the reference sentence). The first two conditions thus require sentence comparisons that are entirely based on “structural” information such as prosody, suprasegmental acoustic modulations, intonation, pitch, etc. The latter two conditions in contrast enable comparisons that are additionally based on lexical-semantic (“propositional”) information provided by the nondegraded reference sentence. Importantly, the propositional match condition evoked an understanding of the degraded target (as established by pretesting). Therefore, this condition allowed for meaning extraction from the degraded (and normally unintelligible) target.

Each of the 25 degraded sentences was presented exactly once as a target in every condition. Therefore, the stimulus material constituting the (crucial) second part of each event was identical across conditions. Thus, the only difference between conditions that could explain differential fMRI results was (1) whether only structural or also

propositional information was provided by the reference sentence, and (2) whether this information matched the target sentence.

Procedure

After receiving task instructions, participants performed a practice run with sentence pairs different from those in the main experiment. The practice run was introduced to familiarize participants with the auditory stimuli and with the sequence of events. After entering the MR scanner, a sequence of test scans was run while examples of practice sentence stimuli were presented. This was done to allow an individual adjustment of the headphone volume for each participant and ensure that the sentence stimuli were well audible with the scanner noise in the background. Subsequently, the experiment started. Following the presentation of each sentence pair, a display was shown for 2 s asking participants to indicate by left or right button press whether or not the sentence pair contained two identical sentences. Participants were instructed to respond as fast as possible. Left/right response assignment was counterbalanced across participants such that half the participants responded with the left hand and the other half responded with the right hand to specify identical sentences. After a jittered intertrial interval of 4–9 s (uniformly distributed), the next sentence pair was presented. The sentences within each pair were separated by an interstimulus interval of 1 s. The sub-blocks lasted about 3 min and were separated by a 20-s resting period from each other. A warning tone in combination with a warning on the display was presented 1–3 s prior to the end of the resting period to prepare participants for the upcoming sub-block. The total time spent in the scanner was ~35 min.

fMRI Data Acquisition and Preprocessing

Imaging was performed on a Siemens Trio 3-T whole-body scanner (Erlangen, Germany) using gradient-echo echo-planar imaging (EPI). T2*-weighted BOLD contrast volumes covering the whole brain were acquired (TR = 2.2 s, in-plane resolution = $3.1 \times 3.1 \text{ mm}^2$, 36 axial slices of 3.1 mm thickness, distance factor = 15%). To allow for magnetic-field saturation, image acquisition was preceded by four dummy images which were discarded prior to data analysis. Images were analyzed using SPM5 (www.fil.ion.ucl.ac.uk/spm). The EPI images were corrected for head movement by affine registration using a two-pass procedure. This included an initial realignment of all images to the first image and a subsequent realignment to the mean of the realigned images. After realignment, the mean EPI image of each participant was spatially normalized to the MNI (Montreal Neurological Institute) single-subject template using the unified segmentation approach (Ashburner and Friston, 2005). The resulting parameters

that define the deformation field necessary to move the participant’s data into the space of the MNI tissue probability maps were then combined with the deformation field transforming between the latter and the MNI single-subject template. The ensuing deformation was subsequently applied to the individual EPI volumes that were thereby transformed into the MNI single-subject space and resampled at $2 \times 2 \times 2 \text{ mm}^3$ voxel size. Finally, these normalized images were spatially smoothed with a Gaussian kernel of 8-mm full width at half-maximum.

Data Analysis

Behavioral data were analyzed using SPSS 18.0.0 (SPSS, Chicago, IL). Reaction time and accuracy were subjected to 2×2 repeated-measures analyses of variance (ANOVAs) to test the effects of the factors Match (matching vs. non-matching sentence pairs) and Type of Prior (propositional vs. structural). Furthermore, reaction time of match and nonmatch trials was separately calculated for correct and incorrect trials (i.e., hits, misses, correct rejections, false alarms) and tested for the effects of signal-detection category and Type of Prior by a 4×2 ANOVA. Note that hits and misses were computed from correct and incorrect responses on match trials, respectively, and correct rejections and false alarms were computed from correct and incorrect responses on mismatch trials, respectively. Post-hoc analyses were Bonferroni-corrected for multiple comparisons. Finally, paired t tests were used to test for group-level differences in sensitivity (d') and decision criterion (c) between the different types of prior. The d' parameter was calculated based on the convention suggested for same-different designs [Macmillan and Creelman, 2005] using the formula

$$d' = 2z(0.5\{1 + [2p(c)\text{max} - 1]/2\})$$

with

$$p(c)\text{max} = \Phi(0.5\{z(H) - z(F)\}),$$

where Φ is the standard normal cumulative density function, H is the hit rate (i.e., proportion of match responses when pairs actually were matches), and F is the false-alarm rate (i.e., proportion of match responses when pairs actually were mismatches). The decision criterion c was calculated by the formula

$$c = -0.5[z(H) + z(F)].$$

Admittedly, typical same-different experiments within the signal-detection framework differ from the current experiment in terms of the number and complexity of stimuli. This analysis, however, was only performed to provide evidence for equivalent levels of difficulty across

both types of prior. For this purpose, applying the same-different convention should provide an acceptable approximation.

Imaging data were analyzed using the general linear model as implemented in SPM5. For each of the six events of interest (presentation of nondegraded or degraded reference sentences, presentation of target sentences from one of the four conditions: structural match, structural mismatch, propositional match, and propositional mismatch), the hemodynamic response was separately modeled by a boxcar reference vector (duration: 4 s) convolved with a canonical hemodynamic response function (HRF) and its first-order temporal derivative. The four target sentence regressors thus defined the four conditions which were identical with regard to sensory input but differed with regard to the type of input provided by the preceding reference sentence. Importantly, we limited our analysis to those target sentences that evoked correct match or mismatch responses (i.e., hits or correct rejections, respectively). Accordingly, a nuisance regressor for target sentences in trials with incorrect responses was included in the first-level model. The reason for restricting the analysis to correct trials was to ensure that participants paid attention to the task at hand during all trials included. However, one disadvantage of this approach is the potential reduction of statistical power due to the exclusion of trials. Furthermore, this exclusion may perturb the a-priori identical distribution of target stimuli across the four conditions because some of the excluded target sentences may still be present in one of the other conditions. We therefore computed a supplementary analysis based on all trials in which we reanalyzed the imaging data from all trials without the nuisance regressor.

Additional nuisance regressors were included for experimental events of no interest: left and right button presses and head movements as reflected by six motion parameters for translation and rotation. Finally, reaction time was included as parametric modulator for the structural match, structural mismatch, propositional match, and propositional mismatch regressors to assess intraindividual variation of brain activity related to performance level. Low-frequency signal drifts were removed by employing a high-pass filter with a cut-off period of 128 s. After correction of the time series for dependent observations according to an autoregressive first-order correlation structure, parameter estimates of the HRF regressors were calculated for each voxel using weighted least squares to provide maximum-likelihood estimators based on the temporal autocorrelation of the data [Kiebel et al., 2003]. The individual first-level contrasts (each condition relative to the implicit baseline) were then fed into a second-level random-effects ANOVA.

In this group analysis, mean parameter estimates over all participants were computed for all six regressors of interest (cf., above) as well as for the four parametric modulators (reflecting reaction times) and the two motor-response nuisance regressors (left/right button press).

Based on these estimates, separate t-contrasts within the ANOVA were calculated for testing differential effects. Furthermore, differential effects were combined into conjunctions based on the minimum t-statistic [Nichols et al., 2005]. Conjunction analysis was chosen because of its higher specificity and more conservative character as compared with a factorial analysis. In particular, by using a conjunction analysis, we constrained inference to those regions that were significantly present in all of the included conditions. All resulting activation maps were thresholded at $P < 0.05$ (family-wise error (FWE)-corrected for multiple comparisons at cluster level; cluster-forming threshold at voxel level: $P < 0.001$) and anatomically localized using probabilistic maps of cytoarchitecturally defined areas [Amunts et al., 2007; Zilles and Amunts, 2010] using version 1.6b of the SPM Anatomy toolbox [Eickhoff et al., 2005; www.fz-juelich.de/inm/inm-1/spm_anatomy_toolbox].

To identify regions implicated in the processing of all six sentence type events, the conjunction “nondegraded reference sentence \cap degraded reference sentence \cap structural match \cap structural mismatch \cap propositional match \cap propositional mismatch” was used. This analysis should thus reflect regions commonly activated by the sound stimuli or recruited by the general task demands (e.g., working memory, decision making). The contrast “degraded reference sentence $>$ nondegraded reference sentence” was employed to isolate regions that are more activated by the unintelligible sounds as compared to meaningful verbal information. The inverse contrast “nondegraded reference sentence $>$ degraded reference sentence” was analyzed to discern regions more tuned to intelligible speech than to (unintelligible) dynamic intonation contour. The latter contrast should thus identify regions that are selectively involved in processing the lexical-semantic aspects of speech.

Three conjunctions were employed to unravel the effects of the propositional prior compared to a purely structural prior, i.e., the effects of a nondegraded reference sentence compared to a degraded reference sentence on the subsequent processing of the degraded target sentence. To ensure that all activations associated with the propositional prior effect were specific for intelligible speech, the contrast “nondegraded reference sentence $>$ degraded reference sentence” was always included in these conjunctions. That is, we compared differential effects of the previously heard sentence on the processing of the identical (precisely the same target stimuli were presented in all four conditions) degraded sentences, but restricted this analysis to those regions that were actually involved in processing nondegraded (i.e., intelligible) speech, as opposed to degraded (i.e., normally unintelligible) speech. Hence, all these analyses should exclusively reveal effects within the brain network subserving lexical-semantic speech processing. First, the conjunction “[propositional match + propositional mismatch] $>$ (structural match + structural mismatch)] \cap (nondegraded reference sentence

> degraded reference sentence)'' aimed at identifying the general effect of exposure to a propositional prior as compared to a structural prior. This conjunction thus should specifically reveal those effects on the processing of the degraded target sentence that stem from any lexical-semantic influence provided by the reference sentence while controlling for (mis)matching of prosody (as this process should affect all target sentences alike, independently of whether the prior was propositional or structural). Second, the conjunction ''(propositional match > structural match) \cap (propositional match > structural mismatch) \cap (nondegraded reference sentence > degraded reference sentence)'' was used to reveal the effects of a propositional match on brain activity within the lexical-semantic network (as defined by the last component of the conjunction). Finally, the conjunction ''(propositional mismatch > structural mismatch) \cap (propositional mismatch > structural match) \cap (nondegraded reference sentence > degraded reference sentence)'' was employed to reveal the effects of a propositional mismatch on brain activity within the lexical-semantic network. Furthermore, we performed an additional analysis of these effects that was not restricted to those regions more responsive to intelligible compared to degraded speech.

Furthermore, we directly tested for differences between propositional matches and mismatches via (i) the contrast ''propositional match > propositional mismatch'' masked inclusively with the above analysis aiming at identifying effects of propositional matches [(propositional match > structural match) \cap (propositional match > structural mismatch) \cap (nondegraded reference sentence > degraded reference sentence)] and (ii) the contrast ''propositional mismatch > propositional match'' masked again inclusively with the above mentioned propositional mismatch effect ''(propositional mismatch > structural mismatch) \cap (propositional mismatch > structural match) \cap (nondegraded reference sentence > degraded reference sentence).''

In addition, we investigated the effect of matches versus mismatches across both types of priors by the conjunctions ''(propositional match > propositional mismatch) \cap (structural match > structural mismatch)'' and ''(propositional mismatch > propositional match) \cap (structural mismatch > structural match).''

RESULTS

Behavioral Results

Overall, the accuracy of identity judgments was comparable for targets following propositional and structural priors (83 and 79% correct responses, respectively). The 2×2 (Match: yes/no \times Type of Prior: propositional/structural) ANOVA of accuracy revealed a significant main effect of Match [$F(1, 28) = 29.93, P < 0.001$] and a significant Match \times Type of Prior interaction [$F(1, 28) = 12.02, P < 0.002$; Fig. 1A]. Type of Prior had no significant main effect

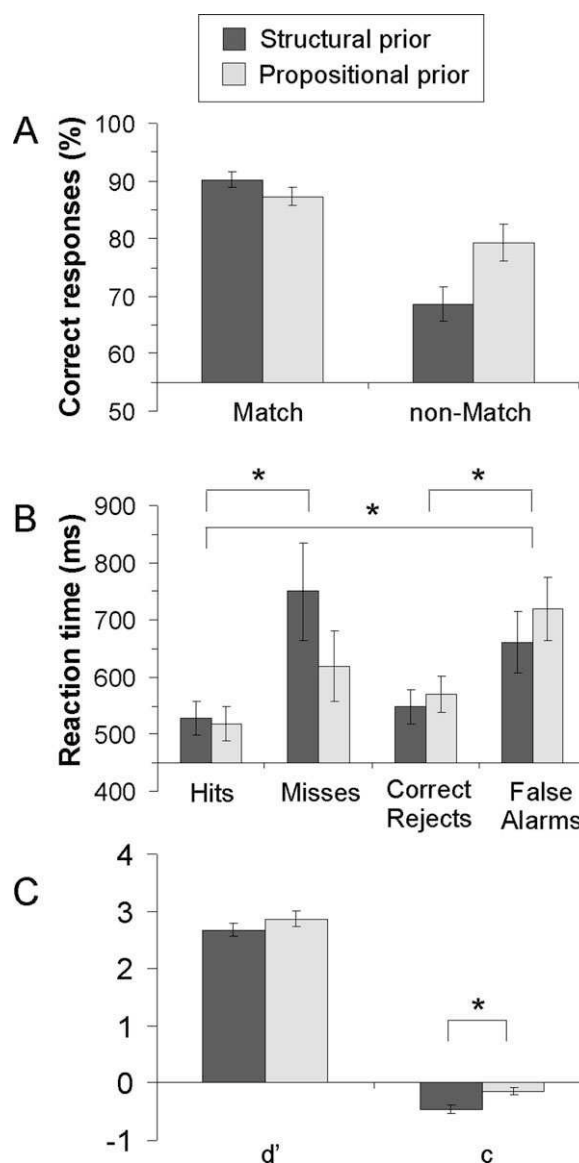


Figure 1.

Behavioral data. Accuracy (A) and reaction time (B) of target sentences following structural (dark gray) and propositional (light gray) priors. Panel C depicts measures of discriminability (d') and bias (c) as derived from same-different signal-detection analyses for the two types of prior. Positive d' values reflect discriminability above chance level. Negative c values indicate a bias toward ''same'' responses (i.e., a more lenient criterion), whereas positive c values signifies a bias toward ''different'' responses. Error bars represent the standard error of the means. * = significant at $P < 0.01$.

[$F(1, 28) = 3.86, p > .05$]. Thus, although accuracy was generally lower on nonmatch than match trials, this drop of accuracy was significantly stronger for targets following structural rather than propositional priors. An ANOVA of reaction time indicated a significant main effect of Match

[$F(1, 28) = 12.91, P = 0.001$]. Responses were faster for matching than nonmatching pairs, independent of Type of Prior (propositional/structural). When splitting match and nonmatch trials into correct and incorrect trials (i.e., hits, misses, correct rejections, false alarms), a 4(Category) \times 2(Type of Prior) ANOVA showed a main effect of Category [$F(3,18) = 10.99, P < 0.001$; Fig. 1B], indicating that in particular incorrect decision trials (misses and false alarms) were associated with slower responses. Specifically, after Bonferroni correction, hits (i.e., correct match decisions) were significantly faster than misses (i.e., incorrect nonmatch decisions), and correct rejections (i.e., correct nonmatch decisions) were faster than false alarms (i.e., incorrect match decisions). Furthermore, hits were also faster than false alarms. These results suggest that the above-reported main effect of Match on reaction time is mainly due to the fast responses on hit trials.

Signal-detection parameters for observer sensitivity (d') and decision criterion (c) were calculated to investigate differences in discriminability and response tendency, respectively (Fig. 1C). Paired t tests revealed no difference in d' between propositional and structural priors [$t(1, 28) = 1.19, P = 0.243$] but showed that c was significantly lower for structural than for propositional priors [$t(1, 28) = 3.89, P < 0.001$]. Thus, discrimination difficulty in trials with structural versus propositional priors was comparable, while responses following structural priors were relatively more biased toward “same” responses (i.e., match decisions) than responses following propositional priors. Finally, no sex differences were observed for any of the behavioral measures.

fMRI Results

General overview

Activations common to all six sentence types (nondegraded reference sentence \cap degraded reference sentence \cap structural match \cap structural mismatch \cap propositional match \cap propositional mismatch) were found bilaterally in temporal and frontal areas, in the supplementary motor area (SMA), premotor cortex, and cerebellum (Fig. 2A). Next, the contrast between nondegraded and degraded reference sentences revealed significant clusters in the left IFG [area 44, 45; Amunts et al., 1999], bilateral MTG/STG [TE1.0, TE 1.1; Morosan et al., 2001], precuneus, posterior cingulate cortex, hippocampus [SUB; Amunts et al., 2005], amygdala [CM; Amunts et al., 2005], thalamus, as well as dorsomedial and ventromedial prefrontal cortex (PFC; Fig. 2B). The inverse contrast (Fig. 2C) revealed higher activation in bilateral insula, middle frontal gyrus, and middle cingulate cortex, in right IFG (area 44), rolandic operculum [OP4; Eickhoff et al., 2006], and inferior parietal cortex, as well as left cerebellum, premotor cortex, and pre-SMA.

Furthermore, reaction times of the sentence comparisons were included as parametric modulators of the BOLD response to target sentence presentation in each of the

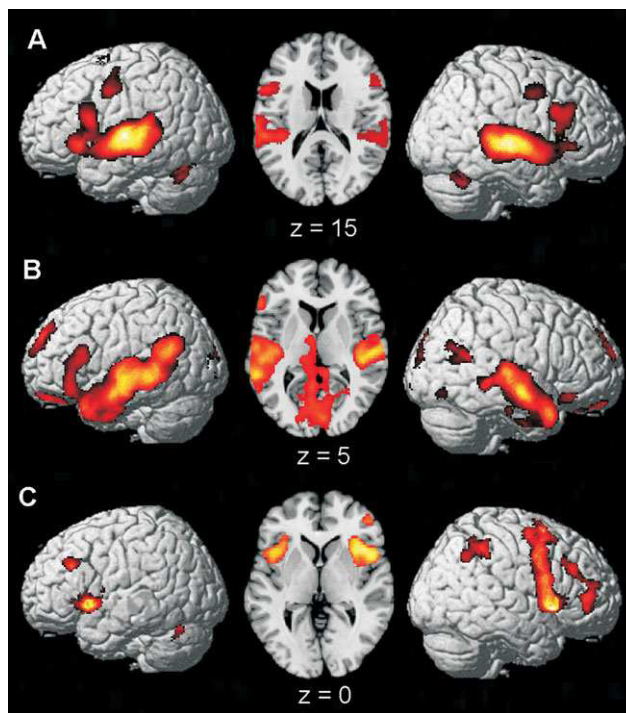


Figure 2.

Overview of the general fMRI findings. (A) The conjunction (nondegraded reference sentence \cap degraded reference sentence \cap structural match \cap structural mismatch \cap propositional match \cap propositional mismatch) revealed bilateral activations reflecting auditory processing common to all six sentence type events. (B) Regions representing the lexical-semantic rather than the prosodic aspects of speech (nondegraded reference sentence $>$ degraded reference sentence) and (C) the inverse contrast (degraded reference sentence $>$ nondegraded reference sentence). All images are thresholded at $P < 0.05$ (FWE-corrected at cluster-level; cluster forming threshold at voxel level: $P < 0.001$).

four conditions. No significant correlations between reaction time and BOLD response were observed in the group analysis.

Effect of propositional priors

To identify the general effect of exposure to propositional priors on the processing of (degraded) targets, we employed the following conjunction: [(propositional match + propositional mismatch) $>$ (structural match + structural mismatch)] \cap (nondegraded reference sentence $>$ degraded reference sentence). Three left-hemispheric clusters localized in the IFG (area 44/45), MTG and AG (PGa/PGp) resulted from this conjunction (Fig. 3A and Table II).

When focusing on activations related to propositional matches [(propositional match $>$ structural match) \cap (propositional match $>$ structural mismatch)] \cap

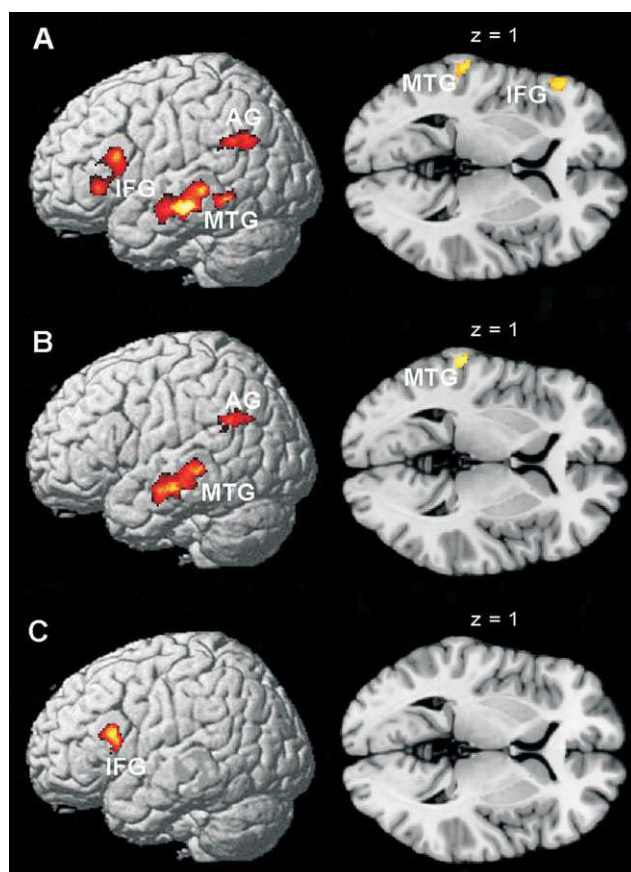


Figure 3.

Effects of propositional prior were all left-lateralized. **A)** Regions within the lexical-semantic network responding more to degraded targets that were preceded by propositional compared to structural priors “[$(\text{propositional match} + \text{propositional mismatch}) > (\text{structural match} + \text{structural mismatch}) \cap (\text{nondegraded reference sentence} > \text{degraded reference sentence})$].” Dissociation of this network into **B)** left MTG and AG for propositional matches [$(\text{propositional match} > \text{structural match}) \cap (\text{propositional match} > \text{structural mismatch}) \cap (\text{nondegraded reference sentence} > \text{degraded reference sentence})$] and **C)** Broca’s area for propositional mismatches [$(\text{propositional mismatch} > \text{structural mismatch}) \cap (\text{propositional mismatch} > \text{structural match}) \cap (\text{nondegraded reference sentence} > \text{degraded reference sentence})$]. All images are thresholded at $P < 0.05$ (FWE-corrected at cluster-level; cluster forming threshold at voxel level: $P < 0.001$). See also Supporting Information Figures S2 and S4.

(nondegraded reference sentence $>$ degraded reference sentence)], the resulting pattern no longer included Broca’s region (area 44/45) but was confined to the left AG and left MTG (Fig 3B and Table II). Broca’s region (area 44/45), however, was the only region associated with propositional mismatches [$(\text{propositional mismatch} > \text{structural$

$\text{match}) \cap (\text{propositional mismatch} > \text{structural mismatch}) \cap (\text{nondegraded reference sentence} > \text{degraded reference sentence})$] (Fig. 3C and Table II). Direct comparison between propositional matches and mismatches revealed that Broca’s region (area 44/45) was the only cluster showing significantly increased activation in response to propositional mismatches compared to propositional matches. No such specific association could be established for the MTG; however, the AG was more strongly activated in response to propositional matches compared to propositional mismatches.

We repeated this analysis without including the contrast “nondegraded reference sentence $>$ degraded reference sentence” in the conjunctions. For the general effect of propositional prior and propositional match, we observed additional activations in some areas including the left inferior temporal gyrus, hippocampus, amygdala, basal ganglia, and cerebellum (see Supporting Information Fig. S2 for details).

Effects of reference–target match versus mismatch

Regions responding more strongly to reference–target matches than mismatches in general comprised the ventromedial PFC (vmPFC) and the bilateral putamen. Conversely, reference–target mismatches selectively activated the pre-SMA bilaterally as well as the right insula and right IFG (see Supporting Information Fig. S3).

Supplementary analysis

In addition to the main analysis based only on correct trials, a supplementary analysis was performed involving all trials. The results (see Supporting Information Table SI for details) were largely comparable to those of the main analysis; however, some interesting differences emerged. When testing for the effect of a propositional (relative to a structural) prior on the processing of a (degraded) target sentence, we again found the left MTG and IFG, but instead of activation in the left AG, we now observed significant activity in the left thalamus. According to the thalamic connectivity atlas (<http://www.fmrib.ox.ac.uk/connect>), 65% of this thalamic activation was localized in a section having connections with the prefrontal cortex, and 29% of the cluster was localized in a section connecting to the temporal cortex. These thalamic areas are thought to include the mediodorsal nucleus and nuclei of the anterior complex [Behrens et al., 2003]. Analogous to the main analysis, the comparison to targets with structural priors revealed that the left MTG and thalamus (60% of the cluster predominantly connecting to the prefrontal cortex, 36% predominantly connecting to the temporal cortex) were responsive to propositional matches, whereas Broca’s region (area 44/45) was responsive to propositional mismatches (see Supporting Information Fig. S4).

TABLE II. Overview of activations

Region	Cytoarchitectonic area (percent overlap)	x	y	z	Z-score	Cluster size
<i>Effect of propositional prior</i>						
L IFG	Area 44 ^a (48% overlap); Area 45 ^a (36% overlap)	-54	20	16	5.29	632
L MTG		-62	-26	-10	4.71	1443
L AG	PGa ^b (41% overlap); PGp ^b (18% overlap)	-46	-62	28	3.96	405
<i>Effect of matching propositional prior</i>						
L MTG		-62	-10	-15	4.68	1085
L AG	PGa ^b (51% overlap); PGp ^b (14% overlap)	-48	-54	30	3.96	297
<i>Effect of nonmatching propositional prior</i>						
L IFG	Area 44 ^a (58% overlap); Area 45 ^a (40% overlap)	-52	18	18	5.00	351

All activations $P < 0.05$ (cluster-level FWE-corrected). x , y , z coordinates refer to the peak voxel in MNI space. R, right; L, left; IFG, inferior frontal gyrus; MTG, middle temporal gyrus; AG, angular gyrus.

^aAmunts et al., 1999.

^bCaspers et al., 2006.

DISCUSSION

This study investigated the behavioral and neural effects of propositional priors carrying lexical-semantic information on the decoding of degraded speech. As noted above, such decoding should reflect an interaction of sensory input and prior information via lexical-semantic predictions and meaning retrieval. We demonstrated that processing physically identical stimuli may result in distinct patterns of neural activation depending on the type of prior information available to the listener. In particular, prior propositional information provided by intelligible speech (compared to purely “structural” information provided by degraded speech) resulted in stronger recruitment of a left-lateralized network comprising the MTG, AG (PGa/PGp), and area 44/45 of Broca’s region. Within this network a direct comparison between propositional matches and mismatches revealed a selective association of activity in Broca’s region with propositional mismatches and a selective association of activity in the AG with propositional matches. A supplementary analysis based on all (instead of correct-only) trials indicated an involvement of the left thalamus (rather than left AG) with propositional priors.

Importantly, reaction time and observer sensitivity did not differ between trials with structural and propositional priors. Therefore, the fMRI results reported here are highly unlikely to be explained by different degrees of task difficulty. Furthermore, we would like to stress that the results are also very unlikely to arise primarily from the matching or recognition of prosody, as this process should be initiated by both types of prior information and is controlled for by the contrasts included in the conjunctions. Rather, the resulting activations most likely stem from the (attempted) lexical-semantic processing of the degraded target sentence when prior propositional information was provided, as this was the only difference between the conditions. Furthermore, in trials with matching propositional priors, this lexical-semantic processing should reflect the

subjective impression of understanding the target sentence. In our view, this perceptual phenomenon did not lead to an observable behavioral benefit compared to structural matches, because the two sentences of propositional match trials were physically not entirely identical, in contrast to structural match trials. This physical difference between reference and target in propositional match trials will have made the matching process more challenging, thereby reducing or even outweighing the (presumably) facilitatory effect of understanding the target sentence. We would moreover suggest that the behavioral benefit observed for propositional mismatches (compared to structural mismatches) might be due to the absence of the “sudden understanding” phenomenon normally associated with propositional matches: while targets in both propositional and structural mismatch conditions were physically different from the reference, the fact that the target could not be understood despite the nondegraded (propositional) prior should have provided a potent clue facilitating the (overall more difficult) mismatch decision under these circumstances, relative to trials with a nonmatching degraded (structural) prior.

According to the dual-stream model of language [Hickok and Poeppel, 2007; Hickok et al., 2011] processing of speech sounds recruits temporal lobe structures in a hierarchical dorsal-to-ventral fashion. While the core and belt auditory areas on the planum temporale process simpler aspects of sounds, the more ventrally located superior temporal gyrus and superior temporal sulcus (STG/STS) are more sensitive to complex amplitude and frequency modulations present in speech sounds. Even further ventrally, the MTG and ITG are thought to be involved in the more abstract analysis of semantic and syntactic features of speech. In accordance with this model, the results of the conjunction across all reference and target sentences indicated the involvement of the STG in response to the complex sound properties present across all sentence types. In contrast, comparing nondegraded with degraded reference sentences yielded activity in the MTG but not in the STG.

Of note, this contrast and the inverse contrast revealed an activity pattern very similar to that reported by Meyer et al. [2004] for comparing nondegraded and degraded speech. Additionally, other areas including the left AG, left IFG, precuneus, and posterior cingulate that resulted from the comparison of nondegraded vs. degraded speech are associated with the lexical-semantic analysis of meaningful speech [Binder et al., 2009; Price, 2010].

Furthermore, the left MTG together with the left AG (or, when considering all trials in the supplementary analysis, the left MTG and the left thalamus) were activated when target sentences matched the propositional prior, i.e., when meaning could potentially be decoded from a degraded sentence. This finding indicated that speech processing in the MTG, in line with Binder and Price [2001], does not depend on the physical properties of speech sounds conveyed by bottom-up signaling because it responded differentially to physically identical target sentences. Rather, the MTG was recruited when more abstract linguistic processing was enabled by a top-down application of stored lexical-semantic information stemming from the matching propositional prior. Indeed, the left MTG has been identified as a key region for semantic processing and meaning extraction [Binder et al., 2009; Price 2010]. Activation of this area has been observed in various lexical-semantic tasks ranging from comprehension of degraded sentences [e.g., Adank and Devlin, 2010; Davis and Johnsruide, 2003] to attempts to derive meaning from gestures supporting spoken speech [Dick et al., 2009; Hubbard et al., 2009]. In line with these findings, lesions of this region are associated with impairments in language comprehension [e.g., Dick et al., 2007; Dronkers et al., 2004].

In addition to the left MTG, also the AG in the left temporo-parietal junction has frequently been associated with semantic processing [Binder et al., 2009]. The AG, which corresponds to the cytoarchitectonic areas PGa and PGp [Caspers et al., 2006], is considered to be a heteromodal association area with access to higher-order concepts and long-term memory. The left AG has been suggested to provide top-down “semantic constraints” in language processing [Price, 2010] and may thus facilitate meaning extraction from ambiguous sentences [Obleser and Kotz, 2010]. Interestingly, Seghier et al. [2010] found that such a function is most likely attributable to the medial or ventral portion of the AG which corresponds well to the AG cluster observed in the current study. Thus, the selective AG activation on correct trials might be the origin of top-down signals mediating predictions that facilitate decoding of the degraded sentences and enabling correct match/non-match decisions based on lexical-semantic content. While both left MTG and AG showed stronger activation when lexical-semantic expectations were present and fulfilled, their specific contribution to the processing of the speech signal is probably not equivalent. The MTG has been proposed to be involved in mapping sound (represented in the STS) to meaning [which is thought to be distributed

throughout the cortex; Hickok and Poeppel, 2007] and thereby enabling comprehension of speech signals.

The left AG, on the other hand, is thought to be a hierarchically higher node [Binder et al., 2009] which aids language processing by top-down modulation [Price, 2010; Seghier et al., 2010]. Potentially, this top-down influence might have been more pronounced on trials with clearer evidence that consequently could be answered correctly. Alternatively however, top-down modulation originating in the AG might also have rendered the evidence clearer and might have been a precondition for correct match/nonmatch decisions.

While the pattern of activation in the AG indicated that activity in this region is mainly linked with correct trials, we observed significant thalamic activation only in the supplementary analysis. This suggests that both correctly and incorrectly answered trials contributed to the observed thalamic activation but that limiting the analysis to the correct trials might have provided insufficient statistical power to detect the thalamic activation. The effect of excluding ~20% of trials in the main analysis may have manifested itself particularly in a small structure such as the thalamus, especially in combination with the cluster threshold we used. Indeed, the thalamic activation was significant in the main analysis, too, when slightly lowering the cluster-forming threshold. Nonetheless, we think that the thalamic activity is an interesting finding that deserves closer attention. Presumably, this activation could be due to top-down modulation of sensory processing by signals from temporal or frontal areas. Indeed, cortico-thalamic feedback is known to influence thalamic responses to auditory stimulation by amplifying those sensory features that optimally represent the signal predicted by cortical areas and inhibit all other response features [Alitto and Usrey, 2003; Suga et al., 2002]. Furthermore, based on patient studies associating thalamic lesions with language deficits, Nadeau and Crosson [1997] proposed that thalamic nuclei can selectively gate and integrate the flow of lexical information between frontal and temporo-parietal cortices and regulate the access to lexical information when semantic input is provided. More recent support for a thalamic involvement in language processing beyond the relay of auditory information has been found in electrophysiological studies implicating cortico-thalamic networks in processing the semantic and syntactic features of spoken sentences [David et al., 2011; Wahl et al., 2008], in fMRI studies reporting stronger thalamic responses to normal compared to (unintelligible) prosodic speech [Kotz et al., 2003] and demonstrating a thalamic contribution to resolving ambiguity of linguistic input [Ketteler et al., 2008].

In contrast to the left MTG, AG and (when considering all trials) the thalamus, the left IFG was selectively activated in response to mismatches between the target sentence and prior propositional information, i.e., when attempts to decode the degraded sentence based on the propositional prior failed. The activation was localized in

a portion of the IFG that has been cytoarchitecturally defined as area 44/45 [Broca's region; Amunts et al., 1999] and is known to play a role in speech perception, in particular when speech is syntactically complex [Friederici, 2011; Friederici et al., 2010]. This region, however, is not restricted to language processing but appears to be generally involved in the sequencing of spatiotemporal structures of various modalities including language, music and action [Fadiga et al., 2009]. Importantly, left IFG activation has also been associated with detecting incompatibility in speech and other hierarchically organized sequences [Embick et al., 2000; Friederici et al., 2010; Myers et al., 2009] which might be interpreted as prediction errors signaling the need for reanalysis to prevent misinterpretation [Christensen and Wallentin, 2011; Novick et al., 2005; Price, 2010]. Furthermore, Giraud et al. [2004] highlighted the role of Broca's region for search of meaningful content in auditory input. Accordingly, the involvement of Broca's region in the "propositional prior" network might arise from the potential meaningful content provided by nondegraded reference sentences compared to degraded ones. In line with the above reasoning, mismatches between the target and the preceding nondegraded sentence might have evoked even stronger activation in Broca's region because the incoming signal was incompatible with the expected sequence of auditory events while the presence of meaningful content was hard to determine. Of interest, activation of Broca's region has also been linked with effects of complexity and task difficulty [Fadiga et al., 2009]. The behavioral data indicated that trials with propositional mismatches were more difficult to discriminate than trials with propositional matches. However, this held also true for structural mismatches. Furthermore, the contrast between all mismatch and match trials demonstrated that in particular the pre-SMA (in addition to the right insula and right IFG) was associated with the overall effect of the higher task difficulty and response conflict associated with mismatches. Therefore, we would suggest that the selective activation of Broca's region in response to propositional mismatches reflects its specific involvement in challenging linguistic tasks, namely when the presence of meaning is hard to determine (search for meaning in noise) and an attempt is made to decode this potential meaning (reanalysis and possibly prevention of misinterpretation).

However, it should also be noted that Broca's region is a multifunctional area [see Rogalsky and Hickok, 2011, for a recent review]. The present study cannot definitively determine the exact mechanism reflected by the activation of Broca's region, and alternative accounts such as the phonological working-memory function of Broca's region cannot completely be ruled out. Nonetheless, if Broca's region merely reflected the storage and inner rehearsal of auditory speech stimuli, the comparison of trials with propositional versus structural priors should not evoke activity in this region because these working-memory processes are also required for matching decisions purely

based on the prosodic speech stimuli. Therefore, it seems more likely that the recruitment of Broca's region is due to the influence of lexical-semantic content provided by (particularly nonmatching) propositional priors on the subsequent processing of the target sentences, as this is the only aspect that distinguishes these conditions.

While Broca's region thus showed higher sensitivity for mismatches with propositional priors, the left MTG and AG (or, when considering all trials, the left MTG and the left thalamus) were implicated in lexical-semantic processing and meaning extraction by means of using prior information. When an informative propositional template is available, originally incomprehensible speech stimuli can be subjected to a more profound analysis. That is, prior exposure to the intelligible original sentence results in a dramatic change in the appraisal of a hitherto meaningless speech-like auditory stimulus that can suddenly be perceived as a salient and meaningful sentence. Such an expectancy-guided reappraisal of formerly noisy and meaningless sensory stimuli corresponds well to the notion of predictive coding which proposes that the brain actively participates in the perceptual process by anticipating upcoming events [Friston, 2005; Rao and Ballard, 1999]. This inferential process may result in striking effects of prior information on perception, even if the perceived stimuli are physically identical [Hunter et al., 2010].

Conceptually, accounts of predictive coding in perception [Friston, 2005; Rao and Ballard, 1999] assert that sensory predictions are generated at each level of the cortical hierarchy based on integration of prior knowledge with neural activity from lower levels. These predictions are thought to be fed back to lower levels where they are compared to the actual neural activity representing the sensory data. Differences between predicted and observed information are fed forward to the hierarchically higher node as the prediction error. This prediction error, in turn, is used to optimize subsequent predictions, as it indicates the fit of the current priors. Therefore, when a prediction fits well with the incoming sensory data, potential ambiguities among the stimuli can be resolved because the perceptual alternatives are weighted by the predicted template. With regard to the current study, propositional templates could only be successfully employed for decoding a degraded target sentence when (1) the reference sentence was a nondegraded sentence (propositional prior) and (2) the target sentence matched that reference sentence. Presumably, interactions within a left-hemispheric network including the AG and the MTG are an important generator of these lexical-semantic predictions. Possibly, these predictions were sent to lower levels of the auditory processing hierarchy and potentially modified the response profile in the left thalamus. Alternatively, it is also possible that top-down feedback from the AG affected the processing in the MTG such that sound could be successfully mapped to meaning, resulting in the percept of an intelligible sentence. The importance of these regions is supported by previous studies reporting involvement of

left temporal areas in successful decoding of originally unintelligibly degraded speech stimuli [Eulitz and Hanne mann, 2010; Giraud et al., 2004; Hannemann et al., 2007]. In contrast, unsuccessful decoding attempts of target sentences following a mismatching propositional prior were selectively associated with activation of Broca's region. This could indicate that Broca's region contributes to speech perception by searching for meaningful content and comparing expected auditory sequences with the actual input. Consequently, activation of Broca's region might represent the prediction error when prior knowledge cannot be used to decode meaningful speech due to mismatches between propositional priors and degraded targets. Alternatively, the comparison between the predicted and the actual signal might also happen elsewhere in the brain. In this case, involvement of Broca's region could reflect the updating of the expectations to be generated. Finally, a response to these mismatches might also signal the need for reanalysis of the auditory sequence to prevent misinterpretation. This signal might then lead to a reduced involvement of the left MTG and AG in processing propositional mismatches. Thus, top-down influences of Broca's region on the MTG in particular but also on the AG might be relevant for the perceptual phenomenon of sudden understanding of a heavily degraded sentence and, at the same time, the lack of comprehension when prior knowledge cannot be applied to such degraded input. However, the exact mechanisms cannot be determined with the current analysis but would ultimately require dynamic causal modeling or related approaches.

Although we interpret our results within the framework of predictive coding, we do not claim that this framework is the only one that can account for the findings. Alternatively, it might also be warranted to refer to priming mechanisms to explain the recognition of degraded sentences by an exposure effect of the original stimulus. However, predictive coding is the more generic framework, encompassing all kinds of contextual effects on perception, ranging from subliminal priming to instructed expectations. Accordingly, we prefer to interpret our findings in the context of this more general model of brain function, although the current experiment did not aim to test the predictive-coding account itself.

CONCLUSION

The current study demonstrated that, in line with the notion of predictive coding, prior information has a decisive effect on speech perception. In particular, the processing of degraded sentences, which were incomprehensible when heard in isolation, was shown to be sensitive to the availability of memory templates ("priors") carrying propositional (i.e., lexical-semantic) information. It may be assumed that this effect results from a combination of direct meaning decoding, based on lexical-semantic predictions, and meaning retrieval, based on a structural match

with previous speech input. Prior propositional information also influenced the neural response to degraded sentences and hence revealed the neural correlates of these processes. Specifically, successful meaning extraction from degraded sentences based on prior information was associated with increased activity in the left MTG and AG. These areas are known to play a role in high-level lexical-semantic processing that presumably modulates more basic speech processing at lower levels including the thalamus. In contrast, unsuccessful decoding due to a misleading propositional prior was selectively associated with stronger activation of Broca's region which may reflect the search for relevant acoustic cues in auditory sequences as well as processing prediction errors, thereby potentially preventing misinterpretation.

REFERENCES

- Adank P, Devlin JT (2010): On-line plasticity in spoken sentence comprehension: Adapting to time-compressed speech. *Neuroimage* 49:1124–1132.
- Alitto HJ, Usrey WM (2003): Corticothalamic feedback and sensory processing. *Curr Opin Neurobiol* 13:440–445.
- Amunts K, Kedo O, Kindler M, Pieperhoff P, Mohlberg H, Shah NJ, Habel U, Schneider F, Zilles K (2005): Cytoarchitectonic mapping of the human amygdala, hippocampal region and entorhinal cortex: Intersubject variability and probability maps. *Anat Embryol (Berl)* 210:343–352.
- Amunts K, Schleicher A, Bürgel U, Mohlberg H, Uylings HB, Zilles K (1999): Broca's region revisited: Cytoarchitectonic and intersubject variability. *J Comp Neurol* 412:319–341.
- Amunts K, Schleicher A, Zilles K (2007): Cytoarchitecture of the cerebral cortex—More than localization. *Neuroimage* 37: 1061–1065.
- Arnal LH, Wyart V, Giraud AL (2011): Transitions in neural oscillations reflect prediction errors generated in audiovisual speech. *Nat Neurosci* 14:797–803.
- Ashburner J, Friston KJ (2005): Unified segmentation. *Neuroimage* 26:839–851.
- Bar M (2007): The proactive brain: Using analogies and associations to generate predictions. *Trends Cogn Sci* 11:280–289.
- Behrens TE, Johansen-Berg H, Woolrich MW, Smith SM, Wheeler-Kingshott CA, Boulby PA, Barker GJ, Sillery EL, Sheehan K, Ciccarelli O, Thompson AJ, Brady JM, Matthews PM (2003): Noninvasive mapping of connections between human thalamus and cortex using diffusion imaging. *Nat Neurosci* 6:750–757.
- Binder JR, Price CJ (2001): Functional imaging of language. In: Cabeza R, Kingstone A, editors. *Handbook on Functional Neuroimaging of Cognition*. Cambridge (MA): MIT Press. pp 187–251.
- Binder JR, Desai RH, Graves WW, Conant LL (2009): Where is the semantic system? A critical review and meta-analysis of 120 functional neuroimaging studies. *Cereb Cortex* 19:2767–2796.
- Blakemore SJ, Wolpert DM, Frith CD (1998): Central cancellation of self-produced tickle sensation. *Nat Neurosci* 1:635–640.
- Caspers S, Geyer S, Schleicher A, Mohlberg H, Amunts K, Zilles K (2006): The human inferior parietal cortex: Cytoarchitectonic parcellation and interindividual variability. *Neuroimage* 33:430–448.

- Christensen KR, Wallentin M (2011): The locative alternation: Distinguishing linguistic processing cost from error signals in Broca's region. *Neuroimage* 56:1622–1631.
- David O, Maess B, Eckstein K, Friederici AD (2011): Dynamic causal modelling of subcortical connectivity of language. *J Neurosci* 31:2712–2717.
- Davis MH, Johnsruide IS (2003): Hierarchical processing in spoken language comprehension. *J Neurosci* 23:3423–3431.
- Davis MH, Johnsruide IS (2007): Hearing speech sounds: Top-down influences on the interface between audition and speech perception. *Hear Res* 229:132–147.
- Davis MH, Johnsruide IS, Hervais-Adelman A, Taylor K, McGettigan C (2005): Lexical information drives perceptual learning of distorted speech: Evidence from the comprehension of noise-vocoded sentences. *J Exp Psychol Gen* 134: 222–241.
- den Ouden HE, Friston KJ, Daw ND, McIntosh AR, Stephan KE (2009): A dual role for prediction error in associative learning. *Cereb Cortex* 19:1175–1185.
- den Ouden HE, Daunizeau J, Roiser J, Friston KJ, Stephan KE (2010): Striatal prediction error modulates cortical coupling. *J Neurosci* 30:3291–3209.
- Dick AS, Goldin-Meadow S, Hasson U, Skipper JL, Small SL (2009): Co-speech gestures influence neural activity in brain regions associated with processing semantic information. *Hum Brain Mapp* 30:3509–3526.
- Dick F, Saygin AP, Galati G, Pitzalis S, Bentrovato S, D'Amico S, Wilson S, Bates E, Pizzamiglio L (2007): What is involved and what is necessary for complex linguistic and nonlinguistic auditory processing: Evidence from functional magnetic resonance imaging and lesion data. *J Cogn Neurosci* 19:799–816.
- Dronkers NF, Wilkins DP, van Valin RD Jr, Redfern BB, Jaeger JJ (2004): Lesion analysis of the brain areas involved in language comprehension. *Cognition* 92:145–177.
- Eickhoff SB, Stephan KE, Mohlberg H, Grefkes C, Fink GR, Amunts K, Zilles K (2005): A new SPM toolbox for combining probabilistic cytoarchitectonic maps and functional imaging data. *Neuroimage* 25:1325–1335.
- Eickhoff SB, Schleicher A, Zilles K, Amunts K (2006): The human parietal operculum. I. Cytoarchitectonic mapping of subdivisions. *Cereb Cortex* 16:254–267.
- Embick D, Marantz A, Miyashita Y, O'Neil W, Sakai KL (2000): A syntactic specialization for Broca's area. *Proc Natl Acad Sci USA* 97:6150–6154.
- Enns JT, Lleras A (2008): What's next? New evidence for prediction in human vision. *Trends Cogn Sci* 12:327–333.
- Eulitz C, Hannemann R (2010): On the matching of top-down knowledge with sensory input in the perception of ambiguous speech. *BMC Neurosci* 11:67.
- Fadiga L, Craighero L, D'Ausilio A (2009): Broca's area in language, action, and music. *Ann N Y Acad Sci* 1169:448–458.
- Friederici AD (2011): The brain basis of language: From structure to function. *Physiol Rev* 91:1357–1392.
- Friederici AD, Kotz SA, Scott SK, Obleser J (2010): Disentangling syntax and intelligibility in auditory language comprehension. *Hum Brain Mapp* 31:448–457.
- Friston K (2005): A theory of cortical responses. *Philos Trans R Soc Lond B Biol Sci* 360:815–836.
- Giraud AL, Kell C, Thierfelder C, Sterzer P, Russ MO, Preibisch C, Kleinschmidt A (2004): Contributions of sensory input, auditory search and verbal comprehension to cortical activity during speech processing. *Cereb Cortex* 14:247–255.
- Grossberg S (2003): Resonant neural dynamics of speech perception. *J Phon* 31:423–445.
- Hall DA, Johnsruide IS, Haggard MP, Palmer AR, Akeroyd MA, Summerfield AQ (2002): Spectral and temporal processing in human auditory cortex. *Cereb Cortex* 12:140–149.
- Hannemann R, Obleser J, Eulitz C (2007): Top-down knowledge supports the retrieval of lexical information from degraded speech. *Brain Res* 1153:134–143.
- Hickok G, Houde J, Rong F (2011): Sensorimotor integration in speech processing: Computational basis and neural organization. *Neuron* 69:407–422.
- Hickok G, Poeppel D (2007): The cortical organization of speech processing. *Nat Rev Neurosci* 8:393–402.
- Hosoya T, Baccus SA, Meister M (2005): Dynamic predictive coding by the retina. *Nature* 436:71–77.
- Hubbard AL, Wilson SM, Callan DE, Dapretto M (2009): Giving speech a hand: Gesture modulates activity in auditory cortex during speech perception. *Hum Brain Mapp* 30:1028–1037.
- Hunter MD, Eickhoff SB, Pheasant RJ, Douglas MJ, Watts GR, Farrow TF, Hyland D, Kang J, Wilkinson ID, Horoshenkov KV, Woodruff PW (2010): The state of tranquillity: Subjective perception is shaped by contextual modulation of auditory connectivity. *Neuroimage* 53:611–618.
- Jakobs O, Wang EW, Dafotakis M, Grefkes C, Zilles K, Eickhoff SB (2009): Effects of timing and movement uncertainty implicate the temporo-parietal junction in the prediction of forthcoming motor actions. *Neuroimage* 47:667–677.
- Kaas JH, Hackett TA (2000): Subdivisions of auditory cortex and processing streams in primates. *Proc Natl Acad Sci USA* 97:11793–11799.
- Ketteler D, Kastrau F, Vohn R, Huber W (2008): The subcortical role of language processing. High level linguistic features such as ambiguity-resolution and the human brain: An fMRI study. *Neuroimage* 39:2002–2009.
- Kiebel SJ, Glaser DE, Friston KJ (2003): A heuristic for the degrees of freedom of statistics based on multiple variance parameters. *Neuroimage* 20:591–600.
- Kotz SA, Meyer M, Alter K, Besson M, von Cramon DY, Friederici AD (2003): On the lateralization of emotional prosody: An event-related functional MR investigation. *Brain Lang* 86: 366–376.
- Ludmer R, Dudai Y, Rubin N (2011): Uncovering camouflage: Amygdala activation predicts long-term memory of induced perceptual insight. *Neuron* 69:1002–1014.
- Macmillan NA, Creelman CD. 2005. *Detection Theory: A User's Guide*. Mahwah, NJ, US: Lawrence Erlbaum Associates Publishers.
- Meyer M, Alter K, Friederici AD, Lohmann G, von Cramon DY (2002): fMRI reveals brain regions mediating slow prosodic modulations in spoken sentences. *Hum Brain Mapp* 17:73–88.
- Meyer M, Steinhauer K, Alter K, Friederici AD, von Cramon DY (2004): Brain activity varies with modulation of dynamic pitch variance in sentence melody. *Brain Lang* 89:277–289.
- Morosan P, Rademacher J, Schleicher A, Amunts K, Schormann T, Zilles K (2001): Human primary auditory cortex: Cytoarchitectonic subdivisions and mapping into a spatial reference system. *Neuroimage* 13:684–701.
- Myers EB, Blumstein SE, Walsh E, Eliassen J (2009): Inferior frontal regions underlie the perception of phonetic category invariance. *Psychol Sci* 20:895–903.
- Nadeau SE, Crosson B (1997): Subcortical aphasia. *Brain Lang* 58:355–402.

- Nichols T, Brett M, Anderson J, Wager T, Poline JB (2005): Valid conjunction inference with the minimum statistic. *Neuroimage* 15:653–660.
- Novick JM, Trueswell JC, Thompson-Schill SL (2005): Cognitive control and parsing: Reexamining the role of Broca's area in sentence comprehension. *Cogn Affect Behav Neurosci* 5:263–281.
- Obleser J, Kotz SA (2010): Expectancy constraints in degraded speech modulate the language comprehension network. *Cereb Cortex* 20:633–640.
- Porter P (1954): Another picture-puzzle. *Am J Psychol* 67:550–551.
- Price CJ (2010): The anatomy of language: A review of 100 fMRI studies published in 2009. *Ann NY Acad Sci* 1191:62–88.
- Rao RP, Ballard DH (1999): Predictive coding in the visual cortex: A functional interpretation of some extra-classical receptive-field effects. *Nat Neurosci* 2:79–87.
- Rauschecker JP, Tian B, Hauser M (1995): Processing of complex sounds in the macaque nonprimary auditory cortex. *Science* 268:111–114.
- Remez RE, Rubin PE, Berns SM, Pardo JS, Lang JM (1994): On the perceptual organization of speech. *Psychol Rev* 101:129–156.
- Rogalsky C, Hickok G (2011): The role of Broca's area in sentence comprehension. *J Cogn Neurosci* 23:1664–1680.
- Saberi K, Perrott DR (1999): Cognitive restoration of reversed speech. *Nature* 398:760–761.
- Scott SK, Blank CC, Rosen S, Wise RJ (2000): Identification of a pathway for intelligible speech in the left temporal lobe. *Brain* 123:2400–2406.
- Seghier ML, Fagan E, Price CJ (2010): Functional subdivisions in the left angular gyrus where the semantic system meets and diverges from the default network. *J Neurosci* 30:16809–16817.
- Shannon RV, Zeng FG, Kamath V, Wygonski J, Ekelid M (1995): Speech recognition with primarily temporal cues. *Science* 270:303–304.
- Sharma J, Dragoi V, Tenenbaum JB, Miller EK, Sur M (2003): V1 neurons signal acquisition of an internal representation of stimulus location. *Science* 300:1758–1763.
- Suga N, Xiao Z, Ma X, Ji W (2002): Plasticity and corticofugal modulation for hearing in adult animals. *Neuron* 36:9–18.
- Wahl M, Marzinzik F, Friederici AD, Hahne A, Kupsch A, Schneider GH, Saddy D, Curio G, Klostermann F (2008): The human thalamus processes syntactic and semantic language violations. *Neuron* 59:695–707.
- Zilles K, Amunts K (2010): Centenary of Brodmann's map—Conception and fate. *Nat Rev Neurosci* 11:139–145.

SUPPLEMENTAL METHODS

Transcription of the sentence stimuli

Block A

Peter verspricht Anna, zu arbeiten und das Büro zu putzen.

Udo verbietet Jutta, zu verschlafen und die Gäste zu enttäuschen.

Heiko verbietet Carla, zu türmen und den Kumpel zu verlassen.

Werner befiehlt Lena, zu schlafen und die Türen zu verriegeln.

Harald hilft Sigrid, zu verschwinden und die Grenze zu erreichen.

Block B

Sascha versichert Maja, zu verweilen und die Reise zu organisieren.

Eckhard bittet Inge, zu verschlafen und den Ausflug zu unterbrechen.

Volker gesteht Lore, zu schummeln und die Regeln zu missachten.

Henning empfiehlt Moni, zu reagieren und den Anwalt zu informieren.

Rosa verspricht Helmut, zu laufen und den Termin zu wahren.

Block C

Heidi verbietet Hartmut, zu quengeln und die Eltern zu nerven.

Petra erlaubt Markus, zu zelten und das Kanu zu mieten.

Ina droht Richard, zu jammern und die Stimmung zu verderben.

Sandra befiehlt Günther, zu jubeln und die Fahnen zu schwenken.

Maga hilft Lukas, zu klettern und den Felsen zu erklimmen.

Block D

Peter verspricht, Anna zu entlasten und das Büro zu putzen.

Udo verbietet, Jutta zu ärgern und die Gäste zu enttäuschen.

Heiko droht, Carla zu knebeln und den Kumpel zu verlassen.

Werner befiehlt, Lena zu suchen und die Türen zu verriegeln.

Harald hilft, Sigrid zu fesseln und die Grenze zu erreichen.

Block E

Sascha versichert, Maja zu sponsern und die Reise zu organisieren.

Eckhard bietet, Inge zu begrüßen und den Ausflug zu unterbrechen.

Erwin rät, Dora zu verlassen und die Chance zu nutzen.

Volker gesteht, Lore zu betrügen und die Regeln zu missachten.

Ina droht, Richard zu tadeln und die Stimmung zu verderben.

SUPPLEMENTAL FIGURES

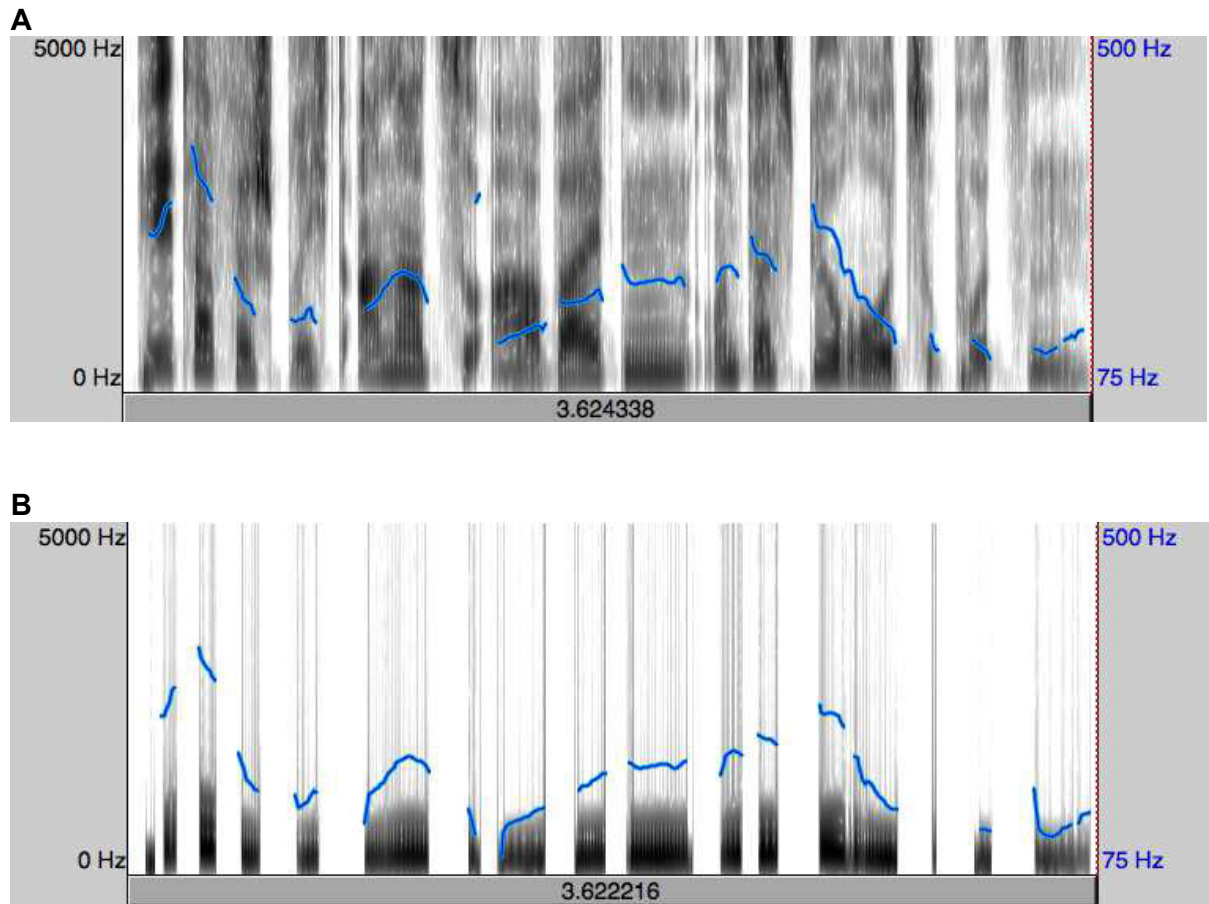


Figure S1: Spectrogram of the sentence stimuli

Spectrogram of a speech stimulus before (A, non-degraded sentence) and after (B, degraded sentence) application of the filtering procedure. While the pitch contour (blue) is not changed by the filtering, the spectral information (black) is reduced to frequencies containing the F0 as well as the 2nd and the 3rd harmonic. Additionally, the duration of degraded sentences is slightly shorter as compared to the normal sentences from which they are derived because of the removal of aperiodic portions. The spectrogram in this example corresponds to the first sentence listed above in Block A.

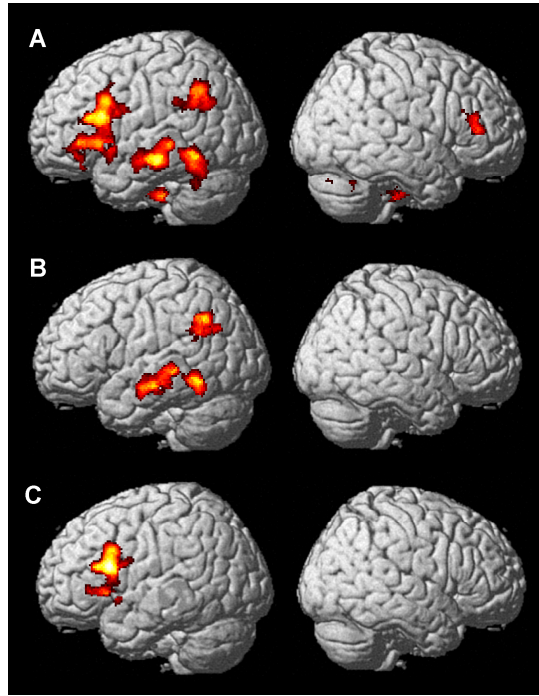


Figure S2: Effect of propositional prior outside the intelligible speech network

(A) The general effect of propositional prior without including the contrast (non-degraded reference sentence > degraded reference sentence) resulted in additional activations in the left inferior temporal gyrus, left hippocampus (CA)/ amygdala (LB), left basal ganglia, right IFG (area 45), in the cerebellum, brainstem, and precuneus/ posterior cingulate cortex. (B) Propositional matches activated the left inferior temporal gyrus, left basal ganglia, left hippocampus (CA)/ amygdala (LB/SF), and right cerebellum when the effects were not restricted to those regions that were actually involved in processing intelligible (compared to degraded) speech in addition to the left MTG and left AG. (C) In contrast, propositional mismatches evoked activation only in the left IFG. All images are thresholded at $p < .05$ (FWE-corrected at cluster level; cluster-forming threshold at voxel level: $p < .001$).

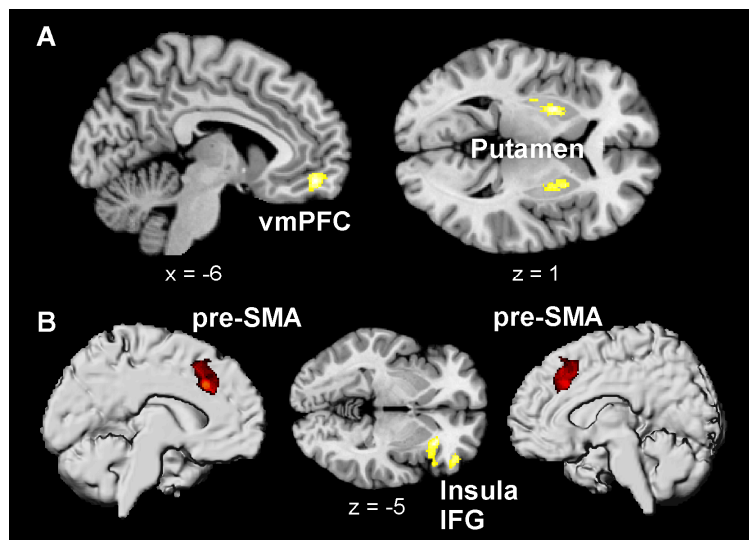


Figure S3: Match and mismatch effects

(A) Reference–target matches compared to reference–target mismatches [(propositional match > propositional mismatch) \cap (structural match > structural mismatch)] based on correct trials led to stronger activation in the ventromedial prefrontal cortex (vmPFC) and bilateral putamen. (B) The inverse mismatch effect [(propositional mismatch > propositional match) \cap (structural mismatch > structural match)] was reflected by significant activations in the pre-SMA, right insula, and right IFG. All images are thresholded at $p < .05$ (FWE-corrected at cluster level; cluster-forming threshold at voxel level: $p < .001$).

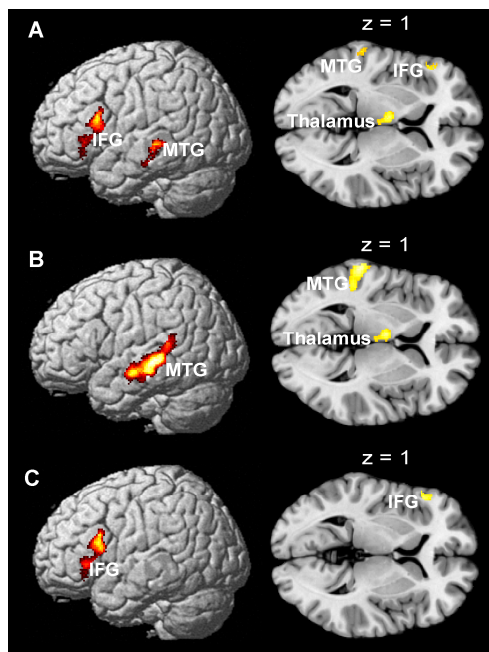


Figure S4: Effect of propositional prior across all trials

Significant results of the supplementary analysis including all trials. Compared to the main analysis based on only correct trials, the results showed one major modification pictured in A and B. (A) Comparing degraded targets preceded by propositional priors to those with structural priors [(propositional match > structural match) \cap (propositional mismatch > structural mismatch) \cap (non-degraded reference sentence > degraded reference sentence)] resulted in activation in Broca's area and left MTG similar to the main analysis, which included only correct trials. However, in contrast to the main analysis, the third significant cluster was in the left thalamus rather than in the left AG. (B) Propositional matches in the lexical-semantic network [(propositional match > structural match) \cap (propositional match > structural mismatch) \cap (non-degraded reference sentence > degraded reference sentence)] evoked activation in the left MTG and left thalamus instead of the analogous network of left MTG and left AG from the main analysis. (C) Paralleling the results of the main analysis, propositional mismatches in the lexical-semantic network [(propositional mismatch > structural mismatch) \cap (propositional mismatch > structural match) \cap (non-degraded reference sentence > degraded reference sentence)] resulted in activation in Broca's area of the left IFG. All images are thresholded at $p < .05$ (FWE-corrected at cluster level; cluster-forming threshold at voxel level: $p < .001$).

SUPPLEMENTAL TABLE

Table S1, related to Table 2: Overview of activations across all trials

Region	Cytoarchitectonic area (% overlap)	x	y	z	Z-score	Cluster size
<i>Effect of propositional prior</i>						
L IFG	Area 44 ¹ (53% overlap) Area 45 ¹ (29% overlap)	-54	18	16	4.74	457
L MTG		-50	-20	-18	4.13	261
L Thalamus		-4	-14	4	3.70	253
<i>Effect of propositional match</i>						
L MTG		-64	-30	0	5.23	2186
L Thalamus		-8	-8	2	4.53	340
<i>Effect of propositional mismatch</i>						
L IFG	Area 44 (50% overlap) Area 45 (30% overlap)	-54	18	18	4.90	615

All activations $p < .05$ (cluster-level FWE-corrected). x, y, z coordinates refer to MNI space. R, right; L, left; IFG, inferior frontal gyrus; MTG, middle temporal gyrus.

¹Amunts et al., 1999.

STUDY 2

Tackling the multifunctional nature of Broca's region meta-analytically: Connectivity-based parcellation of area 44

Mareike Clos¹, Katrin Amunts^{1,2,3,4}, Angela R. Laird⁵, Peter T. Fox⁶, Simon B. Eickhoff^{1,7}

¹Institute of Neuroscience and Medicine (INM-1), Research Center Jülich, Germany

²JARA-BRAIN, Jülich-Aachen Research Alliance, Germany

³Department of Psychiatry, Psychotherapy, and Psychosomatics, RWTH Aachen, Germany

⁴C. and O. Vogt Institute for Brain Research, Heinrich Heine University, Düsseldorf, Germany

⁵Department of Physics, Florida International University, Miami, FL, USA

⁶Research Imaging Institute, University of Texas Health Science Center at San Antonio, TX, USA

⁷Institute of Clinical Neuroscience and Medical Psychology, Heinrich Heine University, Düsseldorf, Germany

Manuscript submitted for publication in Neuroimage

Impact factor (2011): 5.895

Own contributions

Conception and design of experiment

Reviewing and adapting analysis code

Statistical data analysis

Interpretation of results

Preparing figures

Writing the paper

Total contribution: 80%

ABSTRACT

Cytoarchitectonic area 44 of Broca's region in the left inferior frontal gyrus is known to be involved in several functional domains including language, action and music processing. We investigated whether this functional heterogeneity is reflected in distinct modules within cytoarchitectonically defined left area 44 using meta-analytic connectivity-based parcellation (CBP). This method relies on identifying the whole-brain co-activation pattern for each area 44 voxel across a wide range of functional neuroimaging experiments and subsequently grouping the voxels into distinct clusters based on the similarity of their co-activation patterns. This CBP-analysis revealed that five separate clusters exist within left area 44. A post-hoc functional characterization and functional connectivity analysis of these five clusters was then performed. The two posterior clusters were primarily associated with action processes, in particular with phonology and overt speech (posterior-dorsal cluster) and with rhythmic sequencing (posterior-ventral cluster). The three anterior clusters were primarily associated with language and cognition, in particular with working-memory (anterior-dorsal cluster), with detection of meaning (anterior-ventral cluster) and with task switching/cognitive control (inferior frontal junction cluster). These five clusters furthermore showed specific and distinct connectivity patterns. The results demonstrate that left area 44 is heterogeneous, thus supporting anatomical data on the molecular architecture of this region, and provide a basis for more specific interpretations of activations localized in area 44.

Keywords: activation likelihood estimation, functional connectivity, K-means clustering, language, meta-analytic connectivity modeling

INTRODUCTION

Area 44, as mapped cytoarchitectonically by Brodmann (1909), corresponds to the posterior part of Broca's region on the inferior frontal gyrus. More recently, the borders of this area have been redefined cytoarchitectonically using observer-independent techniques in a series of histological sections of 10 postmortem brains (Amunts et al., 1999). Being part of Broca's speech region, left area 44 is known to be involved in both language production and comprehension although its exact contribution to language comprehension is still a matter of debate (Friederici, 2011; Hagoort, 2005). In addition to this core function, however, area 44 also plays a role in several non-language related functions such as working-memory (Buchsbaum et al., 2005; Kaan and Swaab, 2002; Rogalsky and Hickok, 2011; Smith and Jonides, 1999), execution and perception of action (as part of the mirror neuron system; Clerget et al., 2009; Fazio et al., 2009; Heiser et al., 2003; Iacoboni et al., 1999; Rizzolatti and Craighero, 2004;) and the processing of music (Koelsch, 2011; Koelsch et al., 2002; Maess et al., 2001; Platel et al., 1997). This raises the question whether this cytoarchitectonic area may indeed be regarded as a single, homogeneous functional module. Supporting the view of a structural heterogeneity within area 44, a recent postmortem, receptor-based parcellation of Broca's region indicated the presence of distinct subareas within this cytoarchitectonic region (Amunts et al., 2010). In this study left area 44 was divided into an anterior-dorsal area 44d and a posterior-ventral area 44v using multi-receptor mapping. Since transmitter receptors are key molecules for neurotransmission, it can be assumed that this heterogeneity at the molecular level corresponds to a similar differentiation at the level of function and connectivity. Evidence of such a differentiation may be achieved with connectivity-based parcellation (CBP) of functional imaging data. The rationale behind CBP is that functionally homogenous subregions show very similar connectivity patterns, which at

the same time are clearly distinguished from that of other subregions. Connectivity measures employed in CBP approaches include diffusion-tensor imaging (Johansen-Berg et al., 2004), resting state functional connectivity (Zhang and Li, 2012), and meta-analytic connectivity modeling (Cauda et al., 2012; Eickhoff et al., 2011). Previous DTI parcellations targeting Broca's region have demonstrated that area 44 and 45 can be distinguished from each other based on their connectivity patterns (Anwander et al., 2007; Ford et al., 2010; Klein et al., 2007). However, as these studies focused mainly on the inter-area differences, no intra-area subdivisions have been identified.

In order to investigate whether functionally distinct subregions exist within left area 44, we used a MACM based parcellation (Bzdok et al., 2012a; Cieslik et al., 2012). This approach makes use of the BrainMap database (Fox and Lancaster, 2002; Laird et al., 2005; Laird et al., 2009a; Laird et al., 2011) to identify the whole-brain co-activation pattern for each voxel within area 44 across a wide range of neuroimaging experiments. The resulting individual co-activation profiles are then compared between voxels to identify clusters of voxels showing very similar co-activation patterns. Furthermore, a follow-up MACM analysis on the derived clusters was performed to reveal the overall and specific co-activation networks of these clusters. Finally, the function of the clusters in terms of behavioral domains and paradigm classes was determined from the associated BrainMap meta-data. Note that the parcellation was only based on the whole-brain co-activation pattern of the individual voxels and that the decision regarding the optimal parcellation solution was based on external stability criteria. Subsequently, only the most stable parcellation solution was functionally characterized post-hoc based on specific connectivity and BrainMap meta-data of the individual clusters (for an overview of the method see Fig. 1).

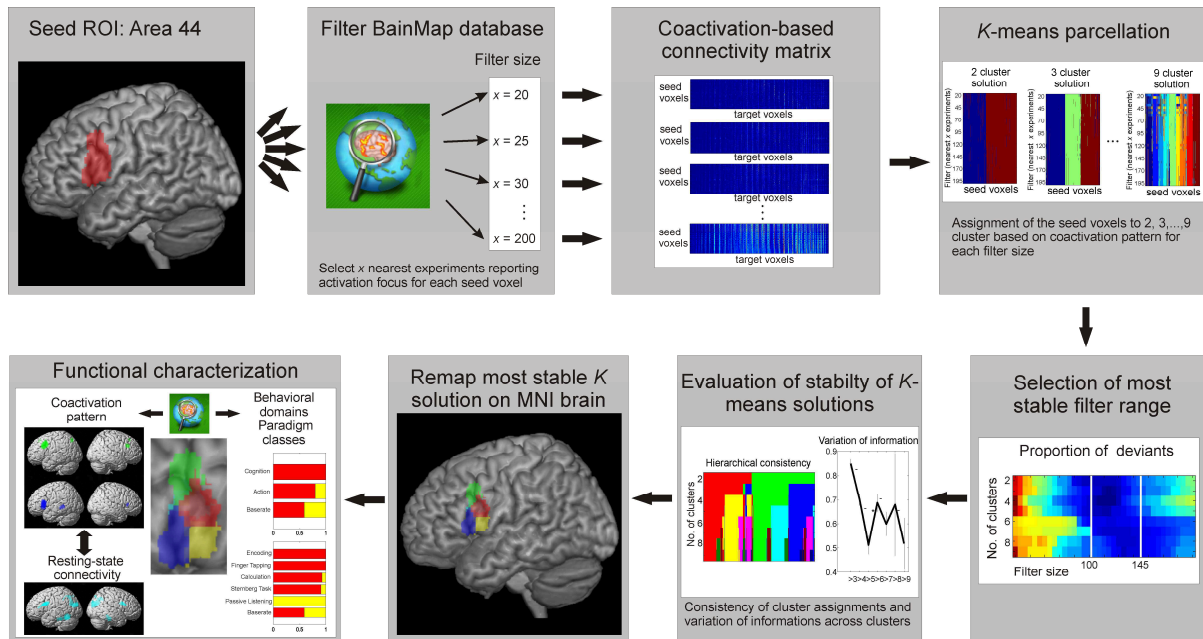


Fig. 1: Summary of analysis steps

For each voxel of area 44, activation foci from the x nearest experiments are selected from the BrainMap database. In the next step, the activation foci from the selected experiments are used to generate the brain-wide co-activation profile for each seed voxel and each filter size x based on meta-analytic co-activation modeling. Subsequent parcellation of the co-activation matrices was performed with K -means. Next, the optimal range of filter sizes was selected based on the consistency of the cluster assignments. The ensuing evaluation of the K -means solutions was limited to the optimal filter range. The most stable K -means solution was mapped back on the brain and the K clusters were functionally characterized based on their connectivity pattern and BrainMap meta-data. See methods for details.

MATERIAL AND METHODS

Meta-analytic connectivity mapping

The volume-of-interest (VOI) for the current CBP analysis was provided by representation of left area 44 in the maximum probability map (MPM) in the SPM Anatomy Toolbox (Eickhoff et al., 2005; Eickhoff et al., 2006a). This MPM was derived from the cytoarchitectonic mapping of 10 postmortem human brains (Amunts et al., 1999) registered to 3D MNI space (Montreal Neurological Institute; Amunts et al., 2004; Evans et al., 2012) and specifies the likelihood that a particular cortical area is localized at each brain voxel. This whole-brain MPM thus provides a continuous, nonoverlapping representation of the microanatomically defined area 44 and allows the user to define a VOI that includes only those voxels which are more likely to represent area 44 than any other cytoarchitectonic area. It should be noted

that normalization into standard space (which is slightly bigger than an average brain) as well as representation of microscopical structures in $2 \times 2 \times 2 \text{ mm}^3$ voxel space may result in a rather liberal definition of area 44 as compared to the stereological volume measured in postmortem data at micrometer histological resolution. Nevertheless, the MPM-based definition of the area 44 seed region has a sound biological basis (cf. Eickhoff et al., 2006a), with currently no available alternative based on in vivo imaging (but see Walters et al., 2007 for a potential future perspective). In addition, we also performed a supplementary parcellation with a more conservative definition of left area 44 based on the 50% probability map that was constrained to the surface of the pars opercularis of the inferior frontal gyrus.

The BrainMap database was used to compute whole brain co-activation maps for each voxel within the VOI (www.brainmap.org; Fox and Lancaster, 2002; Laird et al., 2005; Laird et al., 2009a; Laird et al., 2011). BrainMap is an established database in which the activation foci from of many thousand neuroimaging experiments are recorded. Each experiment is furthermore coded in terms of behavioral domains and paradigm classes using a standardized taxonomy. Only fMRI and PET experiments from “normal mapping” studies (no interventions, no group comparisons) in healthy subjects that reported results as coordinates in stereotaxic space were included in the analysis. Based on these criteria, approximately 7200 functional neuroimaging experiments were available for the current analysis. The idea of the co-activation analysis is to compute the convergence across (all foci of) all BrainMap experiments where the seed voxel in question is reported as active. However, a general problem of this meta-analytic co-activation mapping approach is that usually not every voxel is activated by a sufficiently high number of experiments (Bzdok et al., 2012a; Cieslik et al., 2012). Therefore, to enable a reliable delineation of task-based functional connectivity, we pooled across the neighborhood of each seed voxel and

identified those experiments from the BrainMap database that reported activation closest to the current seed voxel. Importantly, the extent of this spatial filter was systematically varied from including the closest 20 to 200 experiments in steps of five. That is, we selected 20, 25, 30, 35,..., 200 experiments reporting the closest activation at a given seed voxel. This was achieved by calculating and subsequently sorting the Euclidian distances between a given seed voxel and any activation reported in BrainMap. In the following step, the x nearest activation foci were selected, as defined by the spatial filter size. Examination of the resulting distances showed that this procedure identified activation foci within close vicinity of the seed voxel. Specifically, the average distance between the seed voxel and activation foci included for that voxel varied from 3.08 mm (i.e. ~ 1.5 voxels) when 20 experiments were included to 6.53 mm (i.e. ~ 3 voxels) when 200 experiments were included.

The retrieved experiments were then used to compute the brain-wide co-activation profile of a given seed voxel for each the 37 filter sizes. In particular, we performed a coordinate-based meta-analysis over all foci reported in these experiments to quantify their convergence. Since the experiments were identified by activation in or near a particular seed voxel, highest convergence will evidently be found at the location of the seed. Convergence outside the seed, however, indicates co-activation across task-based functional neuroimaging experiments. The brain-wide co-activation pattern for each individual seed voxel thus was computed by activation likelihood estimation (ALE; Eickhoff et al., 2009b; Laird et al., 2009a; Turkeltaub et al., 2002) meta-analysis over the experiments that were associated with that particular voxel by the procedure outlined above. The key idea behind ALE is to treat the foci reported in the associated experiments not as single points, but as centers for 3D Gaussian probability distributions that reflect the spatial uncertainty associated with neuroimaging results. For each experiment, the probability distributions of

all reported foci were then combined into a modeled activation (MA) map for that particular experiment (Turkeltaub et al., 2012). The voxel-wise union of these values (across all experiments associated with a particular seed voxel) then yielded an ALE score for each voxel of the brain that describes the co-activation probability with the current seed voxel of each particular location in the brain. The ALE scores of all voxels within the gray matter (based on 10% probability according to the ICBM [International Consortium on Brain Mapping] tissue probability maps) were then recorded before moving to the next voxel of the seed region. It should be noted that this co-activation profile was not thresholded because no inference was sought at this point of the analysis. Rather, the aim was to record for each seed voxel the “full” individual probability of co-activation with any other voxel and use this profile to parcellate the seed region.

Connectivity-based parcellation

The unthresholded brain-wide co-activation profiles for all seed voxels were then combined into a $N_S \times N_T$ co-activation matrix, where N_S denotes the number of seed voxels in left area 44 (1574 voxels) and N_T the number of target voxels in the reference brain volume at $2 \times 2 \times 2 \text{ mm}^3$ resolution ($\sim 260,000$ voxels located within gray matter). Importantly, we computed 37 individual co-activation maps, each representing the connectivity of the different seed voxels when using the 37 different filter sizes (see above). The parcellation of the VOI was performed using K -means clustering as implemented in Matlab with $K = 2, 3, \dots, 9$ using one minus the correlation between the connectivity patterns of the individual seed voxels as the distance measure (correlation distance). Importantly, this parcellation was performed for each of the 37 filter sizes independently, yielding 8 (K number of clusters) $\times 37$ (filter size) independent cluster solutions. K -means clustering is a non-hierarchical clustering method

that uses an iterative algorithm to separate the seed region into a previously selected number of K non-overlapping clusters (Hartigan and Wong, 1979). K -means aims at minimizing the variance within clusters and maximizing the variance between clusters by first computing the centroid of each cluster and subsequently reassigning voxels to the clusters such that their difference from the centroid is minimal. For each of the 8×37 parcellations we recorded the best solutions from 25 replications with randomly placed initial centroids.

Selection of optimal filter range

For each of the 37 filter sizes, the K -means procedure described above thus yielded eight different solutions parcellating area 44 into two, three, ... up to nine subdivisions. One of the challenges of K -means clustering is the choice of the optimal cluster solution. This problem is even more complex for the current MACM-based parcellation approach because not only the optimal number of K clusters has to be determined. Rather, the use of multiple spatial filter sizes also leads to 37 different solutions that have to be combined into a single parcellation. In previous parcellation studies involving MACM and multiple filters this issue has been dealt with by averaging across all filter sizes (Bzdok et al., 2012a; Cieslik et al., 2012). Here, however, we examined the properties of these various solutions and selected the most stable range of filter sizes. That is, we implement a two-step procedure that involves first a decision on those filter-sizes (from the broad range of processed ones) to be included in the final analysis and subsequently a decision on the optimal cluster-solution. The first step was based on the consistency of the cluster assignment for the individual voxels across the different filter sizes. We selected the filter range with the lowest number of deviants, i.e., voxels that were assigned differently as compared to the solution from the

majority of filters. In other words, we identified those filter sizes which produced solutions most similar to the consensus-solution across all filter sizes. The proportion of deviants (normalized within each cluster-solution K) illustrated in Fig. 2A indicates that most deviants were present in parcellations based on small but also very large filter sizes. We chose the borders of the filter range (100 to 145) based on the increase in (z-normalized) number of deviants before and after these values (Fig. 2B). In all subsequent steps the analysis was restricted to K parcellations based on co-activation in the nearest 100 to 145 experiments. However, since the definition of the filter range is not entirely objective, we additionally examined the impact of broadening and narrowing the range on the cluster assignment.

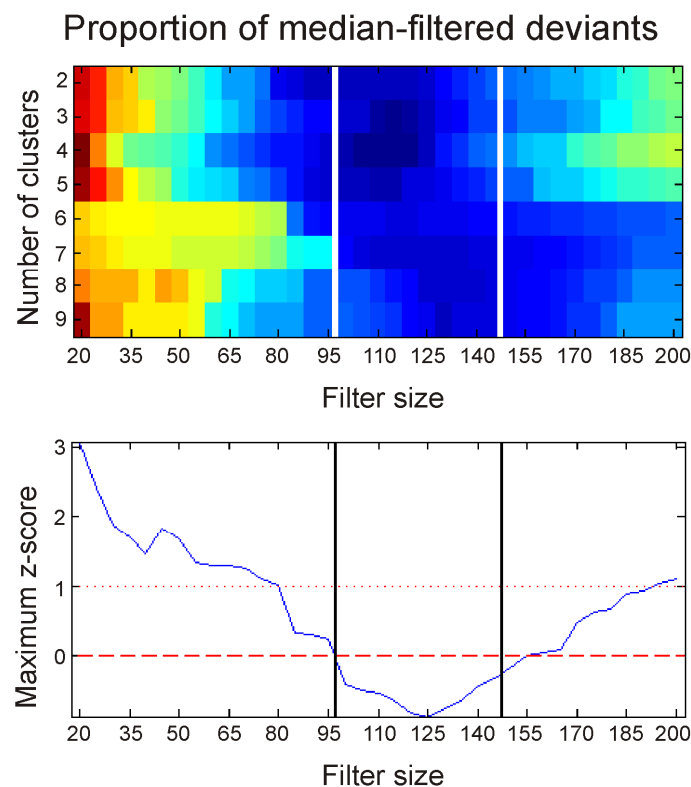


Fig. 2: Deviants and stability

Z-scores on median-filtered deviants (normalized for K). The vertical lines specify the ultimately selected, most stable range of filter size (i.e. range with least deviants across K). A) The proportion of deviants computed across filter size. Warm colours indicate high numbers of deviants, cold colours indicate low numbers of deviants. B) Maximum z-score of median-filtered deviants.

Selection of the optimal number of clusters

Next, we determined the optimal solution of K clusters (restricted to the filter sizes between 100 and 145 as outlined in the previous paragraph). We considered three criteria reflecting topological and information-theoretic characteristics of the respective cluster solutions. The first topological criterion was the percentage of voxels not related to the dominant parent cluster compared to the $K-1$ solution (Fig. 3A). This measure is related to the hierarchy-index (Kahnt et al., 2012) and corresponds to the number of lost voxels when only voxels consistent across the entire hierarchy are considered for the final clustering. That is, voxels assigned e.g. to cluster 3 in the $K = 3$ solution stemming from a subset of voxels previously assigned to cluster 2 (in the $K = 2$ solution) would be excluded if the majority of cluster 3 voxels actually stemmed from cluster 1 (in the $K = 2$ solution). A given K cluster parcellation qualified as a good solution if the percentage of lost voxels was below the median across all

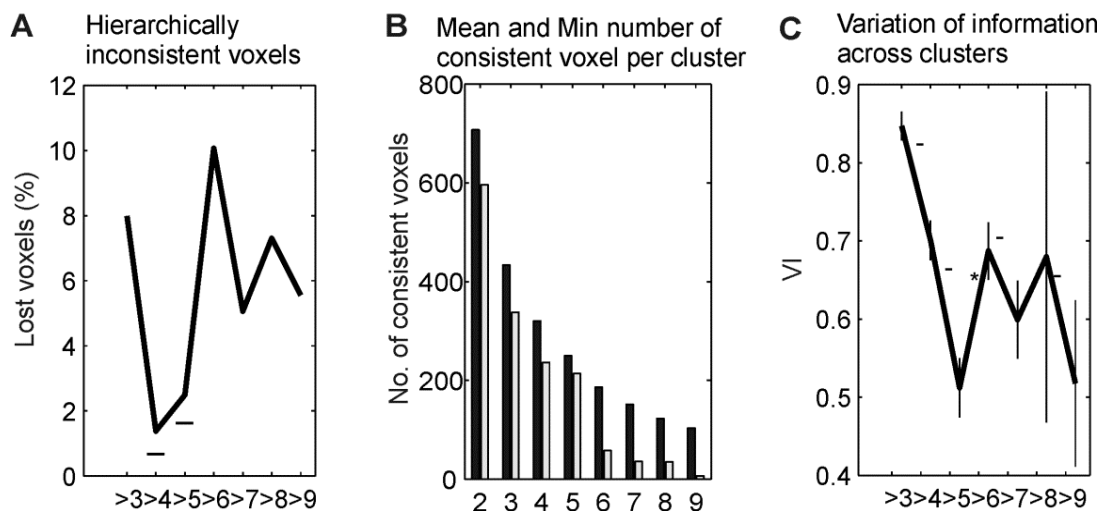


Fig. 3: Cluster criteria

A) Percentage of voxels not related to dominant parent cluster compared to the $K-1$ solution. $K = 4$ and $K = 5$ are considered good solutions (—) because they are located before the maximum and are lower than the median across all k solutions. B) Mean number of consistent voxel across cluster (dark gray) and the number of voxels of the smallest individual cluster (light gray). The ratio between the minimum and the average cluster size was more than 0.5 for $K = 2$, $K = 3$, $K = 4$ and $K = 5$ (good solutions). The ratio was largest for the $K = 5$ solution. C) Variation of information between cluster solutions, significant increase in VI (*) to the subsequent cluster solution only for $K = 5$ (primary criterion); significant decrease (-) from previous cluster solution for $K = 4$, $K = 5$, $K = 7$, $K = 9$ (secondary criterion).

steps and the following clustering-step featured a local maximum in the percentage of lost voxels. For example, if (1) moving from a 3- to a 4-cluster solution resulted in a local maximum of lost voxels and (2) the percentage of lost voxels in the 3-cluster solution is lower than the median value (computed across all K solutions), the 3-cluster solution would be considered a suitable one. The second topological criterion concerned the number of consistent voxels per cluster, i.e., the sizes of the individual cluster after removal of hierarchically inconsistent voxels (previous criterion). K parcellations were evaluated by considering the proportion of the minimum cluster size to the average cluster size provided by a given K solution (Fig. 3B). Good solutions were those where the size of the minimum cluster size was more than half of the average cluster size within the K solution. In particular, however, solutions in which the smallest cluster becomes zero would have been disregarded, as these indicate that at least one cluster did not contain any hierarchically consistent voxels anymore. Finally, as an information-theoretic criterion, we assessed the similarity of cluster assignments between the current solution and the neighbouring ($K-1$ and $K+1$) solutions by using the variation of information (VI) metric (Meila, 2007; Fig. 3C). The VI metric is an established clustering criterion that has previously been used for determining the optimal K -means parcellation of a given brain region by Kelly and colleagues (Kelly et al., 2010) and Kahnt and colleagues (Kahnt et al., 2012). For each filter size, the VI metric was computed between a given K solution and the subsequent $K+1$ solution. The variation of information between the two cluster solutions C and C' was computed as

$$VI(C, C')_k = H(C)_k + H(C')_k - 2I(C, C')_k$$

where H represents the amount of information (entropy) present in the cluster solutions C and C' , respectively, and I is the mutual information shared by the two cluster solutions C and C' . Solutions were considered stable if there was a significant increase in VI from the

current to the subsequent set of solutions (primary criterion) or if there was a significant decrease from the previous to the current clustering step (secondary criterion).

Visualization of the best cluster solution

The above criteria identified a 5-cluster solution as the most stable parcellation of left area 44 based on co-activation differences within this cytoarchitecturally defined area (see Fig. 3). We only considered hierarchically and spatially consistent voxels located in gray matter for the subsequent analyses. These restrictions resulted in a voxel number of 1251 out of the originally 1574 voxels attributed to left area 44 in the MPM (178 voxels were hierarchically not consistent, 144 were located outside the gray matter and one voxel was lost because it was spatially unconnected to its cluster). We used multidimensional scaling (MDS) to visualize the cluster separation (dissimilarity in whole-brain co-activation profiles). MDS allows the visualization of signals residing in an N-dimensional “functional space” in 2D. To this end, we first computed for each of the 10 filter sizes the $N_s \times N_s$ distance matrix represented by one minus the pairwise correlation between the co-activation profiles of the individual seed voxels (correlation distance, as in the K-means cluster analysis). Next, we performed MDS on the eigenimage of the distance matrixes using Sammon’s nonlinear mapping as the goodness-of-fit criterion. In addition, the locations of the five clusters (mode across selected filter size) were mapped back on the brain to visualize their anatomical location.

Post-hoc analysis on task-dependent connectivity: co-activations

To characterize the functional connectivity of the five clusters, a follow-up meta-analytic connectivity modeling (MACM) analysis was performed to determine the co-activation

pattern of the individual clusters. The co-activation pattern for each cluster was obtained by first identifying all experiments in the BrainMap database that featured at least one focus of activation in the particular CBP-derived cluster. Next, an ALE meta-analysis was performed on these experiments as described above. In contrast to the MACM underlying the co-activation-based parcellation, where ALE maps were not thresholded to retain the complete pattern of co-activation likelihoods, statistical inference was now performed. To establish which regions were significantly co-activated with a given cluster, ALE scores for the MACM analysis of this cluster were compared to a null-distribution reflecting a random spatial association between experiments with a fixed within-experiment distribution of foci (Eickhoff et al., 2009b). This random-effects inference assesses above-chance convergence between experiments, not clustering of foci within a particular experiment. The observed ALE scores from the actual meta-analysis of experiments activating within a particular cluster were then tested against the ALE scores obtained under this null-distribution yielding a p-value based on the proportion of equal or higher random values (Eickhoff et al., 2012). The resulting non-parametric p-values were transformed into Z-scores and thresholded at a cluster-level FWE-corrected threshold of $p < 0.05$ (cluster-forming threshold at voxel-level $p < 0.001$).

To identify co-activation common to all clusters, we computed the overlap between the brain-wide co-activation patterns of the five connectivity-derived clusters using a minimum-statistic conjunction, i.e., by computing the intersection of the thresholded ALE-maps (Caspers et al., 2010). Next, we tested for differences in co-activation patterns between all pairs of clusters by performing MACM separately on the experiments associated with either cluster and computing the voxel-wise difference between the ensuing ALE maps. All experiments contributing to either analysis were then pooled and randomly divided into two

groups of the same size as the two original sets of experiments defined by activation in the first or second cluster (Eickhoff et al., 2011). ALE-scores for these two randomly assembled groups were calculated and the difference between these ALE-scores was recorded for each voxel in the brain. Repeating this process 10,000 times then yielded a null-distribution of differences in ALE-scores between the MACM analyses of the two clusters. The “true” difference in ALE scores was then tested against this null-distribution yielding a posterior probability that the true difference was not due to random noise in an exchangeable set of labels based on the proportion of lower differences in the random exchange. The resulting probability values were then thresholded at $p > 0.95$ (95% chance for true difference) and inclusively masked by the respective main effects, i.e., the significant effects in the MACM for the particular cluster. Finally, we computed the specific co-activation pattern for all five clusters, that is, brain regions significantly more co-activated with a given cluster than with any of the other clusters. This was achieved by performing a conjunction analysis over the differences between a given cluster and the other four ones.

Post-hoc analysis on task-independent connectivity: “resting state”

To cross-validate the pattern of task-dependent co-activation for the delineated clusters within left area 44, we additionally assessed their specific functional connectivity in a task-free setting using resting state correlations. Resting state fMRI images of 153 healthy volunteers (mean age 41.1 ± 18.0 years; 92 males) from the NKI/Rockland sample were obtained through the 1000 functional connectomes project (www.nitrc.org/projects/fcon_1000/; Nooner et al., 2012). During the resting state scans subjects were instructed to keep their eyes closed and to think about nothing in particular but not to fall asleep (which was confirmed by post-scan debriefing). For each subject 260

resting state EPI images were acquired on a Siemens TimTrio 3T scanner using blood-oxygen-level-dependent (BOLD) contrast [gradient-echo EPI pulse sequence, TR = 2.5s, TE = 30ms, flip angle = 80°, in plane resolution = 3.0 x 3.0mm², 38 axial slices (3.0 mm thickness) covering the entire brain]. The first four scans were excluded from further processing analysis using SPM8 to allow for magnet saturation. The remaining EPI images were first corrected for movement artifacts by affine registration using a two pass procedure in which the images were first aligned to the initial volumes and subsequently to the mean after the first pass. The obtained mean EPI of each subject was then spatially normalized to the MNI single subject template using the “unified segmentation” approach (Ashburner and Friston, 2005). The ensuing deformation was applied to the individual EPI volumes. To improve signal-to-noise ratio and compensate for residual anatomical variations images were smoothed with a 5-mm FWHM Gaussian.

The time-series data of each voxel were processed as follows (Jakobs et al., 2012; Weissenbacher et al., 2009): In order to reduce spurious correlations, variance that could be explained by the following nuisance variables was removed: i) The six motion parameters derived from the image realignment, ii) the first derivative of the realignment parameters, iii) mean gray matter, white matter and CSF signal per time-point as obtained by averaging across voxels attributed to the respective tissue class in the SPM8 segmentation (Reetz et al., 2012; Sommer et al., 2012). All nuisance variables entered the model as first and second order. Data was then band pass filtered preserving frequencies between 0.01 and 0.08 Hz, since meaningful resting state correlations will predominantly be found in these frequencies given that the BOLD response acts as a low-pass filter (Biswal et al., 1995; Fox and Raichle, 2007; Greicius et al., 2003).

We used the five CBP-derived clusters as seeds for the resting state analysis. Linear (Pearson) correlation coefficients between the time series of the seed regions and all other gray matter voxels in the brain were computed to quantify resting-state functional connectivity (Reetz et al., 2012; zu Eulenburg et al., 2012). These voxel-wise correlation coefficients were then transformed into Fisher's Z-scores and tested for consistency in a flexible factorial model across subjects. The main effect of connectivity for each cluster as well as contrasts between the clusters were tested using the standard SPM8 implementations with the appropriate non-sphericity correction. Correspondingly to the task-dependent MACM co-activation analysis above, we firstly computed a conjunction across the main effect of positive connectivity of the five clusters, i.e., the task-free functional connectivity shared by all five clusters. Secondly, we performed a conjunction analysis for each cluster across the contrasts with the four other clusters corresponding to the specific co-activation pattern of each cluster. These conjunction analyses were based on the minimum t-statistic (Nichols et al., 2005) and thresholded at $p < 0.05$ (FWE corrected at cluster level; cluster-forming threshold at voxel-level $p < 0.001$). For comparison and visualization purposes, the resting-state conjunctions were masked with the corresponding MACM connectivity results.

Post-hoc functional characterization: meta-data

The functional characterization of the CBP-derived clusters was based on the "Behavioral Domain" and "Paradigm Class" meta-data categories available for each neuroimaging experiment included in the BrainMap database. Behavioral domains include the main categories cognition, action, perception, emotion, and interoception, as well as their related

sub-categories. Paradigm classes categorize the specific task employed (see <http://brainmap.org/scribe> for the complete BrainMap taxonomy).

In a first step, we determined the individual functional profile of the five CBP-derived clusters by using forward and reverse inference. Forward inference is the probability of observing activity in a brain region given knowledge of the psychological process, whereas reverse inference is the probability of a psychological process being present given knowledge of activation in a particular brain region. In the forward inference approach, a cluster's functional profile was determined by identifying taxonomic labels, for which the probability of finding activation in the respective cluster was significantly higher than the overall chance (across the entire database) of finding activation in that particular cluster. Significance was established using a binomial test ($p < .05$, corrected for multiple comparisons using Bonferroni's method; Laird et al., 2009b; Eickhoff et al., 2011; Nickl-Jockschat et al., 2012). That is, we tested whether the conditional probability of activation given a particular label [$P(\text{Activation}|\text{Task})$] was higher than the baseline probability of activating the region in question per se [$P(\text{Activation})$]. In the reverse inference approach, a cluster's functional profile was determined by identifying the most likely behavioral domains and paradigm classes given activation in a particular cluster. This likelihood $P(\text{Task}|\text{Activation})$ can be derived from $P(\text{Activation}|\text{Task})$ as well as $P(\text{Task})$ and $P(\text{Activation})$ using Bayes rule. Significance (at $p < 0.05$, corrected for multiple comparisons using Bonferroni's method) was then assessed by means of a chi-squared test.

Secondly, we contrasted the functional profiles of the clusters at each level of splitting up to the most stable 5-cluster solution. More precisely, we always contrasted the newly emerged child cluster with its remaining parent cluster at the same level of K . Thus, we compared cluster $1_{K=2}$ with cluster $2_{K=2}$, cluster $3_{K=3}$ with cluster $2_{K=3}$, cluster $4_{K=4}$ with cluster $1_{K=4}$, and

cluster $5_{K=5}$ with cluster $2_{K=5}$ (cf. Fig. 4B). For each comparison of the splitting cluster, the analysis was constrained to all BrainMap experiments activating either cluster. From this pool of experiments, the baserate is the a priori probability of any focus to lie in either of the two compared clusters. Forward inference here compared the activation probabilities of the clusters given a task compared to the a priori baserate by means of a binomial test ($p < .05$, corrected for multiple comparisons using Bonferroni's method). In the likewise performed reverse inference approach, we compared the occurrence probabilities of the tasks given activation in the one cluster (rather than in the other cluster) and assessed them by means of a chi-squared test ($p < .05$, corrected for multiple comparisons using Bonferroni's method).

RESULTS

Best cluster solution and stability of the clustering

Based on the consistency of the cluster assignment for the individual voxels across the different filter sizes, we only considered the closest 100 to 145 experiments (Fig. 2). The topographical and information-theoretic criteria (Fig. 3) then identified the 5-cluster solution as the best one among the 8 assessed levels of K -means clustering (from $K = 2$ to $K = 9$). The visualization in 2D, the hierarchical splitting of the five clusters and their anatomical location in the brain are displayed in Fig. 4. The clusters were labeled from 1 to 5 based on the hierarchical splitting order. At $K = 2$, left area 44 was composed of a posterior cluster $1_{K=2}$ and an anterior cluster $2_{K=2}$. At the next level $K = 3$, the posterior cluster $1_{K=2}$ remained the same but from the anterior cluster $2_{K=2}$ the ventral portion comprising the final cluster 3 split off. At $K = 4$, the final cluster 4 emerged from the posterior cluster $1_{K=2}$ ventrally. The remaining dorsal portion contained the final cluster 1. At the last split at $K = 5$, the final cluster 5 emerged from the anterior parent cluster $2_{K=3}$. Cluster 5 was located in close vicinity of the inferior frontal junction and the final cluster 2 was located dorsally extending into the inferior frontal sulcus.

To ascertain that the selected definition of the filter range including only the closest 100 to 145 experiments did not overtly impact the results, we additionally examined the effect of both broadening and narrowing the filter range by three steps on both sides, i.e., including 15 additional/fewer experiments per voxel. The results showed that cluster assignments of the individual voxels were identical to the cluster assignment of the selected filter range (100 to 145) for 96.3% of the voxels in the broadened range (85 to 160) and for 94.2% of the voxels in the narrowed range (115 to 130) across all eight parcellation levels ($K = 2$ to $K = 9$).

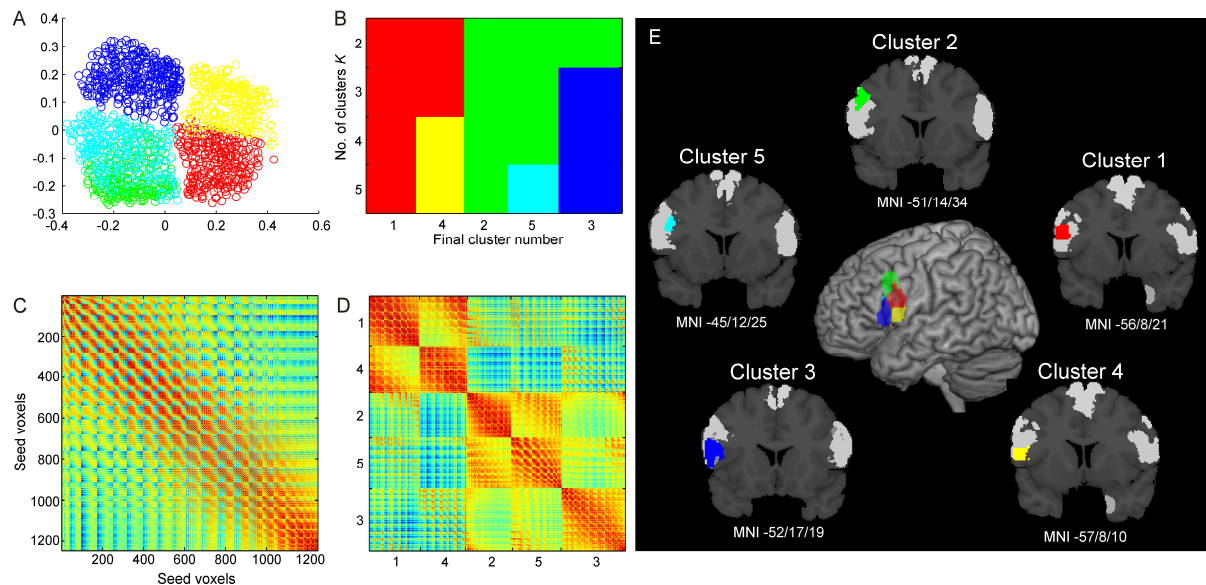


Fig. 4: Visualization and localization of the best cluster solution ($K = 5$)

A) Visualization of the 5 cluster solution by multidimensional scaling. Higher proximity between points (voxels) indicates more similar co-activation patterns of these voxels. B) Pattern of cluster assignment and splitting of clusters across levels of K . C) Original similarity matrix of the seed voxels. D) Similarity matrix of the seed voxels reordered according to the splitting scheme derived from K -means clustering illustrated in B) above. E) The 5 cluster solution is rendered on the brain surface (middle), note that the cyan cluster is located behind the green and the red cluster. The coronal sections display the location of the clusters on the anatomical template of area 44 (left light gray area). Only hierarchically and spatially consistent voxels are included in these visualizations. Colour code in A) and B): red = cluster 1, green = cluster 2, blue = cluster 3, yellow = cluster 4, cyan: cluster 5. MNI coordinates correspond to the centre of gravity of the clusters.

Importantly, the 5-cluster solution was identified as the most optimal solution for both the broadened and the narrowed range. Comparison of the cluster assignments across these selected $K = 2$ to $K = 5$ parcellation levels showed that these were identical to those of the 5-cluster solution based on the selected filter range for 99.0% (broadened range) and 98.4% (narrowed range) of the voxels, respectively. Very similar results with identical cluster assignments between 88% and 99% were obtained when broadening or narrowing the filter range asymmetrically and when broadening and narrowing the filter range by two steps or one step. Together, these results clearly demonstrate that the cluster assignment is extremely stable across choice of filter-ranges for further analysis and accordingly the exact definition of the filter range should not affect the final parcellation results.

Furthermore, we performed a supplementary parcellation based on the 50% probability map of left area 44 to ensure that the parcellation results are not driven by surrounding regions

into which the rather liberal MPM definition may be partly extending. This more conservative VOI was limited to those regions on the opercular surface of the left inferior frontal gyrus in which the probability for area 44 was at least 50%. It was hence considerably smaller and focused on the center of left area 44, accordingly, it did not include the inferior frontal junction anymore (supplementary Fig. S1). The parcellation results demonstrated that a 4-cluster solution was the optimal parcellation for this VOI, the fifth cluster present in the main analysis had disappeared because of the exclusion of the inferior frontal junction part. However, the anatomical location of these four clusters corresponded extremely well to those of cluster 1 to 4 from the main analysis based on the MPM (Fig. S2 and S3). Additionally, we still identified a posterior-anterior splitting at the $K = 2$ level as we did for the 5-cluster solution based on the MPM. Moreover, both the anterior and the posterior cluster were split into a dorsal and ventral part, reflecting the same splitting pattern as in the main analysis. These additional results thus support the validity of the parcellation based on the MPM of left area 44 and confirm that cluster assignments and splitting order are present even when restricting the analysis only to the core of histologically defined left area 44.

Post-hoc analysis of co-activation patterns of the clusters

The follow-up MACM analysis on the final clusters was performed to reveal the co-activation pattern for each cluster. A conjunction across the five co-activation patterns identified co-activated regions common to all five clusters. These common co-activations included bilateral inferior frontal gyrus (IFG)/ precentral gyrus, insula, supplementary motor area (SMA)/ middle cingulate cortex (MCC), thalamus and the left putamen (see Table 1 and Fig. 5A for details including associated cytoarchitectonic areas). This common connectivity was supported by the task-free resting state connectivity analysis (Fig. 5B). In particular, we

found all of these connections likewise present in the analysis of task-free functional connectivity except for the thalamus, which barely missed the statistical threshold.

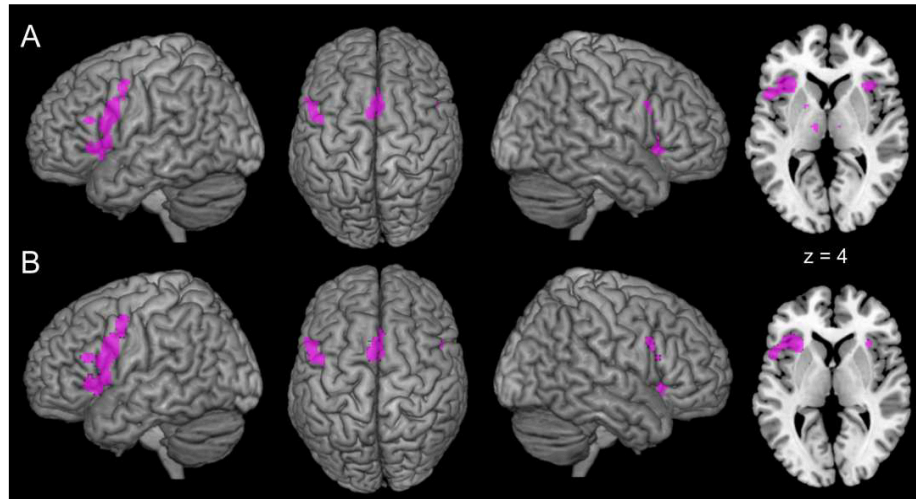


Fig. 5: Conjunction of connectivity across cluster 1-5

A) Regions significantly co-activated with all five clusters. B) Regions showing significant resting-state connectivity with all five clusters (masked with common MACM connectivity from A).

Table 1: Co-activated regions: conjunction across the five clusters

Region	Overlap with cytoarchitectonic area	x	y	z	Cluster size
L IFG/precentral gyrus/ insula	Area 44 ¹ (36% overlap)	-52	10	20	938
R IFG/precentral gyrus		48	10	30	16
R insula		36	20	0	214
L/R SMA/MCC	Area 6 ² (47% overlap)	-2	8	52	647
L thalamus		-12	-14	6	43
R thalamus		10	-12	6	4
L putamen		-20	2	6	15

x, y, z coordinates refer to the peak voxel in MNI space. R, right; L, left.

¹Amunts et al., 1999; ²Geyer, 2004

We furthermore examined the specific connectivity pattern of each cluster, that is, brain regions significantly more coupled with a given cluster than with any of the other ones (see Table 2 and Fig. 6A for details including associated cytoarchitectonic areas). Overall, the specific MACM connectivity indicated high local connectivity surrounding any given cluster. Of note, each cluster's right-sided homotope was also specifically co-activated. Additionally, cluster 1 showed a particular co-activation with the bilateral inferior and superior parietal

cortex including the supramarginal gyrus (SMG) and the postcentral gyrus, with the superior frontal gyrus (SFG), the precentral gyrus and the supplementary motor area (SMA). Cluster 2 was specifically co-activated with the left posterior intraparietal sulcus (IPS) and with the medial superior frontal gyrus (medSFG). Cluster 3 showed specific task-dependent connectivity with the left posterior middle temporal gyrus (MTG) and with the left hippocampus and amygdala. For cluster 4, the specific connectivity included the left anterior superior temporal gyrus (STG), the bilateral insula, putamen and thalamus as well as the right SMA. Specific co-activations with cluster 5 were found bilaterally in the anterior inferior parietal lobule (IPL) and with the right insula and pre-SMA/ MCC. The task-free resting state analysis confirmed this specific connectivity pattern of the clusters (Fig. 6B), even though the connectivity of cluster 3 with the left hippocampus/ amygdala, the connectivity of cluster 4 with the thalamus and the connectivity of cluster 5 with the right insula and with the pre-SMA/ MCC did not quite reach the statistical threshold. Thus, both task-dependent MACM and task-independent resting state connectivity showed converging evidence for functional specific connectivity patterns associated with each of the five clusters.

Post-hoc functional characterization: BrainMap meta-data

The behavioral domains and paradigm classes of the individual clusters emphasized the strong association between activation in left area 44 and language-related processes such as phonology, semantics, overt and covert speech. However, these functional profiles also hint at specific characteristics and hence functional differences between the five clusters identified within this histologically defined area (Fig. 7). In summary, cluster 1 was

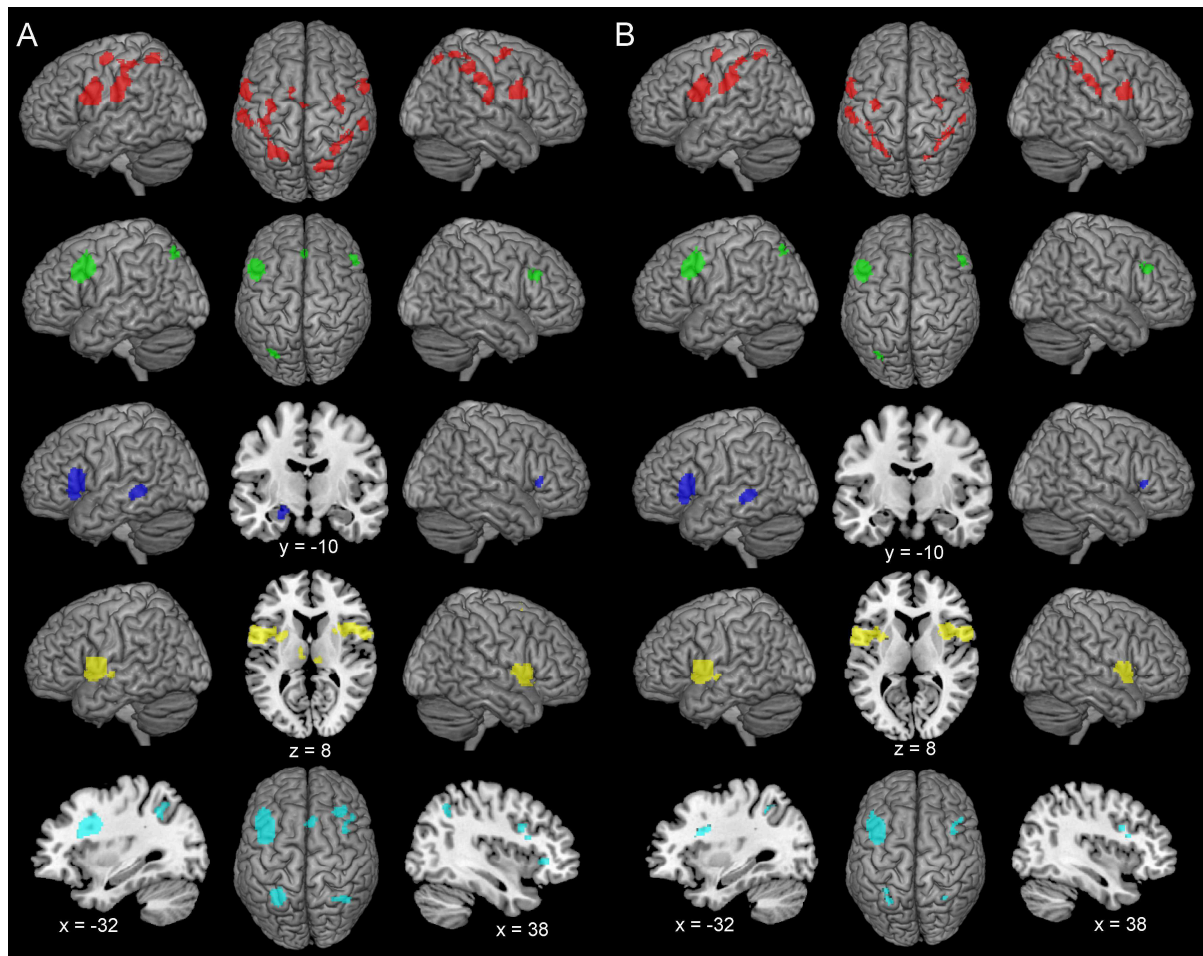


Fig. 6: Specific connectivity pattern of the five clusters

A) Regions significantly more co-activated with a given cluster than with any of the other four clusters. B) Regions showing significantly more resting state connectivity with a given cluster than with any of the other four clusters (masked with specific MACM connectivity from A). Colour code: red = cluster 1, green = cluster 2, blue = cluster 3, yellow = cluster 4, cyan = cluster 5.

significantly associated with phonology, syntax and tasks requiring overt speech but also with action imagination. Cluster 2 was involved in semantics, orthography and covert speech but also in working-memory processes. Cluster 3 was associated with several core aspects of language including overt and covert speech, semantics, phonology and syntax. The profile of cluster 4 indicated primarily a role in action imagination but also in music comprehension and production, making it the only cluster without a significant association to any language related process. Cluster 5 was involved in speech, phonology and semantics but also in working memory processes and paradigms requiring task switching and cognitive control

Table 2: Co-activated regions: Specific connectivity

Region	Overlap with cytoarchitectonic area	x	y	z	Cluster size
<i>Cluster 1</i>					
L IFG/ precentral gyrus	Area 44 ¹ (41% overlap) Area 6 ² (23% overlap)	-60	8	34	582
L postcentral gyrus/ SPL/ SMG	Area PF _t ³ (17% overlap) Area 7A ⁴ (15% overlap)	-66	-20	24	1049
L SFG/ SMA	Area 6 ² (79% overlap)	-16	2	58	119
R IPL/ SPL/ postcentral gyrus	Area hIP2 ⁵ (18% overlap) Area 7PC ⁴ (17% overlap)	42	-40	44	393
R SPL	Area 7P ⁴ (72% overlap) Area 7A ⁴ (23% overlap)	16	-68	56	173
R IFG/ precentral gyrus	Area 44 ¹ (45% overlap)	58	8	26	346
R SMG/ Rolandic operculum	Area OP1 ⁶ (30% overlap) Area PF _t ³ (30% overlap) Area PF ₃ ³ (16% overlap) Area PFop ₃ ³ (16% overlap)	56	-28	38	292
R SFG/ Precentral gyrus	Area 6 ² (28% overlap) Area 4A ⁷ (5% overlap)	32	-10	58	155
<i>Cluster 2</i>					
L IFG/ MFG	Area 44 ¹ (35% overlap) Area 45 ¹ (11% overlap)	-50	12	46	536
L IPS	Area PGa ³ (50% overlap) Area 7A ⁴ (33% overlap)	-32	-74	54	60
L/R medSFG		0	-34	50	54
R IFG	Area 45 ¹ (49% overlap)	54	26	30	90
<i>Cluster 3</i>					
L IFG	Area 44 ¹ (31% overlap) Area 45 ¹ (30% overlap)	-58	25	8	802
L MTG		-60	-40	2	172
L Hippocampus/ amygdala	Area CA ⁸ (49% overlap) Area LB ⁸ (21% overlap) Area SF ⁸ (13% overlap)	-24	-10	-16	77
R IFG	Area 45 ¹ (89% overlap)	48	26	6	78
<i>Cluster 4</i>					
L IFG/ STG/ insula/ putamen	Area 44 ¹ (14% overlap) Area OP4 ⁶ (8% overlap)	-56	12	14	1325
L Thalamus		-8	-12	16	110
R Thalamus		10	-24	4	157
R IFG/ insula/ putamen	Area 44 ¹ (19% overlap)	46	12	8	1311
R SMA (area 6)	Area 6 ² (83% overlap)	6	6	66	166
<i>Cluster 5</i>					
L IFG/ precentral gyrus	Area 44 ¹ (15% overlap) Area 45 ¹ (6% overlap)	-38	8	38	940
R IFG		36	10	30	70
L IPL	Area hIP3 ⁴ (41% overlap) Area hIP1 ⁵ (10% overlap)	-26	-56	40	340
R IPL	Area hIP3 ⁴ (35% overlap) Area hIP1 ⁵ (31% overlap) Area PGa ³ (13% overlap)	40	-56	44	82
R insula		34	30	0	125
R pre-SMA/ MCC	Area 6 ² (7% overlap)	6	18	46	82

All activations $p < .001$; extent threshold of 50 voxels. x, y, z coordinates refer to the peak voxel in MNI space. R, right; L, left. ¹Amunts et al., 1999; ²Geyer, 2004; ³Caspers et al., 2006; ⁴Scheperjans et al., 2008; ⁵Choi et al., 2006; ⁶Eickhoff et al., 2006b; ⁷Geyer et al., 1996; ⁸Amunts et al., 2005.

(e.g. the stroop task). This functional characterization of the final clusters was confirmed by the supplemental parcellation based on the 50% probability map of left area 44. The functional profiles of the resulting Cluster 1 to 4 were very similar to those from the main parcellation (Fig. S4).

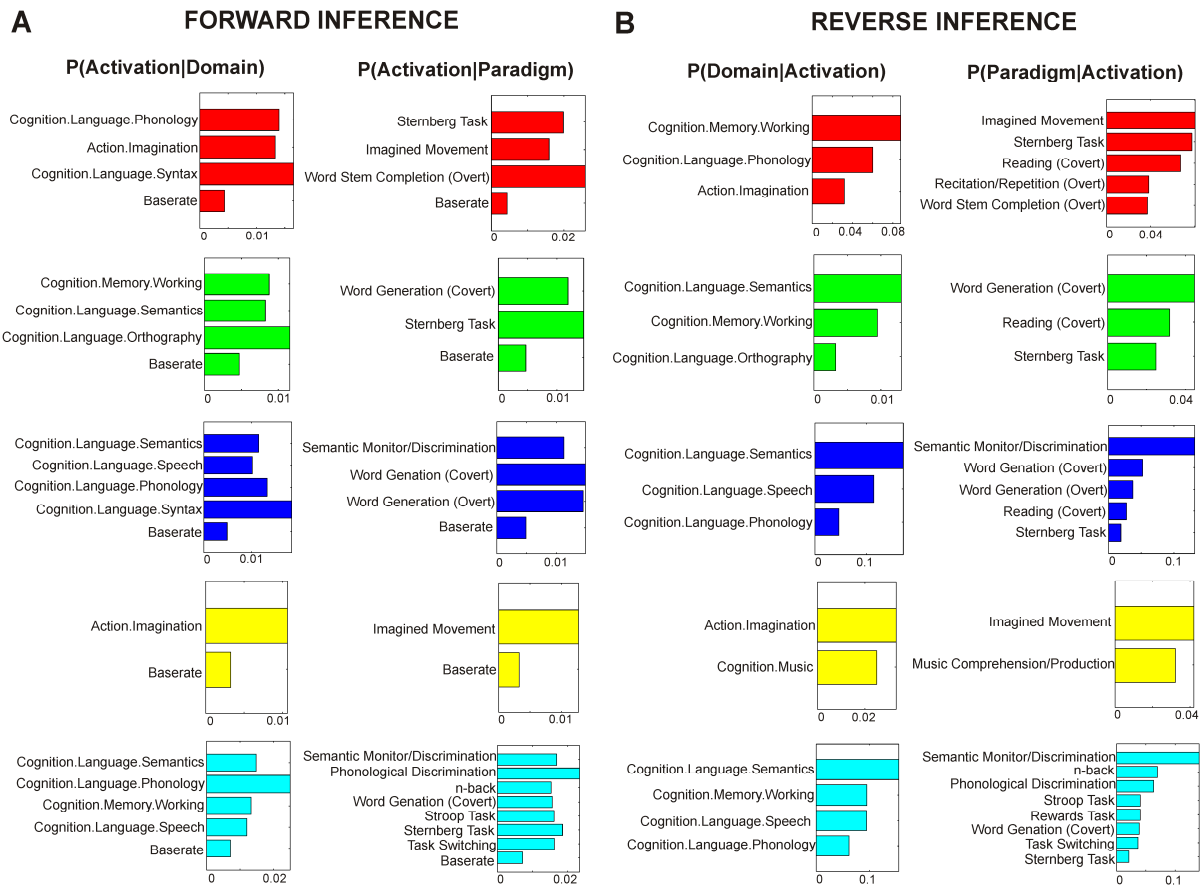


Fig. 7: Behavioral domains and paradigm classes of final clusters

A) Forward inference on final clusters: significant activation probability of the cluster given a certain domain (left column) or paradigm (right column). B) Reverse inference on final clusters: significant probability of domain (left column) or paradigm (right column) occurrence given activation in a cluster. Colour code: red = cluster 1, green = cluster 2, blue = cluster 3, yellow = cluster 4, cyan = cluster 5.

To additionally examine the differences between the splitting clusters (that is, differences between the newly emerged child cluster and its remaining parent cluster) we compared the functional profiles of the clusters at each level of splitting (Fig. 8). In this context, please note that the posterior cluster $1_{K=2}$ and the anterior clusters $2_{K=2}$ and $2_{K=3}$ do not correspond to the final CBP-derived clusters 1 and 2 but rather still contain their children cluster 4, 3 & 5, and

5, respectively. The comparison at $K = 2$ revealed that the posterior cluster $1_{K=2}$ was more associated with action imagination and execution as well as with action and body-related perception than the anterior cluster $2_{K=2}$. In contrast, the anterior cluster $2_{K=2}$ showed a higher activation probability for semantics and working memory. At $K = 3$, splitting this anterior cluster $2_{K=2}$, the ventral cluster $3_{K=3}$ differed significantly from the more dorsal cluster $2_{K=3}$ in its association with social cognition. This cluster $2_{K=3}$ on the other hand, showed a higher probability for working memory and several body-related perceptual and cognitive processes than the ventral cluster $3_{K=3}$. Contrasting the posterior-dorsal cluster $1_{K=4}$ with the posterior-ventral cluster $4_{K=4}$ revealed a stronger link of the former with language, tasks requiring overt speech and working memory. The ventral cluster $4_{K=4}$ in turn showed significantly stronger association than cluster $1_{K=4}$ only with regard to a higher activation probability in passive listening tasks. Finally, the last split at $K = 5$ distinguished a medially located cluster $5_{K=5}$ from cluster $2_{K=5}$ based on a higher activation probability in overt word stem completion tasks of cluster $5_{K=5}$.

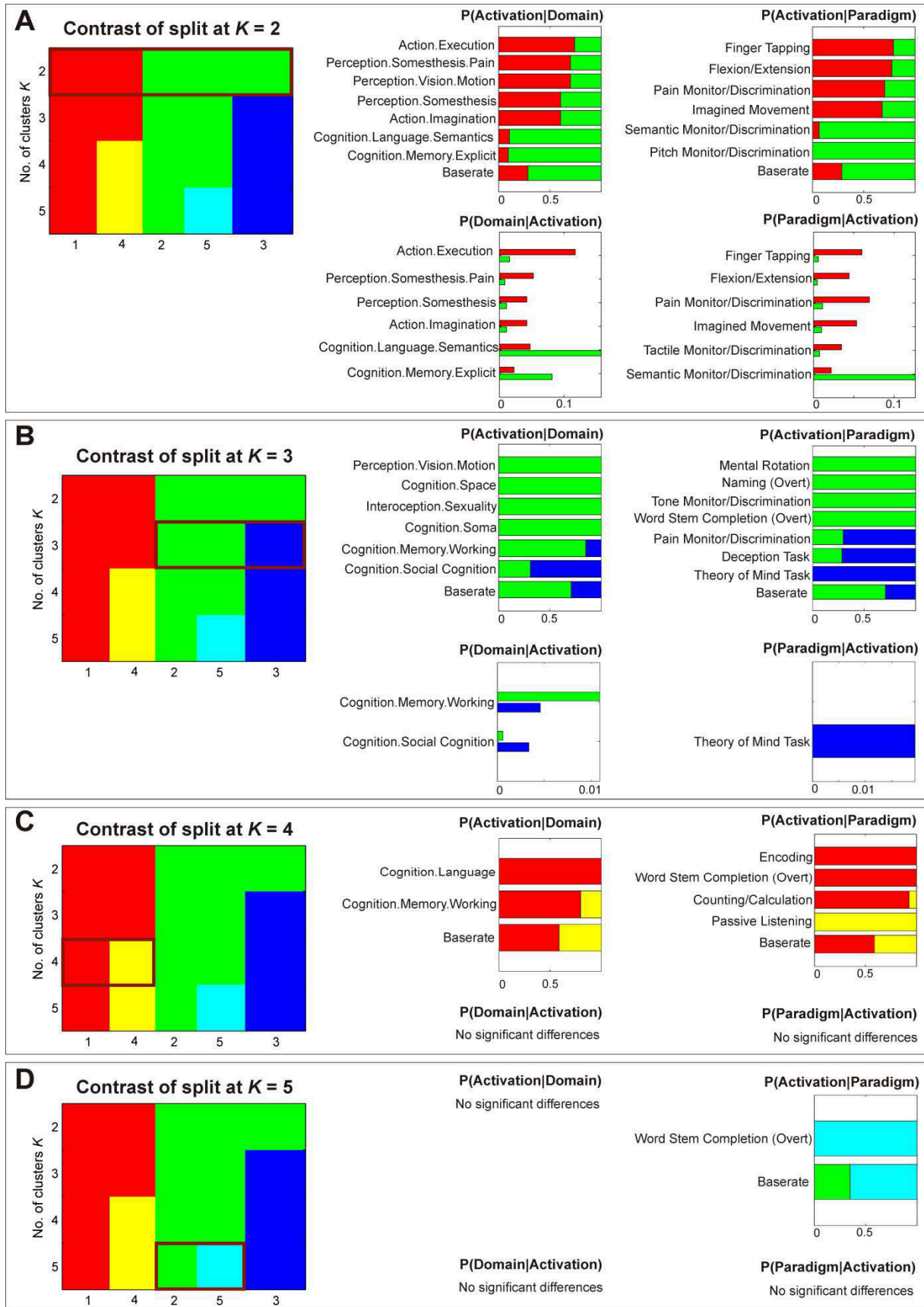


Fig. 8: Differences in behavioral domains and paradigm classes between splitting clusters

Significant differences in forward (upper panels) and reverse (lower panels) inference between A) cluster 1 and cluster 2 at $K = 2$; B) cluster 2 and 3 at $K = 3$; C) cluster 1 and 4 at $K = 4$; D) cluster 2 and 5 at $K = 5$. Colour code: red = cluster 1, green = cluster 2, blue = cluster 3, yellow = cluster 4, cyan = cluster 5.

Post-hoc external validation

In order to validate the functional characterization of the five clusters, we compared activations within left area 44 as observed in previously conducted fMRI studies from our laboratory with the localization of the delineated clusters. For the posterior portion, the results point to a role of the posterior cluster 1 and 4 in the motor network (Kellermann et al., 2012; Fig. 9A), but furthermore they also indicate the specific involvement of the dorsal cluster 1 in phonological word generation (Heim et al., 2008; Fig. 9B) and of the ventral cluster 4 in action imitation (Caspers et al., 2010; Fig. 9C). In addition, search for meaning in degraded speech (Clos et al., 2012; Fig. 9D) and social judgments on faces (Bzdok et al., 2012b; Fig. 9E) both were clearly localized to the anterior-ventral cluster 3. Importantly, these activations were specifically localized to the associated cluster(s) within left area 44, although they partly extended into surrounding regions as well.

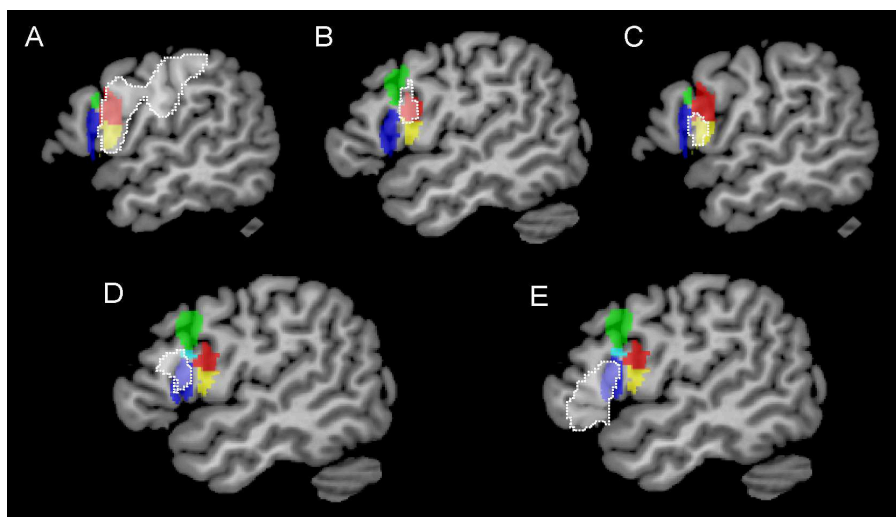


Fig. 9: External validation of functional cluster characterization

A) Activation associated with encoding and retrieval of action sequences (Kellermann et al., 2012), B) phonological word generation (Heim et al., 2008), C) action imitation (Caspers et al., 2010), D) search for meaning in degraded speech (Clos et al., 2012) and E) social evaluation of faces (Bzdok et al., 2012b) superimposed in white on the CBP-derived clusters.

DISCUSSION

We demonstrated that cytoarchitectonic left area 44 of Broca's region can be parcellated into five distinct clusters based on different whole-brain co-activation patterns across the wide range of neuroimaging experiments recorded in the BrainMap database. This approach has the advantage over parcellations based on DTI or resting-state data in that a functional characterization of the resultant clusters can be obtained based on BrainMap meta-data. We identified the best parcellation in a two-step procedure. Firstly, the optimal range of filter sizes (number of foci included for each voxel) was chosen based on the stability of cluster assignments. It is important to note that slight variations of the exact filter range did not make any notable difference in the subsequent clustering. Secondly, the eight different parcellations derived from *K*-means clustering with *K* varying from 2 to 9 enabled us to identify the 5-cluster parcellation as the best solution based on topographical and information-theoretical criteria as employed in previous CBP applications.

Two kinds of post-hoc analyses on this co-activation-based 5-cluster parcellation were then performed. Firstly, the follow-up MACM analysis on the ensuing five clusters revealed co-activation differences underlying the sub-parcellation of left area 44. The subsequent cross-validation by task-independent resting state connectivity indicates convergent functional connectivity differences also in a task-free setting. Secondly, the functions of the delineated clusters were quantitatively characterized using the BrainMap meta-data. These post-hoc analyses showed that although all five subregions were linked with language and showed common connectivity to several regions, they also featured clear differences in connectivity and function.

The strongest differentiation within left area 44 was found at the first level of clustering ($K = 2$) where the posterior part more associated with action, and the anterior part, primarily associated with language, separated from each other. This differentiation is in accordance with the receptor-based mapping of Broca's region (Amunts et al., 2010), which revealed a subdivision of area 44 into an anterior-dorsal (44d) and a posterior-ventral (44v) area based on pronounced differences in the concentration of muscarinic M_2 , glutamatergic AMPA, and adrenergic α_1 receptors. Topographically, our action cluster corresponds to the posterior-ventral area 44v and our language cluster to the anterior-dorsal area 44d.

In addition to this fundamental differentiation within left area 44, the specific co-activations and functional characterization of the final clusters revealed several additional differences within the anterior language and the posterior action part, respectively. In the posterior portion, the ventral cluster 4 was most strongly associated with action-related processing whereas the more dorsal cluster 1 showed a relatively stronger association with cognitive functions, in particular language and working-memory processes. Cluster 1 was furthermore associated with tasks requiring overt speech and showed high evidence for phonological processes. This link with phonological processes in overt speech is supported by studies reporting higher activation of the posterior-dorsal area 44 in tasks requiring phonological word generation as compared to either semantic or syntactic word generation (Costafreda et al., 2006; Heim et al., 2008). The connectivity pattern of cluster 1 suggests that this task is accomplished primarily in concert with its right homotope, the inferior and superior parietal cortex, the superior frontal gyrus (SFG), the precentral gyrus and the supplementary motor area (SMA). Indeed, these regions are known to be involved in production of both speech (Brown et al., 2009; Eickhoff et al., 2009a) but also non-speech sounds involving orofacial

and vocal tracts movements (Chang et al., 2009). Thus, the posterior-dorsal cluster 1 might contribute specifically to phonological processes and overt articulation of speech.

In contrast, cluster 4 showed a stronger association with action and action imagination than any other cluster, including the dorsally adjacent cluster 1. This finding is in agreement with a meta-analysis indicating that in particular the posterior-ventral part of left area 44 is consistently recruited by action imitation and may hence represent part of the mirror-neuron system (Caspers et al., 2010) as a potential homologue to macaque area F5 (Rizzolatti and Arbib, 1998). Furthermore, the reverse inference on cluster 4 provided also a link with music perception and production. Presumably, this cluster might be particularly responsive to sequencing aspects, including rhythm-processing, common to both movements and music. Indeed, activation in the posterior-ventral part of area 44 together with the bilateral insula, thalamus and basal ganglia has been reported in response to musical sequences (Koelsch et al., 2002). Moreover, time-keeping and sequencing of motor and auditory listening tasks is also strongly associated with activations in the SMA, insula, putamen and thalamus (Stevens et al., 2007). These findings match the specific co-activation network of cluster 4 and suggest that the posterior-ventral cluster 4 might play a specific role in the rhythmic sequencing.

Within the anterior “language” part of left area 44, cluster 2 was located more dorsally and showed a significant association with tasks probing working memory, semantics and orthography as well as those involving reading and covert speech. Compared to the more ventrally located cluster 3, cluster 2 was in particular significantly stronger associated with working memory, but also with cognitive and perceptual non-verbal processes. Furthermore, the specific co-activation of cluster 2 with medial superior and middle frontal gyri and the

intraparietal sulcus form a network reliably associated with working-memory across verbal and non-verbal domains (Rottschy et al., 2012). These findings are in accordance with a study demonstrating a shift of activation within area 44 superiorly towards the IFS with increasing demands of working-memory in language processing (Makuuchi et al., 2009). Together, these findings support a role of cluster 2 in working-memory mechanisms required for language-related processes including speech perception and orthography but potentially also for other, non-verbal, domains. Whether this cluster belongs to cytoarchitecturally defined area 44 or to dorsally adjacent regions, which are until now unmapped, remains a future project. The localization of this cluster in the posterior inferior frontal sulcus and its involvement in non-verbal processes may be arguments towards an interpretation as an area outside area 44. A putative candidate might be recently reported areas the inferior frontal sulcus (Bradler et al., 2012). Thus, the region of interest as based of the MPM of area 44 in the present study would include non-area 44 compartments. This seems to be also true for cluster 5 (see below).

Ventral-anterior cluster 3 had a particular association with various key aspects of language processing such as semantics, syntax, phonology and overt as well as covert speech. Contrasting this cluster with cluster 2 demonstrated that cluster 3 was also significantly more involved in social cognition including theory of mind tasks than cluster 2. A possible explanation for the association with both language processes and social cognition might be that most social concepts are rather abstract (Zahn et al., 2007) and therefore most likely represented verbally (Dove, 2010; Wang et al., 2010). Accordingly, tasks involving social cognition might require covert speech mechanisms (Femyhough and Meins, 2009). Alternatively however, it may be the necessity of access to semantics in the form of previously acquired (verbal and non-verbal) conceptual knowledge that both domains have

in common (Binder and Desai, 2011). In particular, social interactions might heavily depend on the recognition of meaningful cues in other people's behavior, gestures and mimic. These non-verbal processes should be phylogenetically much older than verbal mechanisms and therefore might have formed a basis for the ability to decode meaning from speech sounds (Arbib, 2005; Corballis, 2009). Interestingly, in particular the anterior-ventral part of area 44 has been suggested to support speech comprehension by searching for meaning in auditory speech signals (Clos et al., 2012). We would speculate that activations of the anterior-ventral part of area 44 observed in social evaluations of faces (Bzdok et al., 2012b) and in judgments of emotional states of others (Ochsner et al., 2004) reflect a similar search for meaning in the social domain. This interpretation is in accordance with the specific co-activated network of cluster 3 that included besides parts of the cluster's right homotope also the left-sided MTG, amygdala and hippocampus. Firstly, the left MTG has been identified as a key region for semantic processing and meaning extraction (Binder et al., 2009; Price, 2010). Furthermore, the amygdala is not only involved in attribution of social meaning to stimuli (Heberlein and Adolphs, 2004) but also in the recognition of meaningful patterns in degraded images unrelated to emotion or social aspects (Ludmer et al., 2011), indicating a more general role of the amygdala in detection of meaningful stimuli. Finally, the hippocampus might be involved in the retrieval of meaningful semantic concepts and in the comparison with previously encoded semantic information (Burianova and Grady, 2007; Manns et al., 2003). Thus, we propose that the anterior-ventral cluster 3 is specifically involved in meaning extraction from sensory information and semantic processing relevant for both language comprehension and social interactions.

Finally, cluster 5 was located in the region of the inferior frontal junction (IFJ; Brass et al., 2005; Derrfuss et al., 2005; Derrfuss et al., 2009) and might correspond to two recently described areas ifj1 and ifj2 identified at the junction of the inferior frontal and the precentral sulcus by the receptor-architectonic study of Amunts and colleagues (Amunts et al., 2010). Cluster 5 was differentiated from cluster 2 by its higher activation probability in overt word stem completion. However, the functional inference also revealed significant association with task switching and stroop tasks that was not observed for cluster 2, nor for any other cluster in left area 44. Thus, cluster 5 seems to be particularly associated with task switching, attention and cognitive control, matching previous functional concepts of the left IFJ (e.g. Brass et al., 2005; Derrfuss et al., 2005). This functional characterization is furthermore in agreement with the specifically co-activated network. In particular, the pre-SMA/ MCC and the right insula are involved in switching paradigms and stroop tasks (Derrfuss et al., 2005), but also intra-parietal regions are known to contribute to tasks requiring cognitive control (e.g. Brass and von Cramon, 2004; Derrfuss et al., 2004; Tomita et al., 1999) and attention (Corbetta, 1998). Thus, the cluster 5 located at the IFJ seems to be a main node in the cognitive control network composed furthermore of the insula, pre-SMA/ MCC and bilateral intra-parietal sulcus.

In summary, our results demonstrate that area 44 of Broca's region and its dorsal neighbourhood is a heterogeneous region that can be parcellated into five sub-regions based on their co-activation pattern. These sub-regions feature distinct connectivity and functional profiles which suggest a particular role of these in phonology and overt speech (posterior-dorsal cluster), rhythmic sequencing (posterior-ventral cluster), working-memory (anterior-dorsal cluster), detection of meaning (anterior-ventral cluster), and task switching/

cognitive control (inferior frontal junction cluster). While these functions should be highly relevant in the context of language production and comprehension, they will obviously also be recruited by other domains including action or social cognition.

ACKNOWLEDGMENTS

This work was supported by the National Institute of Mental Health (R01-MH074457), the Initiative and Networking Fund of the Helmholtz Association within the Helmholtz Alliance on Systems Biology (Human Brain Model SBE, MC), the BMBF (01GW0771 to KA), and the DFG (IRTG 1328 to SBE).

REFERENCES

- Amunts K, Kedo O, Kindler M, Pieperhoff P, Mohlberg H, Shah NJ, Habel U, Schneider F, Zilles K. 2005. Cytoarchitectonic mapping of the human amygdala, hippocampal region and entorhinal cortex: intersubject variability and probability maps. *Anat.Embryol.(Berl)*. 210:343-352.
- Amunts K, Lenzen M, Friederici AD, Schleicher A, Morosan P, Palomero-Gallagher N, Zilles K. 2010. Broca's region: novel organizational principles and multiple receptor mapping. *PLoS.Biol.* 8:e1000489.
- Amunts K, Schleicher A, Burgel U, Mohlberg H, Uylings HB, Zilles K. 1999. Broca's region revisited: cytoarchitecture and intersubject variability. *J.Comp Neurol.* 412:319-341.
- Amunts K, Weiss PH, Mohlberg H, Pieperhoff P, Eickhoff S, Gurd JM, Marshall JC, Shah NJ, Fink GR, Zilles K. 2004. Analysis of neural mechanisms underlying verbal fluency in cytoarchitectonically defined stereotaxic space--the roles of Brodmann areas 44 and 45. *Neuroimage.* 22:42-56.
- Anwander A, Tittgemeyer M, von Cramon DY, Friederici AD, Knosche TR. 2007. Connectivity-based parcellation of Broca's area. *Cereb.Cortex.* 17:816-825.
- Arbib MA. 2005. From monkey-like action recognition to human language: an evolutionary framework for neurolinguistics. *Behav.Brain Sci.* 28:105-124.
- Ashburner J, Friston KJ. 2005. Unified segmentation. *Neuroimage.* 26:839-851.
- Binder JR, Desai RH. 2011. The neurobiology of semantic memory. *Trends Cogn Sci.* 15:527-536.
- Binder JR, Desai RH, Graves WW, Conant LL. 2009. Where is the semantic system? A critical review and meta-analysis of 120 functional neuroimaging studies. *Cereb.Cortex.* 19:2767-2796.
- Biswal B, Yetkin FZ, Haughton VM, Hyde JS. 1995. Functional connectivity in the motor cortex of resting human brain using echo-planar MRI. *Magn Reson.Med.* 34:537-541.
- Bradler SH, Palomero-Gallagher N, Schleicher A, Zilles K, Amunts K. 2012. Receptorarchitectonic mapping of four new areas in the inferior frontal sulcus of the human brain. Poster 885, 18th Annual Meeting of the Organization of Human Brain Mapping (OHBM), Beijing, China.
- Brass M, Derrfuss J, Forstmann B, von Cramon DY. 2005. The role of the inferior frontal junction area in cognitive control. *Trends Cogn Sci.* 9:314-316.
- Brass M, von Cramon DY. 2004. Decomposing components of task preparation with functional magnetic resonance imaging. *J.Cogn Neurosci.* 16:609-620.
- Brodman K. 1909. Vergleichende Lokalisationslehre der Grobhirnrinde in ihren Prinzipien dargestellt auf Grund des Zellenbaues. Leipzig: Barth JA.
- Brown S, Laird AR, Pfordresher PQ, Thelen SM, Turkeltaub P, Liotti M. 2009. The somatotopy of speech: phonation and articulation in the human motor cortex. *Brain Cogn.* 70:31-41.
- Buchsbaum BR, Olsen RK, Koch P, Berman KF. 2005. Human dorsal and ventral auditory streams subserve rehearsal-based and echoic processes during verbal working memory. *Neuron.* 48:687-697.

- Burianova H, Grady CL. 2007. Common and unique neural activations in autobiographical, episodic, and semantic retrieval. *J.Cogn Neurosci.* 19:1520-1534.
- Bzdok D, Laird AR, Zilles K, Fox PT, Eickhoff SB. 2012a. An investigation of the structural, connectional, and functional subspecialization in the human amygdala. *Hum.Brain Mapp.* Advance online publication. doi:10.1002/hbm.22138
- Bzdok D, Langner R, Hoffstaedter F, Turetsky BI, Zilles K, Eickhoff SB. 2012b. The modular neuroarchitecture of social judgments on faces. *Cereb.Cortex.* 22:951-961.
- Caspers S, Geyer S, Schleicher A, Mohlberg H, Amunts K, Zilles K. 2006. The human inferior parietal cortex: cytoarchitectonic parcellation and interindividual variability. *Neuroimage.* 33:430-448.
- Caspers S, Zilles K, Laird AR, Eickhoff SB. 2010. ALE meta-analysis of action observation and imitation in the human brain. *Neuroimage.* 50:1148-1167.
- Cauda F, Costa T, Torta DM, Sacco K, D'Agata F, Duca S, Geminiani G, Fox PT, Vercelli A. 2012. Meta-analytic clustering of the insular cortex: characterizing the meta-analytic connectivity of the insula when involved in active tasks. *Neuroimage.* 62:343-355.
- Chang SE, Kenney MK, Loucks TM, Poletto CJ, Ludlow CL. 2009. Common neural substrates support speech and non-speech vocal tract gestures. *Neuroimage.* 47:314-325.
- Choi HJ, Zilles K, Mohlberg H, Schleicher A, Fink GR, Armstrong E, Amunts K. 2006. Cytoarchitectonic identification and probabilistic mapping of two distinct areas within the anterior ventral bank of the human intraparietal sulcus. *J. Comp. Neurol.* 495:53-69.
- Cieslik EC, Zilles K, Caspers S, Roski C, Kellermann TS, Jakobs O, Langner R, Laird AR, Fox PT, Eickhoff SB. 2012. Is there "one" DLPFC in cognitive action control? Evidence for heterogeneity from co-activation-based parcellation. *Cereb.Cortex.* Advance online publication. doi:10.1093/cercor/bhs256
- Clerget E, Winderickx A, Fadiga L, Olivier E. 2009. Role of Broca's area in encoding sequential human actions: a virtual lesion study. *Neuroreport.* 20:1496-1499.
- Clos M, Langner R, Meyer M, Oechslin MS, Zilles K, Eickhoff SB. 2012. Effects of prior information on decoding degraded speech: An fMRI study. *Hum.Brain Mapp.* Advance online publication. doi:10.1002/hbm.22151
- Corballis MC. 2009. The evolution of language. *Ann.N.Y.Acad.Sci.* 1156:19-43.
- Corbetta M. 1998. Frontoparietal cortical networks for directing attention and the eye to visual locations: identical, independent, or overlapping neural systems? *Proc.Natl.Acad.Sci.U.S.A.* 95:831-838.
- Costafreda SG, Fu CH, Lee L, Everitt B, Brammer MJ, David AS. 2006. A systematic review and quantitative appraisal of fMRI studies of verbal fluency: role of the left inferior frontal gyrus. *Hum.Brain Mapp.* 27:799-810.
- Derrfuss J, Brass M, Neumann J, von Cramon DY. 2005. Involvement of the inferior frontal junction in cognitive control: meta-analyses of switching and Stroop studies. *Hum.Brain Mapp.* 25:22-34.

- Derrfuss J, Brass M, von Cramon DY. 2004. Cognitive control in the posterior frontolateral cortex: evidence from common activations in task coordination, interference control, and working memory. *Neuroimage*. 23:604-612.
- Derrfuss J, Brass M, von Cramon DY, Lohmann G, Amunts K. 2009. Neural activations at the junction of the inferior frontal sulcus and the inferior precentral sulcus: interindividual variability, reliability, and association with sulcal morphology. *Hum Brain Mapp*. 30:299-311.
- Dove G. 2010. On the need for Embodied and Dis-Embodied Cognition. *Front Psychol*. 1:242.
- Eickhoff SB, Bzdok D, Laird AR, Kurth F, Fox PT. 2012. Activation likelihood estimation meta-analysis revisited. *Neuroimage*. 59:2349-2361.
- Eickhoff SB, Bzdok D, Laird AR, Roski C, Caspers S, Zilles K, Fox PT. 2011. Co-activation patterns distinguish cortical modules, their connectivity and functional differentiation. *Neuroimage*. 57:938-949.
- Eickhoff SB, Heim S, Zilles K, Amunts K. 2006a. Testing anatomically specified hypotheses in functional imaging using cytoarchitectonic maps. *Neuroimage*. 32:570-582.
- Eickhoff SB, Heim S, Zilles K, Amunts K. 2009a. A systems perspective on the effective connectivity of overt speech production. *Philos.Transact.A Math.Phys.Eng Sci*. 367:2399-2421.
- Eickhoff SB, Laird AR, Grefkes C, Wang LE, Zilles K, Fox PT. 2009b. Coordinate-based activation likelihood estimation meta-analysis of neuroimaging data: a random-effects approach based on empirical estimates of spatial uncertainty. *Hum.Brain Mapp*. 30:2907-2926.
- Eickhoff SB, Schleicher A, Zilles K, Amunts K. 2006b. The human parietal operculum. I. Cytoarchitectonic mapping of subdivisions. *Cereb.Cortex*. 16:254-267.
- Eickhoff SB, Stephan KE, Mohlberg H, Grefkes C, Fink GR, Amunts K, Zilles K. 2005. A new SPM toolbox for combining probabilistic cytoarchitectonic maps and functional imaging data. *Neuroimage*. 25:1325-1335.
- Evans AC, Janke AL, Collins DL, Baillet S. 2012. Brain templates and atlases. *Neuroimage*. 62:911-22.
- Fazio P, Cantagallo A, Craighero L, D'Ausilio A, Roy AC, Pozzo T, Calzolari F, Granieri E, Fadiga L. 2009. Encoding of human action in Broca's area. *Brain*. 132:1980-1988.
- Femyhough C, Meins E. 2009. Private speech and theory of mind: Evidence for developing interfunctional relations. In: Winsler A, Fernyhough C, Montero I, editors. *Private speech, executive functioning, and the development of verbal self-regulation*. New York (NY US): Cambridge University Press. p. 95-104.
- Ford A, McGregor KM, Case K, Crosson B, White KD. 2010. Structural connectivity of Broca's area and medial frontal cortex. *Neuroimage*. 52:1230-1237.
- Fox MD, Raichle ME. 2007. Spontaneous fluctuations in brain activity observed with functional magnetic resonance imaging. *Nat.Rev.Neurosci*. 8:700-711.
- Fox PT, Lancaster JL. 2002. Opinion: Mapping context and content: the BrainMap model. *Nat.Rev.Neurosci*. 3:319-321.

- Friederici AD. 2011. The brain basis of language processing: from structure to function. *Physiol Rev.* 91:1357-1392.
- Geyer S. 2004. The microstructural border between the motor and the cognitive domain in the human cerebral cortex. *Adv.Anat.Embryol.Cell Biol.* 174:I-89.
- Geyer S, Ledberg A, Schleicher A, Kinomura S, Schormann T, Burgel U, Klingberg T, Larsson J, Zilles K, Roland PE. 1996. Two different areas within the primary motor cortex of man. *Nature.* 382:805-807.
- Greicius MD, Krasnow B, Reiss AL, Menon V. 2003. Functional connectivity in the resting brain: a network analysis of the default mode hypothesis. *Proc.Natl.Acad.Sci.U.S.A.* 100:253-258.
- Hagoort P. 2005. On Broca, brain, and binding: a new framework. *Trends Cogn Sci.* 9:416-423.
- Hartigan JA, Wong MA. 1979. A k-means clustering algorithm. *Appl Stat* 28:100–108.
- Heberlein AS, Adolphs R. 2004. Impaired spontaneous anthropomorphizing despite intact perception and social knowledge. *Proc.Natl.Acad.Sci.U.S.A.* 101:7487-7491.
- Heim S, Eickhoff SB, Amunts K. 2008. Specialisation in Broca's region for semantic, phonological, and syntactic fluency? *Neuroimage.* 40:1362-1368.
- Heiser M, Iacoboni M, Maeda F, Marcus J, Mazziotta JC. 2003. The essential role of Broca's area in imitation. *Eur.J.Neurosci.* 17:1123-1128.
- Iacoboni M, Woods RP, Brass M, Bekkering H, Mazziotta JC, Rizzolatti G. 1999. Cortical mechanisms of human imitation. *Science.* 286:2526-2528.
- Jakobs O, Langner R, Caspers S, Roski C, Cieslik EC, Zilles K, Laird AR, Fox PT, Eickhoff SB. 2012. Across-study and within-subject functional connectivity of a right temporo-parietal junction subregion involved in stimulus-context integration. *Neuroimage.* 60:2389-2398.
- Johansen-Berg H, Behrens TE, Robson MD, Drobnyak I, Rushworth MF, Brady JM, Smith SM, Higham DJ, Matthews PM. 2004. Changes in connectivity profiles define functionally distinct regions in human medial frontal cortex. *Proc.Natl.Acad.Sci.U.S.A.* 101:13335-13340.
- Kaan E, Swaab TY. 2002. The brain circuitry of syntactic comprehension. *Trends Cogn Sci.* 6:350-356.
- Kahnt T, Chang LJ, Park SQ, Heinzle J, Haynes JD. 2012. Connectivity-based parcellation of the human orbitofrontal cortex. *J.Neurosci.* 32:6240-6250.
- Kellermann TS, Sternkopf MA, Schneider F, Habel U, Turetsky BI, Zilles K, Eickhoff SB. 2012. Modulating the processing of emotional stimuli by cognitive demand. *Soc.Cogn Affect.Neurosci.* 7:263-273.
- Kelly C, Uddin LQ, Shehzad Z, Margulies DS, Castellanos FX, Milham MP, Petrides M. 2010. Broca's region: linking human brain functional connectivity data and non-human primate tracing anatomy studies. *Eur.J.Neurosci.* 32:383-398.
- Klein JC, Behrens TE, Robson MD, Mackay CE, Higham DJ, Johansen-Berg H. 2007. Connectivity-based parcellation of human cortex using diffusion MRI: Establishing reproducibility, validity and observer independence in BA 44/45 and SMA/pre-SMA. *Neuroimage.* 34:204-211.

- Koelsch S. 2011. Toward a neural basis of music perception - a review and updated model. *Front Psychol.* 2:110.
- Koelsch S, Gunter TC, Cramon DY, Zysset S, Lohmann G, Friederici AD. 2002. Bach speaks: a cortical "language-network" serves the processing of music. *Neuroimage.* 17:956-966.
- Laird AR, Eickhoff SB, Fox PM, Uecker AM, Ray KL, Saenz JJ Jr., McKay DR, Bzdok D, Laird RW, Robinson JL, Turner JA, Turkeltaub PE, Lancaster JL, Fox PT. 2011. The BrainMap strategy for standardization, sharing, and meta-analysis of neuroimaging data. *BMC.Res.Notes.* 4:349.
- Laird AR, Eickhoff SB, Kurth F, Fox PM, Uecker AM, Turner JA, Robinson JL, Lancaster JL, Fox PT. 2009a. ALE meta-analysis workflows via the Brainmap database: Progress towards a probabilistic functional brain atlas. *Front Neuroinform.* 3:23.
- Laird AR, Eickhoff SB, Li K, Robin DA, Glahn DC, Fox PT. 2009b. Investigating the functional heterogeneity of the default mode network using coordinate-based meta-analytic modeling. *J.Neurosci.* 29:14496-14505.
- Laird AR, Lancaster JL, Fox PT. 2005. BrainMap: the social evolution of a human brain mapping database. *Neuroinformatics.* 3:65-78.
- Ludmer R, Dudai Y, Rubin N. 2011. Uncovering camouflage: amygdala activation predicts long-term memory of induced perceptual insight. *Neuron.* 69:1002-1014.
- Maess B, Koelsch S, Gunter TC, Friederici AD. 2001. Musical syntax is processed in Broca's area: an MEG study. *Nat.Neurosci.* 4:540-545.
- Makuuchi M, Bahlmann J, Anwender A, Friederici AD. 2009. Segregating the core computational faculty of human language from working memory. *Proc.Natl.Acad.Sci.U.S.A.* 106:8362-8367.
- Manns JR, Hopkins RO, Squire LR. 2003. Semantic memory and the human hippocampus. *Neuron.* 38:127-133.
- Meila M. 2007. Comparing clusterings – an information based distance. *J. Multivar. Anal.* 98:873-895.
- Nichols T, Brett M, Andersson J, Wager T, Poline JB. 2005. Valid conjunction inference with the minimum statistic. *Neuroimage.* 25:653-660.
- Nickl-Jockschat T, Habel U, Michel TM, Manning J, Laird AR, Fox PT, Schneider F, Eickhoff SB. 2012. Brain structure anomalies in autism spectrum disorder--a meta-analysis of VBM studies using anatomic likelihood estimation. *Hum.Brain Mapp.* 33:1470-1489.
- Nooner KB, Colcombe SJ, Tobe RH, Mennes M, Benedict MM, Moreno AL, Panek LJ, Brown S, Zavitz ST, Li Q, Sikka S, Gutman D, Bangaru S, Schlachter RT, Kamiel SM, Anwar AR, Hinz CM, Kaplan MS, Rachlin AB, Adelsberg S, Cheung B, Khanuja R, Yan C, Craddock CC, Calhoun V, Courtney W, King M, Wood D, Cox CL, Kelly AM, Di MA, Petkova E, Reiss PT, Duan N, Thomsen D, Biswal B, Coffey B, Hoptman MJ, Javitt DC, Pomara N, Sidtis JJ, Koplewicz HS, Castellanos FX, Leventhal BL, Milham MP. 2012. The NKI-Rockland sample: A model for accelerating the pace of discovery science in psychiatry. *Front Neurosci.* 6:152.
- Ochsner KN, Knierim K, Ludlow DH, Hanelin J, Ramachandran T, Glover G, Mackey SC. 2004. Reflecting upon feelings: an fMRI study of neural systems supporting the attribution of emotion to self and other. *J.Cogn Neurosci.* 16:1746-1772.

- Platel H, Price C, Baron JC, Wise R, Lambert J, Frackowiak RS, Lechevalier B, Eustache F. 1997. The structural components of music perception. A functional anatomical study. *Brain*. 120 (Pt 2):229-243.
- Price CJ. 2010. The anatomy of language: a review of 100 fMRI studies published in 2009. *Ann.N.Y.Acad.Sci*. 1191:62-88.
- Reetz K, Dogan I, Rolfs A, Binkofski F, Schulz JB, Laird AR, Fox PT, Eickhoff SB. 2012. Investigating function and connectivity of morphometric findings--exemplified on cerebellar atrophy in spinocerebellar ataxia 17 (SCA17). *Neuroimage*. 62:1354-1366.
- Rizzolatti G, Arbib MA. 1998. Language within our grasp. *Trends Neurosci*. 21:188-194.
- Rizzolatti G, Craighero L. 2004. The mirror-neuron system. *Annu.Rev.Neurosci*. 27:169-192.
- Rogalsky C, Hickok G. 2011. The role of Broca's area in sentence comprehension. *J.Cogn Neurosci*. 23:1664-1680.
- Rottschy C, Langner R, Dogan I, Reetz K, Laird AR, Schulz JB, Fox PT, Eickhoff SB. 2012. Modelling neural correlates of working memory: a coordinate-based meta-analysis. *Neuroimage*. 60:830-846.
- Scheperjans F, Hermann K, Eickhoff SB, Amunts K, Schleicher A, Zilles K. 2008. Observer-independent cytoarchitectonic mapping of the human superior parietal cortex. *Cereb.Cortex*. 18:846-867.
- Smith EE, Jonides J. 1999. Storage and executive processes in the frontal lobes. *Science*. 283:1657-1661.
- Sommer IE, Clos M, Meijering AL, Diederer KM, Eickhoff SB. 2012. Resting state functional connectivity in patients with chronic hallucinations. *PLoS.One*. 7:e43516.
- Stevens MC, Kiehl KA, Pearlson G, Calhoun VD. 2007. Functional neural circuits for mental timekeeping. *Hum.Brain Mapp*. 28:394-408.
- Tomita H, Ohbayashi M, Nakahara K, Hasegawa I, Miyashita Y. 1999. Top-down signal from prefrontal cortex in executive control of memory retrieval. *Nature*. 401:699-703.
- Turkeltaub PE, Eden GF, Jones KM, Zeffiro TA. 2002. Meta-analysis of the functional neuroanatomy of single-word reading: method and validation. *Neuroimage*. 16:765-780.
- Turkeltaub PE, Eickhoff SB, Laird AR, Fox M, Wiener M, Fox P. 2012. Minimizing within-experiment and within-group effects in Activation Likelihood Estimation meta-analyses. *Hum.Brain Mapp*. 33:1-13.
- Walters NB, Eickhoff SB, Schleicher A, Zilles K, Amunts K, Egan GF, Watson JD. 2007. Observer-independent analysis of high-resolution MR images of the human cerebral cortex: in vivo delineation of cortical areas. *Hum.Brain Mapp*. 28:1-8.
- Wang J, Conder JA, Blitzer DN, Shinkareva SV. 2010. Neural representation of abstract and concrete concepts: a meta-analysis of neuroimaging studies. *Hum.Brain Mapp*. 31:1459-1468.
- Weissenbacher A, Kasess C, Gerstl F, Lanzenberger R, Moser E, Windischberger C. 2009. Correlations and anticorrelations in resting-state functional connectivity MRI: a quantitative comparison of preprocessing strategies. *Neuroimage*. 47:1408-1416.

Zahn R, Moll J, Krueger F, Huey ED, Garrido G, Grafman J. 2007. Social concepts are represented in the superior anterior temporal cortex. *Proc.Natl.Acad.Sci.U.S.A.* 104:6430-6435.

Zhang S, Li CS. 2012. Functional connectivity mapping of the human precuneus by resting state fMRI. *Neuroimage.* 59:3548-3562.

zu Eulenburg P, Caspers S, Roski C, Eickhoff SB. 2012. Meta-analytical definition and functional connectivity of the human vestibular cortex. *Neuroimage.* 60:162-169.

SUPPLEMENT

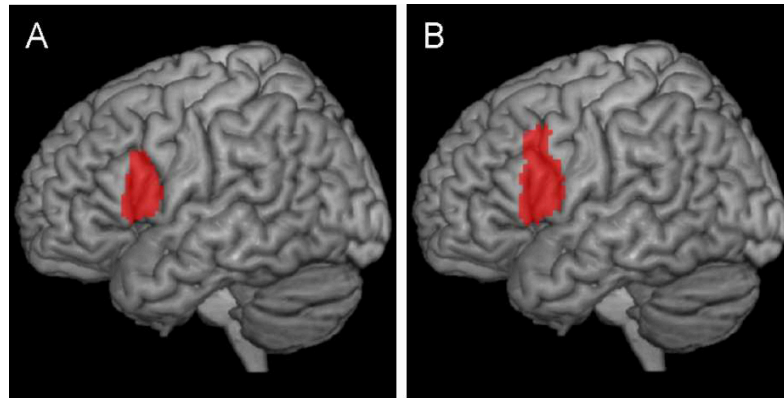


Figure S1: Comparison of the rendered VOIs

A) Rendering of the VOI based on the 50% probability map of area 44 used in the supplemental analysis. B) Rendering of the VOI based on the MPM of area 44 used in the main analysis.

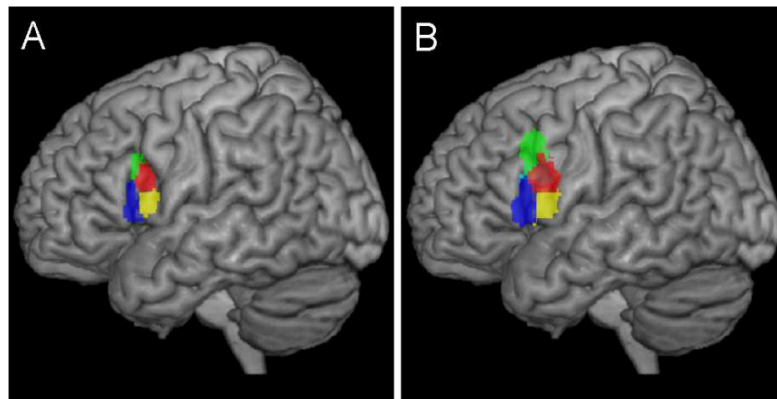


Figure S2: Comparison of the rendered cluster solutions

A) Rendering of the best cluster solution (four clusters) derived from the VOI based on the 50% probability map of area 44. B) Rendering of the best cluster solution (five clusters) derived from the MPM of area 44.

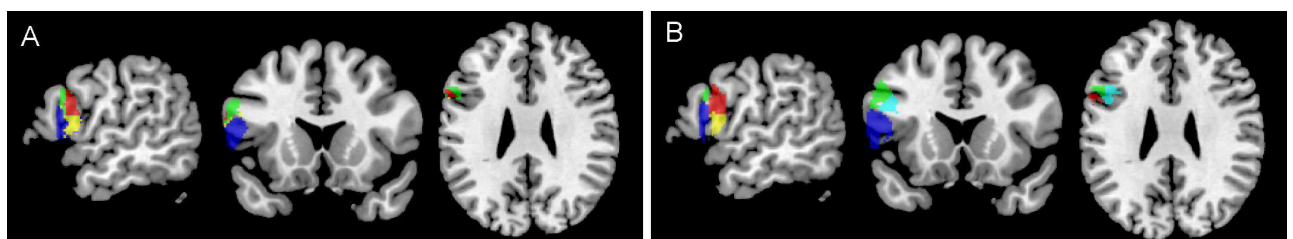


Figure S3: Comparison of the cluster solutions on sagittal, coronal, and transverse sections

A) Sections of the best cluster solution (four clusters) derived from the VOI based on the 50% probability map of area 44. B) Corresponding sections of the best cluster solution (five clusters) derived from the MPM of area 44.

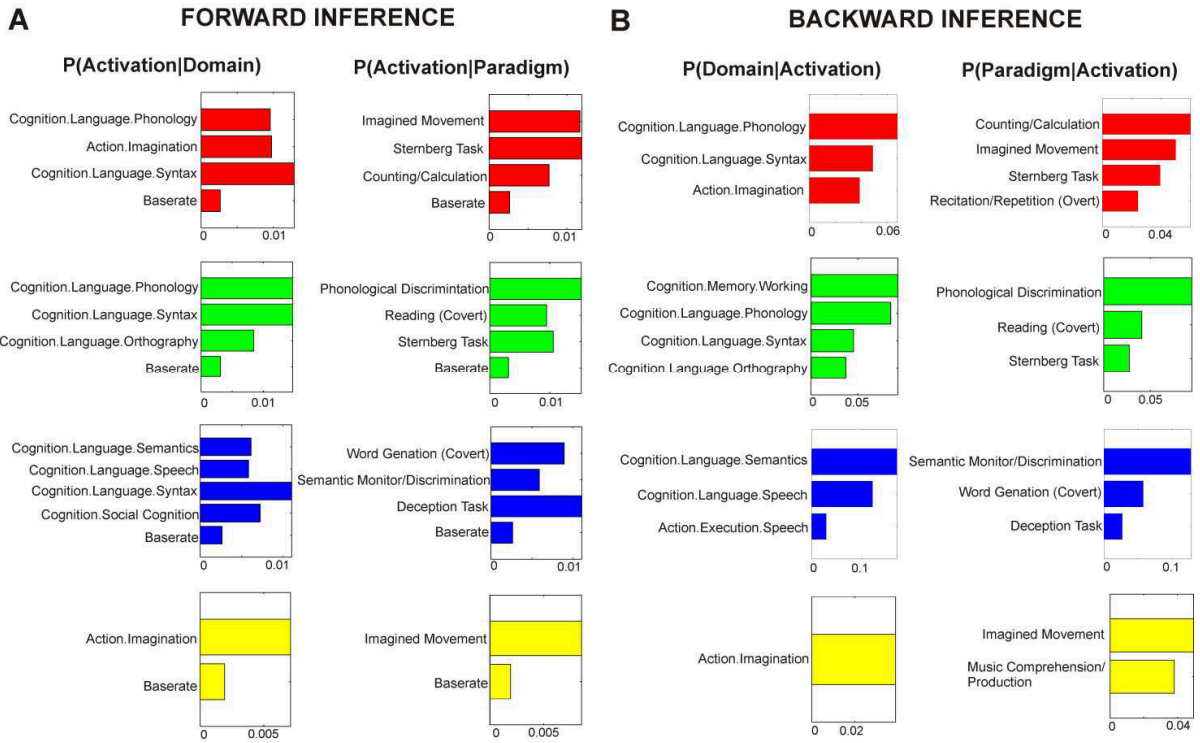


Fig. S4: Behavioral domains and paradigm classes of final clusters based on 50% probability map
 A) Forward inference on final clusters: significant activation probability of the cluster given a certain domain (left column) or paradigm (right column). B) Backward inference on final clusters: significant probability of domain (left column) or paradigm (right column) occurrence given activation in a cluster.

STUDY 3

Aberrant connectivity of areas for decoding degraded speech in patients with auditory verbal hallucinations

Mareike Clos¹, Kelly M. J. Diederer², Anne Lotte Meijering², Iris E. Sommer^{2*}, Simon B. Eickhoff^{1,3*}

¹Institute of Neuroscience and Medicine (INM-1; INM-2), Research Center Jülich, Germany

²Neuroscience Division, University Medical Center Utrecht & Rudolf Magnus Institute for Neuroscience, Netherlands

³Institute of Clinical Neuroscience and Medical Psychology, Heinrich Heine University, Düsseldorf, Germany

*These authors contributed equally to the work

Brain Structure and Function (2013) Advance online publication

doi: 10.1007/s00429-013-0519-5

Impact factor (2011): 5.628

Own contributions

Conception and design of experiment
Reviewing and adapting analysis code
Statistical data analysis
Interpretation of results
Preparing figures
Writing the paper
Total contribution 80%

Aberrant connectivity of areas for decoding degraded speech in patients with auditory verbal hallucinations

Mareike Clos · Kelly M. J. Diederer ·
Anne Lotte Meijering · Iris E. Sommer ·
Simon B. Eickhoff

Received: 27 July 2012 / Accepted: 2 February 2013
© Springer-Verlag Berlin Heidelberg 2013

Abstract Auditory verbal hallucinations (AVH) are a hallmark of psychotic experience. Various mechanisms including misattribution of inner speech and imbalance between bottom-up and top-down factors in auditory perception potentially due to aberrant connectivity between frontal and temporo-parietal areas have been suggested to underlie AVH. Experimental evidence for disturbed connectivity of networks sustaining auditory-verbal processing is, however, sparse. We compared functional resting-state connectivity in 49 psychotic patients with frequent AVH and 49 matched controls. The analysis was seeded from the left middle temporal gyrus (MTG), thalamus, angular gyrus (AG) and inferior frontal gyrus (IFG) as these regions are implicated in extracting meaning from impoverished speech-like sounds. Aberrant connectivity was found for all seeds. Decreased connectivity was observed between the left MTG and its right homotope, between the left AG and the surrounding inferior parietal cortex (IPC) and the left

inferior temporal gyrus, between the left thalamus and the right cerebellum, as well as between the left IFG and left IPC, and dorsolateral and ventrolateral prefrontal cortex (DLPFC/VLPFC). Increased connectivity was observed between the left IFG and the supplementary motor area (SMA) and the left insula and between the left thalamus and the left fusiform gyrus/hippocampus. The predisposition to experience AVH might result from decoupling between the speech production system (IFG, insula and SMA) and the self-monitoring system (DLPFC, VLPFC, IPC) leading to misattribution of inner speech. Furthermore, decreased connectivity between nodes involved in speech processing (AG, MTG) and other regions implicated in auditory processing might reflect aberrant top-down influences in AVH.

Keywords Functional connectivity · Psychosis · Resting state · Schizophrenia · Speech monitoring

I. E. Sommer and S. B. Eickhoff contributed equally to the work.

Electronic supplementary material The online version of this article (doi:10.1007/s00429-013-0519-5) contains supplementary material, which is available to authorized users.

M. Clos (✉) · S. B. Eickhoff
Institute of Neuroscience and Medicine (INM-1, INM-2),
Research Centre Jülich, 52425 Jülich, Germany
e-mail: m.clos@fz-juelich.de

K. M. J. Diederer · A. L. Meijering · I. E. Sommer
Neuroscience Division, University Medical Center Utrecht
and Rudolf Magnus Institute for Neuroscience,
Utrecht, Netherlands

S. B. Eickhoff
Institute of Clinical Neuroscience and Medical Psychology,
Heinrich Heine University, Düsseldorf, Germany

Introduction

Auditory verbal hallucinations (AVH), i.e. perceiving speech in the absence of an external stimulation, are a common symptom of various psychiatric disorders, but in particular of schizophrenia and related psychotic syndromes (Hugdahl 2009). Several neuro-cognitive mechanisms have been suggested to contribute to this highly distressing psychopathology, including dysfunction in verbal self-monitoring resulting in misattribution of inner speech as external voices, dysfunctions in episodic memory, or imbalances between top-down and bottom-up factors contributing to auditory perception (for a review see Hugdahl 2009). According to the latter hypothesis, aberrant dominance of top-down predictions might lead to spontaneous percepts in

the absence of actual sensory stimulation which are experienced as (auditory-verbal) hallucinations (Grossberg 2000). Indeed, research has demonstrated that an increased tendency to hear messages in meaningless noise is associated with a subsequent conversion to schizophrenia in individuals with prodromal symptoms (Hoffman et al. 2007) and that semantic expectations can induce misperceptions in healthy but hallucination-prone individuals (Vercammen and Aleman 2008).

While excessive weighting of top-down predictions may thus contribute to the experience of hallucinations, predictive mechanisms are an integral component of sensory processing. In particular in speech perception, where bottom-up signalling is often ambiguous, expectations acting as priors in the processing of auditory stimuli are known to support perceptual processes, e.g. by facilitating the processing of degraded speech (Sohoglu et al. 2012; Wild et al. 2012). In a previous study (Clos et al. 2012), we showed that such predictions in the form of lexical-semantic expectations led to a sudden percept of an understandable sentence from a degraded sentence rather than hearing unintelligible noise. In this large group of 29 healthy participants four brain regions were associated with this phenomenon, which might approximate the abnormal interactions between top-down and bottom-up factors presumably involved in AVH. (1) The left middle temporal gyrus (MTG) which is thought to map sound to meaning and is known to be a key region in semantic processing (Binder et al. 2009). (2) The left angular gyrus (AG) that might contribute to speech processing by providing top-down semantic constraints (Price 2010; Seghier et al. 2010). (3) The left thalamus that might filter those signals present in the auditory signal that have been predicted by the cortex (Alitto and Usrey 2003). (4) Finally, Broca's region in the left inferior frontal gyrus (IFG) was particularly responsive when incorrect lexical-semantic expectations resulted in an unsuccessful attempt to decode the degraded speech. This response pattern suggests that Broca's region performs a search for meaningful information in ambiguous auditory signals (Giraud et al. 2004) and potentially prevents misinterpretation in the presence of misleading expectations (Price 2010).

If disturbed integration of top-down and bottom-up auditory processing is indeed involved in the pathophysiology of AVH, we would expect that such disturbances should be reflected in aberrant interactions of these regions. We therefore investigated resting-state functional connectivity of the left MTG, AG, thalamus and IFG in patients with chronic AVH relative to healthy controls. When addressing the pathophysiology of AVH, imaging network connectivity in a task free "resting-" state may provide a particularly promising approach for several reasons. First, psychotic symptoms have been suggested to arise from

dysconnectivity between distinct brain regions (e.g. Friston 1998; Stephan et al. 2009). Second, spontaneous correlations between brain regions in the absence of structured external stimulation have been linked with predictive processes reflecting anticipation and interpretation of external events to prepare appropriate responses to these events (Deco et al. 2011; Raichle 2010). Third, as a fundamental characteristic of AVH is their emergence in absence of external driving inputs, resting-state connectivity might be more sensitive to reveal differences in network connectivity underlying the predisposition towards experiencing AVH than paradigms involving sensory stimulation. Finally, it has recently been suggested that abnormally elevated levels of resting state activity (Northoff and Qin 2011) and instability of the default mode network (Jardri et al. 2012) might play a role in the generation of AVH. Furthermore, approaches investigating networks rather than concentrating on isolated regions might be particularly suited to understand pathophysiology of AVH (Allen et al. 2012).

Previous resting state connectivity studies in patients with AVH have found evidence for aberrant functional connectivity between frontal and temporoparietal (Hoffman et al. 2011; Vercammen et al. 2010) and between temporal language areas (Gavrilescu et al. 2010). However, these studies employed a network approach of functional connectivity limited to pre-defined regions that were chosen based on previously observed activation during the experience of AVH. In contrast, we computed a whole-brain connectivity analysis seeded from regions that were associated with decoding degraded speech based on prior expectations. Top-down influences from higher-order cortical regions have been suggested to influence speech perception at lower auditory processing areas such as primary auditory cortex or thalamus (Davis and Johnsrude 2007). These higher-order regions are very likely to include the left MTG and AG, since they are form-independent semantic regions (Davis and Johnsrude 2003) that contribute to speech restoration by means of prior knowledge (Heinrich et al. 2008; Shahin et al. 2009). In particular the left AG has been demonstrated to be involved in top-down activation of semantic concepts (Obleser et al. 2007; Obleser and Kotz 2010; Seghier 2012; Seghier et al. 2010). Accordingly, we hypothesised that disturbed interactions in auditory processing would be reflected in altered coupling of 'higher' nodes in speech processing such as the left AG and MTG with other, 'lower' auditory speech processing areas. However, it has been suggested that a single neurocognitive deficit by itself is unlikely sufficient to account for a multifaceted phenomenon such as AVH (Jones 2010; Seal et al. 2004). Therefore, additional neurocognitive mechanisms such as dysfunctional monitoring of self-produced speech (Allen et al. 2007a) might also be involved.

Verbal self-monitoring and misattribution of speech has been linked with activations left fronto-temporal regions and anterior cingulate cortex (Allen et al. 2005, 2007b; Simons et al. 2010). Likewise, involvement of the parietal cortex in speech monitoring has also been proposed (Danckert et al. 2004). Generation of inner speech and auditory-verbal imagery on the other hand is associated with the (particularly left) IFG/insula, supplementary motor area, temporo-parietal cortex and cerebellum (Shergill et al. 2001). Therefore, we would expect that misattribution of inner speech due to dysfunctional verbal self-monitoring should be mirrored in disturbed connectivity between the left IFG and areas involved in speech articulation and associated monitoring processes.

Materials and methods

Participants

Forty-nine patients with chronic psychosis, as diagnosed according to DSM-IV criteria by an independent psychiatrist using the “Comprehensive Assessment of Symptoms and History (CASH)” (Andreasen et al. 1992), who all experienced AVH several times a day for at least 1 year were included in the study (see Table 1 for clinical and demographic details). The medication types and medication levels as well as the overall symptomatology of the patients were unfortunately too diverse to allow matching of the patients. Psychopathology was assessed on the day of scanning with the Positive and Negative Syndrome Scale (PANSS; Kay et al. 1987). For comparison, 49 healthy (as confirmed by the CASH interview) individuals matched for age, sex and handedness were also included. All participants provided written informed consent into the study, which was approved by the Humans Ethics Committee of the University Medical Center Utrecht. Note that an analysis of these resting state data (addressing a different question) has previously been performed and published (Sommer et al. 2012). In particular, this previous analysis examined connectivity of the left superior temporal gyrus and right inferior frontal gyrus as activity in these two regions was associated with the acute experience of AVH in psychotic patients.

Data acquisition and processing

Resting state scans were obtained on a Philips Achieva 3T MRI scanner using the following parameter: 40 (coronal) slices, TR/TE 21.75/32.4 ms, flip angle 10°, FOV 224 × 256 × 160, matrix 64 × 64 × 40, voxel-size 4 mm isotropic (PRESTO scans typically have shorter TR than TE times, as the whole head is scanned with each volume

in stead of the slab-wise read-out of EPI scans). This scan sequence achieves full brain coverage within 609 ms (yielding 600 images in approximately 6 min) by combining a 3D-PRESTO pulse sequence with parallel imaging (SENSE) in two directions, using a commercial 8-channel SENSE headcoil (Negggers et al. 2008). Participants were instructed to lie in the scanner as still as possible with their eyes closed yet stay awake (which was confirmed by post-scan debriefing). After scanning, all participants were asked whether they had experienced AVH during the scan. We did not instruct the subjects before the scan to keep track of any other aspects of their hallucinations (such as duration, content, frequency, etc.) because we did not want the participants to focus on the AVH during the resting state scan as this may have recruited additional attentional processes. Moreover, spontaneous reports by the patients did not yield specific or reliable information on, in particular, the duration or frequency of the experienced hallucinations.

The resting state scans were first corrected for head movement by affine registration using a two-pass procedure. The mean PRESTO image for each subject was then spatially normalised to the MNI single subject template (Holmes et al. 1998) using the unified segmentation approach (Ashburner and Friston 2005) and the ensuing deformation was applied to the individual PRESTO volumes. Finally, images were smoothed by a 5-mm FWHM Gaussian kernel. Regions of interest (ROIs) used as seeds for the functional connectivity analysis were based on the activation clusters obtained from Clos et al. (2012, cf. introduction and Table 2). Voxel time courses were extracted for all voxels within a 5-mm radius sphere around the centre of the particular clusters.

Resting state fMRI connectivity analyses can be confounded by physiological noise stemming from cardiac or respiratory signals but in particular also motion-related effects (Bandettini and Bullmore 2008; Fox et al. 2009). In order to reduce the potential of these effects to induce spurious correlations, variance explained by the following nuisance variables was removed from the time series (cf. Bandettini and Bullmore 2008; Eickhoff et al. 2011; Fox et al. 2009): (1) motion parameters derived from image realignment and their first derivative; (2) mean grey, white matter and CSF signal intensity per time-point which should account for the global signal changes of non-interest; (3) coherent signal drifts reflected by the first five PCA components on the entire whole-brain data (CompCor approach, cf. Behzadi et al. 2007). All nuisance variables entered the model as first and all but the PCA components also as second-order terms as previously described by Behzadi et al. (2007) and shown by Chai et al. (2012) to increase specificity and sensitivity of the analyses and detect valid correlation and anti-correlations during rest,

Table 1 Demographic and clinical description of participants

Group	Patients, <i>n</i> = 49	Control subjects, <i>n</i> = 49
Age ^a	37.3 years ± 11.9	39.5 years ± 14.8
Sex ^b	22 males, 27 females	19 males, 30 females
Handedness ^c	43 right, 6 non-right	38 right, 11 non-right
Mean time with AVH	13.9 years ± 12.2	No AVH
Diagnosis	43 schizophrenia 4 schizoaffective disorder 1 schizophreniform disorder 1 psychosis NOS	No psychiatric Diagnosis
Antipsychotic medication	10 clozapine, mean dose 464 mg 3 flufenazine, mean dose 30 mg 7 risperidon, mean dose 3.6 mg 8 olanzapine, mean dose 14.2 mg 7 quetiapine, mean dose 514 mg 1 penfluridol 10 mg 5 haloperidol, mean dose 4 mg 1 aripiprazol, 15 mg 7 medication-free	All medication-free
Mean PANSS scores	Positive scale 16.2 ± 3.7 Negative scale 16.3 ± 5.2 Total 63 ± 13.3	
Years of education after primary school ^d	5.8 years ± 2.2	

± denotes the standard deviation

^a $T(2,96) = -0.92, p = 0.41$

^b $\chi^2(1) = 0.38, p = 0.54$

^c $\chi^2(1) = 1.78, p = 0.18$

^d Information missing for 15 patients

Table 2 Overview of seed regions

Region	Cytoarchitectonic area (percent overlap)	<i>x</i>	<i>y</i>	<i>z</i>
L MTG		-57	-27	-5
L IFG (Broca's region)	Area 44 ^a (56 % overlap) Area 45 ^a (44 % overlap)	-51	20	15
L Thalamus		-6	-11	5
L AG	PGa ^b (78 % overlap) PFm ^b (9 % overlap) PF ² (3 % overlap)	-48	-56	29

x, *y*, *z* coordinates refer to the centre of gravity in MNI space, *L* left

^a Amunts et al. (1999)

^b Caspers et al. (2006)

which are not an artefact of the preprocessing method, but may reflect valid biological signals. The data were then band-pass filtered preserving frequencies between 0.01 and 0.08 Hz (Biswal et al. 1995; Greicius et al. 2003). The time course of each ROI was expressed as the first eigenvariate of the processed time series of all voxels associated with that region.

The use of global signal regression as a preprocessing step in fMRI connectivity analyses has recently evoked some criticism that is not only limited to the potential introduction of artificial anticorrelations (Murphy et al.

2009) but furthermore this correction has been discussed to potentially alter interregional correlations within a group and change differences in connectivity between groups because the true noise may vary systematically (Saad et al. 2012). Therefore, we performed a supplementary analysis in which we repeated the analysis without the global signal regression step to evaluate the impact of this correction method on observed group differences of connectivity. This supplementary analysis was thus not performed to establish secondary findings but only to ensure that the results of the main analysis were not confounded by the

preprocessing. As the purpose of the supplementary analysis was thus solely to confirm that the results remain stable when changing the preprocessing parameters, there is no problem with circularity although these two analyses are not independent from each other.

Data analysis

For each subject we computed linear (Pearson) correlation coefficients between the time series of the seeds and any other grey matter voxel, which were then transformed into Fisher's *Z* scores. Group analysis was then performed on these by an analysis of variance (ANOVA) across subjects using appropriate non-sphericity correction. In the ANOVA, both the main effect of functional connectivity and the group-difference between patients and controls were modelled for each seed. Inference on this random-effects analysis was then sought using linear contrasts. First, main effects of connectivity (across both groups) were calculated for each seed and a conjunction analysis over the four seeds was performed on these to reveal regions showing significant coupling common to all four seeds. Subsequently, functional connectivity maps of the left MTG, AG, IFG and thalamus were assessed for significant differences between patients and controls using *t* tests testing for increased or decreased connectivity in patients compared with controls. For all analyses, results were regarded as significant if they passed $p < 0.05$ (FWE-corrected at cluster-level for multiple comparisons; cluster-forming threshold at voxel-level: $p < 0.001$). Anatomical localizations in cytoarchitectonically defined areas were obtained using the SPM Anatomy Toolbox (Eickhoff et al. 2005, 2007).

We computed a follow-up analysis to test for state vs. trait effects of AVH on functional connectivity with our seed regions. We divided the patients into those who actually experienced hallucinations during the scan and those who did not. We extracted individual functional connectivity between the seed regions and 5 mm spheres centred on the peak voxel of those clusters that had shown significant aberrant connectivity in the main analysis. Subsequently, we computed a one-way ANOVA on these individual functional connectivity scores between the subgroups. It should be noted that this inference procedure is not circular, as targets were defined by a main-effect of aberrant connectivity across the entire group of patients and then evaluated for differences between two subsets (acutely hallucinating/not hallucinating) within it. In a second follow-up analysis we assessed whole-brain correlations between functional connectivity to the seeds and the PANSS positive score (reflecting psychotic psychopathology), the PANSS negative score (reflecting impairments in emotional and cognitive processes) as well as the PANSS

item P3 (reflecting hallucinations). To this end, the Fisher's *Z*-images of all patients were correlated with this clinical score and inference was sought on the whole-brain level. Again results were regarded as significant if they passed $p < 0.05$ (FWE-corrected at cluster-level; cluster-forming threshold at voxel-level: $p < 0.001$).

Results

All participants reported that they had stayed awake during the resting-state scan. While none of the healthy controls reported experiences of AVH during the scan, 31 of the 49 patients did. The main effects of connectivity of the four seeds computed across all participants are displayed in Fig. S1. The conjunction over these main effects of connectivity revealed no single cluster that was significantly correlated with all seeds.

Differences between patients and controls

Attenuated coupling in patients compared with controls was observed for all four seeds (Fig. 1 and Table 3). First, the left MTG showed a reduced connectivity with a cluster including parts of the right superior temporal gyrus, the superior temporal sulcus and the middle temporal gyrus (STG/STS/MTG). Second, the left AG showed a reduced local connectivity with the surrounding inferior parietal cortex (IPC) overlapping with the cytoarchitectonic areas PFm/PGa/PGp (Caspers et al. 2006) and with the left inferior temporal gyrus (ITG). Third, for the left IFG, reduced coupling was observed with the bilateral ventrolateral prefrontal cortex (VLPFC; parts of the IFG anterior-ventrally to area 45), with the left dorso-lateral prefrontal cortex (DLPFC; part of the middle frontal gyrus extending to the dorsal portion of area 44/45; Amunts et al. 1999) and with the left inferior parietal cortex (IPC; area PFm/PF and HIP1/HIP2; Caspers et al. 2006; Choi et al. 2006). Finally, the thalamic seed displayed decreased connectivity with the right cerebellum. Additionally, also increased connectivity was observed between the left IFG and the supplementary motor area (area 6; Geyer 2004) and the left insula/putamen, and between the thalamic seed and the left fusiform gyrus/hippocampus (area SUB and hOC4v; Amunts et al. 2005; Rottschy et al. 2007); see Fig. 2 and Table 3.

In order to assure that global signal regression did not introduce any systematic confounds we repeated the analysis on the same dataset but pre-processed without the removal of global signals. The results were well comparable to the group differences reported above. In particular, even though additional regions showed aberrant connectivity, we could replicate the previously observed

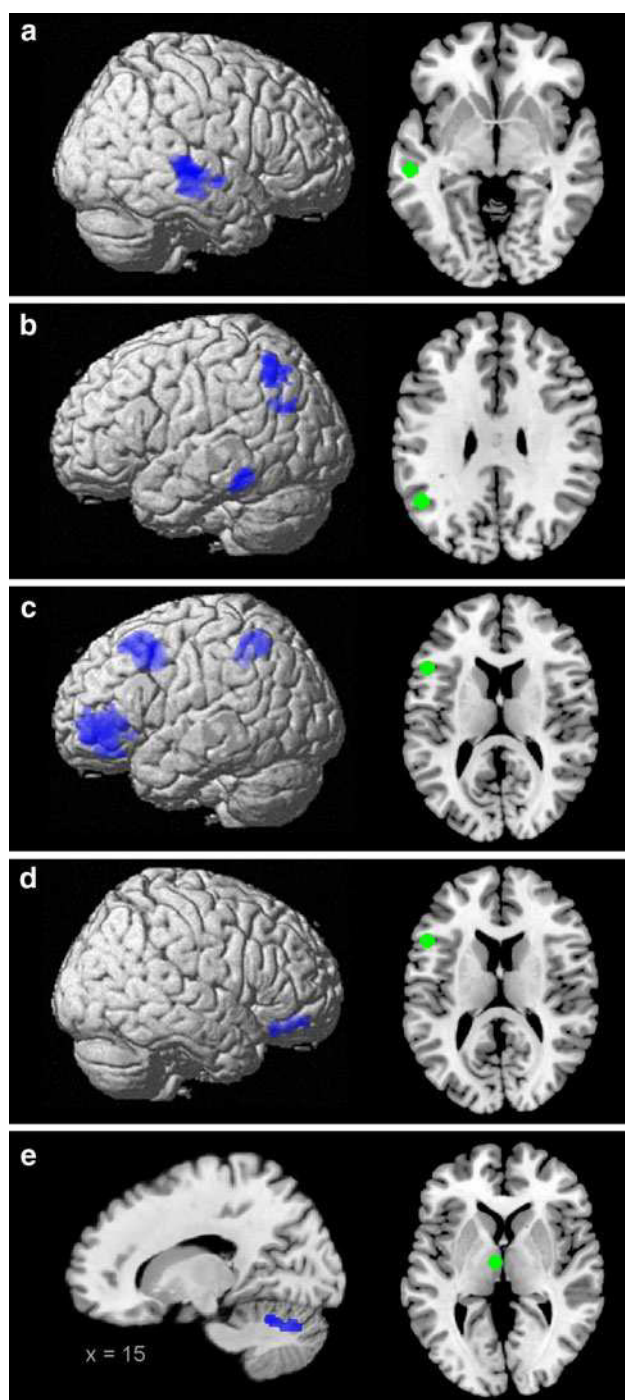


Fig. 1 Decreased connectivity in patients. Regions displaying decreased connectivity with the four seeds (*green*) in patients. **a** MTG, **b** AG, **c** and **d** IFG, **e** thalamus. All images are thresholded at $p < 0.05$ (FWE-corrected at cluster-level; cluster forming threshold at voxel level: $p < 0.001$)

differences in functional connectivity of all seeds (see Fig. S2 and S3). Accordingly, these group differences are very unlikely to be an artefact of the global signal correction.

In order to assess state-effects of acute AVH on functional connectivity with our seed regions, we performed

follow-up analyses for those regions that showed the disturbed connectivity in the overall group of trait carriers as reported above. This analysis revealed that the reduction in connectivity between the AG and the surrounding left inferior parietal cortex and the increase in connectivity between the thalamus and the left fusiform gyrus/hippocampus were more pronounced in those patients who hallucinated during scanning compared with those that did not (Fig. 3). That is, the connectivity linking these regions provided evidence for both trait and state-effects. For the remaining regions, no systematic differences were found between acutely hallucinating patients and those showing merely the trait to experience AVH. As it might be conceivable that the two subgroups (acutely vs. non-acutely hallucinating patients) showed a difference with respect to their medication status, we directly tested for these. We did not find a significant difference between groups with respect to the current medication ($\chi^2 = 6.0973$, $p = 0.53$). Therefore, the subgroups and the associated connectivity differences are unlikely to arise from medication confounds.

Correlations with PANSS-scores

No significant correlations between PANSS-positive score and the connectivity of any of the seed regions to other brain areas were found. However, when correlating only the score on the P3 item of the PANSS (i.e. hallucinatory behaviour), a significant positive relationship was observed with the connectivity between the left IFG and the ventromedial prefrontal cortex (VMPFC; Fig. 4a), indicating that higher connectivity between these two areas is associated with more severe hallucinations. Furthermore, connectivity between the thalamic seed and the right parahippocampal gyrus (area CA/SUB; Amunts et al. 2005) and between the thalamus and the right precentral gyrus was negatively correlated to the severity of hallucinations (Fig. 4b). Thus, reduced thalamic coupling was associated with more severe hallucinations. Finally, the PANSS summary score of negative symptoms showed a negative correlation with the connectivity between the seed in the left AG and the left superior parietal lobe/precuneus (area 7 M/7P; Scheperjans et al. 2008) See Fig. 4c and Table 4 for details.

Discussion

Here we examined whether patients with auditory verbal hallucinations show aberrant whole-brain connectivity of regions that previously have been associated with degraded speech based on prior expectations (Clos et al. 2012). To this end, we assessed resting-state connectivity

Table 3 Overview of regions showing altered functional connectivity in patients

Region	Overlap with cytoarchitectonic area	<i>x</i>	<i>y</i>	<i>z</i>	<i>Z</i> score	Cluster size
Decreased connectivity with left MTG						
R STG/STS/MTG		66	-24	-2	5.64	1,307
Decreased connectivity with left AG						
L IPC	PFm ^a (14 % overlap) PGa ^a (13 % overlap) PGp ^a (11 % overlap)	-50	-59	57	4.81	659
L ITG		-71	-41	-18	5.02	422
Decreased connectivity with Broca's region						
L VLPFC	Area 45 ^b (13 % overlap)	-56	42	-5	6.27	1,913
R VLPFC		44	39	-15	4.84	452
L DLPFC	Area 44 ^b (6 % overlap)	-35	20	51	5.65	1,612
L IPC	PFm ^a (24 % overlap) PF ^a (13 % overlap) hIP1 ^c (9 % overlap) hIP2 ^c (21 % overlap)	-45	-45	45	4.33	658
Increased connectivity with Broca's region						
SMA	Area 6 ^d (83 % overlap)	0	-5	59	5.27	667
L insula/putamen		-32	-5	2	4.14	918
Decreased connectivity with left thalamus						
R cerebellum		5	-78	-27	4.96	632
Increased connectivity with left thalamus						
L hippocampus/fusiform gyrus	SUB ^e (16 % overlap) hOC4v ^f (8 % overlap)	-12	-35	-11	5.61	1,656

All activations $p < 0.05$ (cluster-level FWE corrected)

x, *y*, *z* coordinates refer to the peak voxel in MNI space, *R* right, *L* left

^a Caspers et al. (2006)

^b Amunts et al. (1999)

^c Choi et al. (2006)

^d Geyer (2004)

^e Amunts et al. (2005)

^f Rottschy et al. (2007)

seeded from the left MTG, AG, IFG and thalamus in 49 psychotic patients with frequent AVH and 49 matched healthy controls to reveal disturbances in networks implicated in top-down/bottom-up interactions in speech processing. Predictions should be particularly important for speech perception because of the transient and often ambiguous nature of auditory signals; however, excessive influence of these expectations might lead to experiences of AVH (Grossberg 2000). The crucial role of predictive processes in speech perception could explain why perception in the auditory-verbal domain is particularly vulnerable to hallucinations, as AVH are the most frequent variant of hallucinations in schizophrenia (Hugdahl 2009).

The results indicated several neurocognitive mechanisms that might underlie AVH. In particular, our analysis revealed (1) aberrant coupling in the speech processing

system (connections of the left MTG, AG and the thalamus with regions involved in auditory-verbal processing), (2) increased coupling in the speech production system (connections between the left IFG and regions involved in speech production/articulation) and (3) attenuated coupling in the auditory monitoring system (connections between the left IFG and regions implicated in attentional control). Since these potential deficits are not mutually exclusive and most likely all contribute to the pathophysiology of AVH, these findings are in accordance with a multidimensional framework of AVH (Seal et al. 2004). Furthermore, connectivity with the left IFG and with the left thalamus showed a relationship with hallucination severity as assessed by the P3 item of the PANSS. We subsequently interpret these results in the light of previous findings and proposed models of AVH. Note, however, that the exact

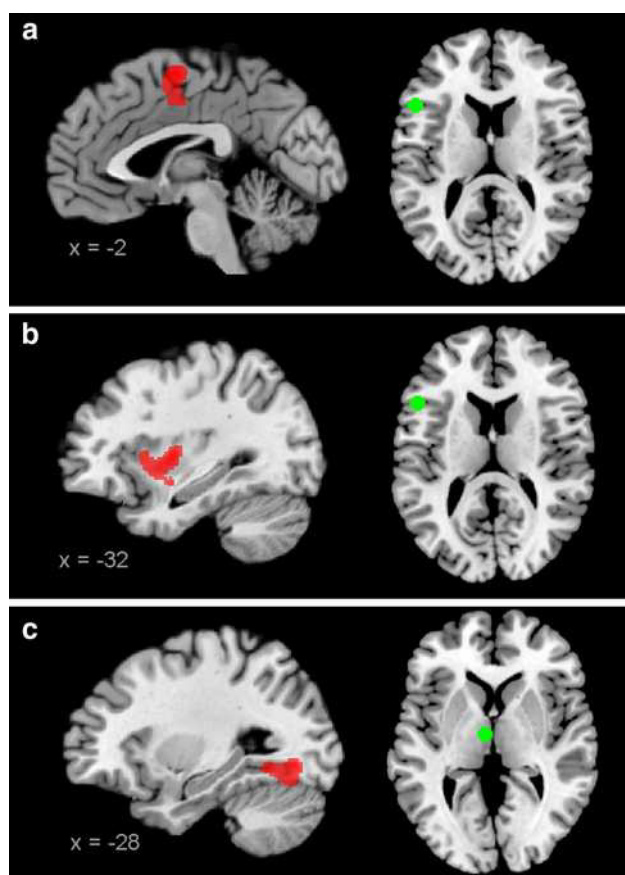


Fig. 2 Increased connectivity in patients. Regions displaying increased connectivity with the seeds (*green*) in patients. **a** and **b** IFG, **c** thalamus. All images are thresholded at $p < 0.05$ (FWE-corrected at cluster-level; cluster forming threshold at voxel level: $p < 0.001$)

mechanisms and causal interactions underlying AVH can of course not be derived from correlational methods such as resting-state connectivity. Therefore, these interpretations represent merely a reasoning on the most likely underlying processes, given our current findings and previous results on AVH as found in the literature.

Speech processing

Decreased connectivity was observed between the left MTG and the right MTG/STG. While the left MTG is known to be especially important for semantic processing of speech (Binder et al. 2009), its right-sided homotope is particularly tuned to process emotional prosody in speech (Mitchell et al. 2003). Furthermore, the right temporal cortex has been reported to be more recruited with increasing semantic complexity of language (Jung-Beeman 2005; Pugh et al. 1996). In particular, the right hemisphere might be involved in integrating context information (Kircher et al. 2001) and be more sensitive to distant

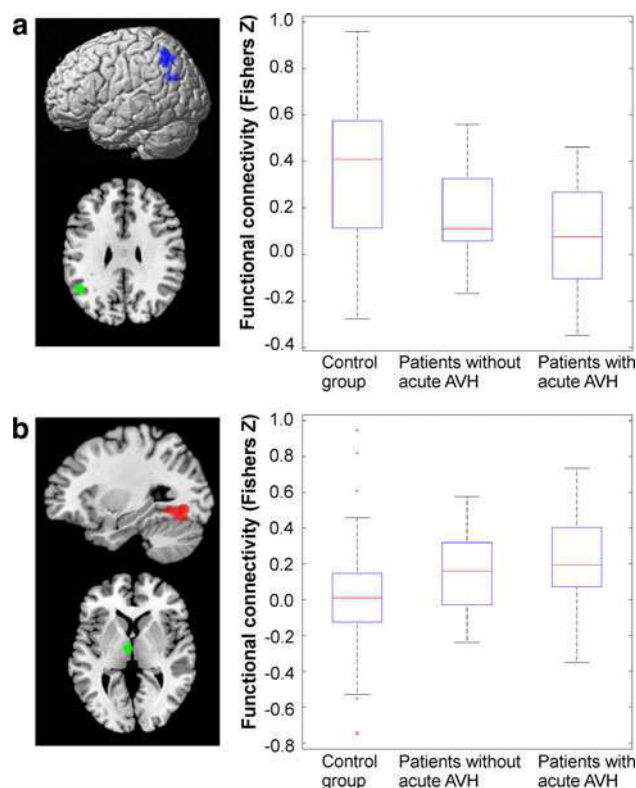


Fig. 3 State-trait effects. **a** The reduction in connectivity between the left AG and the left IPC is more pronounced in patients with acute AVH. **b** The increase in connectivity between the left thalamus and the left fusiform gyrus is more pronounced in patients with acute AVH. *Red crosses* represent data points outside $1.5 \times$ IQR, i.e. outliers

semantic relations (Sass et al. 2009) required for understanding figurative language and metaphors (Bottini et al. 1994; Nichelli et al. 1995; Mashal et al. 2007). Their attenuated coupling in patients with AVH suggests that disturbed balance of the interhemispheric connectivity linking left and right MTG/STG contributes to AVH, potentially through disturbed semantic processing. Indeed, interhemispheric projections to homotopic regions are known to be particularly dominant in the auditory system (Cipolloni and Pandya 1989) and reduced interhemispheric functional connectivity between auditory areas has previously been noted in schizophrenic patients with AVH (Gavrilescu et al. 2010). Furthermore, observations of right MTG activation prior to the onset of AVH (Shergill et al. 2004) and more bilateral language dominance in patients with AVH when listening to speech rather than the usual left-lateralized pattern in healthy controls (Sommer et al. 2001) suggest that this interhemispheric decoupling could lead to hyperactivity of the right node that ultimately plays a role in experiences of AVH. However, it has been suggested that decreased lateralization might actually be linked more with psychosis than with the experience AVH

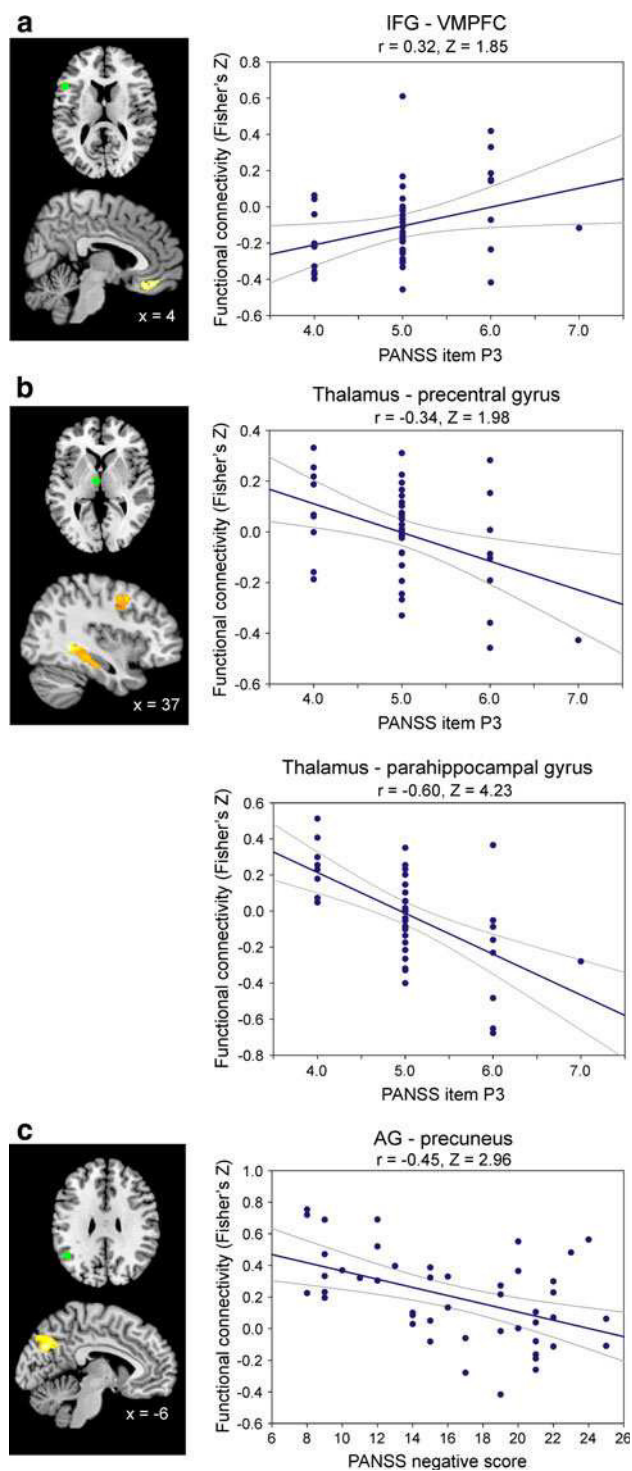


Fig. 4 Correlations with PANSS-scores. Connectivity between the seeds (green) and brain regions showing a significant relationship with hallucination severity (a, b) and with negative symptoms (c) as measured by the PANSS. All images are thresholded at $p < 0.05$ (FWE-corrected at cluster-level; cluster forming threshold at voxel level: $p < 0.001$)

per se (Diederens et al. 2010a). Since we do not have a psychotic control group without AVH, we cannot infer

from the present data whether this decreased interplay between left and right MTG is indeed contributing to AVH rather than reflecting more general aspects of psychosis.

The left AG also showed a decreased connectivity with regions involved in speech processing, namely the surrounding left IPC and the left ITG. The left AG is known to be a hierarchically high node in the speech processing system with access to higher-order concepts and long-term memory that has been suggested to provide top-down semantic constraints in language processing (Price 2010; Seghier et al. 2010). Since both the left IPC and the left ITG are involved in semantic analysis and speech processing (Binder et al. 2009; Price 2010) the decreased connectivity with the left AG might potentially reflect disturbances between bottom-up and top-down aspects in the speech processing system.

Furthermore, decreased connectivity between the thalamic seed and the cerebellum and increased connectivity between the thalamic seed and the left fusiform gyrus/hippocampus in patients with AVH was observed. The left fusiform and the adjacent parahippocampal gyrus are implicated in semantic processing of language (Binder et al. 2009). The additional role of hippocampal structures in verbal memory recollection has previously been linked with AVH (Diederens et al. 2010b). The aberrant thalamic connectivity with these regions could hence reflect disturbed feedback of semantic-verbal memory recollection which might influence the filtering and amplification processes of auditory signals in the thalamus.

Together, these results point toward an association between AVH and disturbed top-down and bottom-up interactions in auditory-verbal processing. Moreover, the pattern of reduced connectivity between the left AG and the surrounding IPC and the pattern of increased connectivity between the left thalamus and the left fusiform gyrus/hippocampus differentiated between state and trait. This observation suggests that aberrant coupling between these areas is particularly important for the acute experience of AVH. However, the state vs. trait analysis may have actually been underpowered because the acutely hallucinating patients (most likely) were not experiencing AVH during the entire scanning period. Unfortunately, however, reports on the nature and extent of hallucinations were not precise and reliable enough to quantitatively assess these aspects and, e.g. correct for the duration spent hallucinating. Therefore, the lack of state vs. trait connectivity differences for the other disturbed connections might potentially be due to the low power.

Inner speech production

In addition to these aberrant connectivity patterns in the speech processing system, Broca's region in the left IFG

Table 4 Overview of regions connected to seeds showing significant correlations with the PANSS

Region	Overlap with cytoarchitectonic area	<i>x</i>	<i>y</i>	<i>z</i>	<i>Z</i> score	Cluster size
Connections with Broca's region positively correlated with item P3 (hallucination severity)						
vmPFC		3	38	-20	4.25	377
Connections with the thalamus negatively correlated with item P3 (hallucination severity)						
R parahippocampal gyrus	CA ^a (13 % overlap) SUB ^a (7 % overlap)	41	-38	-12	5.31	467
R precentral gyrus	Area 6 ^b (3 % overlap)	42	-3	41	4.34	485
Connections with the AG negatively correlated with the negative scale						
L precuneus/SPL	7 M ^c (16 % overlap) 7P ^c (12 % overlap)	-6	-75	29	4.99	693

All activations $p < 0.05$ (cluster-level FWE corrected)

x, *y*, *z* coordinates refer to the peak voxel in MNI space, *R* right, *L* left

^a Amunts et al. (2005)

^b Geyer (2004)

^c Scheperjans et al. (2008)

showed increased coupling with the SMA and with the left insula in the patient group. Activation of these three areas is associated with generation of (inner) speech (Price 2010) and auditory imagery of alien speech (Shergill et al. 2001). Therefore, increased connectivity of this network might potentially reflect increased recruitment of these pathways in AVH. This interpretation would be in accordance with accounts hypothesising that AVH are caused by dysfunctional monitoring of self-produced speech (Frith 1995). Previously, observations of reduced SMA response in AVH compared with deliberate imagining alien speech (Shergill et al. 2000) and in verbal imagery in schizophrenic patients with AVH compared with healthy controls and schizophrenic patients without AVH (McGuire et al. 1996) have been reported. These reduced SMA responses could be reconciled with the increased connectivity observed in our study if this connection with Broca's region results in higher tonic SMA recruitment and, accordingly, attenuated phasic responses. Moreover, a recent study by Linden et al. (2011) revealed that auditory verbal imagery was associated with SMA activity, clearly preceding activity in Broca's region and the STS. In contrast, in non-clinical persons with AVH these areas became active nearly coincidentally. This coincidence of activations is in line with the increased connectivity we observed between Broca's region and the SMA. In sum, these findings suggest that the increased coupling between Broca's region with the SMA and with the insula might underlie an increased generation of inner speech/inner dialogue of alien voices in psychotic patients.

Monitoring and misattribution of inner speech

However, an increased frequency of inner dialogues alone is not sufficient for AVH because the voices in AVH are

perceived as externally generated and intrusive unlike inner speech. Furthermore, psychotic patients can distinguish between their self-produced inner speech and the voices in AVH (Hoffman et al. 2008). It has been suggested that self-produced inner speech is actually misattributed to an external source in psychotic patients due to impairments in verbal self-monitoring. As a result, the self-produced verbal thoughts are erroneously experienced as coming from another person's voice (Allen et al. 2007a). This hypothesised impairment in verbal self-monitoring might be represented in the reduced coupling between Broca's region and the DLPFC, VLPFC and IPC since accurate self-monitoring has been previously associated with a frontoparietal network (Danckert et al. 2004). Importantly, schizophrenic patients were shown to have a specific impairment in self-monitoring but not dysfunctional attentional control processes in general (Turken et al. 2003). This finding suggests that the network underlying self-monitoring might not be identical to the frontoparietal network associated with attentional control (Danckert et al. 2004). Alterations of right IPC function have been associated with delusions of control, i.e. the impression that one's movements are unintended and externally caused due to impairments of the action self-monitoring system (Blakemore 2003). Furthermore, VLPFC activation is linked to the executive control network by being the place of interaction between short-term memory and executive processing (Owen et al. 1996). In particular, the left side of this network is not only associated with language production and processing (Price 2010) but also with auditory-verbal imagery (Shergill et al. 2001) and might therefore preferentially monitor language-related processes. Therefore, aberrant connectivity in this network might cause misattributions of inner speech and auditory verbal imagery equivalent to delusions in action control

resulting from dysfunction of the right-sided action-monitoring system.

AVH would thus, at least in part, result from imbalance in connectivity with Broca's region. First, increased coupling with the SMA and the left insula would lead to aberrant recruitment of pathways subserving inner speech. Second, the resulting dialogues are experienced as alien because of relative decoupling of the verbal monitoring system (VLPFC, DLPF and IPC) from Broca's region.

Correlations with the PANSS

Finally, we observed correlations between altered connectivity and hallucination severity. First, higher connectivity between Broca's region and the VMPFC was associated with increased hallucination severity. The VMPFC is implicated in anticipation of upcoming stimuli (Stephens et al. 2010), perceptual set (Summerfield et al. 2006) and importantly, was found in our previous study (Clos et al. 2012) to be especially responsive when prior information matched with the following stimuli. In contrast, Broca's region was particularly responsive to mismatches of stimuli when the presence of meaning was hard to determine which might reflect search for meaning and the prevention of misinterpretation (Novick et al. 2005; Price 2010). The observation that increased connectivity between these two regions is associated with higher hallucination behaviour might point to a mechanism where expectations in the VMPFC override bottom-up sensory evidence and/or that the mismatch detection usually performed by Broca's region is dysfunctional. This could, in consequence, lead to detection of perceptual matches when these are not supported by sensory information.

Furthermore, attenuated coupling between the thalamus and both the right parahippocampal gyrus as well as the right precentral gyrus was associated with higher hallucination severity. This again suggests the extent of hallucinations is linked with effects of memory retrieval in verbal imagery (Diederer et al. 2010b) and auditory attention (Westernhausen et al. 2010) on auditory processing in the thalamus.

Finally, we observed a negative relationship between the connectivity between the left AG and the left precuneus/superior parietal lobe with negative symptoms. This finding is interesting given the involvement of both areas in the 'default mode' network (e.g. Binder et al. 2009) and abnormalities in this network observed in schizophrenia (Skudlarski et al. 2010; Whitfield-Gabrieli et al. 2009).

Limitations and technical considerations

By using regions as seeds that are important for top-down guided speech decoding, we employed a model-based approach for assessing differences in connectivity between

patients and controls. While such an approach has limited sensitivity to discover aberrations that might equally contribute to AVH but were not connected to our seed regions, it provides higher specificity with regard to the functional interpretation of the implicated network. Furthermore, one must acknowledge that the observed differences between patients and controls might also be due to other symptoms than AVH as patients and controls also differed in variables such as the presence of other psychotic or cognitive symptoms. Since we did not use a psychotic patient group without AVH as an additional control group, we cannot be entirely certain that the observed differences are indeed specifically due to AVH. A similar argument holds true for a potential medication confound as the types and levels of antipsychotic medication used by the patients were too heterogeneous to test for effects of medication on overall connectivity patterns. However, the a-priori selection of regions specifically involved in decoding of degraded speech sounds should reduce the influence of variables other than AVH on the observed connectivity pattern. Moreover, these factors should only vary unsystematically between acutely and non-acutely hallucinating patients. Still, it should be noted that this last state vs. trait analysis might possibly have been underpowered because the acute hallucinations were not present continuously during scanning.

Conclusions

The observed differences in connectivity point towards two main, complementary mechanisms that might underlie AVH rather than to a single unidimensional neurocognitive deficit. First, decoupling between Broca's area and the verbal monitoring system might lead to misattribution of auditory verbal imagery produced by the increased interaction of Broca's area with the SMA and the left insula. Furthermore, abnormal connectivity between nodes involved in speech processing (AG, MTG) and other regions implicated in auditory-verbal processing might reflect aberrant interactions that can elicit percepts in the absence of stimulation. In particular, the aberrant coupling with the left AG and the left thalamus might represent a more specific contribution to the acute state of AVH. Finally, these disturbed connections might be possible targets for future repetitive transcranial magnetic stimulation (rTMS) or transcranial direct current stimulation (tDCS) intervention studies. We would hypothesise that inhibitory stimulation of the speech production network and excitatory stimulation of the verbal monitoring system might be particularly promising given that stimulation of the temporo-parietal speech perception system has received more attention but only provided rather mixed evidence for reduction of hallucination severity (Slotema et al. 2012).

Acknowledgments This work was supported by the Human Brain Project (R01-MH074457-01A1 to SBE), the Initiative and Networking Fund of the Helmholtz Association within the Helmholtz Alliance on Systems Biology (Human Brain Model SBE, MC), and the DFG (IRTG 1328 to SBE).

Conflict of interest The authors declare that they have no conflict of interest.

References

- Alitto HJ, Usrey WM (2003) Corticothalamic feedback and sensory processing. *Curr Opin Neurobiol* 13:440–445
- Allen PP, Amaro E, Fu CH, Williams SC, Brammer M, Johns LC, McGuire PK (2005) Neural correlates of the misattribution of self-generated speech. *Hum Brain Mapp* 26:44–53
- Allen P, Aleman A, McGuire PK (2007a) Inner speech models of auditory verbal hallucinations: evidence from behavioural and neuroimaging studies. *Int Rev Psychiatry* 19:407–415
- Allen P, Amaro E, Fu CH, Williams SC, Brammer MJ, Johns LC, McGuire PK (2007b) Neural correlates of the misattribution of speech in schizophrenia. *Br J Psychiatry* 190:162–169
- Allen P, Modinos G, Hubl D, Shields G, Cachia A, Jardri R, Thomas P, Woodward T, Shotbolt P, Plaze M, Hoffman R (2012) Neuroimaging auditory hallucinations in schizophrenia: from neuroanatomy to neurochemistry and beyond. *Schizophr Bull* 38:695–703
- Amunts K, Schleicher A, Bürgel U, Mohlberg H, Uylings HB, Zilles K (1999) Broca's region revisited: cytoarchitecture and inter-subject variability. *J Comp Neurol* 412:319–341
- Amunts K, Kedo O, Kindler M, Pieperhoff P, Mohlberg H, Shah NJ, Habel U, Schneider F, Zilles K (2005) Cytoarchitectonic mapping of the human amygdala, hippocampal region and entorhinal cortex: intersubject variability and probability maps. *Anat Embryol (Berl)* 210:343–352
- Andreassen NC, Flaum M, Arndt S (1992) The comprehensive assessment of symptoms and history (CASH): an instrument for assessing psychopathology and diagnosis. *Arch Gen Psychiatry* 49:615–623
- Ashburner J, Friston KJ (2005) Unified segmentation. *Neuroimage* 26:839–851
- Bandettini PA, Bullmore E (2008) Endogenous oscillations and networks in functional magnetic resonance imaging. *Hum Brain Mapp* 29:737–739
- Behzadi Y, Restom K, Liu J, Liu TT (2007) A component based noise correction method (CompCor) for BOLD and perfusion based fMRI. *Neuroimage* 37:90–101
- Binder JR, Desai RH, Graves WW, Conant LL (2009) Where is the semantic system? A critical review and meta-analysis of 120 functional neuroimaging studies. *Cereb Cortex* 19:2767–2796
- Biswal B, Yetkin FZ, Haughton VM, Hyde JS (1995) Functional connectivity in the motor cortex of resting human brain using echo-planar MRI. *Magn Reson Med* 34:537–541
- Blakemore SJ (2003) Deluding the motor system. *Conscious Cogn* 12:647–655
- Bottini G, Corcoran R, Sterzi R, Paulesu E, Schenone P, Scarpa P, Frackowiak RS, Frith CD (1994) The role of the right hemisphere in the interpretation of figurative aspects of language. A positron emission tomography activation study. *Brain* 117:1241–1253
- Caspers S, Geyer S, Schleicher A, Mohlberg H, Amunts K, Zilles K (2006) The human inferior parietal cortex: cytoarchitectonic parcellation and interindividual variability. *NeuroImage* 33:430–448
- Chai XJ, Castañón AN, Öngür D, Whitfield-Gabrieli S (2012) Anticorrelations in resting-state networks without global signal regression. *Neuroimage* 59:1420–1428
- Choi HJ, Zilles K, Mohlberg H, Schleicher A, Fink GR, Armstrong E, Amunts K (2006) Cytoarchitectonic identification and probabilistic mapping of two distinct areas within the anterior ventral bank of the human intraparietal sulcus. *J Comp Neurol* 495:53–69
- Cipolloni PB, Pandya DN (1989) Connectional analysis of the ipsilateral and contralateral afferent neurons of the superior temporal region in the rhesus monkey. *J Comp Neurol* 281:567–585
- Clos M, Langner R, Meyer M, Oechslin MS, Zilles K, Eickhoff SB (2012) Effects of prior information on decoding degraded speech: an fMRI study. *Hum Brain Mapp* (Advance online publication). doi:10.1002/hbm.22151
- Danckert J, Saoud M, Maruff P (2004) Attention, motor control and motor imagery in schizophrenia: implications for the role of the parietal cortex. *Schizophr Res* 70:241–261
- Davis MH, Johnsrude IS (2003) Hierarchical processing in spoken language comprehension. *J Neurosci* 23:3423–3431
- Davis MH, Johnsrude IS (2007) Hearing speech sounds: top-down influences on the interface between audition and speech perception. *Hear Res* 229:132–147
- Deco G, Jirsa VK, McIntosh AR (2011) Emerging concepts for the dynamical organization of resting-state activity in the brain. *Nat Rev Neurosci* 12:43–56
- Diederen KM, De Weijer AD, Daalman K, Blom JD, Neggers SF, Kahn RS, Sommer IE (2010a) Decreased language lateralization is characteristic of psychosis, not auditory hallucinations. *Brain* 133:3734–3744
- Diederen KM, Neggers SF, Daalman K, Blom JD, Goekoop R, Kahn RS, Sommer IE (2010b) Deactivation of the parahippocampal gyrus preceding auditory hallucinations in schizophrenia. *Am J Psychiatry* 167:427–435
- Eickhoff SB, Stephan KE, Mohlberg H, Grefkes C, Fink GR, Amunts K, Zilles K (2005) A new SPM toolbox for combining probabilistic cytoarchitectonic maps and functional imaging data. *Neuroimage* 25:1325–1335
- Eickhoff SB, Paus T, Caspers S, Grosbas MH, Evans AC, Zilles K, Amunts K (2007) Assignment of functional activations to probabilistic cytoarchitectonic areas revisited. *Neuroimage* 36:511–521
- Eickhoff SB, Bzdok D, Laird AR, Roski C, Caspers S, Zilles K, Fox PT (2011) Co-activation patterns distinguish cortical modules, their connectivity and functional differentiation. *Neuroimage* 57:938–949
- Fox MD, Zhang D, Snyder AZ, Raichle ME (2009) The global signal and observed anticorrelated resting state brain networks. *J Neurophysiol* 101:3270–3283
- Friston KJ (1998) The disconnection hypothesis. *Schizophr Res* 30:115–125
- Frith CD (1995) The cognitive abnormalities underlying the symptomatology and the disability of patients with schizophrenia. *Int Clin Psychopharmacol* 10(Suppl. 3):87–98
- Gavrilescu M, Rossel S, Stuart GW, Shea TL, Innes-Brwon H, Henshall K, McKay C, Sergejew AA, Copolov D, Egan GF (2010) Reduced connectivity of the auditory cortex in patients with auditory hallucinations: a resting state functional magnetic resonance imaging study. *Psychol Med* 40:1149–1158
- Geyer S (2004) The microstructural border between the motor and the cognitive domain in the human cerebral cortex. *Adv Anat Embryol Cell Biol* 174:1–92
- Giraud AL, Kell C, Thierfelder C, Sterzer P, Russ MO, Preibisch C, Kleinschmidt A (2004) Contributions of sensory input, auditory

- search and verbal comprehension to cortical activity during speech processing. *Cereb Cortex* 14:247–255
- Greicius MD, Krasnow B, Reiss AL, Menon V (2003) Functional connectivity in the resting brain: a network analysis of the default mode hypothesis. *Proc Natl Acad Sci USA* 100:253–258
- Grossberg S (2000) How hallucinations may arise from brain mechanisms of learning, attention, and volition. *J Int Neuropsychol Soc* 6:583–592
- Heinrich A, Carlyon RP, Davis MH, Johnsrude IS (2008) Illusory vowels resulting from perceptual continuity: a functional magnetic resonance imaging study. *J Cogn Neurosci* 20:1737–1752
- Hoffman RE, Woods SW, Hawkins KA, Pittman B, Tohen M, Preda A, Breier A, Glist J, Addington J, Perkins DO, McGlashan TH (2007) Extracting spurious messages from noise and risk of schizophrenia-spectrum disorders in a prodromal population. *Br J Psychiatry* 191:355–356
- Hoffman RE, Varanko M, Gilmore J, Mishara AL (2008) Experiential features used by patients with schizophrenia to differentiate ‘voices’ from ordinary verbal thought. *Psychol Med* 38:1167–1176
- Hoffman RE, Fernandez T, Pittman B, Hampson M (2011) Elevated functional connectivity along a corticostriatal loop and the mechanism of auditory/verbal hallucinations in patients with schizophrenia. *Biol Psychiatry* 69:407–414
- Holmes CJ, Hoge R, Collins L, Woods R, Toga AW, Evans AC (1998) Enhancement of MR images using registration for signal averaging. *J Comput Assist Tomogr* 22:324–333
- Hugdahl K (2009) “Hearing voices”: auditory hallucinations as failure of top-down control of bottom-up perceptual processes. *Scand J Psychol* 50:553–560
- Jardri R, Thomas P, Delmaire C, Delion P, Pins D (2012) The neurodynamic organization of modality-dependent hallucinations. *Cereb Cortex* (Advance online publication). doi: [10.1093/cercor/bhs082](https://doi.org/10.1093/cercor/bhs082)
- Jones SR (2010) Do we need multiple models of auditory verbal hallucinations? Examining the phenomenological fit of cognitive and neurological models. *Schizophr Bull* 36:566–575
- Jung-Beeman M (2005) Bilateral brain processes for comprehending natural language. *Trends Cogn Sci* 9:512–518
- Kay S, Fiszbein A, Opler L (1987) The positive and negative syndrome scale (PANSS) for schizophrenia. *Schizophr Bull* 13:261–276
- Kircher TT, Brammer M, Tous Andreu N, Williams SC, McGuire PK (2001) Engagement of right temporal cortex during processing of linguistic context. *Neuropsychologia* 39:798–809
- Linden DE, Thornton K, Kuswanto CN, Johnston SJ, van de Ven V, Jackson MC (2011) The brain’s voices: comparing nonclinical auditory hallucinations and imagery. *Cereb Cortex* 21:330–337
- Mashal N, Faust M, Hendler T, Jung-Beeman M (2007) An fMRI investigation of the neural correlates underlying the processing of novel metaphoric expressions. *Brain Lang* 100:115–126
- McGuire PK, Silbersweig DA, Wright I, Murray RM, Frackowiak RS, Frith CD (1996) The neural correlates of inner speech and auditory verbal imagery in schizophrenia: relationship to auditory verbal hallucinations. *Br J Psychiatry* 169:148–159
- Mitchell RL, Elliott R, Barry M, Cruttenden A, Woodruff PW (2003) The neural response to emotional prosody, as revealed by functional magnetic resonance imaging. *Neuropsychologia* 41:1410–1421
- Murphy K, Birm RM, Handwerker DA, Jones TB, Bandettini PA (2009) The impact of global signal regression on resting state correlations: are anti-correlated networks introduced? *Neuroimage* 44:893–905
- Neggers SF, Hermans EJ, Ramsey NF (2008) Enhanced sensitivity with fast three-dimensional blood-oxygen-level-dependent functional MRI: comparison of SENSE-PRESTO and 2D-EPI at 3 T. *NMR Biomed* 21:663–676
- Nichelli P, Grafman J, Pietrini P, Clark K, Lee KY, Miletich R (1995) Where the brain appreciates the moral of a story. *NeuroReport* 6:2309–2313
- Northoff G, Qin P (2011) How can the brain’s resting state activity generate hallucinations? A ‘resting state hypothesis’ of auditory verbal hallucinations. *Schizophr Res* 127:202–214
- Novick JM, Trueswell JC, Thompson-Schill SL (2005) Cognitive control and parsing: reexamining the role of Broca’s area in sentence comprehension. *Cogn Affect Behav Neurosci* 5:263–281
- Obleser J, Kotz SA (2010) Expectancy constraints in degraded speech modulate the language comprehension network. *Cereb Cortex* 20:633–640
- Obleser J, Wise RJ, Alex Dresner M, Scott SK et al (2007) Functional integration across brain regions improves speech perception under adverse listening conditions. *J Neurosci* 27:2283–2289
- Owen AM, Evans AC, Petrides M (1996) Evidence for a two-stage model of spatial working memory processing within the lateral frontal cortex: a positron emission tomography study. *Cereb Cortex* 6:31–38
- Price CJ (2010) The anatomy of language: a review of 100 fMRI studies published in 2009. *Ann NY Acad Sci* 1191:62–88
- Pugh KR, Shaywitz BA, Shaywitz SE, Constable RT, Skudlarski P, Fulbright RK, Bronen RA, Shankweiler DP, Katz L, Fletcher JM, Gore JC (1996) Cerebral organization of component processes in reading. *Brain* 119:1221–1238
- Raichle ME (2010) Two views of brain function. *Trends Cogn Sci* 14:180–190
- Rottschy C, Eickhoff SB, Schleicher A, Mohlberg H, Kujovic M, Zilles K, Amunts K (2007) Ventral visual cortex in humans: cytoarchitectonic mapping of two extrastriate areas. *Hum Brain Mapp* 28:1045–1059
- Saad ZS, Gotts SJ, Murphy K, Chen G, Jo HJ, Martin A, Cox RW (2012) Trouble at rest: how correlation patterns and group differences become distorted after global signal regression. *Brain Connect* 2:25–32
- Sass K, Krach S, Sachs O, Kircher T (2009) Lion–tiger–stripes: neural correlates of indirect semantic priming across processing modalities. *Neuroimage* 45:224–236
- Scheperjans F, Hermann K, Eickhoff SB, Amunts K, Schleicher A, Zilles K (2008) Observer-independent cytoarchitectonic mapping of the human superior parietal cortex. *Cereb Cortex* 18:846–867
- Seal ML, Aleman A, McGuire PK (2004) Compelling imagery, unanticipated speech and deceptive memory: neurocognitive models of auditory verbal hallucinations in schizophrenia. *Cogn Neuropsychiatry* 9:43–72
- Seghier ML (2012) The Angular Gyrus: multiple Functions and Multiple Subdivisions. *Neuroscientist* (Advance online publication). doi: [10.1177/1073858412440596](https://doi.org/10.1177/1073858412440596)
- Seghier ML, Fagan E, Price CJ (2010) Functional subdivisions in the left angular gyrus where the semantic system meets and diverges from the default network. *J Neurosci* 30:16809–16817
- Shahin AJ, Bishop CW, Miller LM (2009) Neural mechanisms for illusory filling-in of degraded speech. *Neuroimage* 44:1133–1143
- Shergill SS, Brammer MJ, Williams SC, Murray RM, McGuire PK (2000) Mapping auditory hallucinations in schizophrenia using functional magnetic resonance imaging. *Arch Gen Psychiatry* 57:1033–1038
- Shergill SS, Bullmore ET, Brammer MJ, Williams SC, Murray RM, McGuire PK (2001) A functional study of auditory verbal imagery. *Psychol Med* 31:241–253
- Shergill SS, Brammer MJ, Amaro E, Williams SC, Murray RM, McGuire PK (2004) Temporal course of auditory hallucinations. *Br J Psychiatry* 185:516–517

- Simons CJ, Tracy DK, Sanghera KK, O'Daly O, Gilleen J, Dominguez MD, Krabbendam L, Shergill SS (2010) Functional magnetic resonance imaging of inner speech in schizophrenia. *Biol Psychiatry* 67:232–237
- Skudlarski P, Jagannathan K, Anderson K, Stevens MC, Calhoun VD, Skudlarska BA, Pearlson G (2010) Brain connectivity is not only lower but different in schizophrenia: a combined anatomical and functional approach. *Biol Psychiatry* 68:61–69
- Slotema CW, Aleman A, Daskalakis ZJ, Sommer IE (2012) Meta-analysis of repetitive transcranial magnetic stimulation in the treatment of auditory verbal hallucinations: update and effects after one month. *Schizophr Res* 142:40–45
- Sohoglu E, Peelle JE, Carlyon RP, Davis MH (2012) Predictive top-down integration of prior knowledge during speech perception. *J Neurosci* 32:8443–8453
- Sommer IE, Ramsey NF, Kahn RS (2001) Language lateralization in schizophrenia, an fMRI study. *Schizophr Res* 52:57–67
- Sommer IE, Clos M, Meijering AL, Diederer KM, Eickhoff SB (2012) Resting state functional connectivity in patients with chronic hallucinations. *PLoS ONE* 7:e43516
- Stephan KE, Friston KJ, Frith CD (2009) Dysconnection in schizophrenia: from abnormal synaptic plasticity to failures of self-monitoring. *Schizophr Bull* 35:509–527
- Stephens GJ, Silbert LJ, Hasson U (2010) Speaker-listener neural coupling underlies successful communication. *Proc Natl Acad Sci USA* 107:14425–14430
- Summerfield C, Egner T, Greene M, Koechlin E, Mangels J, Hirsch J (2006) Predictive codes for forthcoming perception in the frontal cortex. *Science* 314:1311–1314
- Turken AU, Vuilleumier P, Mathalon DH, Swick D, Ford JM (2003) Are impairments of action monitoring and executive control true dissociative dysfunctions in patients with schizophrenia? *Am J Psychiatry* 160:1881–1883
- Vercammen A, Aleman A (2008) Semantic expectations can induce false perceptions in hallucination-prone individuals. *Schizophr Bull* 36:151–156
- Vercammen A, Kneegtering H, den Boer JA, Liemburg EJ, Aleman A (2010) Auditory hallucinations in schizophrenia are associated with reduced functional connectivity of the temporo-parietal area. *Biol Psychiatry* 67:912–918
- Westernhausen R, Moosmann M, Alho K, Belsby SO, Hämäläinen H, Medvedev S, Hugdahl K (2010) Identification of attention and cognitive control networks in a parametric auditory fMRI study. *Neuropsychologia* 48:2075–2081
- Whitfield-Gabrieli S, Thermenos HW, Milanovic S, Tsuang MT, Faraone SV, McCarley RW, Shenton ME, Green AI, Nieto-Castanon A, LaViolette P, Wojcik J, Gabrieli JD, Seidman LJ (2009) Hyperactivity and hyperconnectivity of the default network in schizophrenia and in first-degree relatives of persons with schizophrenia. *Proc Natl Acad Sci USA* 106:1279–1284
- Wild CJ, Davis MH, Johnsrude IS (2012) Human auditory cortex is sensitive to the perceived clarity of speech. *Neuroimage* 60:1490–1502

SUPPLEMENTAL FIGURES

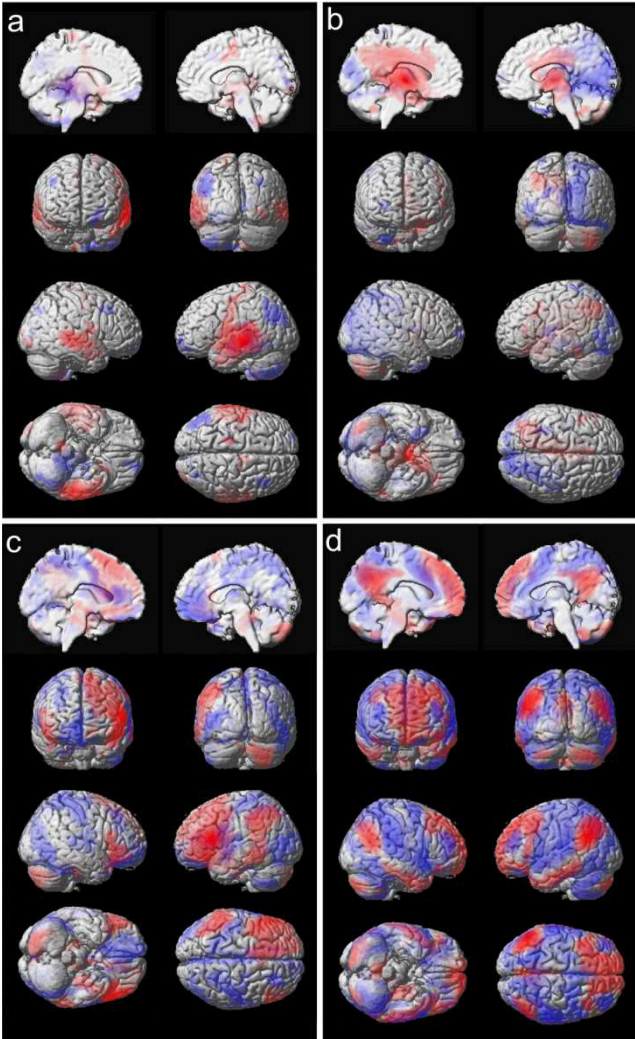


Fig. S1: Main effects of connectivity of the seeds
a) left MTG, b) left Thalamus, c) Broca's region, d) left AG. Red-coloured voxels indicate significant positive correlations, blue significant negative correlations. All images are thresholded at $p < .05$ (FWE-corrected at cluster-level; cluster forming threshold at voxel level: $p < .001$)

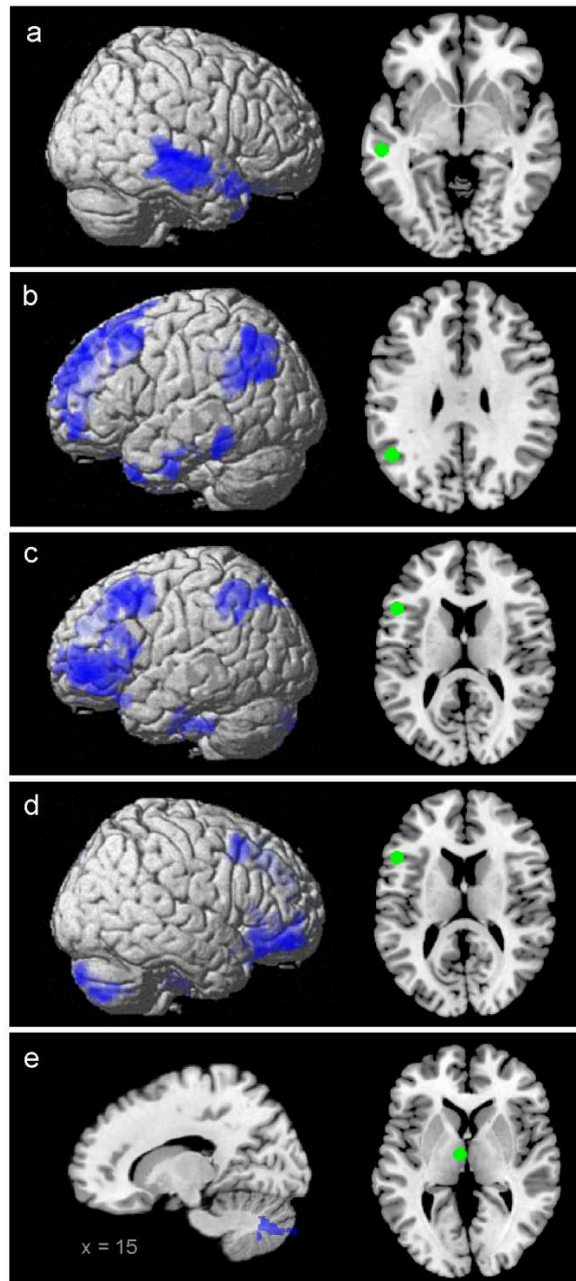


Fig. S2: Pattern of decreased connectivity without global signal regression

Regions displaying decreased connectivity with the four seeds (green) in patients. a) MTG, b) AG, c) & d) IFG, e) thalamus. All images are thresholded at $p < .01$ with an extent threshold of 500 voxels. Note that all regions displayed in Fig. 1 are replicated in this analysis.

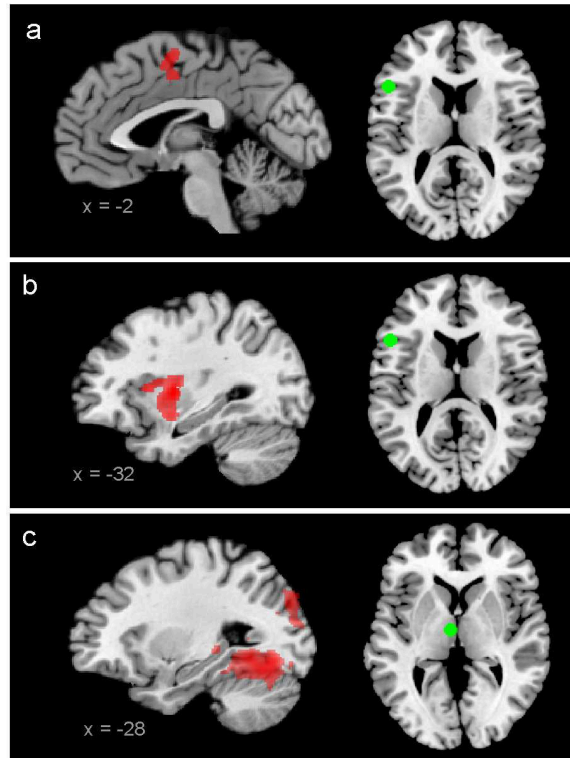


Fig. S3: Pattern of increased connectivity without global signal regression

Regions displaying increased connectivity with the seeds (green) in patients. a) & b) IFG, c) thalamus. All images are thresholded at $p < .01$ with an extent threshold of 500 voxels. Note that all regions displayed in Fig. 2 are replicated in this analysis.

STUDY 4

Resting state functional connectivity in patients with chronic hallucinations

Iris E. Sommer¹, Mareike Clos², Anne Lotte Meijering¹, Kelly M. J. Diederer¹, Simon B. Eickhoff^{2,3,4}

¹Psychiatry Department, University Medical Center Utrecht & Rudolf Magnus Institute for Neuroscience, The Netherlands

²Institute of Neuroscience and Medicine (INM-1; INM-2), Research Center Jülich, Germany

³Department of Psychiatry, Psychotherapy, and Psychosomatics, Medical School, RWTH Aachen University, Germany

⁴Institute of Clinical Neuroscience and Medical Psychology, Heinrich Heine University, Düsseldorf, Germany

PLoS One (2012) 7(9):e43516

doi: 10.1371/journal.pone.0043516

Impact factor (2011): 4.092

Own contributions

Reviewing and adapting analysis code

Statistical data analysis

Preparing figures

Writing parts of the methods section of the paper

Correcting the introduction, results and discussion sections

Total contribution: 30%

Resting State Functional Connectivity in Patients with Chronic Hallucinations

Iris E. Sommer^{1*}, Mareike Clos², Anne Lotte Meijering¹, Kelly M. J. Dieren¹, Simon B. Eickhoff^{2,3,4}

1 Psychiatry Department, University Medical Center Utrecht & Rudolf Magnus Institute for Neuroscience, Utrecht, The Netherlands, **2** Institute of Neurosciences and Medicine (INM-1, INM-22), Research Centre Jülich, Jülich, Germany, **3** Department of Psychiatry, Psychotherapy, and Psychosomatics, Medical School, RWTH Aachen University, Aachen, Germany, **4** Institute for Clinical Neuroscience and Medical Psychology, Heinrich-Heine University, Düsseldorf, Germany

Abstract

Auditory verbal hallucinations (AVH) are not only among the most common but also one of the most distressing symptoms of schizophrenia. Despite elaborate research, the underlying brain mechanisms are as yet elusive. Functional MRI studies have associated the experience of AVH with activation of bilateral language-related areas, in particular the right inferior frontal gyrus (rIFG) and the left superior temporal gyrus (ISTG). While these findings helped to understand the neural underpinnings of hearing voices, they provide little information about possible brain mechanisms that predispose a person to experience AVH, i.e. the *traits* to hallucinate. In this study, we compared resting state connectivity between 49 psychotic patients with chronic AVH and 49 matched controls using the rIFG and the ISTG as seed regions, to identify functional brain systems underlying the predisposition to hallucinate. The right parahippocampal gyrus showed increased connectivity with the rIFG in patients as compared to controls. Reduced connectivity with the rIFG in patients was found for the right dorsolateral prefrontal cortex. Reduced connectivity with the ISTG in patients was identified in the left frontal operculum as well as the parietal opercular area. Connectivity between the ISTG and the left hippocampus was also reduced in patients and showed a negative correlation with the severity of hallucinations. Concluding, we found aberrant connectivity between the seed regions and medial temporal lobe structures which have a prominent role in memory retrieval. Moreover, we found decreased connectivity between language-related areas, indicating aberrant integration in this system potentially including corollary discharge mechanisms.

Citation: Sommer IE, Clos M, Meijering AL, Dieren KMJ, Eickhoff SB (2012) Resting State Functional Connectivity in Patients with Chronic Hallucinations. PLoS ONE 7(9): e43516. doi:10.1371/journal.pone.0043516

Editor: Bogdan Draganski, Centre Hospitalier Universitaire Vaudois Lausanne - CHUV, UNIL, Switzerland

Received: April 27, 2012; **Accepted:** July 23, 2012; **Published:** September 6, 2012

Copyright: © 2012 Sommer et al. This is an open-access article distributed under the terms of the Creative Commons Attribution License, which permits unrestricted use, distribution, and reproduction in any medium, provided the original author and source are credited.

Funding: This work was supported by NWO/ZonMW (Dutch Scientific Research Organization) Clinical Fellowship [40-00703-97-270] and by NWO/ZonMW Innovation Impulse (VIDI) [017.106.301]. The funders had no role in study design, data collection and analysis, decision to publish, or preparation of the manuscript.

Competing Interests: The authors have declared that no competing interests exist.

* E-mail: I.Sommer@umcutrecht.nl

Introduction

Auditory verbal hallucinations (AVH) are among the most common and distressing symptoms of schizophrenia and also affect persons with affective psychosis and some (e.g., borderline and schizotypic) personality disorders. While AVH are thus a highly prevalent feature of psychiatric illnesses, their underlying brain mechanisms remain elusive. Models proposed for their pathophysiology include the misattribution of inner speech [1,2], increased top-down processing [3], recollection of verbal memory fragments [4,5] and sensory-based bottom-up deviations [6,7]. Functional MRI studies demonstrated activation of inferior-frontal and temporo-parietal areas during the experience of AVH [5,8,9] together with deactivation of medial temporal lobe structures at the onset of AVH [5,10]. However, these symptom-capture studies do not provide information about brain mechanisms predisposing a person to experience AVH, i.e. the *trait* to hallucinate. Insight into aberrations of neuronal networks underlying such vulnerability, in turn, may be particularly relevant for guiding the development and evaluation of treatment strategies.

It could be hypothesized that a predisposition to AVH may be instantiated by aberrant connectivity between inferior frontal and temporo-parietal areas leading to a misattribution of inner speech

[1,2]. If this were to be the case, we would expect reduced functional connectivity at rest between the inferior frontal and the temporo-parietal areas of both hemispheres, reflecting disturbances within the language network underlying aberrant processing of ambiguous bottom-up signals [11]. This hypothesized reduced couplings between inferior frontal and temporo-parietal areas may render a person vulnerable to hallucinate in the auditory verbal domain. At the structural level, deviations in the fiber-tracts connecting these areas have been demonstrated with Magnetic Transfer Imaging (MTI) in schizophrenia patients [12] and in non-psychotic individuals with frequent hallucinations [13]. However, it is currently unclear if these structural deficiencies also lead to functionally decreased connectivity.

Alternatively, deviant connectivity between speech-related areas and the medial temporal lobe could give rise to spontaneous verbal memory recollection [4,5]. A predisposition for intrusive memory fragments may be reflected in anomalous functional connectivity between cortical association areas such as the frontal, temporal and parietal cortex and memory related structures such as the hippocampus and parahippocampal gyrus. Such increased vulnerability for intrusive memory fragments may predispose a person for hallucinations per se, as the hippocampal-parahippocampal complex is involved in the recollection of memories from

Table 1. Demographic and clinical description of participants.

Group	Patients, n = 49	Control subjects, n = 49
Age	38.5 years \pm 11.72	39.5 years \pm 14.9
Sex	20 males, 29 females	18 males, 31 females
Handedness	41 right, 8 non-right	41 right, 7 non-right
Mean time with AVH	13.9 \pm 12.2 years	No AVH
Diagnosis	43 Schizophrenia, 4 Schizoaffective Disorder, 1 Schizophreniform Disorder, 1 Psychosis NOS	No psychiatric diagnosis
Antipsychotic Medication	10 clozapine, mean dose 464 mg, 3 flufenazine, mean dose 30 mg, 7 risperidon, all medication-free mean dose 3.6 mg, 8 olanzapine, mean dose 14.2 mg, 7 quetiapine, mean dose 514 mg, 1 penfluridol 10 mg, 5 haloperidol, mean dose 4 mg, 1 aripiprazol, 15 mg, 7 medication-free	
Mean PANSS scores	Positive scale	16.2 \pm 3.7,
	Negative scale	16.3 \pm 5.2,
	Total	63 \pm 13.3

doi:10.1371/journal.pone.0043516.t001

several modalities. Increased vulnerability to memory intrusions could result from either increased connectivity between the cortical and the medial temporal structures, or decreased (inhibitory) connectivity, or a combination of both.

Either of these hypothesized dysconnectivities may become evident in the absence of external tasks, given that the latter may override the endogenous dynamics of AVH. Therefore, aberrations in functional coupling that may predispose a person to hearing voices may become evident by examining resting state connectivity data. Resting state fMRI connectivity measures low-frequency fluctuations in the cerebral haemodynamics (around 0.01–0.1 Hz). Recently, attention has been focused on the possible origins of these slow variations. Various investigations suggested that these signal variations are of neuronal origin and characterize the neuronal baseline activity of the human brain in the absence of externally stimulated neuronal activity.

Resting state connectivity can be assessed by using Regions of Interest (ROIs); areas that are thought to play a major role in the trait under investigation, or without the predefinition of ROIs as in an independent component analysis (ICA). In this paper, we used the first approach as there is good evidence for the essential contribution of certain well-defined areas in AVH. In contrast, the data-driven ICA approach may also pick up other differences in resting state between the groups that may not be related to hallucinations given that lack of focus on a specific system. In this study we aim to investigate the vulnerability to experience AVH in patients who have experienced AVH.

A recent meta-analysis indicated consistent activation of the right inferior frontal gyrus (rIFG) and the left superior temporal gyrus (lSTG) during the experience of AVH [14], these regions therefore provide a strong model to assess dysfunctional connectivity underlying AVH. In the present study we thus compare resting state connectivity of these regions between 49 psychotic patients with chronic AVH and a group of well-matched controls in order to unravel network aberrations underlying the predisposition to AVH. For practical reasons, we selected the Regions of Interest (ROIs) from a single large fMRI study [5], as meta-analytic studies provide rather large ROIs. As the study by Diederer et al. was by far the largest study included in the meta-analysis, results of the meta-analysis are largely in agreement with this study. We selected the two seeds that showed the largest areas of activation, namely the left superior temporal gyrus and the right inferior frontal gyrus. These two seeds also have functional

significance as the left superior temporal gyrus may be involved in the auditory component of AVH; i.e. the fact that voices are being heard aloud, while the right inferior frontal area may be the place where the words and sentences that are later perceived as voices could be generated [15].

Materials and Methods

Participants

Forty-nine patients with psychosis, as diagnosed according to DSM-IV criteria by an independent psychiatrist using the “Comprehensive Assessment of Symptoms and History (CASH)” [16], who all experienced AVH with a frequency of at least several times a day during at least one year were included in the study (cf. Table 1 for clinical and demographic details). Psychopathology was assessed at the day of scanning with the Positive and Negative Syndrome Scale [17]. For comparison, 49 healthy (as confirmed by the CASH interview) individuals matched for age, sex and handedness were also included. After complete description of the study to the subjects, the participants provided written informed consent into the study, which was approved by the Humans Ethics Committee of the University Medical Center Utrecht.

Data acquisition and processing

Resting state scans of eight minutes duration (600 blood-oxygenation-level-dependent (BOLD) fMRI images) were obtained on a Philips Achieva 3 T MRI scanner using the following parameter: 40 (coronal) slices, TR/TE 21.75/32.4 ms, flip angle 10°, FOV 224 \times 256 \times 160, matrix 64 \times 64 \times 40, voxel-size 4 mm isotropic. (PRESTO scans typically have shorter TR than TE times, as the whole head is scanned with each volume in stead of the slab-wise read-out of EPI scans). This scan sequence achieves full brain coverage within 609 ms by combining a 3D-PRESTO pulse sequence with parallel imaging (SENSE) in two directions, using a commercial 8-channel SENSE headcoil [18]. Participants were instructed to lie in the scanner as still as possible with their eyes closed yet stay awake (which was confirmed by post-scan debriefing). After scanning, patients were asked whether or not they had experienced AVH during the resting state scan. Likewise, healthy subjects were asked for AVH, which were denied by all of them.

The resting state scans were first corrected for head movement by affine registration using a two pass procedure. The mean

PRESTO image for each subject was then spatially normalized to the MNI single subject template [19] using the unified segmentation approach [20] and the ensuing deformation was applied to the individual PRESTO volumes. Finally, images were smoothed by a 5-mm FWHM Gaussian kernel. Regions of interest (ROIs) used as seeds for the functional connectivity analysis were based on two activation clusters reliably associated with the state of AVH obtained from Diederer et al. [5] (table 2.): the right inferior frontal gyrus, MNI coordinates: 44,16,12 and the left superior temporal gyrus, MNI coordinates $-48, 0, 0$. We selected regions from this large fMRI study rather than using seeds from the meta-analysis [21] because the latter would have provided very large and unspecific clusters.

Voxel time courses were extracted for all voxels within a 5 mm sphere around the centre of the particular clusters that were located in the grey matter of the individual subject.

Variance explained by the following nuisance variables was removed from the time series to reduce spurious correlations [22–24]: i) motion parameters derived from image realignment and their first derivative; ii) mean grey, white matter and CSF signal intensity per time-point; iii) coherent signal drifts reflected by the first five PCA components on the entire whole-brain data. All nuisance variables entered the model as first and all but the PCA components also as second order terms, as previously described by Behzadi et al. [25] and shown by Chai et al. [26] to increase specificity and sensitivity of the analyses. Data was then band pass filtered preserving frequencies between 0.01 and 0.08 Hz [27,28]. The time course of each ROI was then expressed as the first eigenvariate of the processed time series of all voxels associated with that region. A recent study showed that this method is able to detect valid correlation and anti-correlations during rest, which are not an artefact of the preprocessing method, but may reflect valid biological signals [29]. Moreover, it should be emphasized, that the current analysis focussed on differences between the two groups of subjects, which should not be affected by potentially confounds induced by preprocessing steps, even if these were to be present, as long as they do not systematically vary in effect between groups.

Data analysis

For each subject we computed linear (Pearson) correlation coefficients between the time series of the seeds and any other grey matter voxel, which were then transformed into Fisher's Z-scores. Group analysis was then performed on these by an analysis of variance (ANOVA) across subjects using appropriate non-sphericity correction. In the ANOVA, both the main effect of functional connectivity as well as the group-difference between patients and controls were modelled for each seed. Inference on this random-effects analysis was then sought using linear contrasts. First, main effects of connectivity (across both groups) were calculated for both seeds and a conjunction analysis was

performed on these to reveal regions showing significant coupling. Subsequently, functional connectivity maps of rIFG and ISTG were assessed for significant differences between patients and controls using unilateral T-tests. These differences in connectivity were evaluated by testing for either significant *positive* coupling across both groups (main effect) in conjunction with a *reduced* coupling in patients or significant *negative* coupling across both groups (main effect) in conjunction with *enhanced* coupling in patients as compared to controls indicating enhanced and reduced coupling. For all analyses, results were regarded as significant if they passed $p < 0.05$, cluster-level FDR-corrected for multiple comparisons. Anatomical localizations were obtained using the SPM Anatomy Toolbox [30].

Statistical analyses

To test whether the observed differences between patients and controls were additionally related to psychopathology, we extracted individual functional connectivity between the seeds and the peak voxels of the clusters showing significant differences. We then performed a Spearman rank-correlation between these and the individual scores on the “Hallucinatory behaviour” (P3) PANSS item to test for significant ($p < 0.05$) associations. In a second follow-up analysis we divided the patients into those who actually experienced hallucinations during the scan and those who did not. Subsequently, we computed a one-way ANOVA between the groups on the individual functional connectivity scores between the seed and the peak of a significant cluster.

Results

All participants stayed awake during the resting state scan. Thirty-one out of the 49 patients reported the experience of hallucinations during the resting state scan. None of the controls experienced hallucinations during the scan.

The analysis of the main effects for both seeds across both groups is provided in Supplementary Material S1. When resting state connectivity was compared between the patients and the controls, the following differences emerged.

Increased connectivity

The right parahippocampal gyrus showed significantly increased connectivity with the rIFG (Figure 1) in the patient group.

Decreased connectivity

Reduced connectivity with the rIFG in the patients was found for the right dorsolateral prefrontal cortex (DLPFC) just anterior to and slightly encroaching cytoarchitectonically defined Area 45 (Figure 2).

Two regions showed significantly (whole-brain corrected) reduced connectivity to the ISTG in patients (Figure 3). The first was located on the left frontal operculum, extending into the anterior insula areas as well as the parietal opercular areas OP 3 and OP 4. The second was located in the left hippocampus, allocated predominantly to the subiculum and to a smaller extent the entorhinal cortex. Connectivity between the ISTG and the left hippocampus was not only reduced in patients but furthermore showed a significant negative correlation with the item P3 (hallucinations) of the PANSS rating scale.

In order to assess state-effects of AVH on functional connectivity with our seed regions, we performed a follow-up analysis for those regions that showed disturbed connectivity in the overall group of trait carriers (i.e., the regions reported above) which assessed differences between controls, trait and state/trait-groups, i.e. individuals with acute AVH during scanning. For this purpose,

Table 2. Areas used for seed regions.

Lobe	Area	MNI Coordinates			T-value	Cluster size
R Frontal	Inferior Frontal gyrus	44	16	12	4.31	243
L Temporal	Superior Temporal gyrus	-48	0	0	3.46	40

T-values, cluster sizes and locations of local maxima of activation during AVH in 24 patients, taken from Diederer et al. 2011. Threshold set at $p < 0.05$ whole-brain FDR corrected.

doi:10.1371/journal.pone.0043516.t002

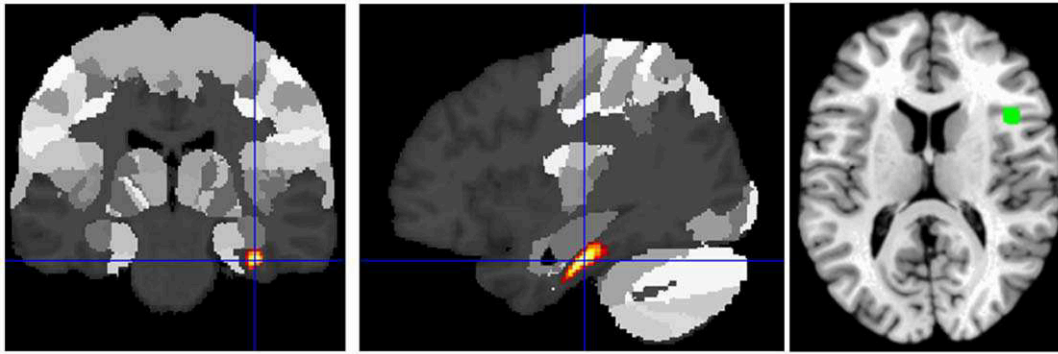


Figure 1. Increased connectivity with rIFG in patients as compared to controls. Increased connectivity with rIFG in patients as compared to controls was found in the right parahippocampal gyrus ($p < 0.05$ cluster-level FDR-corrected). doi:10.1371/journal.pone.0043516.g001

we divided the patients into one group who hallucinated during the resting state scan, and those who did not. This analysis revealed that the reduction in connectivity between the ISTG and the left hippocampus was significantly stronger in those patients who hallucinated during scanning (Figure 4). That is, in these regions both trait (as demonstrated by the lower connectivity in non-acutely hallucinating patients compared to controls) and state-effects (as evidenced by the further reduction in the acutely hallucinating patients) were evident. For the remaining regions, including those showing abnormal connectivity with the rIFG, no differences were found between acutely hallucinating patients and those showing merely the trait to experience AVH.

Discussion

We compared resting state functional connectivity of 49 psychotic patients experiencing chronic auditory verbal hallucinations (AVH) to 49 healthy controls. Analysis was seeded from the left superior temporal gyrus (ISTG) and the right inferior frontal gyrus (rIFG) as these areas are consistently activated during the state of AVH [5,21] and are therefore expected to play a crucial role in AVH. In patients, the rIFG showed increased connectivity with the right parahippocampal gyrus and decreased connectivity with the right dorsolateral prefrontal cortex (DLPFC). Decreased connectivity with the ISTG in patients was revealed in the left frontal operculum and the left temporo-parietal operculum. Both opercular areas are considered part of the general neuronal frame work for language [28]. Furthermore, the ISTG

showed decreased connectivity with the left hippocampus, this connectivity correlated significantly with the severity of hallucinations as measured in the PANSS interview.

To differentiate between trait and state aspects of AVH we divided the patient group into those who acutely hallucinated during scanning and those who did not. Here, only coupling of the ISTG with the left temporo-parietal operculum and hippocampus was more strongly decreased in the patients who actually hallucinated, indicating that these deviations may result from a combination of state and trait characteristics. Increased connectivity between the rIFG and the parahippocampus was equally strong in both patient groups.

Dys-connectivity with the medial temporal lobe

Our analysis revealed disturbed interactions between both seeds and medial temporal lobe (MTL) structures, including increased connectivity between the rIFG and the right parahippocampal gyrus. This observation resonates strongly with a previous symptom capture study which revealed that cortical activations during AVH were preceded by significant signal changes in the parahippocampal gyrus [5]. The MTL structures, especially the hippocampus [31], play important roles in both the consolidation and the retrieval of memories. This latter function may be involved in hallucinations, as hallucinations may be triggered by inappropriate recollections from memory. The parahippocampal gyri have a gatekeeper function as they integrate and transfer information from neocortical association areas to the hippocampus [32]. When this delicate interplay becomes deranged by aberrant connectivity, incidental information from memory may be recollected, giving rise to hallucinations [33]. The finding of both increased and decreased coupling between neocortical and MTL regions represents an important notion about the differentiated organization of the MTL and its interactions, challenging simple notions of “more” or “less integration”. Rather, deregulation of the usually well-balanced interactions between hippocampus, parahippocampal gyrus and neocortical association areas may represent a crucial pathomechanism for hallucinations. Since the hippocampus and parahippocampus regulate retrieval of memories in all modalities, we expect that deregulation between MTL and cortical association areas constitutes a predisposition to hallucinations in general and not specifically for hallucinations in the auditory verbal domain. Indeed, most of these patients who experience chronic AVH also experienced hallucinations in other modalities and can thus be expected prone to hallucinations in general.

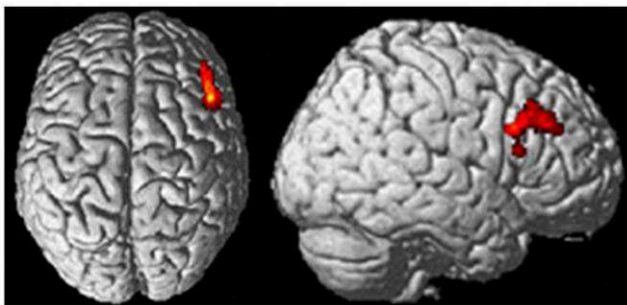


Figure 2. Reduced connectivity with rIFG in patients as compared to controls. Reduced connectivity with rIFG in patients as compared to controls was found in the right DLPFC/area 45 ($p < 0.05$ cluster-level FDR-corrected). doi:10.1371/journal.pone.0043516.g002

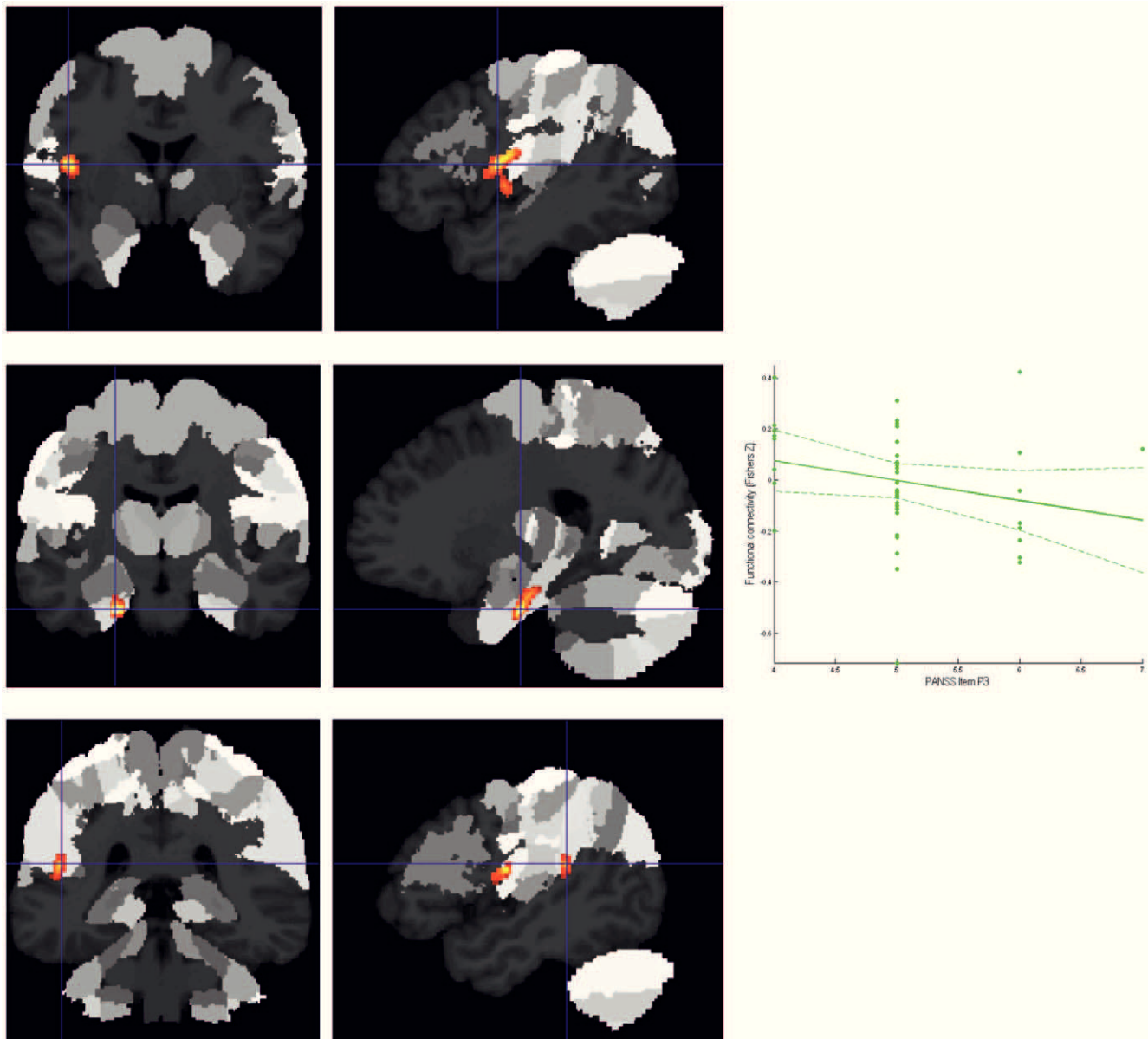


Figure 3. Decreased connectivity to ISTG in patients as compared to controls. A. Cluster of significantly ($p < 0.05$ corrected) decreased connectivity with the ISTG in patients in the left frontal operculum/anterior insula shown on the MPM of the SPM Anatomy Toolbox. **B.** Cluster of significantly ($p < 0.05$ corrected) decreased connectivity with the ISTG in patients in the left hippocampus (subiculum/entorhinal cortex) shown on the MPM of the SPM Anatomy Toolbox. **C.** Cluster of decreased connectivity (as a strong statistical trend) with the ISTG in patients in the left temporo-parietal operculum/retroinsular cortex. doi:10.1371/journal.pone.0043516.g003

Dysconnectivity within the neocortical areas

Secondly, decreased connectivity in the patient group between the ISTG and the left frontal operculum was observed. We also found decreased connectivity between the rIFG and the right DLPFC. These findings may reflect decreased integration between areas mainly associated with the generation (rIFG) and interpretation (ISTG) of language, suggesting misattribution of inner speech as a potential pathomechanism. Furthermore, these regions are often found active during acute hallucinations [5,21]. Mechanistically, such misattribution may be well reconciled with decreased connectivity by the notion of aberrant corollary discharge [34] failing to suppress the sensory consequences of self-generated actions. A possible mechanism would be that

insufficient corollary discharge in the language system as reflected by decreased functional connectivity could result from microstructural alterations in the arcuate fasciculi, the most important fibre bundle between Broca's area and Wernicke's area [35] as observed by de Weijer and co-workers [12,13]. Flaws or disintegration in the corollary discharge system of language networks may be specifically related to the attribution of internally generated speech to an external origin, which posed a predisposition specifically to hallucinate in the auditory verbal domain.

Comparison to previous functional connectivity studies

Seeding from Wernicke's area (in close vicinity to our ISTG seed), Hoffman and colleagues [36] found increased connectivity

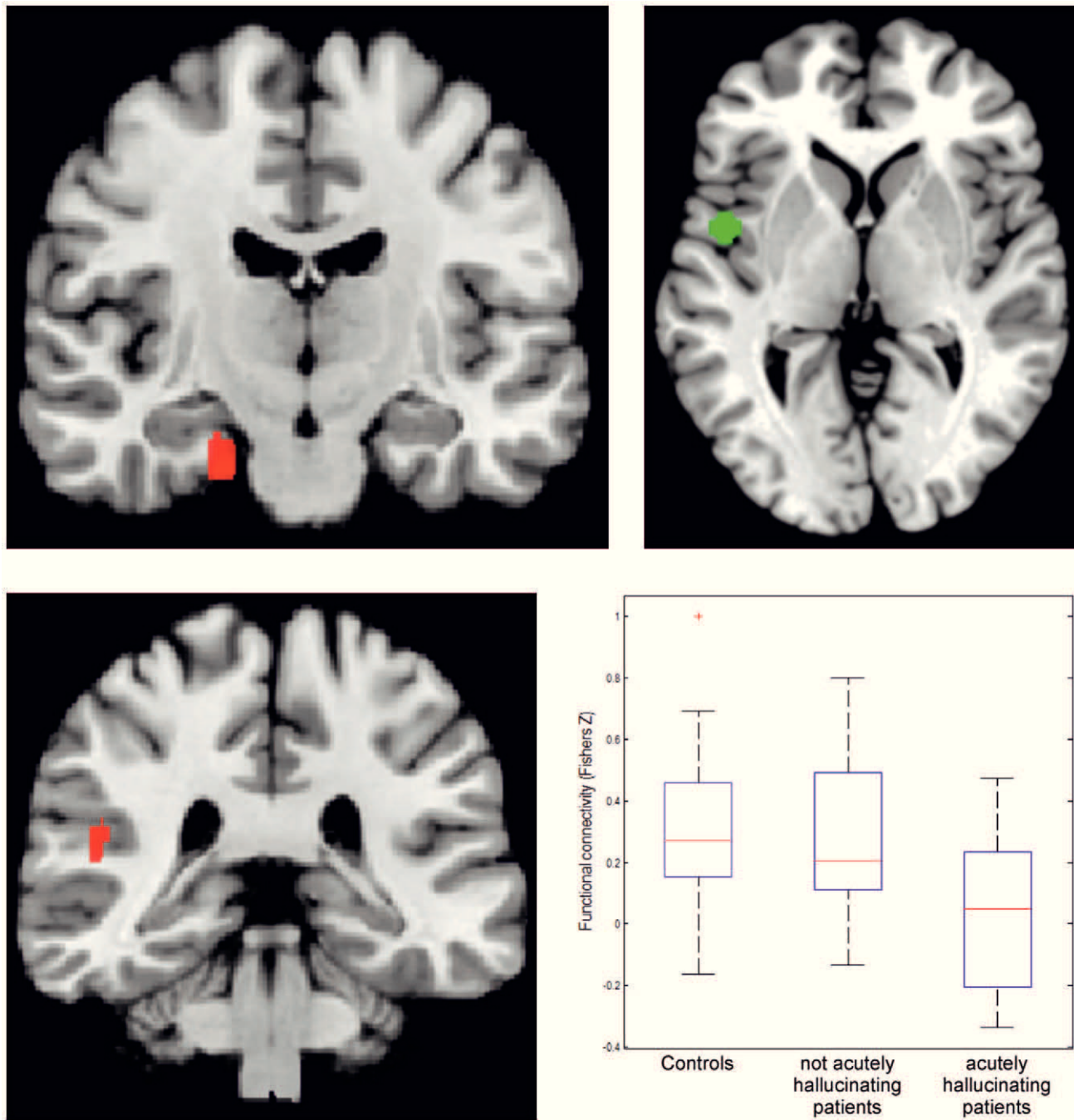


Figure 4. Differences in connectivity with ISTG, specified for patients who hallucinated during the scans and those who did not. A. Aberrations in functional connectivity between ISTG and the left entorhinal cortex gyrus differentiate between healthy controls. Separate findings are shown for patients showing the AVH trait and those acutely experiencing AHV (state). **B.** Aberrations in functional connectivity between ISTG and the left temporo-parietal operculum/retroinsular cortex differentiate between healthy controls. Separate findings are shown for the patients showing the AVH trait and those patients acutely experiencing AHV during the scan (state). The red crosses in these box plots represent data points outside 1.5 * IQR, i.e. outliers.
doi:10.1371/journal.pone.0043516.g004

in schizophrenia patients with a large subcortical cluster including the thalamus, midbrain and putamen, which is supported by the more localized findings of increased connectivity with the parahippocampal gyrus in the present analysis. Vercammen et al. [37] observed reduced functional connectivity between the left temporo-parietal junction and the right homologue of Broca's area in patients, while Gavrilescu et al. [38] demonstrated reduced

connectivity of the bilateral auditory system. These studies thus point to decreased connectivity within the network of language-related areas in patients with AVH, a finding that was confirmed and extended in the present study. Rotarska-Jagiela et al. [39] found that the severity of positive symptoms correlated with functional connectivity of fronto-temporal and auditory networks in schizophrenia patients using an independent component

analysis (ICA). In spite of the different approach taken in the present analysis, we could add evidence for the trait-specific aspect of this finding. We thus conclude that the present work is well in line with previous evidence but may provide more specific insights into disturbed circuits by seeding from areas shown to be engaged in AVH, separating state- and trait-dependent dysconnectivity and assessing the association between disturbed coupling and the severity of clinical symptoms.

Limitations and technical considerations

A limitation of this study is the absence of a patient group without the trait to hallucinate. However, to our opinion, all patients with schizophrenia have a predisposition to hallucinate given their psychotic liability. The fact that a small proportion of schizophrenia patients have not experienced hallucinations may reflect adequate pharmacotherapy, rather than an absence of the trait.

The current approach of assessing functional connectivity of regions that have previously been implicated in the pathophysiology of hallucinations allowed for a model-based assessment of dysfunctional circuitry in patients suffering from AVH. This may represent a considerable advantage in terms of functional specificity as compared to purely data-driven approaches such as ICA, as ICA would also identify other differences between the groups unrelated to AVH. In turn, however, analyses based on a-priori information evidently have low sensitivity to aberrations in non-probed circuits.

The removal of noise from resting-state fMRI data as part of the preprocessing has been criticized because this process can introduce artificial anti-correlations [40,41,42]. However, component based methods such as PCA have been shown to be less susceptible to this effect while effectively reducing spurious correlations caused by noise [43,44].

It must also be acknowledged, that the observed differences may not be absolutely specific to hallucinations, as patients and controls also differed in variables such as the presence of other psychotic symptoms, negative symptoms and medication status. While all these factors may have influenced connectivity patterns, the specific, localized aberrations of connectivity with areas activated during AVH should point to a pathophysiological contribution. This is in particular the case for those connections showing a

significant state effect or an association with the severity of hallucinations as assessed with the PANSS rating.

In sum, we found two clear deviations in resting state connectivity in the patients with chronic AVH as compared to the controls. The first was aberrant connectivity between the seed regions that are active during AVH and MTL structures which have a prominent role in memory retrieval. The second deviation was decreased connectivity between language-related areas in the neocortex.

Aberrations between neocortical association areas and MTL structures may underlie a liability to experience hallucinations in general. In turn, reduced connectivity within the neocortical language network may indicate deficits in corollary discharge mechanisms as another potentially important pathophysiological mechanism for hallucination in the language domain specifically.

Supporting Information

Supplementary Material S1 The analysis of the main effects for both seeds across both groups. The analysis of the main effects for both seeds across both groups demonstrated significant positive coupling between both seed regions with (in particular the left) inferior frontal lobes and anterior insula, dorso-lateral prefrontal cortex, inferior parietal lobules, right anterior temporal lobe and the posterior medial frontal cortex. In turn, both regions were significantly anti-correlated with anterior and posterior cingulate regions, the precuneus, right posterior inferior parietal lobule, bilateral inferior temporal lobe and right cerebellum. Positive coupling, i.e., functional connectivity, with the seeds is shown in green, negative coupling in red. Significantly decreased connectivity with the seeds in patients is superimposed on the main effect in cyan, significantly increased connectivity in patients is superimposed on the main effect in yellow below (all effects significant at $p < 0.05$ cluster-level FDR-corrected). (TIF)

Author Contributions

Conceived and designed the experiments: IS SE. Performed the experiments: MC AM KD. Analyzed the data: MC. Contributed reagents/materials/analysis tools: KD IS. Wrote the paper: IS SE. Helped to gather nd: AM. Analysed the data: AM. Helped with the design of the study: AM. Helped with the writing of the study: AM.

References

- Allen P, Aleman A, McGuire PK (2007) Int Rev Psychiatry. 2007 Aug;19(4):407–15.
- Waters F, Woodward T, Allen P, Aleman A, Sommer I (2010) Self-recognition Deficits in Schizophrenia Patients With Auditory Hallucinations: A Meta-analysis of the Literature. *Schizophr Bull* doi: 10.1093/schbul/sbq144
- Vercammen A, Aleman A (2010) Semantic expectations can induce false perceptions in hallucination-prone individuals. *Schizophr Bull* 36: 151–156.
- Copolov DL, Seal ML, Maruff P, Uluosoy R, Wong MTH, et al. (2003) Cortical activation associated with the experience of auditory hallucinations and perception of human speech in schizophrenia: a PET correlation study. *Psychiatry Res* 122: 139–152.
- Diederer KM, Neggess SF, Daalman K, Blom JD, Goekoop R, et al. (2010) Deactivation of the parahippocampal gyrus preceding auditory hallucinations in schizophrenia. *Am J Psychiatry* 167: 427–735.
- Hunter MD, Eickhoff SB, Pheasant RJ, Douglas MJ, Watts GR, et al. (2010) The state of tranquility: Subjective perception is shaped by contextual modulation of auditory connectivity. *Neuro Image* 53: 611–618.
- Hunter MD, Eickhoff SB, Miller TW, Farrow TF, Wilkinson ID, et al. (2006) Neural activity in speech-sensitive auditory cortex during silence. *Proc Natl Acad Sci USA* 103: 189–194.
- Sommer IE, Weijer de AD, Daalman K, Neggess SF, Somers M, et al. (2007) Can fMRI-guidance improve the efficacy of rTMS treatment for auditory verbal hallucinations? *Schizophr Res* 93: 406–408.
- Sommer IE, Diederer KM, Blom JD, Willems A, Kushan L, et al. (2008) Auditory verbal hallucinations predominantly activate the right inferior frontal area. *Brain* 131: 3169–3177.
- Hoffman RE, Anderson AW, Varanko M, Gore JC, Hampson M (2008) Time course of regional brain activation associated with onset of auditory/verbal hallucinations. *Br J Psychiatry* 193: 424–425.
- Northoff G, Qin P (2011) How can the brain's resting state activity generate hallucinations? A 'resting state hypothesis' of auditory verbal hallucinations. *Schizophr Res* 127: 202–214.
- Weijer de AD, Neggess SF, Daalman K, Kahn RS, Sommer IE (2011) Microstructural alterations of the arcuate fasciculus in schizophrenia patients with frequent auditory verbal hallucinations. *Schizophr Res* 130: 68–77.
- Weijer de AD, Neggess SF, Diederer KM, Mandl RCW, Kahn RS, et al. (2011) Aberrations in the arcuate fasciculus in psychotic and non-psychotic individuals with auditory verbal hallucinations. *Human Brain Mapping* doi: 10.1002/hbm.21463
- Bandettini PA, Bullmore E (2008) Endogenous oscillations and networks in functional magnetic resonance imaging. *Human Brain Mapping* 29: 737–739.
- Sommer IE, Selten JP, Diederer KM, Blom JD (2010) Dissecting auditory verbal hallucinations into two components: audibility (Gedankenlautwerden) and alienation (thought insertion). *Psychopathology* 43(2):137–40.
- Andreasen NC, Flaum M, Arndt S (1992) The comprehensive assessment of symptoms and history (CASH): An instrument for assessing psychopathology and diagnosis. *Arch Gen Psychiatry* 49: 615–623.
- Kay S, Fiszbein A, Opler L (1987) The positive and negative syndrome scale (PANSS) for schizophrenia. *Schizophrenia Bulletin* 13: 261–276.
- Neggess SF, Hermans EJ, Ramsey NF (2008) Enhanced sensitivity with fast three-dimensional blood-oxygen-level-dependent functional MRI: comparison of SENSE-PRESTO and 2D-EPI at 3 T. *NMR Biomed* 21: 663–676.

19. Holmes CJ, Hoge R, Collins L, Woods R, Toga AW, et al. (1998) Enhancement of MR images using registration for signal averaging. *J Comput Assist Tomogr* 22: 324–333.
20. Ashburner J, Friston KJ (2005) Unified segmentation. *Neuroimage* 26: 839–851.
21. Jardri R, Pouchet A, Pins D, Thomas P (2011) Cortical activations during auditory verbal hallucinations in schizophrenia: a coordinate-based meta-analysis. *Am J Psychiatry* 168: 73–81.
22. Fox MD, Zhang D, Snyder AZ, Raichle ME (2009) The global signal and observed anticorrelated resting state brain networks. *J of Neurophysiology* 101: 3270–3283.
23. Weissenbacher A, Kasess C, Gerstl F, Lanzenberger R, Moser E, et al. (2009) Correlations and anticorrelations in resting-state functional connectivity MRI: A quantitative comparison of preprocessing strategies. *Neuro Image* 47: 1408–1416.
24. Eickhoff SB, Bzdok D, Laird AR, Roski C, Caspers S, et al. (2011) Co-activation patterns distinguish cortical modules, their connectivity and functional differentiation. *Neuro Image* 57: 938–949.
25. Behzadi Y, Restom K, Liau J, Liu TT (2007) A component based noise correction method (CompCor) for BOLD and perfusion based fMRI. *Neuroimage* 37: 90–101.
26. Chai XJ, Castañón AN, Ongür D, Whitfield-Gabrieli S (2011) Anticorrelations in resting-state networks without global signal regression. *Neuroimage* 29: 1420–1428.
27. Biswal B, Yetkin FZ, Haughton VM, Hyde JS (1995) Functional connectivity in the motor cortex of resting human brain using echo-planar MRI. *Magn Reson Med* 34: 537–541.
28. Greicius MD, Krasnow B, Reiss AL, Menon V (2003) Functional connectivity in the resting brain: a network analysis of the default mode hypothesis. *Proc Natl Acad Sci USA* 100: 253–258.
29. Murphy K, Birn RM, Handwerker DA, Jones TB, Bandettini PA (2009) The impact of global signal regression on resting state correlations: Are anti-correlated networks introduced? *Neuro Image* 44: 893–905.
30. Eickhoff SB, Paus T, Caspers S, Grosbras MH, Evans AC, et al. (2007) Assignment of functional activations to probabilistic cytoarchitectonic areas revisited. *Neuro Image* 36: 511–521.
31. Bartsch T, Döhning J, Rohr A, Jansen O, Deuschl G (2011) CA1 neurons in the human hippocampus are critical for autobiographical memory, mental time travel, and autoegetic consciousness. *Proc Natl Acad Sci USA* 108: 17562–17567.
32. Bauer EP, Paz R, Paré D (2007) Gamma oscillations coordinate amygdalorhinal interactions during learning. *J Neurosci* 27: 9369–9379.
33. Badcock JC, Waters FA, Maybery MT, Michie PT (2005) Auditory hallucinations: failure to inhibit irrelevant memories. *Cogn Neuropsychiatry* 10: 125–36.
34. Ford JM, Mathalon DH (2005) Corollary discharge dysfunction in schizophrenia: can it explain auditory hallucinations? *Int J Psychophysiol* 58: 179–189.
35. Lichtheim L (1885) On Aphasia. *Brain* 7: 433–484.
36. Hoffman RE, Fernandez T, Pittman B, Hampson M (2011) Elevated functional connectivity along a corticostriatal loop and the mechanism of auditory/verbal hallucinations in patients with schizophrenia. *Biol Psychiatry* 69: 407–414.
37. Vercammen A, Knegeter H, den Boer JA, Liemburg EJ, Aleman A (2010) Auditory hallucinations in schizophrenia are associated with reduced functional connectivity of the temporo-parietal area. *Biol Psychiatry* 67: 912–918.
38. Gavrilescu M, Rossell S, Stuart GW, Shea TL, Innes-Brown H, et al. (2010) Reduced connectivity of the auditory cortex in patients with auditory hallucinations: a resting state functional magnetic resonance imaging study. *Psychol Med* 40: 1149–1158.
39. Rotarska-Jagiela A, van de Ven V, Oertel-Knöchel V, Uhlhaas PJ, Vogeley K, et al. (2010) Resting-state functional network correlates of psychotic symptoms in schizophrenia. *Schizophr Res* 117: 21–30.
40. Saad ZS, Gotts SJ, Murphy K, Chen G, Jo HJ, et al. (2012) Trouble at rest: how correlation patterns and group differences become distorted after global signal regression. *Brain Connect* 2(1):25–32.
41. Bellec P, Perlberg V, Jbabdi S, Pelegrini-Issac M, Anton JL, et al. (2006) Identification of large-scale networks in the brain using fMRI. *Neuroimage* 29, 1231–1243.
42. Birn RM, Diamond JB, Smith MA, Bandettini PA (2006) Separating respiratory-variation-related fluctuations from neuronal-activity-related fluctuations in fMRI. *Neuroimage* 31(4):1536–48.
43. Weissenbacher A, Kasess C, Gerstl F, Lanzenberger R, Moser E, et al. (2009) Correlations and anticorrelations in resting-state functional connectivity MRI: A quantitative comparison of preprocessing strategies. *Neuroimage* 47(4):1408–16.
44. Lohmann G, Hoehl S, Brauer J, Danielmeier C, Bornkessel-Schlesewsky I, et al. (2010) Setting the frame: the human brain activates a basic low-frequency network for language processing. *Cereb Cortex* 20: 1286–1292.

SUPPLEMENTAL FIGURE

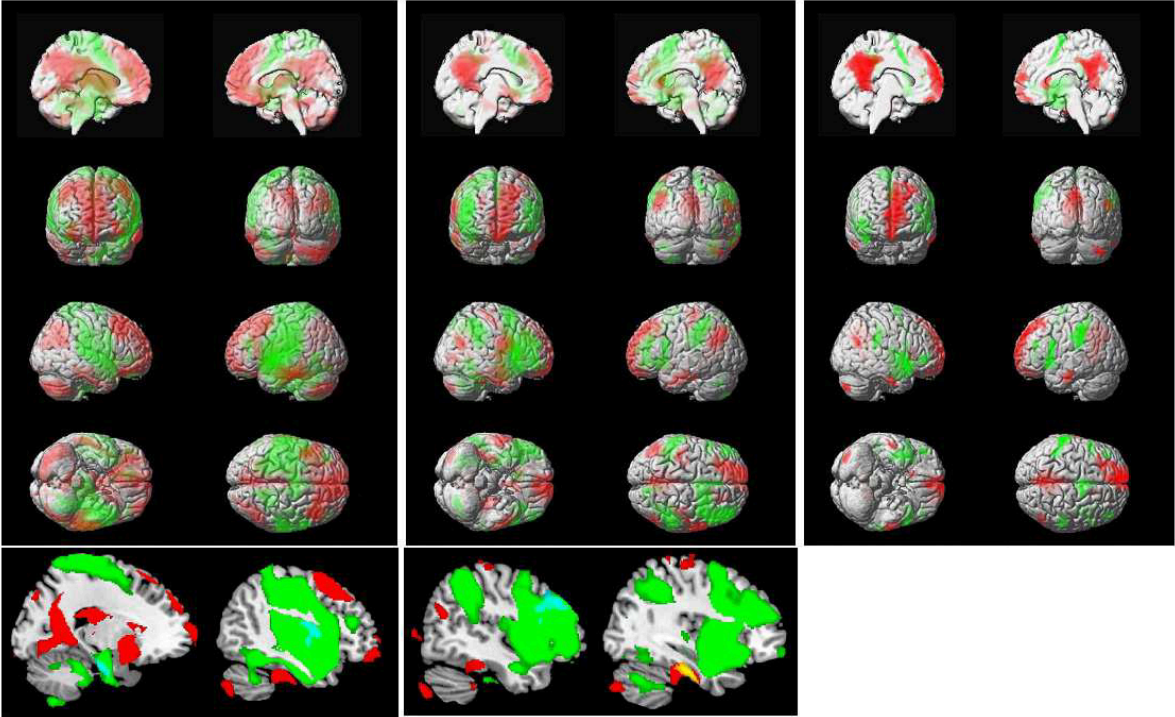


Figure S1
Main effect of functional connectivity for ISTG (left), rIFG (middle) and their conjunction (right) across all subjects. Positive coupling, i.e., functional connectivity, with the seeds is shown in green, negative coupling in red. Significantly decreased connectivity with the seeds in patients is superimposed on the main effect in cyan, significantly increased connectivity in patients is superimposed on the main effect in yellow below (all effects significant at $p < 0.05$ cluster-level FDR-corrected)

STUDY 5

Aberrant resting-state connectivity in non-psychotic individuals with auditory hallucinations

Kelly M. J. Diederer¹, Sebastiaan F. W. Neggers¹, Antoin D. de Weijer¹, Remko van Lutteveld¹, Kirstin Daalman¹, Simon B. Eickhoff^{2,3,4}, Mareike Clos², Rene S. Kahn¹, Iris E. Sommer¹

¹Neuroscience Division, University Medical Center Utrecht & Rudolf Magnus Institute for Neuroscience, The Netherlands

²Institute of Neuroscience and Medicine (INM-1; INM-2), Research Center Jülich, Germany

³Department of Psychiatry, Psychotherapy, and Psychosomatics, Medical School, RWTH Aachen University, Germany

⁴Institute of Clinical Neuroscience and Medical Psychology, Heinrich Heine University, Düsseldorf, Germany

Psychological Medicine (2013) 43(8): 1685-1696

doi:10.1017/S0033291712002541

Impact factor (2011): 6.159

Own contributions

Statistical data analysis

Discussion of results

Correcting the paper

Total contribution: 10%

Aberrant resting-state connectivity in non-psychotic individuals with auditory hallucinations

K. M. J. Dieren^{1*}, S. F. W. Neggers¹, A. D. de Weijer¹, R. van Lutterveld¹, K. Daalman¹,
S. B. Eickhoff^{2,3,4}, M. Cios², R. S. Kahn¹ and I. E. C. Sommer¹

¹ Neuroscience Division, University Medical Centre Utrecht and Rudolf Magnus Institute for Neuroscience, Utrecht, The Netherlands

² Institute of Neuroscience and Medicine (INM-1, INM-2), Research Centre Jülich, Germany

³ Department of Psychiatry, Psychotherapy, and Psychosomatics, Medical School, RWTH Aachen University, Germany

⁴ Institute for Clinical Neuroscience and Medical Psychology, Heinrich-Heine University, Düsseldorf, Germany

Background. Although auditory verbal hallucinations (AVH) are a core symptom of schizophrenia, they also occur in non-psychotic individuals, in the absence of other psychotic, affective, cognitive and negative symptoms. AVH have been hypothesized to result from deviant integration of inferior frontal, parahippocampal and superior temporal brain areas. However, a direct link between dysfunctional connectivity and AVH has not yet been established. To determine whether hallucinations are indeed related to aberrant connectivity, AVH should be studied in isolation, for example in non-psychotic individuals with AVH.

Method. Resting-state connectivity was investigated in 25 non-psychotic subjects with AVH and 25 matched control subjects using seed regression analysis with the (1) left and (2) right inferior frontal, (3) left and (4) right superior temporal and (5) left parahippocampal areas as the seed regions. To correct for cardiorespiratory (CR) pulsatility rhythms in the functional magnetic resonance imaging (fMRI) data, heartbeat and respiration were monitored during scanning and the fMRI data were corrected for these rhythms using the image-based method for retrospective correction of physiological motion effects RETROICOR.

Results. In comparison with the control group, non-psychotic individuals with AVH showed increased connectivity between the left and the right superior temporal regions and also between the left parahippocampal region and the left inferior frontal gyrus. Moreover, this group did not show a negative correlation between the left superior temporal region and the right inferior frontal region, as was observed in the healthy control group.

Conclusions. Aberrant connectivity of frontal, parahippocampal and superior temporal brain areas can be specifically related to the predisposition to hallucinate in the auditory domain.

Received 6 January 2012; Revised 5 October 2012; Accepted 8 October 2012; First published online 16 November 2012

Key words: Functional connectivity, functional magnetic resonance imaging, hallucinations, language, memory, psychosis, schizophrenia.

Introduction

Auditory verbal hallucinations (AVH) can be observed in several psychiatric disorders including schizophrenia, psychotic depression, psychotic mania and borderline personality disorder and also in non-psychotic subjects in the general population (Aleman & Laroi, 2008). Patients typically experience AVH as highly distressing, decreasing their quality of life (Daalman *et al.* 2011). Moreover, these hallucinations are refractory to pharmacological treatment in 25–30% of patients, stressing the need for development of new

treatment options (Shergill *et al.* 1998). This is, however, hampered by the fact that the pathophysiology of AVH is only partly known.

Over the past decades numerous studies have investigated brain activation during AVH as a first step to elucidating the neurobiological origin of this symptom. These studies revealed AVH-related activation in inferior frontal, parahippocampal and temporoparietal regions comprising the inferior frontal gyri, insula, pre- and postcentral gyri, frontal and parietal operculum, middle and superior temporal gyri, inferior parietal lobule and hippocampus/parahippocampal region (Sommer *et al.* 2008b; Jardri *et al.* 2010; Kuhn & Gallinat, 2010; Dieren *et al.* 2011, 2012). Involvement of these areas presumably reflects the role of language and memory processes in the experience of AVH. However, these studies do not

* Address for correspondence: K. M. J. Dieren, Ph.D., Department of Physiology, Development and Neuroscience, University of Cambridge, Downing Place, Cambridge CB2 3DY, UK. (Email: kmjd2@cam.ac.uk)

provide information about the brain mechanisms that predispose a person to experience AVH. Such a pathogenic mechanism has been hypothesized to consist of dysfunctional connectivity between frontal and superior temporal regions involved in the production and perception of language (Frith *et al.* 1995; McGuire & Frith, 1996; Spence *et al.* 2000; Allen *et al.* 2007; Ford *et al.* 2007; Heinks-Maldonado *et al.* 2007; Shergill *et al.* 2007). Alternatively, AVH could result from the re-experience of verbal memories, which may be instantiated by aberrant connectivity of cortical association areas and the parahippocampal gyrus (Copolov *et al.* 2003; Diederer *et al.* 2010*b*).

Studies have addressed these hypotheses by investigating functional connectivity in patients suffering from AVH during a task-free 'resting' state because aberrations in connectivity may be specifically present in the absence of external tasks (Gavrilescu *et al.* 2010; Hoffman *et al.* 2010; Rotarska-Jagiela *et al.* 2010; Vercammen *et al.* 2010; Liemburg *et al.* 2012). Altered integration of frontal and superior temporal regions, and also subcortical regions, was indeed observed in schizophrenia patients with AVH (Gavrilescu *et al.* 2010; Hoffman *et al.* 2010; Rotarska-Jagiela *et al.* 2010; Vercammen *et al.* 2010; Liemburg *et al.* 2012). However, the results of these studies are inconsistent as some found reduced connectivity (Gavrilescu *et al.* 2010; Rotarska-Jagiela *et al.* 2010; Vercammen *et al.* 2010) whereas others reported increased connectivity (Hoffman *et al.* 2010), or found both increases and decreases in connectivity (Liemburg *et al.* 2012; Sommer *et al.* 2012). Moreover, the exact loci of aberrant connectivity varied among studies.

This discrepancy could result from the fact that previous studies did not correct for cardiorespiratory (CR) processes, which may have led to artificially increased correlation strengths (Noll & Schneider, 1994; Glover & Lee, 1995; Dagli *et al.* 1999; Birn *et al.* 2006). Moreover, the mere presence of AVH episodes during scanning could have influenced the results as most studies did not exclude patients with active AVH, or did not report if AVH were present during scanning (Hoffman *et al.* 2010; Rotarska-Jagiela *et al.* 2010; Vercammen *et al.* 2010). This is of particular importance as increased connectivity within the hallucination network could arise from simultaneous AVH-induced activation of brain regions implicated in AVH. Finally, previous investigations included patients with schizophrenia who presented with other symptoms, such as delusions, affective and negative symptoms, and were treated with antipsychotic medication (Honey *et al.* 1999).

To determine whether AVH are indeed related to dysfunctional connectivity, these hallucinations

should be studied in isolation. Of note, previous studies have shown that AVH in the non-clinical population frequently occur in the absence of other psychiatric symptoms (Tien, 1991; Sommer *et al.* 2008*a*). AVH in these individuals are phenomenologically somewhat different from AVH in psychotic patients as the first group typically experiences AVH with a neutral to positive content, experiences AVH less frequently, has some control over the voices and started hearing them at a younger age (Daalman *et al.* 2011). Of these characteristics, negative emotional content of the voices seemed to be an important feature for diagnosing a psychotic disorder as this characteristic could accurately predict the presence of a psychotic disorder in 88% of the participants. Other aspects of the AVH, such as the perceived location of the voices, the number of voices, loudness and personification, were similar for both groups.

These non-psychotic individuals display similar AVH-related brain activation as psychotic patients, suggesting the same neurobiological mechanism (Diederer *et al.* 2011). Consequently, these individuals provide an ideal opportunity to investigate a more isolated form of AVH. A major advantage is that these subjects do not use psychoactive medication (Sommer *et al.* 2008*a*).

The present study investigated resting-state connectivity in 25 non-psychotic individuals with AVH. As AVH were hypothesized to result from aberrant integration of frontal, parahippocampal and superior temporal regions, these areas provided the starting point for investigating resting-state connectivity. Bilateral frontal and superior temporal regions of interest (ROIs) were defined by the location of AVH-related activation in a separate group of non-psychotic individuals (Diederer *et al.* 2011). The parahippocampal region was based on a previous study by our group in which it was shown that AVH are preceded by consistent deactivation of this area (Diederer *et al.* 2010*b*).

Heartbeat and respiration were monitored during scanning to allow for corrections of CR rhythms. To circumvent the influence of 'active' AVH episodes, individuals experiencing AVH during scanning were excluded from analyses. Connectivity of memory and language areas was hypothesized to be aberrant (i.e. either increased or decreased), as both increases and decreases in resting-state connectivity were observed in previous studies.

Method

Subjects

Thirty-seven non-psychotic individuals with AVH and 44 healthy control subjects were recruited through

a website: www.verkenuwgeest.nl ('explore your mind'). An extended description of the recruitment and selection procedure is provided in prior studies by our group (Sommer *et al.* 2008a; Diederens *et al.* 2010a, 2011; van Lutterveld *et al.* 2010; Daalman *et al.* 2011). In brief, inclusion criteria were: (1) the absence of any Axis I psychiatric disorder other than anxiety or depressive disorder in full remission, as assessed by a psychiatrist using the Comprehensive Assessment of Symptoms and History (CASH; Andreasen *et al.* 1992); (2) no chronic somatic disorder; and (3) no alcohol or drug abuse for at least 3 months prior to the assessments. To confirm the absence of drug abuse, urine samples were collected and tested for opiates, amphetamines/ecstasy, cocaine and cannabis. Additional inclusion criteria for the non-psychotic individuals with AVH comprised the following: (4) voices were distinct from thoughts and had a perceptual quality; (5) voices occurred at least once a week; (6) drug or alcohol abuse did not precede the first experience of AVH; and (7) an absence of AVH during the resting-state scan. All participants were required to complete the Schizotypal Personality Questionnaire (SPQ; Raine, 1991).

Although the hallucinating subjects experienced little discomfort from their AVH, the absence of a major psychiatric diagnosis in these individuals can be disputed. If strict DSM-IV criteria for Axis I were applied, all subjects with AVH would meet criteria for psychosis not otherwise specified (NOS), as all participants met the criterion persistent hallucinations, which in itself is sufficient for this classification. However, the DSM general terms state that a person has to be bothered by their symptoms and/or dysfunction on social, psychological and professional domains should be present to make a diagnosis. The fact that the hallucinating subjects showed no social, affective or professional dysfunction, were not bothered by the AVH and were not in need of treatment indicates that the diagnoses psychosis NOS is clinically inappropriate (Sommer *et al.* 2008a). Although the combination of hallucinations (perceptual aberrations) and magical ideation present in most subjects with hallucinations made them score on at least three items on the DSM-IV criteria for schizotypal personality disorder, the individuals with AVH did not reach criteria for schizotypal personality disorder as there was no lack in social capacity, nor did the subjects have inadequate or constrained affect as determined by a trained psychiatrist using the CASH and SCID-II (Spitzer *et al.* 1992; Williams *et al.* 1992) and the global assessment of functioning (GAF) scale (Endicott *et al.* 1976). Other key arguments why the subjects did not meet criteria for schizotypy were that their magical beliefs were largely socially

accepted (mainly spiritual ideas) and that they were functioning well. Finally, these individuals did not use psychoactive medication.

In this study, non-psychotic individuals with AVH were considered to hold an intermediate position on a psychosis continuum, with healthy individuals at one end and individuals with a psychotic disorder at the other. Being an intermediate on this continuum, the hallucinating individuals are expected to be affected by psychotic symptoms to some extent, as expressed by the presence of subclinical levels of suspicion, formal thought disorder and a tendency for magical ideation.

This study was approved by the Humans Ethics Committee of the University Medical Centre Utrecht. After complete description of the study to the subjects, written informed consent was obtained.

Data acquisition

Resting-state functional magnetic resonance imaging (fMRI) scans were acquired while participants kept their eyes closed but stayed awake. During scan acquisition, CR (Glover *et al.* 2000) processes were monitored by affixing four electrocardiogram electrodes to the subject's chest and by placing a respiration band at the level of the abdomen. The measured CR data consisted of a heartbeat signal with a trigger marking times at which an R-peak was detected, and a respiratory signal measuring the expansion of the respiration band (Glover *et al.* 2000; van Buuren *et al.* 2009). Inclusion criteria for these data were that both cardiac and respiratory signals were measured throughout the scan (i.e. no interruptions in the data), and that the trigger marking times at which an R-peak was detected did not miss more than 25 R-peaks within a scan session.

Following acquisition of the resting-state scan, participants were asked if they had experienced hallucinations. Subjects experiencing AVH during scanning were excluded from analyses.

fMRI time-series data were obtained using a Philips Achieva 3-T Clinical MRI scanner (Philips Medical Systems, The Netherlands). Six hundred blood oxygenation level-dependent (BOLD) fMRI images were acquired per patient with the following parameter settings: 40 (coronal) slices, repetition time (TR)/echo time (TE) 21.75/32.4 ms, flip angle 10°, field of view (FOV) 224 × 256 × 160 mm, matrix 64 × 64 × 40, voxel size 4 mm isotropic. This scan sequence achieves full brain coverage within 609 ms by combining a 3D-PRESTO pulse sequence with parallel imaging (SENSE) in two directions using a commercial eight-channel SENSE headcoil (Neggens *et al.* 2008) rendering scans of approximately 6 min (i.e. 600

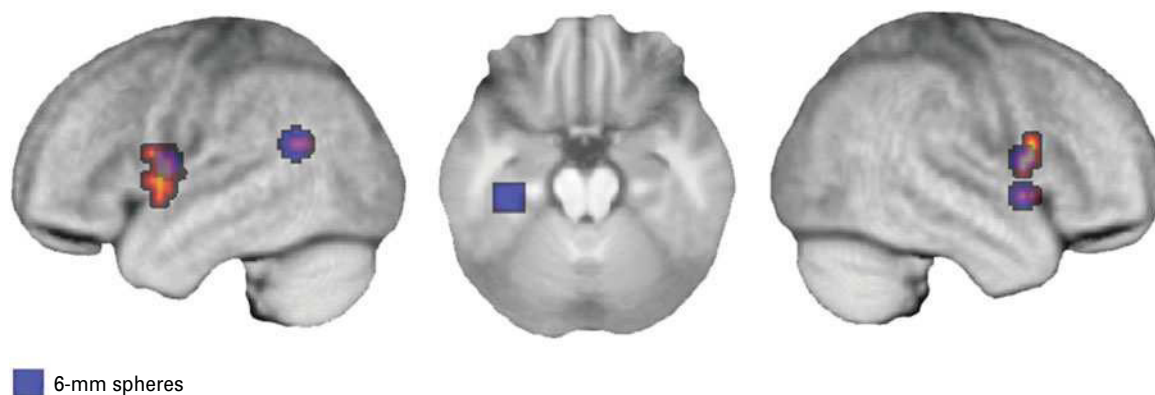


Fig. 1. SPM T values for the group-wise analysis revealing brain activation during auditory verbal hallucinations (AVH) and 6-mm spheres centred on local maxima in the inferior frontal, superior temporal and parahippocampal regions. Seeds: (1) left inferior frontal gyrus ($-48, 0, 12$), (2) right inferior frontal gyrus ($60, 8, 12$), (3) left superior temporal region ($-60, -56, 20$), (4) right superior temporal region ($60, 8, -4$) and (5) left parahippocampal region ($-36, -24, -1$). Threshold for the group-wise analysis: $p=0.05$ false discovery rate (FDR) corrected for multiple comparisons within a region of interest (ROI) comprising Brodmann area (BA) 22, corresponding to Wernicke's area of language perception, BAs 44 and 45 containing Broca's area of language production and BAs 27, 28, 34, 35 and 36, which intersect with the parahippocampal gyrus.

images $\times 0.609$ s). As these PRESTO SENSE images have little anatomical contrast, 40 identical scans, but with a flip angle of 27° (fa27), were acquired to improve realignment and co-registration during preprocessing. After the functional scans, a high-resolution anatomical scan (TR/TE 9.86/4.6 ms, $0.875 \times 0.875 \times 1$ voxels, slice thickness 1 mm, flip angle 8° , FOV $224 \times 160 \times 168$ mm, 160 slices) was acquired to improve localization of the functional data.

Data preprocessing

Preprocessing and data analysis were conducted using statistical parametric mapping (SPM5; Wellcome Department of Cognitive Neurology, London, UK). Within-subject image realignment with the mean fa27 as the reference was used to correct for the effects of head motion. The T1-weighted anatomical image was then co-registered to the mean fa27. Using unified segmentation (Ashburner & Friston, 2005), the structural scan was then segmented, which includes estimation of normalization parameters. These parameters were subsequently used to register all scans (T1 and fMRI) to the Montreal Neurological Institute (MNI) template as present in SPM5. Finally, images were smoothed using an 8-mm full-width at half-maximum (FWHM) Gaussian kernel.

Seed selection

To identify seed regions for seed regression analysis, we used data from two fMRI studies published by our group. In the first study 21 non-psychotic individuals and 21 matched psychotic patients indicated the presence of AVH during fMRI scanning (Diederer

et al. 2011). Six of the 21 non-psychotic subjects also participated in the current study (for a detailed description see Diederer *et al.* 2011). In that study we identified a common pattern of AVH-related activation for the psychotic and non-psychotic individuals. Activation patterns per group were not described in the previous study. The inferior frontal and superior temporal seeds were centred on local maxima of significant AVH-related activation in the group of non-psychotic individuals, and the results from this group are displayed in Fig. 1. The analysis was thresholded at $p < 0.05$ false discovery rate (FDR) corrected for multiple comparisons within a small volume containing Brodmann area (BA) 22, BA 44 and BA 45, which correspond to Wernicke's area of language perception and Broca's area of language production. The location of the parahippocampal seed was based on another study by our group in which we identified significant signal changes in this area prior to the onset of AVH (Diederer *et al.* 2010*b*). The five seed regions (left and right inferior frontal gyrus, left and right superior temporal gyrus and left parahippocampal area) are also shown in Fig. 1.

Data analysis

After preprocessing, fMRI time courses were extracted for all voxels in a seed for each subject. Next, the first eigenvariate of the voxel time series contained in each seed was calculated and entered as a covariate of interest in a whole-brain regression analysis (van Marle *et al.* 2010). A regression analysis was conducted for each seed, resulting in five analyses per subject, that is one for each seed. This approach is generally referred

Table 1. Demographic description of all participants

	Healthy control subjects (<i>n</i> = 25)		Non-psychotic subjects with AVH (<i>n</i> = 25)		Statistics
	<i>n</i>	Mean (S.D.)	<i>n</i>	Mean (S.D.)	
Age (years)	25	39.8 (15.9)	25	41.6 (13.5)	KS <i>Z</i> = 0.85, <i>p</i> = 0.47
Sex (male/female)	7/18		7/18		$\chi^2 = 0.11$, <i>p</i> = 1
Handedness (right/left)	19/6		18/6		$\chi^2 = 0.11$, <i>p</i> = 1
Years of education	25	14.0 (2.4)	25	13.5 (2.0)	KS <i>Z</i> = 0.57, <i>p</i> = 0.91
SPQ total score	24	7.5 (6.1)	25	29.6 (10.6)	$t_{38.46} = -8.95$, <i>p</i> < 0.001*

AVH, Auditory verbal hallucinations; SPQ, Schizotypal Personality Questionnaire; KS, Kolmogorov–Smirnov; S.D., standard deviation.

* Significant at *p* < 0.001.

to as seed-based resting-state fMRI, or functional connectivity (Greicius *et al.* 2003; Fox *et al.* 2005; Cole *et al.* 2010).

fMRI time series can be severely contaminated by (non-white) noise factors including head movement-induced image noise and CR noise. Such signals may induce spurious correlations in a seed-based analysis, as these global signals often occur similarly in regions throughout the brain and hence cause correlations between regions based on non-neuronal signals (Lund *et al.* 2006). Consequently, some covariates of no interest were also included in the model to correct for these confounding temporal signals. First, the average white matter and cerebrospinal fluid (CSF) signals were used as covariates of no interest as these tissues may carry physiological or thermal signal fluctuations that are similar to those affecting grey matter, while containing little contribution from neural activity (Chang & Glover, 2009). Average white matter and CSF signals were obtained by extracting the average signal per time point of two additional 6-mm spheres that were placed in white matter (MNI coordinates: 0, 28, 5) and CSF (MNI coordinates: -4, 13, 9). The global signal was not entered as a covariate in the analysis as it has been shown that this may induce spurious negative correlations (Murphy *et al.* 2009). Second, the realignment parameters, consisting of six-parameter rigid-body transformations (three translations and three rotations), were entered to model movement artefacts. Third, CR processes were corrected for using the image-based retrospective correction method for physiological motion effects in fMRI (RETROICOR; Glover *et al.* 2000). RETROICOR extracts cardiac- and respiratory-related noise effects from the MR signal by assigning cardiac and respiratory phases to each image in a time series. The CR noise is then modelled as the linear combination of a set of sinusoid functions, which can be used to correct

for this noise. In the current study, CR noise was modelled using 10 sinusoid functions for cardiac noise and 10 for respiratory noise, which were entered as covariates of no interest in the analysis. Data were also high-pass filtered with a cut-off of 100 s to remove non-global low-frequency noise.

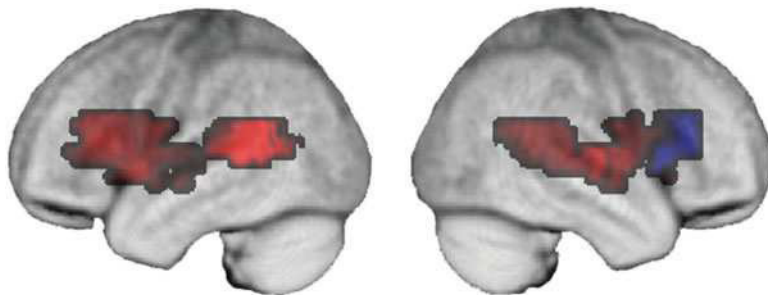
Following analysis, individual *T* maps were created for the covariates of interest and converted to *R* maps, which represent the correlation coefficient of the time-series signal in each voxel with the signal from the seed regions. Correlation coefficients were subsequently *Z*-transformed and entered in five separate (i.e. one for each seed) random-effects two-sample *T* tests to enable comparisons between groups. These tests comprised the main outcome measure of this study. As it was hypothesized that aberrant connectivity in the non-psychotic individuals with AVH would be present between inferior frontal, superior temporal and parahippocampal regions, a small volume correction (SVC) for multiple comparisons was applied using an ROI (Allen *et al.* 2008). The ROI was defined anatomically and comprised BA 22, corresponding to Wernicke's area of language perception, BAs 44 and 45 containing Broca's area of language production and BAs 27, 28, 34, 35 and 36, which intersect with the parahippocampal gyrus. Analyses were thresholded at *p* = 0.05 FDR corrected for all voxels within the ROI, with an extended threshold of four voxels.

Results

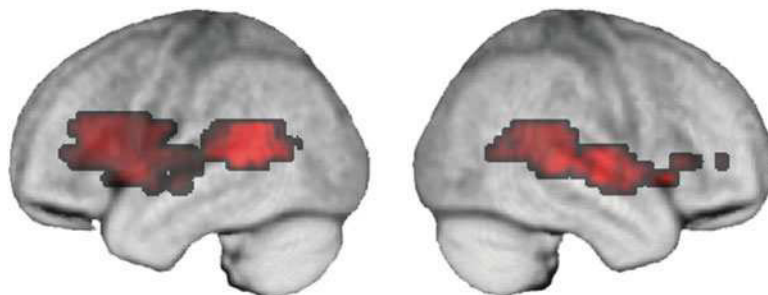
Exclusions

After scanning 37 AVH participants and 44 healthy controls, 12 non-psychotic individuals with AVH and 13 control subjects were found unsuitable for inclusion, resulting in 25 valid scans of non-psychotic

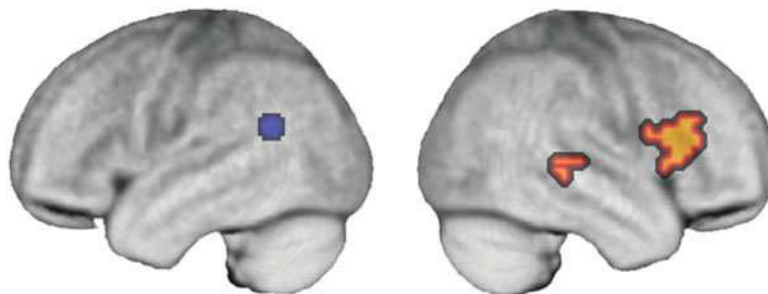
(a) Healthy control subjects



(b) Non-psychotic subjects with AVH



(c) Non-psychotic with AVH > Healthy control subjects



(d) Average *R* values

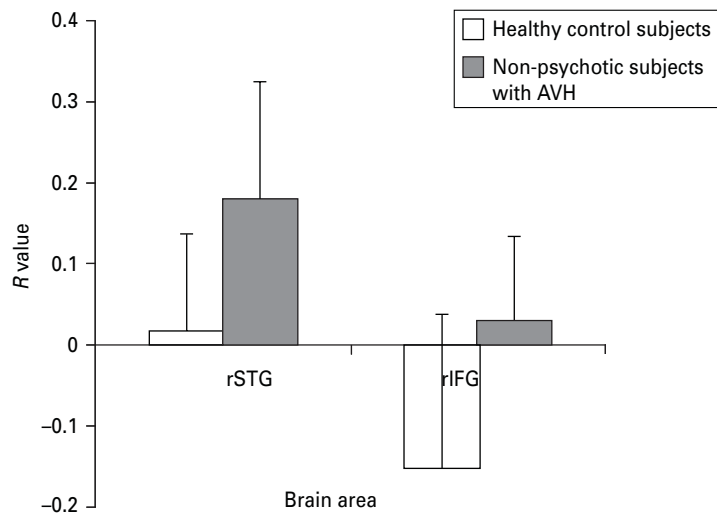


Fig. 2. SPM *T* values revealing areas displaying significant connectivity with the left superior temporal seed in (a) healthy control subjects and (b) non-psychotic subjects with auditory verbal hallucinations (AVH). (c) Significantly increased connectivity with the left superior temporal seed in non-psychotic subjects with AVH in comparison to the control group. (d) Average *R* values and standard deviation of clusters showing significantly increased connectivity with the left superior

Table 2. Cluster sizes, *T* values and locations of local maxima for the two-sample *T* test with (a) the left superior temporal region and (b) the left parahippocampal region as the seed region

Cluster size	<i>p</i> value	<i>T</i> value	MNI coordinates	Area
<i>(a)</i> Left superior temporal seed region				
4	0.036	4.05	44, -28, 4	Right superior temporal gyrus
38	0.036	3.88	48, 24, 16	Right inferior frontal gyrus
<i>(b)</i> Left parahippocampal seed region				
33	0.45	3.81	-44, 16, 12	Left inferior frontal gyrus
	0.45	3.97	-44, 4, 8	Left insula/precentral gyrus

MNI, Montreal Neurological Institute.

The results are from random-effects two-sample *T* tests on *Z*-transformed correlation coefficients. Thresholded at $p=0.05$, false discovery rate (FDR) corrected for multiple comparisons with an extended threshold of four voxels.

subjects with AVH and 31 scans of healthy control subjects. Nine of the 12 excluded non-psychotic subjects were excluded because they had experienced AVH during the resting state, and three were excluded as a result of the poor quality of the CR data obtained. The poor quality of the CR data also resulted in the exclusion of 13 control subjects. Twenty-five of the 31 control subjects were then selected to enable the best match with the remaining non-psychotic individuals with AVH based on age, sex, handedness and years of education. Data on these 25 non-psychotic individuals with AVH and 25 healthy control subjects were then used for further analyses.

Demographic variables

The groups did not differ significantly with respect to age, sex, handedness and years of education. As expected, the non-psychotic individuals with AVH scored significantly higher on the SPQ. Table 1 provides a demographic description of the participants, including SPQ scores.

Left superior temporal seed

The left superior temporal seed showed significantly increased connectivity with the right superior temporal and the right inferior frontal regions in the non-psychotic individuals. Inspection of the average *R* values of the right superior temporal gyrus revealed an average correlation coefficient of 0.02 (s.d. = 0.12) in the healthy control subjects and 0.18 (s.d. = 0.15) in the non-psychotic individuals with AVH. For the right

inferior frontal gyrus, the healthy controls showed a negative correlation with the left temporoparietal region (mean $R = -0.15$, s.d. = 0.19), which was absent in the non-psychotic individuals with AVH (mean $R = 0.03$, s.d. = 0.11). Figure 2 shows the SPM *T* values and average *R* values of the clusters displaying significantly different connectivity with the left superior temporal seed in the non-psychotic individuals compared to the healthy control subjects. Coordinates, *T* values and cluster sizes of these regions are listed in Table 2a.

Left parahippocampal seed

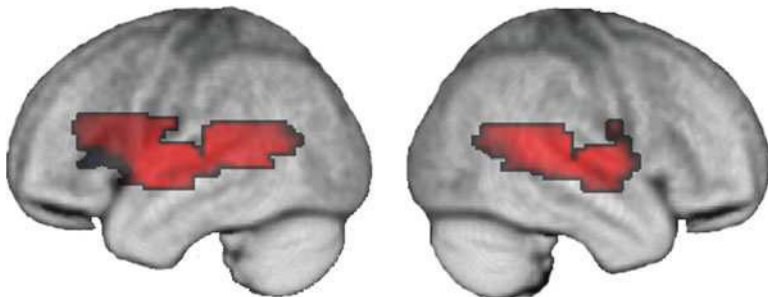
The left parahippocampal gyrus displayed significantly increased connectivity with the left inferior frontal region in the non-psychotic individuals with AVH. Although the non-psychotic individuals displayed a small positive correlation between the left parahippocampal region and the left inferior frontal gyrus (mean $R = 0.05$, s.d. = 0.22), this was absent in the healthy control subjects (mean $R = 0.00$, s.d. = 0.05). Figure 3 shows the SPM *T* values and average *R* values of the voxels displaying significantly increased connectivity with the left parahippocampal seed in the non-psychotic individuals with AVH. Coordinates, *T* values and cluster sizes are listed in Table 2b.

Right superior temporal and bilateral inferior frontal seeds

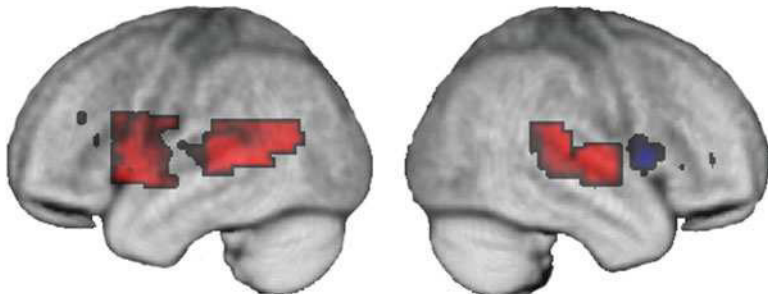
No significant differences in connectivity between the right superior temporal and the left and right inferior

temporal seed in non-psychotic subjects with AVH. In (a) and (b), red indicates positive correlations, blue indicates negative correlations. In (c), the left superior temporal seed is shown in blue. The results are from random-effects two-sample *T* tests on *Z*-transformed correlation coefficients. Thresholded at $p=0.05$ false discovery rate (FDR) corrected for multiple comparisons within the *a priori* hypothesized regions with an extend threshold of four voxels.

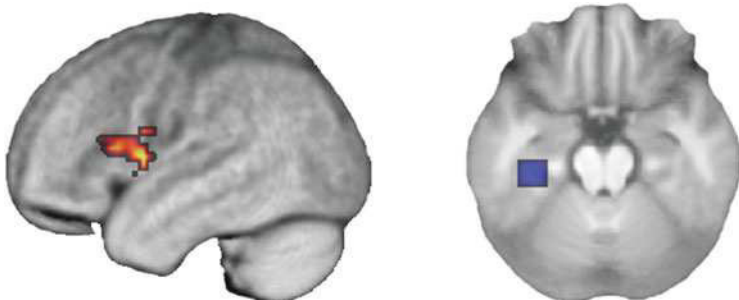
(a) Healthy control subjects



(b) Non-psychotic subjects with AVH



(c) Non-psychotic with AVH > Healthy control subjects



(d) Average *R* values

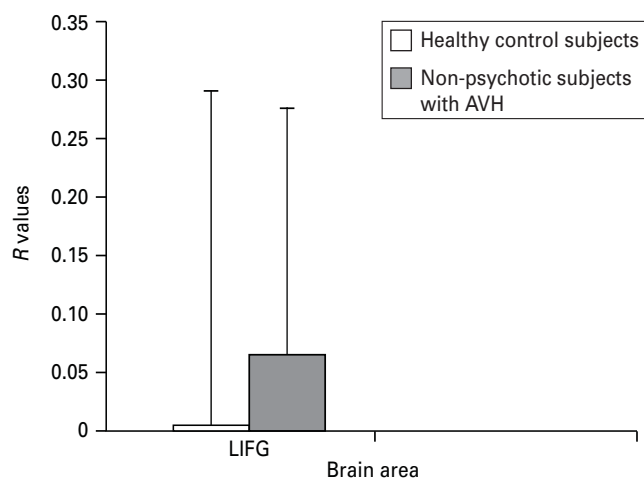


Fig. 3. SPM *T* values revealing areas displaying significant connectivity with the left parahippocampal seed in (a) healthy control subjects and (b) non-psychotic subjects with auditory verbal hallucinations (AVH). (c) Significantly increased connectivity with the left parahippocampal seed in non-psychotic subjects with AVH in comparison to the control group. (d) Average *R* values and standard deviation of the cluster showing significantly increased connectivity with the left

frontal seeds on the one hand and voxels within the *a priori* hypothesized regions on the other hand could be observed between the healthy control group and the group of non-psychotic individuals with AVH.

Discussion

In this study we investigated whether a direct link could be established between AVH and aberrant connectivity between inferior frontal, parahippocampal and superior temporal brain regions. Resting-state connectivity was studied in a group of 25 non-psychotic individuals who experience AVH in the absence of other psychiatric symptoms and are free of medication. Individuals who hallucinated during the scan were excluded from analysis to prevent effects of symptom-related activation. In the non-psychotic individuals, increased connectivity was observed between the left and right superior temporal regions and also between the left parahippocampal and the inferior frontal regions. Moreover, this group did not show the negative correlation between the left superior temporal area and the right inferior frontal region as was observed in the healthy control group.

Aberrant connectivity of frontal and superior temporal regions may well reflect erroneous interaction of language production and perception processes in individuals with AVH. Consequently, language production areas in the frontal lobes may not be able to signal to superior temporal language processing regions that fragments of inner speech are self-generated (Frith *et al.* 1995; Spence *et al.* 2000; Ford *et al.* 2007; Heinks-Maldonado *et al.* 2007). As a result, this inner speech may acquire an acoustic quality and be misattributed to an external source. This finding is in line with previous task-based and resting-state fMRI studies that have reported faulty integration of frontal and superior temporal regions in subjects with AVH (Frith *et al.* 1995; Silbersweig *et al.* 1995; Spence *et al.* 2000; Rotarska-Jagiela *et al.* 2010; Vercammen *et al.* 2010). Such dysfunctional interaction has been suggested to result from alterations of the arcuate fasciculi, the most important fibre bundles between frontal and superior temporal language areas. Indeed, alterations of the arcuate fasciculi were previously observed in hallucinating patients with schizophrenia and in non-psychotic subjects with AVH (de Weijer *et al.* 2011*a, b*).

Our results differ from most other studies because dysfunctional connectivity was observed between the left superior temporal and the right inferior frontal regions whereas previous studies mainly found aberrant connectivity between the left frontal and superior temporal regions. Involvement of the right inferior frontal region is, however, in line with previous studies that have revealed prominent activation of this area during the experience of AVH (Jardri *et al.* 2010; Kuhn & Gallinat, 2010; Diederer *et al.* 2011). Although no direct anatomical connection exists between the right inferior frontal and left superior temporal areas, integration of these areas should be enabled through involvement of a third area. This third region may consist of the right temporal region because this area has a direct connection with the left superior temporal and right inferior frontal regions. Moreover, the right superior temporal region displayed increased connectivity with the left superior temporal area in the subjects with AVH.

Increased functional connectivity was also observed between the left parahippocampal and the left inferior frontal regions in non-psychotic individuals with AVH. The parahippocampal region fulfils a prominent role in memory processes in which it mediates information flow between the hippocampus and neocortical regions such as the language areas (Van Hoesen, 1982; Eichenbaum *et al.* 1996, 2007; Eichenbaum, 2000). When a memory is retrieved, the parahippocampal gyri are hypothesized to reinstate activation in neocortical association areas involved in the original experience (Wheeler *et al.* 2000; Johnson & Rugg, 2007). Activation of the latter regions presumably enables the re-experience of the retrieved memory.

Increased connectivity between association areas such as the left inferior frontal region area and the parahippocampal gyrus may thus represent an enhanced redistribution of memory fragments to language production areas. This may lead to erroneous activation of association cortices and hence to incorrect recognition (Diederer *et al.* 2010*b*). Support for this hypothesis is provided by studies reporting significant signal changes in the parahippocampal gyrus preceding AVH (Hoffman *et al.* 2008, 2011; Diederer *et al.* 2010*b*). Based on these findings it is conceivable that AVH do not result from a single deficit, but rather from the integration of multiple deficits.

parahippocampal seed in non-psychotic subjects with AVH. In (a) and (b), red indicates positive correlations, blue indicates negative correlations. In (c), the left parahippocampal seed is shown in blue. The results are from random-effects two-sample *T* tests on Z-transformed correlation coefficients. Thresholded at $p=0.05$ false discovery rate (FDR) corrected for multiple comparisons within the *a priori* hypothesized regions with an extended threshold of four voxels.

Although this is the first study to investigate resting-state functional connectivity in a group of non-psychotic individuals with AVH, some studies have investigated resting-state connectivity in relation to AVH in schizophrenia patients (Gavrilescu *et al.* 2010; Hoffman *et al.* 2010; Rotarska-Jagiela *et al.* 2010; Vercammen *et al.* 2010). The present study is partly in line with previous studies that observed aberrant connectivity between the left temporoparietal junction and the right inferior frontal gyrus (Vercammen *et al.* 2010) and also between bilateral superior temporal areas (Gavrilescu *et al.* 2010). Furthermore, it was shown that the severity of hallucinations correlated negatively with the functional connectivity of fronto-temporal and auditory networks in schizophrenia (Rotarska-Jagiela *et al.* 2010). Whereas most of these studies reported reduced connectivity, the present study found increased connectivity. This may reflect the general decrease in connectivity observed in schizophrenia, which is presumably not related specifically to AVH. Indeed, the only study to date to compare hallucinating schizophrenia patients to non-hallucinating patients, which can therefore assess characteristics that are specifically related to AVH, also reported increased connectivity, in this case between Wernicke's area in the left temporoparietal region (the seed region) and a large subcortical region including the medial temporal region (Hoffman *et al.* 2010).

Discrepancies between the findings of previous studies and the present study may well be explained by the fact that previous studies included patients with schizophrenia who present with additional psychiatric symptoms such as delusions, negative and cognitive symptoms, and mostly use antipsychotic medication. Furthermore, most studies did not exclude patients with active AVH from analyses or did not report whether AVH were present during scanning (Hoffman *et al.* 2010; Rotarska-Jagiela *et al.* 2010; Vercammen *et al.* 2010). Finally, these studies did not correct for CR rhythms, known to contaminate resting-state connectivity analyses (Noll & Schneider, 1994; Glover & Lee, 1995; Dagli *et al.* 1999; Glover *et al.* 2000; Birn *et al.* 2006). As the subjects included in this study experienced AVH in relative isolation and did not actively hallucinate during the scans, these results suggest that dysfunctional connectivity of frontal, parahippocampal and superior temporal regions is specifically related to the predisposition to hallucinate in the auditory modality.

Limitations

A limitation of this study is that the method used provides no information on the directionality of

connectivity. Furthermore, this method does not account for any temporal variation in connectivity. Another limitation is that, although aberrant connectivity was observed between frontal, superior temporal and parahippocampal regions, the sites of most of these regions do not fully correspond with the *a priori* defined seed regions. This may, however, be due to high inter-individual differences in the exact location of brain regions observed in AVH (Ojemann, 1991). Consequently, the sites of AVH-related brain activation probably differ somewhat between the current group and the group on which the seed regions were based (Diederer *et al.* 2011). The latter explanation may also account for the fact that, although the left superior temporal seed showed aberrant connectivity with the right superior temporal and the right inferior frontal regions, no significant differences in connectivity with the superior temporal region (the current seed) between the groups were observed when the right superior temporal and inferior frontal regions were used as seed regions, that is when the logic of the current analysis is reversed. This does, however, not pose a major limitation as the selected seed regions in the right superior temporal and inferior frontal regions do not exactly correspond with loci of aberrant connectivity in the right inferior frontal and superior temporal areas as observed in this study.

In summary, the presence of increased connectivity of frontal, parahippocampal and superior temporal areas in individuals with isolated AVH suggests that dysfunctional integration of these regions is specifically related to the propensity to hallucinate in the auditory domain.

Declaration of Interest

None.

References

- Aleman A, Laroi F (2008). *Hallucinations: The Science of Idiosyncratic Perception*. American Psychological Association: Washington, DC.
- Allen P, Amaro E, Fu CH, Williams SC, Brammer MJ, Johns LC, McGuire PK (2007). Neural correlates of the misattribution of speech in schizophrenia. *British Journal of Psychiatry* **190**, 162–169.
- Allen P, Laroi F, McGuire PK, Aleman A (2008). The hallucinating brain: a review of structural and functional neuroimaging studies of hallucinations. *Neuroscience and Biobehavioral Reviews* **32**, 175–191.
- Andreasen NC, Flaum M, Arndt S (1992). The Comprehensive Assessment of Symptoms and History (CASH). An instrument for assessing diagnosis and psychopathology. *Archives of General Psychiatry* **49**, 615–623.

- Ashburner J, Friston KJ (2005). Unified segmentation. *NeuroImage* 26, 839–851.
- Birn RM, Diamond JB, Smith MA, Bandettini PA (2006). Separating respiratory-variation-related fluctuations from neuronal-activity-related fluctuations in fMRI. *NeuroImage* 31, 1536–1548.
- Chang C, Glover GH (2009). Effects of model-based physiological noise correction on default mode network anti-correlations and correlations. *NeuroImage* 47, 1448–1459.
- Cole DM, Smith SM, Beckmann CF (2010). Advances and pitfalls in the analysis and interpretation of resting-state fMRI data. *Frontiers in Systems Neuroscience* 4, 8.
- Copolov DL, Seal ML, Maruff P, Ulusoy R, Wong MT, Tochon-Danguy HJ, Egan GF (2003). Cortical activation associated with the experience of auditory hallucinations and perception of human speech in schizophrenia: a PET correlation study. *Psychiatry Research* 122, 139–152.
- Daalman K, Boks MP, Diederer KM, de Weijer AD, Blom JD, Kahn RS, Sommer IE (2011). The same or different? A phenomenological comparison of auditory verbal hallucinations in healthy and psychotic individuals. *Journal of Clinical Psychiatry* 72, 320–325.
- Dagli MS, Ingeholm JE, Haxby JV (1999). Localization of cardiac-induced signal change in fMRI. *NeuroImage* 9, 407–415.
- de Weijer AD, Mandl RC, Diederer KM, Neggers SF, Kahn RS, Hulshoff Pol HE, Sommer IE (2011a). Microstructural alterations of the arcuate fasciculus in schizophrenia patients with frequent auditory verbal hallucinations. *Schizophrenia Research* 130, 68–77.
- de Weijer AD, Neggers SF, Diederer KM, Mandl RC, Kahn RS, Hulshoff Pol HE, Sommer IE (2011b). Aberrations in the arcuate fasciculus are associated with auditory verbal hallucinations in psychotic and in non-psychotic individuals. *Human Brain Mapping*. Published online: 23 November 2011. doi:10.1002/hbm.21463.
- Diederer KM, Daalman K, de Weijer AD, Neggers SF, van Gastel W, Blom JD, Kahn RS, Sommer IE (2011). Auditory hallucinations elicit similar brain activation in psychotic and nonpsychotic individuals. *Schizophrenia Bulletin* 38, 1074–1082.
- Diederer KM, De Weijer AD, Daalman K, Blom JD, Neggers SF, Kahn RS, Sommer IE (2010a). Decreased language lateralization is characteristic of psychosis, not auditory hallucinations. *Brain* 133, 3734–3744.
- Diederer KM, Neggers SF, Daalman K, Blom JD, Goekoop R, Kahn RS, Sommer IE (2010b). Deactivation of the parahippocampal gyrus preceding auditory hallucinations in schizophrenia. *American Journal of Psychiatry* 167, 427–435.
- Diederer KM, van Lutterveld R, Sommer IE (2012). Neuroimaging of voice hearing in non-psychotic individuals: a mini review. *Frontiers in Human Neuroscience* 6, 111.
- Eichenbaum H (2000). A cortical-hippocampal system for declarative memory. *Nature Reviews. Neuroscience* 1, 41–50.
- Eichenbaum H, Schoenbaum G, Young B, Bunsey M (1996). Functional organization of the hippocampal memory system. *Proceedings of the National Academy of Sciences USA* 93, 13500–13507.
- Eichenbaum H, Yonelinas AP, Ranganath C (2007). The medial temporal lobe and recognition memory. *Annual Reviews of Neuroscience* 30, 123–152.
- Endicott J, Spitzer RL, Fleiss JL, Cohen J (1976). The Global Assessment Scale: a procedure for measuring overall severity of psychiatric disturbance. *Archives of General Psychiatry* 33, 766–771.
- Ford JM, Roach BJ, Faustman WO, Mathalon DH (2007). Synch before you speak: auditory hallucinations in schizophrenia. *American Journal of Psychiatry* 164, 458–466.
- Fox MD, Snyder AZ, Vincent JL, Corbetta M, Van Essen DC, Raichle ME (2005). The human brain is intrinsically organized into dynamic, anticorrelated functional networks. *Proceedings of the National Academy of Sciences USA* 102, 9673–9678.
- Frith CD, Friston KJ, Herold S, Silbersweig D, Fletcher P, Cahill C, Dolan RJ, Frackowiak RS, Liddle PF (1995). Regional brain activity in chronic schizophrenic patients during the performance of a verbal fluency task. *British Journal of Psychiatry* 167, 343–349.
- Gavrilescu M, Rossell S, Stuart GW, Shea TL, Innes-Brown H, Henshall K, McKay C, Sergejew AA, Copolov D, Egan GF (2010). Reduced connectivity of the auditory cortex in patients with auditory hallucinations: a resting state functional magnetic resonance imaging study. *Psychological Medicine* 40, 1149–1158.
- Glover GH, Lee AT (1995). Motion artifacts in fMRI: comparison of 2DFT with PR and spiral scan methods. *Magnetic Resonance in Medicine* 33, 624–635.
- Glover GH, Li TQ, Ress D (2000). Image-based method for retrospective correction of physiological motion effects in fMRI: RETROICOR. *Magnetic Resonance in Medicine* 44, 162–167.
- Greicius MD, Krasnow B, Reiss AL, Menon V (2003). Functional connectivity in the resting brain: a network analysis of the default mode hypothesis. *Proceedings of the National Academy of Sciences USA* 100, 253–258.
- Heinks-Maldonado TH, Mathalon DH, Houde JF, Gray M, Faustman WO, Ford JM (2007). Relationship of imprecise corollary discharge in schizophrenia to auditory hallucinations. *Archives in General Psychiatry* 64, 286–296.
- Hoffman RE, Anderson AW, Varanko M, Gore JC, Hampson M. (2008). Time course of regional brain activation associated with onset of auditory/verbal hallucinations. *British Journal of Psychiatry* 193, 424–425.
- Hoffman RE, Fernandez T, Pittman B, Hampson M (2010). Elevated functional connectivity along a corticostriatal loop and the mechanism of auditory/verbal hallucinations in patients with schizophrenia. *Biological Psychiatry* 69, 407–414.
- Hoffman RE, Pittman B, Constable RT, Bhagwagar Z, Hampson M (2011). Time course of regional brain activity accompanying auditory verbal hallucinations in schizophrenia. *British Journal of Psychiatry* 198, 277–283.
- Honey GD, Bullmore ET, Soni W, Varatheesan M, Williams SC, Sharma T (1999). Differences in frontal cortical activation by a working memory task after substitution of risperidone for typical antipsychotic drugs

- in patients with schizophrenia. *Proceedings of the National Academy of Sciences USA* **96**, 13432–13437.
- Jardri R, Pouchet A, Pins D, Thomas P** (2010). Cortical activations during auditory verbal hallucinations in schizophrenia: a coordinate-based meta-analysis. *American Journal of Psychiatry* **168**, 73–81.
- Johnson JD, Rugg MD** (2007). Recollection and the reinstatement of encoding-related cortical activity. *Cerebral Cortex* **17**, 2507–2515.
- Kuhn S, Gallinat J** (2010). Quantitative meta-analysis on state and trait aspects of auditory verbal hallucinations in schizophrenia. *Schizophrenia Bulletin* **38**, 779–786.
- Liemburg EJ, Vercammen A, Ter Horst GJ, Curcic-Blake B, Knegtering H, Aleman A** (2012). Abnormal connectivity between attentional, language and auditory networks in schizophrenia. *Schizophrenia Research* **135**, 15–22.
- Lund TE, Madsen KH, Sidaros K, Luo W-L, Nichols TE** (2006). Non-white noise in fMRI: does modelling have an impact? *NeuroImage* **29**, 54–66.
- McGuire PK, Frith CD** (1996). Disordered functional connectivity in schizophrenia. *Psychological Medicine* **26**, 663–667.
- Murphy K, Birn RM, Handwerker DA, Jones TB, Bandettini PA** (2009). The impact of global signal regression on resting state correlations: are anti-correlated networks introduced? *NeuroImage* **44**, 893–905.
- Neggers SF, Hermans EJ, Ramsey NF** (2008). Enhanced sensitivity with fast three-dimensional blood-oxygen-level-dependent functional MRI: comparison of SENSE-PRESTO and 2D-EPI at 3 T. *Nuclear Magnetic Resonance in Biomedicine* **21**, 663–676.
- Noll DC, Schneider W** (1994). Theory, simulation, and compensation of physiological motion artifacts in functional MRI. *Image Processing, 1994. Proceedings. ICIP-94, IEEE International Conference* **3**, 40–44.
- Ojemann GA** (1991). Cortical organization of language. *Journal of Neuroscience* **11**, 2281–2287.
- Raine A** (1991). The SPQ: a scale for the assessment of schizotypal personality based on DSM-III-R criteria. *Schizophrenia Bulletin* **17**, 555–564.
- Rotarska-Jagiela A, van de Ven V, Oertel-Knochel V, Uhlhaas PJ, Voegeley K, Linden DE** (2010). Resting-state functional network correlates of psychotic symptoms in schizophrenia. *Schizophrenia Research* **117**, 21–30.
- Shergill SS, Kanaan RA, Chitnis XA, O'Daly O, Jones DK, Frangou S, Williams SC, Howard RJ, Barker GJ, Murray RM, McGuire P** (2007). A diffusion tensor imaging study of fasciculi in schizophrenia. *American Journal of Psychiatry* **164**, 467–473.
- Shergill SS, Murray RM, McGuire PK** (1998). Auditory hallucinations: a review of psychological treatments. *Schizophrenia Research* **32**, 137–150.
- Silbersweig DA, Stern E, Frith C, Cahill C, Holmes A, Grootoank S, Seaward J, McKenna P, Chua SE, Schnorr L, Jones T, Frackowiak RSJ** (1995). A functional neuroanatomy of hallucinations in schizophrenia. *Nature* **378**, 176–179.
- Sommer IE, Clos M, Meijering AL, Diederens KMJ, Eickhoff SB** (2012). Resting state functional connectivity in patients with chronic hallucinations. *PLoS ONE* **7**, e43516.
- Sommer IE, Daalman K, Rietkerk T, Diederens KM, Bakker S, Wijkstra J, Boks MP** (2008a). Healthy individuals with auditory verbal hallucinations; who are they? Psychiatric assessments of a selected sample of 103 subjects. *Schizophrenia Bulletin* **36**, 633–641.
- Sommer IE, Diederens KM, Blom JD, Willems A, Kushan L, Slotema K, Boks MP, Daalman K, Hoek HW, Neggers SF, Kahn RS** (2008b). Auditory verbal hallucinations predominantly activate the right inferior frontal area. *Brain* **131**, 3169–3177.
- Spence SA, Liddle PF, Stefan MD, Hellewell JS, Sharma T, Friston KJ, Hirsch SR, Frith CD, Murray RM, Deakin JF, Grasby PM** (2000). Functional anatomy of verbal fluency in people with schizophrenia and those at genetic risk. Focal dysfunction and distributed disconnectivity reappraised. *British Journal of Psychiatry* **176**, 52–60.
- Spitzer RL, Williams JB, Gibbon M, First MB** (1992). The Structured Clinical Interview for DSM-III-R (SCID). I: History, rationale, and description. *Archives of General Psychiatry* **49**, 624–629.
- Tien AY** (1991). Distributions of hallucinations in the population. *Social Psychiatry and Psychiatric Epidemiology* **26**, 287–292.
- van Buuren M, Gladwin TE, Zandbelt BB, van den Heuvel M, Ramsey NF, Kahn RS, Vink M** (2009). Cardiorespiratory effects on default-mode network activity as measured with fMRI. *Human Brain Mapping* **30**, 3031–3042.
- Van Hoeseen GW** (1982). The parahippocampal gyrus: new observations regarding its cortical connections in the monkey. *Trends in Neurosciences* **5**, 345–350.
- van Lutterveld R, Oranje B, Kemner C, Abramovic L, Willems AE, Boks MP, Glenthøj BY, Kahn RS, Sommer IE** (2010). Increased psychophysiological parameters of attention in non-psychotic individuals with auditory verbal hallucinations. *Schizophrenia Research* **121**, 153–159.
- van Marle HJF, Hermans EJ, Qin S, Fernández G** (2010). Enhanced resting-state connectivity of amygdala in the immediate aftermath of acute psychological stress. *NeuroImage* **53**, 348–354.
- Vercammen A, Knegtering H, den Boer JA, Liemburg EJ, Aleman A** (2010). Auditory hallucinations in schizophrenia are associated with reduced functional connectivity of the temporo-parietal area. *Biological Psychiatry* **67**, 912–918.
- Wheeler ME, Petersen SE, Buckner RL** (2000). Memory's echo: vivid remembering reactivates sensory-specific cortex. *Proceedings of the National Academy of Sciences USA* **97**, 11125–11129.
- Williams JB, Gibbon M, First MB, Spitzer RL, Davies M, Borus J, Howes MJ, Kane J, Pope Jr. HG, Rounsaville B, Wittchen HU** (1992). The Structured Clinical Interview for DSM-III-R (SCID). II. Multisite test-retest reliability. *Archives of General Psychiatry* **49**, 630–636.

STUDY 6

Model-based analyses of resting state fMRI reveal hyperconnectivity in an introspective socio-affective network in major depression

Leo Schilbach^{1,2}, Veronika I. Müller^{3,4,5}, Felix Hoffstaedter^{3,5}, Mareike Clos³, Roberto Goya-Maldonado⁶, Oliver Gruber^{6*}, Simon B. Eickhoff^{3,4*}

¹Department of Psychiatry, University of Cologne, Germany

²Max-Planck-Institute for Neurological Research, Cologne, Germany

³Institute of Neuroscience and Medicine (INM-1), Research Center Jülich, Germany

⁴Institute of Clinical Neuroscience and Medical Psychology, Heinrich Heine University, Düsseldorf, Germany

⁵Department of Psychiatry, Psychotherapy and Psychosomatics, Medical School, RWTH Aachen University, Germany

⁶Center for Translational Research in Systems Neuroscience and Psychiatry, Department of Psychiatry and Psychotherapy, Georg August University Göttingen, Germany

*Both authors contributed equally to the work

Manuscript submitted for publication

Own contributions

Help with data analysis

Discussion of the results

Writing parts of the methods and results sections

Correcting the introduction and discussion sections

Total contribution: 15%

ABSTRACT

Alterations of social cognition and dysfunctional interpersonal expectations are thought to play an important role in the etiology of depression and have, thus, become a key target of psychotherapeutic interventions. The underlying neurobiology, however, remains elusive. Based upon the idea of a close link between affective and introspective processes relevant for social interactions and alterations thereof in states of depression, we used a model-based analysis approach to investigate resting state functional connectivity in an introspective socio-affective (ISA) network in individuals with and without depression. Results of this analysis demonstrate significant differences between groups with depressed individuals showing hyperconnectivity of the ISA network, in part as a function of symptom severity. These findings demonstrate that neurofunctional alterations exist in individuals with depression in a socio-affective network, which may contribute to the interpersonal difficulties that are linked to depressive symptomatology.

Key words: depression, functional connectivity, model-based analysis, resting state fMRI, social brain

INTRODUCTION

Depression is a highly prevalent mental disorder, whose underlying neurobiology is still only partially understood. It is characterized by a broad range of cognitive (Hammar and Ardal 2009), psychomotor (Sobin and Sackeim 1997) and somatic symptoms (Simon et al. 1999; cf. WHO 1992). Affective symptoms such as low mood, anhedonia and loss of perspective constitute the psychopathological core of the disorder. Furthermore, depression is characterized by abnormally increased introspective thoughts and self-referential concerns, which may contribute to dysfunctional interpersonal expectations and make successful participation in social interaction increasingly difficult (Kashdan and Roberts 2007; McCullough et al. 2010, 2011). Since social interactions are normally experienced as intrinsically rewarding (e.g. Schilbach et al. 2010), unsuccessful or reduced social interactions can further contribute to the depressive symptomatology and eventually its chronification (Liu et al. 2006; McCullough et al. 2010, 2011; Cusi et al. 2011; Niven et al. 2012; Venzala et al. 2012). The neurobiology that may mediate the relationship between affective, self-referential and introspective processes, however, is poorly understood.

Several recent findings point towards aberrant functional connectivity between specific brain regions in depression (Greicius et al. 2007; Sheline et al. 2010) and have provided evidence for an alteration of cortico-limbic connections in individuals vulnerable to this disorder (Goulden et al. 2012). From a methodological point of view, resting state fMRI analyses -as an indicator of functional connectivity- may provide a powerful approach to investigate network dysfunctions in major depression. In contrast to traditional task-based neuroimaging, such analyses should be less confounded by cognitive and/or motivational impairments, which are commonly observed in patient populations and often impair sufficient task performance (e.g. Greicius et al. 2003, 2007). Yet, the reliable identification of

functional connectivity networks is complicated by various methodological drawbacks (cf. Zuo et al. 2010). While data-driven approaches allow a robust definition of key networks of covariant activity, their representation is directly dependent on the used data, i.e. the networks to be investigated as well as their disturbances are estimated from the same measurements (cf. Kriegeskorte et al. 2009). In seed-based approaches, on the other hand, the observed patterns of functional connectivity are largely dependent upon the choice of the seed regions and, hence, potentially open to bias. Moreover, in both these approaches functional meaning is usually assigned to the derived components or networks by subjective reverse inference, i.e. inferring the presence of certain cognitive processes based on the involvement of certain brain regions (Poldrack 2006; 2011).

The present study aims to circumvent these methodological problems by applying a hypothesis-driven and model-based analysis of functional connectivity. In particular, we used inter-regional correlations in resting state fMRI data to estimate connectivity within a meta-analytically derived network model. Given the above considerations concerning the pathophysiology of depression and its relationship to self-referential or social cognition and affective processes, we focused on parts of the so-called “default mode network” that are also engaged by affective processing. While the default mode network plays a major role in self-referential thoughts and introspection (Schilbach et al., 2008; Schilbach et al. 2012; Timmermans et al. 2012), the “affective network” is especially relevant for emotion perception and regulation (Schilbach et al. 2012; Zeng et al. 2012). As both aspects not only contribute to social cognition but are also likely to be disturbed in depression, we were interested to examine the combination of both circuits, which we refer to as the “introspective socio-affective” (ISA) network. The ISA network comprises anterior and subgenual cingulate regions relevant for interpersonal action control and the generation of

predictions concerned with another person's behavior (e.g. Behrens et al. 2008; Schilbach et al. 2011; Chester et al. 2012). Furthermore, it includes the dorsomedial prefrontal cortex and the precuneus, both of which has been implicated in mental state attribution relevant for understanding others' behavior as well as prospective meta-cognition (Fleming et al. 2010; Timmermans et al. 2012). Lastly, the ISA network includes the amygdala, whose role in fear conditioning has been well established (for a review see Jacobs et al. 2012) and through which anxiety may contribute to the social interaction-based development of depression (Cremers et al. 2010; McCullough et al. 2011).

Taken together, the current study is based on the idea that aberrant functional connectivity in a network for affective, introspective and social processing represents a key pathophysiological aspect of depressive symptomatology. To investigate this, a meta-analytically derived network model is used to interrogate resting state connectivity between nodes of this network in a large group of patients with major depression and a cohort of matched controls. In line with recent findings suggestive of a "hyperconnectivity hypothesis" of depression (Perrin et al. 2012), we hypothesized to find more pronounced neurofunctional coupling within the ISA network in depressed patients as compared to healthy controls.

METHODS

Meta-analytically derived network model

The ISA network model was based on two previous meta-analyses (Schilbach et al. 2012). The meta-analytic approach to the definition of brain regions reliably involved in affective and introspective tasks has been described in detail elsewhere (Schilbach et al. 2012). In brief, we used the revised version of the activation likelihood estimation (ALE) approach for coordinate-based meta-analyses of neuroimaging results (Turkeltaub et al. 2002; Eickhoff et al. 2009, 2012) to identify brain regions that are consistently implicated in affective and introspective processing, respectively, across a large number of experiments, resulting in a robust functional-anatomic model of the ISA network. In particular, we performed a conjunction analysis across two meta-analyses which investigated statistical convergence of functional neuroimaging results for the so-called “default mode network” relevant for self-referential cognition or introspection (DMN) and emotional processing (EMO) across a large number of studies (DMN: $n = 1474$; EMO: $n = 533$) (for details see Schilbach et al. 2012). The resulting ISA network included the anterior cingulate cortex (ACC), left amygdala (AmyL), dorsomedial prefrontal cortex (dmPFC), precuneus (PrC) and subgenual cingulate cortex (SGC; see Figure 1A and Table 1). We furthermore performed a control analysis to ensure that the differences in connectivity between patients and controls were specific to affect processing and introspection and not part of a more general disease pattern. To this end, we used a network that previously has been associated with decoding degraded speech based on prior expectations (Clos et al. 2012) as speech perception should not be related to socio-affective aspects of depression. This network was composed of the left inferior frontal gyrus (IFG, area 44/45), the left middle temporal gyrus (MTG), the left angular gyrus (AG) and the left thalamus.

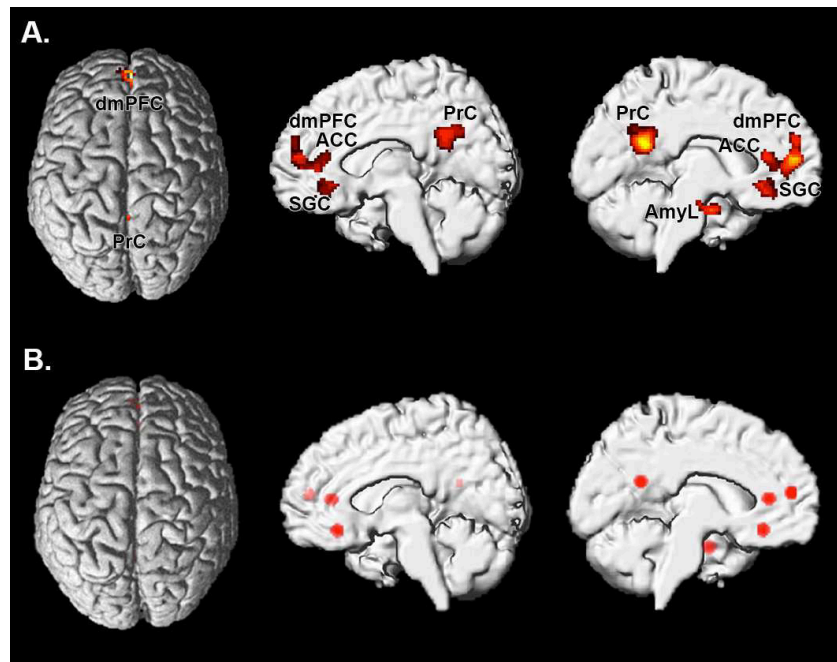


Figure 1

Significant results of the ALE meta-analysis (A) and volumes of interest (VOIs) used for the functional connectivity analysis in healthy controls and patients based on the results of the ALE meta-analysis (B) ACC: anterior cingulate cortex; AmyL: left Amygdala; dmPFC: dorsomedial prefrontal cortex; PrC: precuneus; SGC: subgenual cingulate cortex.

Table 1: Activation peaks of ALE meta-analysis

Macroanatomical location	MNI coordinates		
	x	y	z
Subgenual cingulate cortex (SGC)	0	32	-12
Anterior cingulate cortex (ACC)	0	36	10
Amygdala (AmyL)	-22	-6	-24
Precuneus (PrC)	-4	-54	22
Dorsomedial prefrontal cortex (dmPFC)	-2	52	14

Resting state fMRI data: imaging & preprocessing

Functional connectivity of the ISA and the control network was investigated using resting state fMRI images acquired in 57 patients with major depression and 57 age-matched, healthy volunteers without any record of neurological or psychiatric disorders (for group characteristics see Table 2). Diagnosis was confirmed by clinical examination of the attending psychiatrist in accordance with the International Classification of Diseases (ICD-10), the Hamilton Rating Scale for Depression (HAM-D; Hedlung & Vieweg 1979) or the Montgomery-

Asberg Depression Rating Scale (MADRS; Montgomery et al. 1979), as well as the Beck Depression Inventory (BDI-II; Hautzinger et al., 2006) as a self-report measurement of symptom severity. All subjects gave written consent to participate in the study as approved by the ethics committees of the University of Aachen and the University of Goettingen. Participants were instructed to lie still during the scan session and to let their mind wander, but not to fall asleep. The latter was confirmed during a post-scan debriefing interview.

For each subject 250 (Aachen) or 156 (Goettingen) resting state EPI images were acquired using blood-oxygen-level-dependent (BOLD) contrast [gradient-echo EPI pulse sequence, Aachen: TR=2.2 s, TE=30 ms, flip angle=90°, in-plane resolution=3.1 x 3.1 mm², 36 axial slices (3.1 mm thickness) and Goettingen: TR=2.0 s, TE=30 ms, flip angle=70°, in-plane resolution=3.0 x 3.0 mm², 33 axial slices (3.0 mm thickness), each covering the entire brain]. Prior to further processing (using SPM8, www.fil.ion.ucl.ac.uk/spm) the first four images were discarded allowing for magnetic field saturation. The EPI images were first corrected for head movement by affine registration using a two-pass procedure. The mean EPI image for each subject was then spatially normalized to the MNI single subject template using the "unified segmentation" approach (Ashburner and Friston, 2005), the ensuing deformation field was applied to the individual EPI volumes and the output images were smoothed by a 5-mm FWHM Gaussian kernel. In order to reduce spurious correlations by confounds such as physiological noise and motion (cf. Bandettini & Bullmore, 2008), variance that could be explained by first- or second-order effects of the following nuisance variables was removed from each voxel's time series: i) the six motion parameters derived from the image realignment ii) their first derivative iii) mean grey, white matter and CSF signal intensity (Reetz et al., 2012; Jakobs et al., 2012). These corrections have been shown (Chai et al. 2012) to increase specificity and sensitivity of the analyses and may be used to robustly identify

group-differences in resting-state functional connectivity (cf. Sommer et al., 2012). Data was then band pass filtered preserving frequencies between 0.01 and 0.08 Hz (Fox & Raichle 2007; zu Eulenburg et al., 2012). The time course for each of the regions identified in the meta-analysis described above (Figure 1A, Table 1) or in the control analysis (language processing) was then extracted for each subject as the first eigenvariate of all grey-matter voxels located within 5 mm of the respective peak coordinate (Figure 1B).

Table 2: Group characteristics

	Control group	Patient group
Number of participants	57	57
Gender ratio	M: 30; F: 27	M: 30; F: 27
Mean age (SD)	36.74 (11.48)	36.89 (11.40)
Mean years of education (SD)	13.78 (2.93)	13.81 (3.39)
Mean BDI score (SD)	1.33 (2.34)	20.12 (9.18)
Mean HRSD (SD) Aachen (n = 30)	-	12.20 (8.01)
Mean MADRS (SD) Goettingen (n = 27)	-	15.17 (8.07)
Mean age of depression onset (SD)	-	25.74 (10.36)
Mean depression duration in years (SD)	-	9.09 (9.35)
Mean number of depressive episodes (SD)	-	3.23 (3.03)

SD: standard deviation; M: male; F: female; BDI: Beck Depression Inventory II; HRSD: Hamilton Rating Scale for Depression; MADRS: Montgomery-Asberg Depression Rating Scale.

Resting state fMRI data: individual & group level analysis

For each subject [and analysis, ISA or language network] we computed linear (Pearson) correlation coefficients between extracted time series. These voxel-wise correlation coefficients were then transformed into Fisher's z scores representing the functional connectivity for each connection in each subject. Variance that could be explained by the factor "site" (Aachen / Goettingen) or its interaction with the factor "diagnosis" was then removed from these scores to accommodate potential differences between sites caused, e.g., by scanner setup, in spite of identical hardware and very similar protocols. Group comparison between patients and controls was then performed by a "pseudo-exact" non-parametric approach using 10,000 realizations of the null hypothesis (label exchangeability)

in a Monte-Carlo simulation (Kennedy 1995; Nichols & Holmes 2002). Results were thresholded at a global posterior probability threshold of $P > 0.95$, i.e. 95% confidence for true differences between groups.

To assess a possible relationship between functional connectivity and symptom severity -as indexed by BDI scores- Spearman rank-correlation analyses were performed. Spearman rank-correlations were chosen as the majority of the data violated normal distribution. In order to assess the possible effects of disease onset and duration we performed additional analyses, which compared functional connectivity in subgroups of our patient sample. The subgroups were assembled by using a median split procedure which differentiates between those patients with early and late depression onset and, secondly, with short and long disease duration. Finally, in a supplementary analysis, we performed a median split on the patients based on the MADRS or HAMD scores to test for differences between more or less severely affected as deemed by these clinical rating inventories.

RESULTS

Resting-state functional connectivity differences between patients with major depression and healthy controls were assessed between all nodes of the introspective socio-affective (ISA; Figure 1) network, namely between anterior cingulate cortex (ACC), left amygdala (AmyL), dorsomedial prefrontal cortex (dmPFC), precuneus (PrC) and subgenual cingulate cortex (SGC). Significant differences in resting state functional connectivity between patients and controls were found along several edges of this network, with patients showing higher neurofunctional coupling than control participants in all cases. In particular, patients with depression demonstrated higher functional connectivity (less negative) between ACC and the AmyL ($P>0.996$, Cohen's d : 0.49). Furthermore increased functional connectivity (more positive) in patients compared to controls could be found between ACC and the PrC ($P>0.984$, Cohen's d : 0.41), AmyL and PrC ($P>0.995$, Cohen's d : 0.46), SGC and ACC ($P>0.991$, Cohen's d : 0.44) and between SGC and PrC ($P>0.996$, Cohen's d : 0.47) (see Figure 2 and 4).

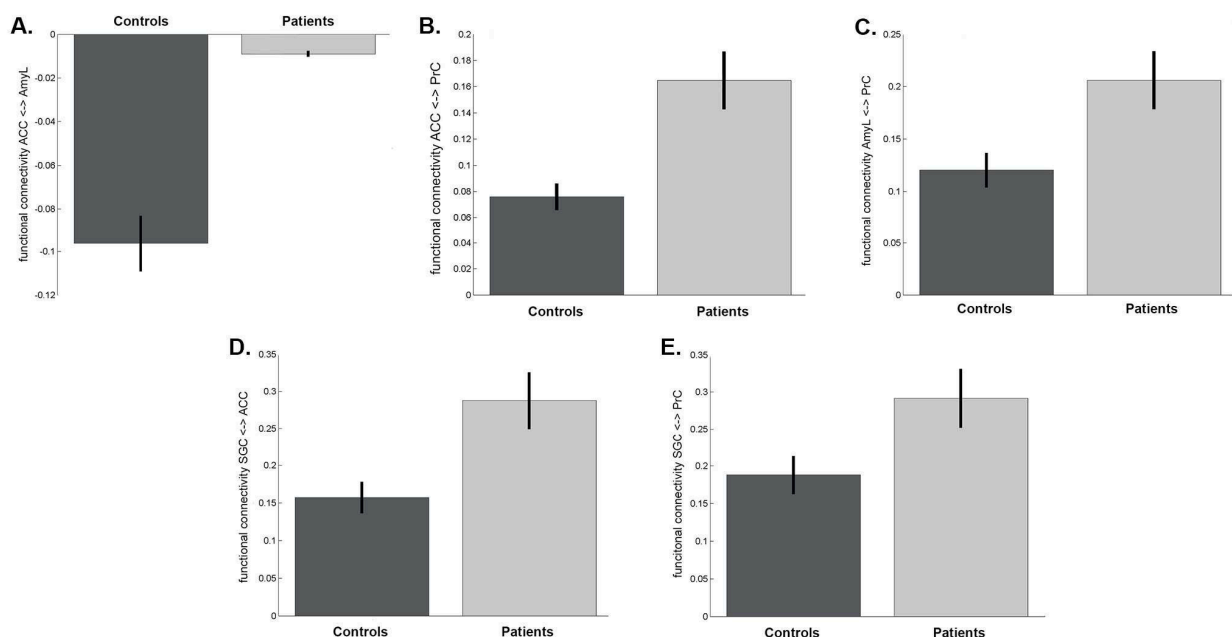


Figure 2

Significant results of the functional connectivity analysis in the control and patient group between: (A) anterior cingulate cortex (ACC) and amygdala (AmyL); (B) ACC and precuneus (PrC); (C) AmyL and PrC; (D) subgenual cingulate cortex (SGC) and ACC; (E) SGC and the precuneus PrC. Error bars depict standard error of the mean.

Group differences between the remaining connections did not reach the posterior probability threshold of $P > 0.95$ for true differences. All these effects were extremely similar across sites (Aachen/Goettingen; see supplementary Figure S1). For the control network, no differences in connectivity between patients and controls were observed (all $P < 0.72$, maximum Cohen's d value = 0.11; see supplementary Figure S2).

The second aim was to investigate a possible relationship of symptom severity –as measured by the BDI– and functional connectivity in the ISA network. This additional analysis demonstrated a positive and statistically significant relationship between BDI scores and functional connectivity for the connection of dmPFC and ACC ($p < 0.036$, $r = 0.23$) and of SGC and ACC ($p < 0.032$, $r = 0.23$) across all subjects (Figure 3A, 3B and 4. The correlation of functional connectivity of dmPFC and ACC with BDI scores remained significant when calculated in the patient group alone ($p < 0.041$, $r = 0.28$; Figure 3C). For the control network, no significant correlations between the BDI score and functional connectivity were observed (all p -values > 0.43 , maximum $r = 0.09$).

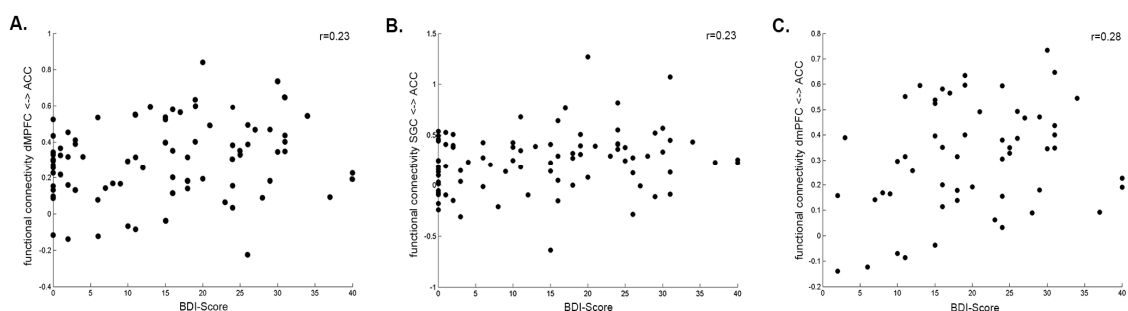


Figure 3

Correlation plots of functional connectivity and BDI scores across all subjects (A and B) and only in the patient group (C). A and C: Correlation with functional connectivity between dorsomedial prefrontal cortex (dmPFC) and anterior cingulate cortex (ACC); B: Correlation with functional connectivity between subgenual cingulate cortex (SGC) and ACC.

When comparing patient subgroups of short and long duration (≥ 5 years) of illness (Figure S3), functional connectivity between ACC and PrC and between ACC and SGC was significantly higher in the subgroup with longer disease history. Patients with later onset

(age ≥ 24) of depression showed higher connectivity between SGC and PrC in comparison to the group with early onset. Only, functional coupling between PrC and AmyL was increased for both groups with long duration and late onset of disease. Finally, when comparing patients with low vs high scores on the MADRS and HAMD scales, we observed that for most connections patients with higher clinical scores trended to also show more extreme differences relative to healthy controls, but the difference between both subgroups did not meet the statistical threshold (see supplementary Figure S4).

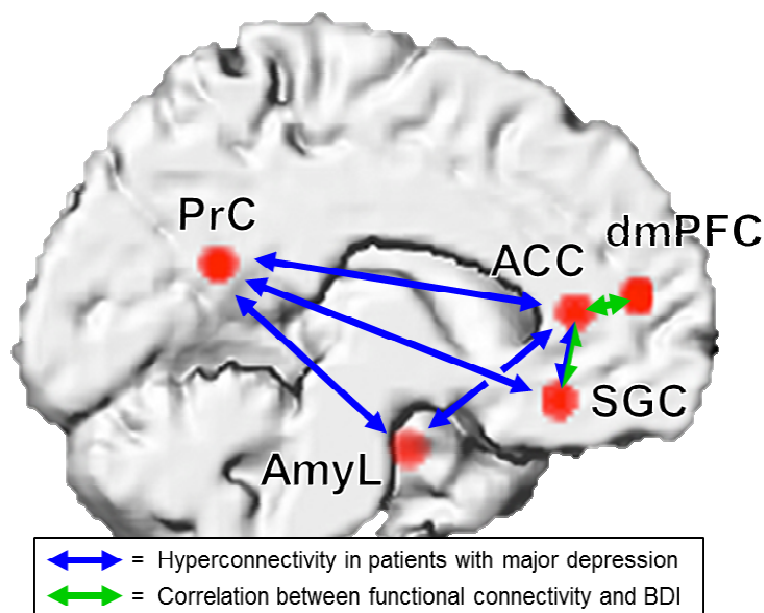


Figure 4

Schematic depiction of functional connectivity differences in patients and controls and correlation between functional connectivity and BDI scores.

DISCUSSION

Here, we made use of a novel, model-based approach to investigate resting state functional connectivity in the ISA network in patients with depression. This investigation was based on the idea that depression is characterized by affective symptoms and alterations of self-referential cognition and introspection, which impair successful participation in social interaction, thereby further contributing to depressive symptomatology (Liu et al. 2006; McCullough et al. 2010, 2011; Cusi et al. 2011). Our analysis approach allows circumventing problems to robustly identify relevant connectivity networks in an unbiased fashion (cf. Zuo et al. 2010), which have hampered the use and reliability of fMRI resting state studies in the past. Furthermore, it is often unclear whether the derived functional interpretations of network alterations are valid since non-standardized approaches cannot allow for the specific investigation of a functional system. In order to provide a robust and standardized assessment of possible alterations of functional connectivity in depression, we have employed a hypothesis-driven and model-based approach, which investigates functional connectivity of an introspective socio-affective (ISA) network. Our network analysis demonstrates striking, region-specific differences in functional connectivity profiles of the ISA network when comparing the control and the patient group. As a key finding, our analysis demonstrates markedly higher connectivity in individuals with depression as compared to healthy individuals, which is consistent with an emerging “hyperconnectivity hypothesis” of depression (Figure 4; cf. Perrin et al. 2012). Importantly, the non-significant group comparison as part of a control analysis demonstrates that the observed differences are specific to the introspection- and affect-related network and not manifestations of a more general pathology. Furthermore, the control analysis indicates that preprocessing did not introduce any artificial group differences. If the global signal regression employed in the

preprocessing of the resting state data had, indeed, differentially affected the resting state data as proposed by simulation studies (e.g. Saad et al. 2012), these effects should equally have introduced differences within the control network of areas involved in language processing.

With respect to the ISA network, our study demonstrates higher (less negative) connectivity between ACC and the AmyL in the patient as compared to the control group. Functional coupling of these two regions is known to play a crucial role in the experience and modulation of affect (e.g. Banks et al. 2007) and may, hence, relate to negative affect and deficits in emotion regulation as key factors in affective disorders (e.g. Kanske et al. 2012). In line with this view, personality traits related to affective disorders have been shown to correlate with aberrant ACC-amygdala connectivity (Cremers et al. 2010; Cisler et al. 2012; Fulwiler et al. 2012). Our finding of hyperconnectivity between these regions is moreover consistent with recent MEG evidence for increased ACC-amygdala connectivity in major depression (Lu et al. 2012). Conversely, antidepressant drugs, which affect the serotonergic or noradrenergic system, have been shown to reduce resting state connectivity between the amygdala and frontal regions compared to placebo (McCabe et al. 2011), which might help to return to a functional optimum of interregional connectivity. Furthermore, it has been shown that genetic polymorphisms, which impact cerebral serotonin turnover, also influence cingulate-amygdala interactions (Pezewas et al. 2005). The suggestion of a functional optimum of interregional connectivity may also help to explain why a connectivity increase in the case of pathology -as observed in our patient sample- may actually lead to a decrease in function.

The increased connectivity between ACC and the PrC in patients is consistent with previous research demonstrating elevated resting state connectivity within the so-called “default

mode" network in depression (Sheline et al. 2010; Gaffrey et al. 2012; Lasalle-Lagadec et al. 2012; Alexopoulos et al. 2012). Based on an analysis rooted in a Bayesian perspective on the brain, which assumes that the brain uses internal hierarchical models to predict its sensory inputs and tries to minimize the ensuing prediction error (Carhart-Harris & Friston 2010), activity in this network has been related to self-referential cognition and prospective cognition (Timmermans et al. 2012). The evaluation of internal and external cues, remembering the past and planning of the future are deemed important for and may also be shaped by the participation in social interactions (Buckner & Carroll 2007; Schilbach et al. 2008, 2010; Timmermans et al. 2012). Therefore, hyperconnectivity of this network may specifically contribute to alterations of introspection and rumination in depression: Following the idea by Schacter et al. (2007) that "prospective memory", i.e. the imagination and projection of future events, may be mediated by these regions, the observed aberrations may well also relate to loss of perspective, another core symptom of depression. Following the idea of "prospective memory" served by the posterior midline, in particular dysconnectivity of the PrC may thus underlie the difficulties with optimistic future-oriented thoughts and the ruminations typical of affective disorders (Whitfield-Gabrieli & Ford 2012; Zhu et al. 2012). An additional analysis targeting the effect of disease duration demonstrated that long as compared to short duration leads to a more pronounced increase in functional connectivity of this region, which is consistent with the notion that chronic forms of depression might be most strongly linked to the feeling of helplessness extending to future thoughts and social interactions (McCullough et al. 2011). Similar findings were also observed for the connections between SGC and ACC and AmyL and the PrC.

In patients, the PrC also showed increased coupling with the amygdala, a result that resembles previous findings on the effect of social stress on functional connectivity (Veer et

al. 2011). Here the authors suggested that the increased connectivity between amygdala, posterior cingulate cortex and precuneus in response to social stress, could be interpreted as the “processing and regulation of emotions”. Connectivity changes between these regions might, therefore, serve as a neural marker for vulnerability to stress (Veer et al. 2011). On the other hand, the precuneus has also been linked to autobiographical memory, self-reflection and mentalization, processes which are known to contribute to emotion regulation (e.g. Koenigsberg et al. 2010; Strawn et al. 2012). Consequently, the idea of a functional optimum in connectivity profiles might seem tempting and could help to explain why increasing levels of connectivity could first contribute to regulatory processes, while further increases could lead to functional deficits.

Finally, our analysis demonstrated hyperconnectivity between SGC and ACC as well as SGC and the PrC. Importantly, we also found evidence for a significant positive relationship between BDI scores and functional connectivity for the connection of SGC and ACC. The SGC, has been implicated as a neurofunctional “hot spot” in affective disorders. Seminal studies by Mayberg and colleagues (2005) have demonstrated evidence for hyperactivity of SGC in treatment-resistant populations of depressed patients (Johansen-Berg et al. 2008; Konarski et al. 2009) and have documented that deep brain stimulation (DBS) of subgenual cingulate white matter results in dramatic remission in some previously treatment-resistant patients. Consistently, recent evidence demonstrates that electroconvulsive therapy (ECT) in major depression weakens symptomatology while reducing serotonin-1A receptor binding in the subgenual part of cingulate cortex (Lanzenberger et al. 2012) as well as decreasing left dorsolateral prefrontal connectivity (Perrin et al. 2012). Similarly, transcranial magnetic stimulation over dorsolateral prefrontal cortex (DLPFC) appears to be effective by influencing SGC, whose activity is anti-correlated to DLPFC (Fox et al. 2012). Furthermore,

differences in the serotonin transporter genotype (5-HTTLPR) have been shown to modulate brain responses to emotional faces such that non-depressed, short variant homozygotes demonstrate an absence of subgenual deactivation, which parallels findings in clinically depressed individuals (O’Nions et al. 2011). Activation differences in response to social stimuli also appear to be linked to differences in empathic concern (Zahn et al. 2009), which may, in turn, perpetuate social interaction difficulties. Therefore, the results of the current study extend previous results by showing that depression is not only associated with SGC hyperactivity but also with hyperconnectivity to ACC and PrC.

Our results also demonstrated a relationship between symptom severity and functional connectivity of the ACC with the SGC and the dmPFC (Figure 3A, 3B and 4) across all participants. These additional findings add weight to the argument that connectivity of the ISA is altered in states of depression and that such neurofunctional alterations might actually fall on to a spectrum similar to how this is assumed to be the case in other psychiatric disorders. With regard to the correlation of dmPFC-ACC connectivity with symptom severity within the patient group, it is interesting to note that these two regions co-activate during tasks that require an automatic adjustment of one’s actions to that of another agent (Schilbach et al. 2011). States of depression might, therefore, interfere with such rapid interpersonal adjustments by altering the underlying neurocircuitry, thereby producing disorder-related social impairments (e.g. Erickson & Hellerstein 2011). Furthermore, alterations of frontopolar brain activity have been discussed as indexing a trait abnormality in socio-emotional processing that might be associated with a vulnerability to depression (Elliott et al. 2012).

In terms of an outlook to future research, we suggest that using model-based analyses of resting state fMRI data could be a clinically feasible, robust, standardized and, therefore,

powerful way to document treatment-induced changes at the neural level in order to further explore the relationship between clinical symptoms (low mood, ruminations, social interaction) and functional connectivity changes in the ISA network (cf. Frewen et al. 2008; Marroquin 2011; Gaffrey et al. 2012). Furthermore, this approach might help to shed new light on the effectiveness and selection criteria of psychotherapeutic, drug-based and electroconvulsive treatments and could, therefore, be developed towards the prediction of treatment outcome.

ACKNOWLEDGEMENTS

L.S. was supported by the Koeln Fortune Program of the Medical Faculty at the University of Cologne and by the Volkswagen Foundation.

S.B.E. was funded by the Human Brain Project (R01-MH074457-01A1), the DFG (IRTG 1328) and the Initiative and Networking Fund of the Helmholtz Association within the Helmholtz Alliance on Systems Biology (Human Brain Model).

We thank Maria Keil, Kristina Weber, Sarah Trost and Peter Dechent for help in data acquisition in Goettingen.

REFERENCES

- Alexopoulos, G. S., Hoptman, M. J., Kanellopoulos, D., Murphy, C. F., Lim, K. O., & Gunning, F. M. (2012). Functional connectivity in the cognitive control network and the default mode network in late-life depression. *J Affect Disord*, *139*(1), 56-65.
- Ashburner, J., & Friston, K. J. (2005). Unified segmentation. *Neuroimage*, *26*(3), 839-851.
- Bandettini, P. A., & Bullmore, E. (2008). Endogenous oscillations and networks in functional magnetic resonance imaging. *Hum Brain Mapp*, *29*(7), 737-739.
- Banks, S. J., Eddy, K. T., Angstadt, M., Nathan, P. J., & Phan, K. L. (2007). Amygdala-frontal connectivity during emotion regulation. *Soc Cogn Affect Neurosci*, *2*(4), 303-312.
- Behrens, T. E., Hunt, L. T., & Rushworth, M. F. (2009). The computation of social behavior. *Science*, *324*(5931), 1160-1164.
- Bistricky, S. L., Ingram, R. E., & Atchley, R. A. (2011). Facial affect processing and depression susceptibility: cognitive biases and cognitive neuroscience. *Psychol Bull*, *137*(6), 998-1028.
- Carhart-Harris, R. L., & Friston, K. J. (2010). The default-mode, ego-functions and free-energy: a neurobiological account of Freudian ideas. *Brain*, *133*(Pt 4), 1265-1283.
- Chai, X. J., Castanon, A. N., Ongur, D., & Whitfield-Gabrieli, S. (2012). Anticorrelations in resting state networks without global signal regression. *Neuroimage*, *59*(2), 1420-1428.
- Chester, D. S., Pond, R. S. J., Richman, S. B., & Dewall, C. N. (2012). The optimal calibration hypothesis: how life history modulates the brain's social pain network. *Front Evol Neurosci*, *4*, 10.
- Cisler, J. M., James, G. A., Tripathi, S., Mletzko, T., Heim, C., Hu, X. P. et al. (2012). Differential functional connectivity within an emotion regulation neural network among individuals resilient and susceptible to the depressogenic effects of early life stress. *Psychol Med*, 1-12.
- Clos, M., Langner, R., Meyer, M., Oechslin, M. S., Zilles, K., & Eickhoff, S. B. (2012). Effects of prior information on decoding degraded speech: An fMRI study. *Hum Brain Mapp*.
- Cremers, H. R., Demenescu, L. R., Aleman, A., Renken, R., van Tol, M. J., van der Wee, N. J. et al. (2010). Neuroticism modulates amygdala-prefrontal connectivity in response to negative emotional facial expressions. *Neuroimage*, *49*(1), 963-970.
- Cusi, A. M., Macqueen, G. M., Spreng, R. N., & McKinnon, M. C. (2011). Altered empathic responding in major depressive disorder: relation to symptom severity, illness burden, and psychosocial outcome. *Psychiatry Res*, *188*(2), 231-236.
- Derntl, B., Seidel, E. M., Eickhoff, S. B., Kellermann, T., Gur, R. C., Schneider, F. et al. (2011). Neural correlates of social approach and withdrawal in patients with major depression. *Soc Neurosci*, *6*(5-6), 482-501.
- Eickhoff, S. B., Bzdok, D., Laird, A. R., Kurth, F., & Fox, P. T. (2012). Activation likelihood estimation meta-analysis revisited. *Neuroimage*, *59*(3), 2349-2361.

- Eickhoff, S. B., Bzdok, D., Laird, A. R., Roski, C., Caspers, S., Zilles, K. et al. (2011). Co-activation patterns distinguish cortical modules, their connectivity and functional differentiation. *Neuroimage*, 57(3), 938-949.
- Eickhoff, S. B., Laird, A. R., Grefkes, C., Wang, L. E., Zilles, K., & Fox, P. T. (2009). Coordinate-based activation likelihood estimation meta-analysis of neuroimaging data: a random-effects approach based on empirical estimates of spatial uncertainty. *Hum Brain Mapp*, 30(9), 2907-2926.
- Erickson, G., & Hellerstein, D. J. (2011). Behavioral activation therapy for remediating persistent social deficits in medication-responsive chronic depression. *J Psychiatr Pract*, 17(3), 161-169.
- Fleming, S. M., Weil, R. S., Nagy, Z., Dolan, R. J., & Rees, G. (2010). Relating introspective accuracy to individual differences in brain structure. *Science*, 329(5998), 1541-1543.
- Fox, M. D., Buckner, R. L., White, M. P., Greicius, M. D., & Pascual-Leone, A. (2012). Efficacy of Transcranial Magnetic Stimulation Targets for Depression Is Related to Intrinsic Functional Connectivity with the Subgenual Cingulate. *Biol Psychiatry*.
- Fox, M. D., & Raichle, M. E. (2007). Spontaneous fluctuations in brain activity observed with functional magnetic resonance imaging. *Nat Rev Neurosci*, 8(9), 700-711.
- Frewen, P. A., Dozois, D. J., & Lanius, R. A. (2008). Neuroimaging studies of psychological interventions for mood and anxiety disorders: empirical and methodological review. *Clin Psychol Rev*, 28(2), 228-246.
- Fulwiler, C. E., King, J. A., & Zhang, N. (2012). Amygdala-orbitofrontal resting-state functional connectivity is associated with trait anger. *Neuroreport*, 23(10), 606-610.
- Gaffrey, M. S., Luby, J. L., Botteron, K., Repovs, G., & Barch, D. M. (2012). Default mode network connectivity in children with a history of preschool onset depression. *J Child Psychol Psychiatry*.
- Goulden, N., McKie, S., Thomas, E. J., Downey, D., Juhasz, G., Williams, S. R. et al. (2012). Reversed Frontotemporal Connectivity During Emotional Face Processing in Remitted Depression. *Biol Psychiatry*.
- Greicius, M. D., Flores, B. H., Menon, V., Glover, G. H., Solvason, H. B., Kenna, H. et al. (2007). Resting-state functional connectivity in major depression: abnormally increased contributions from subgenual cingulate cortex and thalamus. *Biol Psychiatry*, 62(5), 429-437.
- Greicius, M. D., Krasnow, B., Reiss, A. L., & Menon, V. (2003). Functional connectivity in the resting brain: a network analysis of the default mode hypothesis. *Proc Natl Acad Sci U S A*, 100(1), 253-258.
- Hammar, A., & Ardal, G. (2009). Cognitive functioning in major depression--a summary. *Front Hum Neurosci*, 3, 26.
- Jacobs, R. H., Renken, R., Aleman, A., & Cornelissen, F. W. (2012). The amygdala, top-down effects, and selective attention to features. *Neurosci Biobehav Rev*.
- Johansen-Berg, H., Gutman, D. A., Behrens, T. E., Matthews, P. M., Rushworth, M. F., Katz, E. et al. (2008). Anatomical connectivity of the subgenual cingulate region targeted with deep brain stimulation for treatment-resistant depression. *Cereb Cortex*, 18(6), 1374-1383.

- Kanske, P., Heissler, J., Schonfelder, S., & Wessa, M. (2012). Neural correlates of emotion regulation deficits in remitted depression: the influence of regulation strategy, habitual regulation use, and emotional valence. *Neuroimage*, 61(3), 686-693.
- Kashdan, T. B., & Roberts, J. E. (2007). Social anxiety, depressive symptoms, and post-event rumination: affective consequences and social contextual influences. *J Anxiety Disord*, 21(3), 284-301.
- Koenigsberg, H. W., Fan, J., Ochsner, K. N., Liu, X., Guise, K., Pizzarello, S. et al. (2010). Neural correlates of using distancing to regulate emotional responses to social situations. *Neuropsychologia*, 48(6), 1813-1822.
- Konarski, J. Z., Kennedy, S. H., Segal, Z. V., Lau, M. A., Bieling, P. J., McIntyre, R. S. et al. (2009). Predictors of nonresponse to cognitive behavioural therapy or venlafaxine using glucose metabolism in major depressive disorder. *J Psychiatry Neurosci*, 34(3), 175-180.
- Kriegeskorte, N., Simmons, W. K., Bellgowan, P. S., & Baker, C. I. (2009). Circular analysis in systems neuroscience: the dangers of double dipping. *Nat Neurosci*, 12(5), 535-540.
- Lanzenberger, R., Baldinger, P., Hahn, A., Ungersboeck, J., Mitterhauser, M., Winkler, D. et al. (2012). Global decrease of serotonin-1A receptor binding after electroconvulsive therapy in major depression measured by PET. *Mol Psychiatry*.
- Lassalle-Lagadec, S., Sibon, I., Dilharreguy, B., Renou, P., Fleury, O., & Allard, M. (2012). Subacute default mode network dysfunction in the prediction of post-stroke depression severity. *Radiology*, 264(1), 218-224.
- Lederbogen, F., Kirsch, P., Haddad, L., Streit, F., Tost, H., Schuch, P. et al. (2011). City living and urban upbringing affect neural social stress processing in humans. *Nature*, 474(7352), 498-501.
- Liu, Y. L. (2006). Paternal/maternal attachment, peer support, social expectations of peer interaction, and depressive symptoms. *Adolescence*, 41(164), 705-721.
- Lu, Q., Li, H., Luo, G., Wang, Y., Tang, H., Han, L. et al. (2012). Impaired prefrontal-amygdala effective connectivity is responsible for the dysfunction of emotion process in major depressive disorder: A dynamic causal modeling study on MEG. *Neurosci Lett*.
- Marroquin, B. (2011). Interpersonal emotion regulation as a mechanism of social support in depression. *Clin Psychol Rev*, 31(8), 1276-1290.
- Mayberg, H. S., Lozano, A. M., Voon, V., McNeely, H. E., Seminowicz, D., Hamani, C. et al. (2005). Deep brain stimulation for treatment-resistant depression. *Neuron*, 45(5), 651-660.
- McCullough, J. P. J. (2003). Treatment for chronic depression using Cognitive Behavioral Analysis System of Psychotherapy (CBASP). *J Clin Psychol*, 59(8), 833-846.
- McCullough, J. P. J., Lord, B. D., Conley, K. A., & Martin, A. M. (2010). A method for conducting intensive psychological studies with early-onset chronically depressed patients. *Am J Psychother*, 64(4), 317-337.
- McCullough, J. P. J., Lord, B. D., Martin, A. M., Conley, K. A., Schramm, E., & Klein, D. N. (2011). The significant other history: an interpersonal-emotional history procedure used with the early-onset chronically depressed patient. *Am J Psychother*, 65(3), 225-248.

- Niven, K., Totterdell, P., Holman, D., & Headley, T. (2012). Does regulating others' feelings influence people's own affective well-being? *J Soc Psychol*, 152(2), 246-260.
- O'Nions, E. J., Dolan, R. J., & Roiser, J. P. (2011). Serotonin transporter genotype modulates subgenual response to fearful faces using an incidental task. *J Cogn Neurosci*, 23(11), 3681-3693.
- Perrin, J. S., Merz, S., Bennett, D. M., Currie, J., Steele, D. J., Reid, I. C. et al. (2012). Electroconvulsive therapy reduces frontal cortical connectivity in severe depressive disorder. *Proc Natl Acad Sci U S A*, 109(14), 5464-5468.
- Pezawas, L., Meyer-Lindenberg, A., Drabant, E. M., Verchinski, B. A., Munoz, K. E., Kolachana, B. S. et al. (2005). 5-HTTLPR polymorphism impacts human cingulate-amygdala interactions: a genetic susceptibility mechanism for depression. *Nat Neurosci*, 8(6), 828-834.
- Poldrack, R. A. (2006). Can cognitive processes be inferred from neuroimaging data? *Trends Cogn Sci*, 10(2), 59-63.
- Poldrack, R. A. (2011). Inferring mental states from neuroimaging data: from reverse inference to large-scale decoding. *Neuron*, 72(5), 692-697.
- Saad, Z. S., Gotts, S. J., Murphy, K., Chen, G., Jo, H. J., Martin, A. et al. (2012). Trouble at rest: how correlation patterns and group differences become distorted after global signal regression. *Brain Connect*, 2(1), 25-32.
- Schacter, D. L., Addis, D. R., & Buckner, R. L. (2007). Remembering the past to imagine the future: the prospective brain. *Nat Rev Neurosci*, 8(9), 657-661.
- Schilbach, L., Bzdok, D., Timmermans, B., Fox, P. T., Laird, A. R., Vogeley, K. et al. (2012). Introspective minds: using ALE meta-analyses to study commonalities in the neural correlates of emotional processing, social & unconstrained cognition. *PLoS One*, 7(2), e30920.
- Schilbach, L., Eickhoff, S. B., Cieslik, E., Shah, N. J., Fink, G. R., & Vogeley, K. (2011). Eyes on me: an fMRI study of the effects of social gaze on action control. *Soc Cogn Affect Neurosci*, 6(4), 393-403.
- Schilbach, L., Wilms, M., Eickhoff, S. B., Romanzetti, S., Tepest, R., Bente, G. et al. (2010). Minds made for sharing: initiating joint attention recruits reward-related neurocircuitry. *J Cogn Neurosci*, 22(12), 2702-2715.
- Schilbach, L., Eickhoff, S. B., Rotarska-Jagiela, A., Fink, G. R., & Vogeley, K. (2008). Minds at rest? Social cognition as the default mode of cognizing and its putative relationship to the "default system" of the brain. *Conscious Cogn*, 17(2), 457-467.
- Shehzad, Z., Kelly, A. M., Reiss, P. T., Gee, D. G., Gotimer, K., Uddin, L. Q. et al. (2009). The resting brain: unconstrained yet reliable. *Cereb Cortex*, 19(10), 2209-2229.
- Sheline, Y. I., Price, J. L., Yan, Z., & Mintun, M. A. (2010). Resting-state functional MRI in depression unmasks increased connectivity between networks via the dorsal nexus. *Proc Natl Acad Sci U S A*, 107(24), 11020-11025.
- Simon, G. E., VonKorff, M., Piccinelli, M., Fullerton, C., & Ormel, J. (1999). An international study of the relation between somatic symptoms and depression. *N Engl J Med*, 341(18), 1329-1335.

- Sobin, C., & Sackeim, H. A. (1997). Psychomotor symptoms of depression. *Am J Psychiatry*, 154(1), 4-17.
- The ICD-10 classification of mental and behavioural disorders: clinical descriptions and diagnostic guidelines (1992). Geneva: World Health Organization (WHO).
- Timmermans, B., Schilbach, L., Pasquali, A., & Cleeremans, A. (2012). Higher order thoughts in action: consciousness as an unconscious re-description process. *Philos Trans R Soc Lond B Biol Sci*, 367(1594), 1412-1423.
- Turkeltaub, P. E., Eden, G. F., Jones, K. M., & Zeffiro, T. A. (2002). Meta-analysis of the functional neuroanatomy of single-word reading: method and validation. *Neuroimage*, 16(3 Pt 1), 765-780.
- Veer, I. M., Oei, N. Y., Spinhoven, P., van Buchem, M. A., Elzinga, B. M., & Rombouts, S. A. (2011). Beyond acute social stress: increased functional connectivity between amygdala and cortical midline structures. *Neuroimage*, 57(4), 1534-1541.
- Venzala, E., Garcia-Garcia, A. L., Elizalde, N., Delagrangé, P., & Tordera, R. M. (2012). Chronic social defeat stress model: behavioral features, antidepressant action, and interaction with biological risk factors. *Psychopharmacology (Berl)*.
- Whitfield-Gabrieli, S., & Ford, J. M. (2012). Default mode network activity and connectivity in psychopathology. *Annu Rev Clin Psychol*, 8, 49-76.
- Zahn, R., de Oliveira-Souza, R., Bramati, I., Garrido, G., & Moll, J. (2009). Subgenual cingulate activity reflects individual differences in empathic concern. *Neurosci Lett*, 457(2), 107-110.
- Zeng, L. L., Shen, H., Liu, L., Wang, L., Li, B., Fang, P. et al. (2012). Identifying major depression using whole-brain functional connectivity: a multivariate pattern analysis. *Brain*, 135(Pt 5), 1498-1507.
- Zhang, S., & Li, C. S. (2012). Functional connectivity mapping of the human precuneus by resting state fMRI. *Neuroimage*, 59(4), 3548-3562.
- Zhu, X., Wang, X., Xiao, J., Liao, J., Zhong, M., Wang, W. et al. (2012). Evidence of a dissociation pattern in resting-state default mode network connectivity in first-episode, treatment-naive major depression patients. *Biol Psychiatry*, 71(7), 611-617.
- Zuo, X. N., Kelly, C., Adelstein, J. S., Klein, D. F., Castellanos, F. X., & Milham, M. P. (2010). Reliable intrinsic connectivity networks: test-retest evaluation using ICA and dual regression approach. *Neuroimage*, 49(3), 2163-2177.
- zu Eulenburg, P., Caspers, S., Roski, C., & Eickhoff, S. B. (2012). Meta-analytical definition and functional connectivity of the human vestibular cortex. *Neuroimage*, 60(1), 162-169.

SUPPLEMENTAL FIGURES

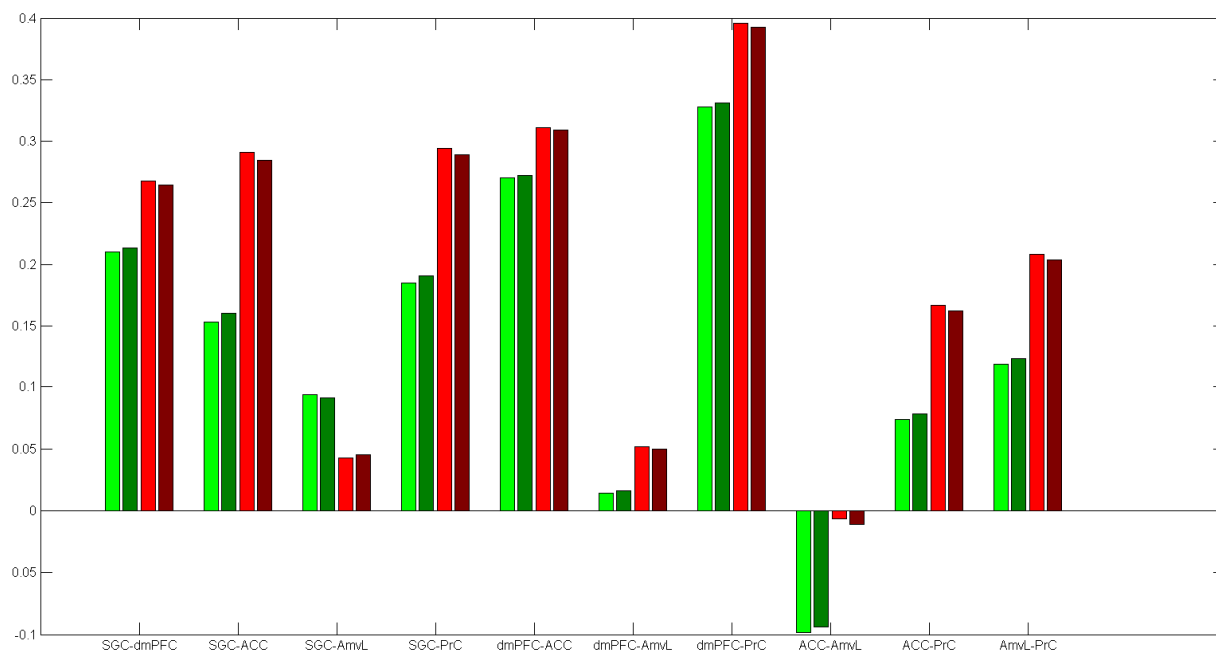


Figure S1: All results of the functional connectivity analysis of the ISA network across measurement sites
 Red bars depict the functional connectivity of the patients, green bars represent the functional connectivity of the controls. Light colours: Aachen; Dark colours: Goettingen

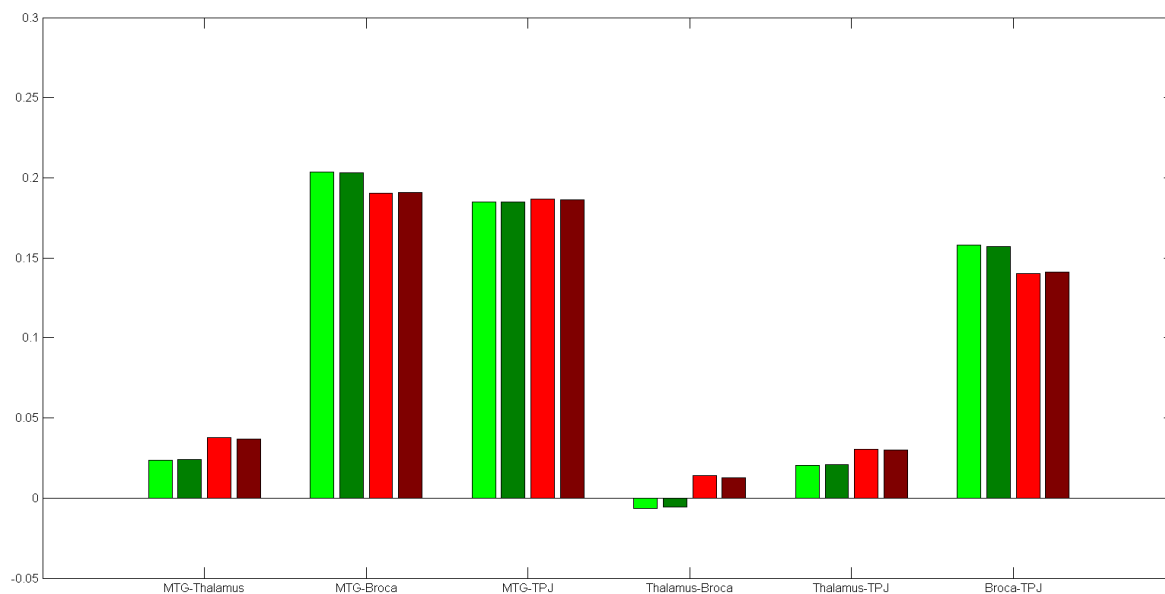


Figure S2: All results of the functional connectivity analysis of the control network across measurement sites
 Red bars depict the functional connectivity of the patients, green bars represent the functional connectivity of the controls. Light colours: Aachen; Dark colours: Goettingen. No significant differences were observed.

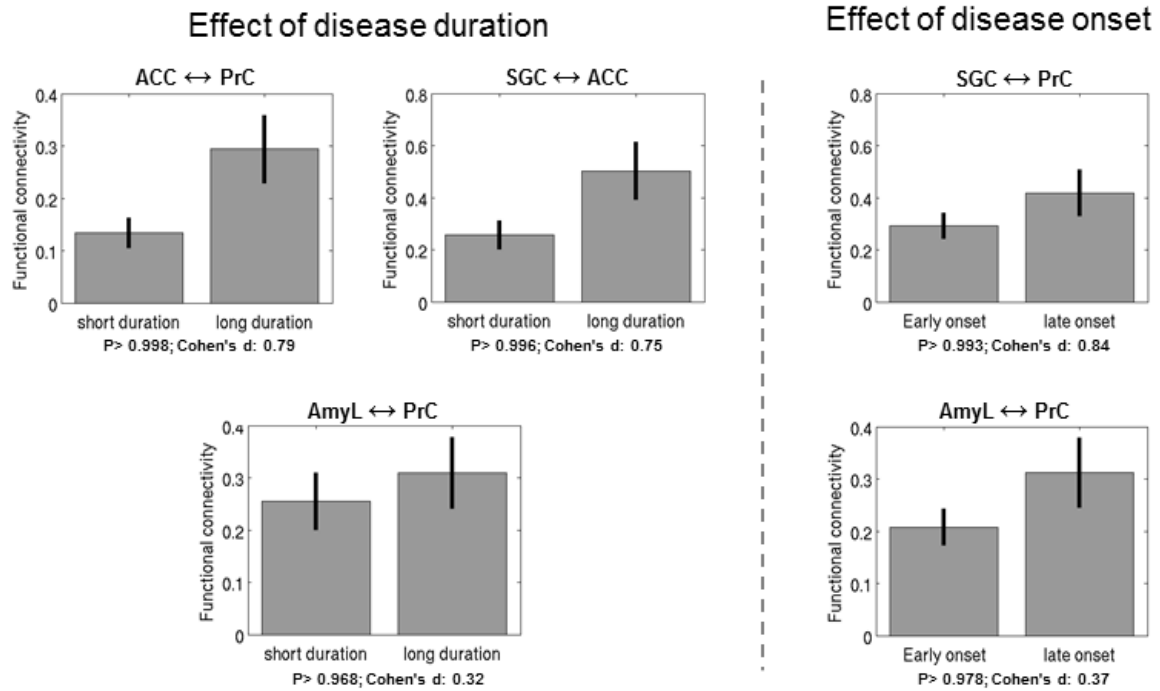


Figure S3
 Significant results of the comparison of functional connectivity between patient subgroups of short and long disease duration and early and late onset of illness. Subgroups were defined each by a median split of the patient group with ≥ 5 years for long duration and ≥ 24 years of age for late disease onset. ACC: anterior cingulate cortex; PrC: precuneus; SGC: subgenual cingulate cortex; AmyL: left Amygdala.

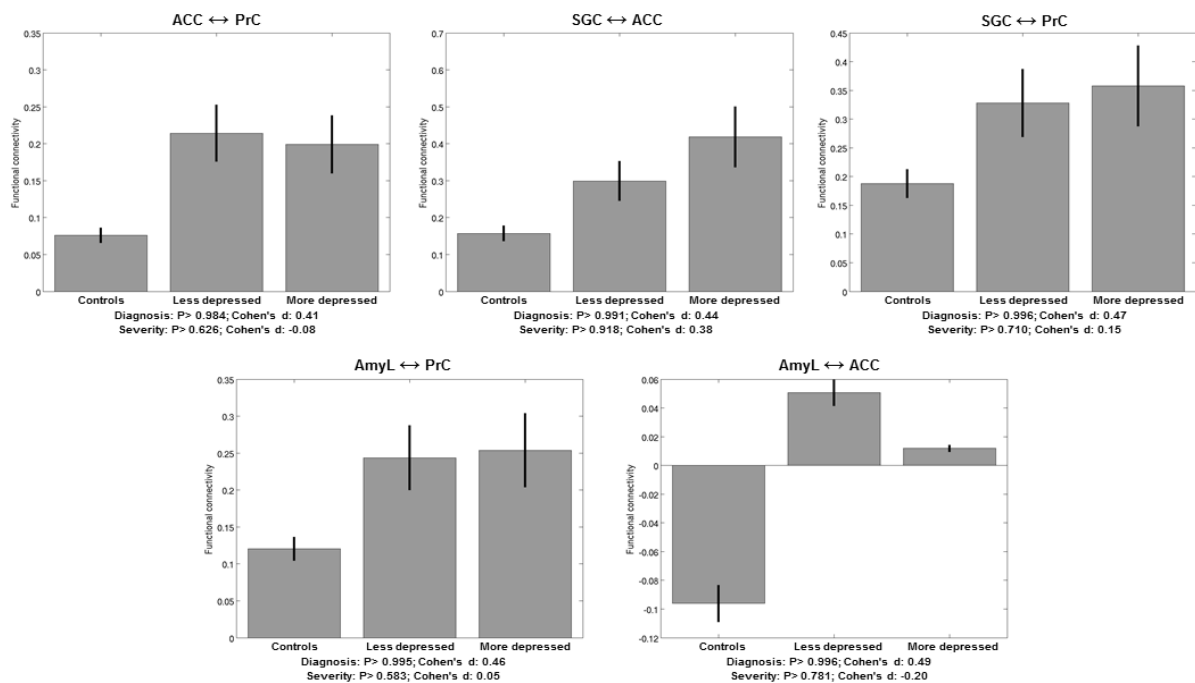


Figure S4
 Significant results of the comparison of functional connectivity between controls and patient subgroups of less and more depression severity. Subgroups were defined by a median split of the patients severity scores (HRSD= 8,5; MADRS= 15). ACC: anterior cingulate cortex; PrC: precuneus; SGC: subgenual cingulate cortex; AmyL: left Amygdala.

SUMMARY & GENERAL DISCUSSION

The six studies presented here investigated the mechanisms and network interactions underlying normal and pathological (auditory verbal hallucinations, AVH) speech perception. Study 1 examined the perception of ambiguous speech sounds in the healthy brain and the role of prior information in decoding such degraded speech. Study 2 further probed the connectivity and functional organization of area 44 of Broca's region as a key hub in this speech processing network. Study 3, 4 and 5 investigated disturbed connectivity patterns associated with pathological voice hearing in psychotic patients and in non-psychotic individuals, respectively. Finally, the last study demonstrated that disturbed connectivity within the healthy speech perception network is not present in "affective psychosis", i.e., depression. Abnormal connectivity within this network should therefore represent aberrations specific to the symptomatology of AVH rather than more general psychopathology.

Contributions of Broca's region to degraded speech perception

The first study used an fMRI paradigm to probe the effect of prior lexical-semantic information on the perception of degraded speech. The results demonstrated that a priori available (matching) lexical-semantic information facilitated the decoding of degraded sentences and was associated with activation of the left middle temporal gyrus (MTG) and the left angular gyrus (AG). The left thalamus was observed instead of the left AG when all trials rather than only correct trials were included in the analysis. Mismatching lexical-semantic information, which resulted in unsuccessful attempts to decode the degraded sentence, was associated with activity in area 44/45 of Broca's region in the left inferior

frontal gyrus (IFG). Although these findings cannot prove that the facilitation of degraded speech decoding based on prior lexical-semantic information involves predictive coding mechanisms, they are in very good agreement with the predictive coding framework. In particular, the prior lexical-semantic information most likely provided a predictive template that subsequently could be applied to the degraded target sentence. In the propositional match condition, the perceptual ambiguity of the degraded sentence could be resolved because possible subjective percepts of the degraded sentence were weighted by the predictive template. This weighting hence favored the percept of an intelligible sentence over meaningless, speech-like noise, which is in agreement with the participants' reported experience. The left AG might be particularly important for the generation of lexical-semantic predictions, as it is a hierarchically high node that has been suggested to provide semantic constraints to lower areas (Price, 2010; Seghier et al., 2010). Possibly, these predictions influence the semantic processing in the left MTG and other lower regions involved in auditory speech processing. These feedback signals might furthermore filter and amplify the predicted auditory signals in the thalamus (Alitto and Usrey, 2003). Moreover, this study highlighted a role for Broca's region in speech perception particularly under conditions when potential meaning is hidden in a noisy auditory signal, that is, when decoding of degraded speech was unsuccessfully attempted as it did not match with the prior lexical-semantic information. Such a response pattern indicates that Broca's region contributes to speech perception by searching for meaningful information (see also Giraud et al., 2004) and compares incoming sound sequences with the predicted sequences. In line with reports showing that Broca's region is particularly sensitive to incompatible speech stimuli (e.g. Friederici et al., 2010; Myers et al., 2009), the strong response to mismatches between the predicted signal (based on the lexical-semantic template) and the actual

degraded speech signal might be interpreted as prediction errors, potentially preventing misinterpretation (Novick et al., 2005). Therefore, it may be assumed that Broca's region exerts top-down influence on the MTG and AG when prior information cannot be applied to the degraded speech signal. Still, it should be noted that the dynamic interactions between these regions presumably underlying the phenomenon of sudden understanding of degraded speech in the propositional match condition and the absence of this phenomenon in the propositional mismatch condition would require the additional modeling of effective connectivity (Friston, 2002). However, this was not attempted in the current study due to the technical characteristics of the design. In particular, the long trials of sentence pair presentation would be problematic for the analysis of effective connectivity.

The first study thus indicated that Broca's region is involved in speech perception by searching for meaningful semantic signals in speech-like signals. However, Broca's region is not only implicated in language processes but also but also contributes to working memory, action and music processes (Grodzinsky and Santi, 2008; Fadiga et al., 2009). This multifunctional character was the starting point for study 2 in which we delineated several functional subunits in the posterior part of Broca's region, i.e., area 44, based on the functional interaction patterns. The results of study 2 demonstrated that left area 44 is functionally heterogeneous as it contains five subunits with distinct whole-brain co-activation patterns across a wide range of neuroimaging experiments. The functional characterization based on the BrainMap meta-data indicated a most prominent segregation of area 44 into a posterior "action-related" and an anterior "language/cognition – related" part. In particular, the posterior (action) portion contained two clusters mainly associated with phonology and overt speech articulation (posterior-dorsal cluster) and with rhythmic sequencing of movement (posterior-ventral cluster), respectively. The language and

cognition portion included three distinct clusters primarily involved in working-memory processes (anterior-dorsal cluster), in detection of meaning in language and in social contexts (anterior-ventral cluster) and in cognitive control (inferior frontal junction cluster), respectively. Furthermore, these five clusters also demonstrated specific and distinct co-activation with networks implicated in the respective functions. These specific connectivity patterns were moreover confirmed by resting state functional connectivity which highlighted very similar networks for the respective clusters. Thus, task-dependent co-activation and task-independent resting state connectivity converged on functional connectivity patterns specifically associated with the five clusters.

These findings provide strong evidence for the view that Broca's region is not a single functional unit and are in accordance with observations of anatomical (Amunts et al., 2010) and functional (Fedorenko et al., 2012) heterogeneity in this region. Furthermore, this parcellation can also be used to arrive at more specific interpretations of activations from neuroimaging studies localized in left area 44. For example, the activation observed in Broca's region in study 1 was overlapping in the anterior-ventral cluster of area 44 (and extended further anteriorly into area 45). Importantly, the strong link of this area 44 cluster with semantic processing of language and of social cognition tasks supports the presumed role of Broca's region in study 1 as essentially searching for a meaningful pattern in the degraded speech signals.

Aberrant connectivity of Broca's region in pathological voice hearing

Based on the above reasoning, it may be hypothesized that Broca's region also plays an important role in AVH as hallucinations might be regarded as an inappropriate detection of meaningful auditory verbal patterns in the absence of such bottom-up stimulation. Since the

top-down expectation-based extraction of meaning from speech signals furthermore involved the left AG, MTG and thalamus, these regions might equally contribute to the perception of voices in AVH. Accordingly, we examined whether disturbed network interactions at rest seeded from these outcome regions of study 1 are linked with the experience of AVH in psychotic patients. Given the importance of the connectivity pattern of a brain region for the determination of its function (Friston, 2002) and the multifaceted character of hallucinations (Seal et al., 2004), resting state connectivity analyses should be very well suited to unravel the pathomechanisms underlying AVH. In study 3, the comparison of psychotic patients with AVH to healthy controls highlighted several dysconnections. In particular, the seed in Broca's region showed a striking pattern of aberrant connectivity in psychotic patients. Firstly, increased connectivity was observed between Broca's region and the supplementary motor area (SMA) and the left insula/putamen, which might represent increased interactions within the articulation network involved in generation of overt and covert speech. Secondly, Broca's region demonstrated decreased connectivity with the dorsolateral and ventrolateral prefrontal cortex as well as with the inferior parietal cortex, which potentially reflects decreased coupling with the verbal self-monitoring system. This aberrant connectivity pattern of Broca's region thus points to misattribution of self-generated verbal imagery to external sources due to dysfunctional verbal monitoring as an important pathomechanism of AVH (Allen et al., 2007). Furthermore, the left MTG and AG displayed decreased connectivity with lateral temporal and inferior parietal regions involved in auditory verbal processing. Given that the left AG and MTG were associated with providing lexical-semantic expectations and extracting meaning from degraded speech in study 1, respectively, these interactions might represent overt dominance of top-down expectations on speech

perception that has been proposed to elicit verbal percepts in the absence of actual stimulation (Grossberg, 2000). Finally, the left thalamus showed increased connectivity with the left fusiform and parahippocampal gyrus. As these regions are associated with semantic processes and memory function, this increased connectivity possibly reflects effects of semantic memory recollection on thalamic auditory processing. Hence, also intrusions from verbal memory (Badcock et al., 2005; Diederer et al., 2010) seem to contribute to AVH.

These results thus provide evidence for several complementary mechanisms involved in AVH and are in accordance with a multidimensional account of hallucinations (Seal et al., 2004). Furthermore, study 4 indicated that not only networks connected with the four seed regions from study 1 are abnormal in psychotic patients with AVH. Rather, this analysis, which was seeded from two regions activated during acute AVH in psychotic patients, showed abnormal interactions of Broca's right-sided homotope and the left superior temporal gyrus with regions associated with memory (hippocampus and parahippocampal gyrus) and language processes (dorsolateral prefrontal cortex and the frontal operculum). Thus, not only Broca's region but also its right homotope, which is in particular associated with the processing of emotional prosody (Gandour et al., 2003; Wildgruber et al., 2005; Rota et al., 2009), might contribute to AVH. Moreover, the deviant coupling with memory structures in the medial temporal lobe observed in study 4 emphasize the role of involuntary memory retrieval in AVH. Possibly, dysfunction of memory recollection represents a more general mechanism of hallucinations independent of the modality in question. The abnormal interactions within the language system observed in study 3 and 4 on the other hand might point to mechanisms more specific for hallucinations in the auditory verbal domain. In particular, both studies agree on abnormal connectivity of regions involved in speech perception (the MTG as well as the AG and the STG,

respectively), speech articulation (Broca's region and its right homotope, respectively) and speech monitoring (especially the dorsolateral prefrontal cortex). These disturbances therefore suggest that misattribution of self-generated speech and top-down effects on speech perception can lead to hallucinations with auditory verbal content.

Disturbed connectivity with Broca's region and Broca's right homotope was moreover associated with AVH in non-psychotic subjects as demonstrated in study 5. In particular, we found increased coupling between the left parahippocampal gyrus and Broca's region as well as between the left superior temporal region and Broca's right homotope in non-psychotic individuals with AVH. This pattern of disturbed connectivity between language and memory regions again points to misattribution of self-generated speech and inappropriate memory retrieval as potential pathomechanisms of AVH. Together, these three resting state analyses thus suggest that disturbed interactions between regions involved in production and perception of speech (in particular Broca's region) and medial temporal lobe regions are associated with AVH in both psychotic patients and non-psychotic individuals. These results are in accordance with a multidimensional account of AVH featuring several proposed mechanisms including misattribution of inner speech (Allen et al., 2007), imbalances between top-down and bottom-up factors in speech perception (Grossberg, 2000) as well as intrusive verbal memories (Badcock et al., 2005).

These findings furthermore indicate that analogous mechanisms may be involved in psychotic and non-psychotic AVH. In support of this, a previous study reported similar activation patterns for psychotic patients and otherwise healthy individuals during the experience of AVH (Diederer et al., 2012). However, this hypothesis needs further testing, as a direct comparison of resting state connectivity would be required to establish a common aberrant connectivity pattern in psychotic and non-psychotic AVH. Future studies

comparing resting state connectivity seeded from the same regions in psychotic patients and non-psychotic individuals are thus needed to shed more light on this issue. However, it should also be noted that psychotic and non-psychotic AVH are associated with different degrees of control and emotional valence (Daalman et al., 2011). Therefore, it is still unclear whether psychotic and non-psychotic AVH represent indeed the same phenomenon and are caused by similar mechanisms. For example, it has been suggested that psychotic and non-psychotic AVH might share the same perceptual bottom-up component but involve different top-down inhibitory control processes over the hallucinations (Hugdahl, 2009). Accordingly, potential differences in connectivity patterns associated with psychotic and non-psychotic AVH might be attributable to (a) different mechanisms underlying experiences of psychotic and non-psychotic AVH or to (b) effects of medication and unspecific psychiatric symptoms not present in the healthy individuals. In the end, the problem of the specificity of the aberrant connectivity in AVH may not be entirely resolved by examining non-psychotic individuals with AVH either.

Finally, however, the resting state analysis of depressed patients and healthy controls reported in study 6 is elucidating with regard to the question of the specificity of the above findings. While we observed that major depression is linked specifically with increased connectivity within an introspective-socio-affective network, no differences between patients and controls were found between the regions of the degraded speech perception network derived from study 1. These findings demonstrate that disturbed connectivity of regions associated with speech perception is not a general manifestation of psychopathology as it is not present in patients with affective psychosis but rather seems to be specific to the symptom of AVH in psychotic patients and non-psychotic individuals.

Conclusions

Lexical-semantic expectations from higher order areas such as the left angular gyrus can facilitate the extraction of meaning from degraded speech in the left middle temporal gyrus and the left thalamus. Broca's region might contribute to the decoding of speech by searching for meaningful content in ambiguous auditory signals. However, the connectivity-based parcellation demonstrated that area 44 of Broca's region is functionally heterogeneous as it contains five subunits with distinct connectivity patterns and functions. In particular, merely the anterior-ventral part of area 44 is involved in meaning detection while the other four subunits are primarily associated with working-memory (anterior-dorsal cluster), cognitive control (inferior frontal junction cluster), rhythmic sequencing (posterior-ventral cluster) and phonology and overt speech (posterior-dorsal cluster).

Furthermore, resting state connectivity patterns indicated that auditory verbal hallucinations (AVH) might be caused by abnormal interactions of Broca's region and its right-sided homotope with regions involved in speech production and monitoring, aberrant interactions in the speech perception system as well as dysconnectivity of medial temporal lobe memory structures. AVH might thus result from mechanisms involving misattribution of self-generated speech, intrusions from verbal memory and an imbalance between top-down and bottom-up processing in speech perception. Furthermore, such deviant functional connectivity between Broca's region and the speech perception network is not merely an unspecific reflection of psychopathology as it was not observed in patients with major depression. Together, these studies demonstrate that although Broca's region is functionally heterogeneous, it is an important hub in both degraded speech perception where meaning can be extracted based on top-down expectations and in pathological voice hearing where speech is perceived in the absence of bottom-up signals.

REFERENCES

- Alitto, H.J., Usrey, W.M. 2003. Corticothalamic feedback and sensory processing. *Curr.Opin.Neurobiol.* 13: 440-445.
- Allen, P., Aleman, A., McGuire, P.K. 2007. Inner speech models of auditory verbal hallucinations: evidence from behavioural and neuroimaging studies. *Int.Rev.Psychiatry.* 19: 407-415.
- Amunts, K., Lenzen, M., Friederici, A.D., Schleicher, A., Morosan, P., Palomero-Gallagher, N., Zilles, K. 2010. Broca's region: novel organizational principles and multiple receptor mapping. *PLoS.Biol.* 8.
- Badcock, J.C., Waters, F.A., Maybery, M.T., Michie, P.T. 2005. Auditory hallucinations: failure to inhibit irrelevant memories. *Cogn Neuropsychiatry.* 10: 125-136.
- Daalman, K., Boks, M.P., Diederer, K.M., de Weijer, A.D., Blom, J.D., Kahn, R.S., Sommer, I.E. 2011. The same or different? A phenomenological comparison of auditory verbal hallucinations in healthy and psychotic individuals. *J.Clin.Psychiatry.* 72: 320-325.
- Diederer, K.M., Daalman, K., de Weijer, A.D., Neggers, S.F., van, G.W., Blom, J.D., Kahn, R.S., Sommer, I.E. 2012. Auditory hallucinations elicit similar brain activation in psychotic and nonpsychotic individuals. *Schizophr.Bull.* 38: 1074-1082.
- Diederer, K.M., Neggers, S.F., Daalman, K., Blom, J.D., Goekoop, R., Kahn, R.S., Sommer, I.E. 2010. Deactivation of the parahippocampal gyrus preceding auditory hallucinations in schizophrenia. *Am.J.Psychiatry.* 167: 427-435.
- Fadiga, L., Craighero, L., D'Ausilio, A. 2009. Broca's area in language, action, and music. *Ann.N.Y.Acad.Sci.* 1169: 448-458.
- Fedorenko, E., Duncan, J., Kanwisher, N. 2012. Language-selective and domain-general regions lie side by side within Broca's area. *Curr.Biol.* 22: 2059-2062.
- Friederici, A.D., Kotz, S.A., Scott, S.K., Obleser, J. 2010. Disentangling syntax and intelligibility in auditory language comprehension. *Hum.Brain Mapp.* 31: 448-457.
- Friston, K. 2002. Functional integration and inference in the brain. *Prog.Neurobiol.* 68: 113-143.
- Gandour, J., Wong, D., Dziedzic, M., Lowe, M., Tong, Y., Li, X. 2003. A cross-linguistic fMRI study of perception of intonation and emotion in Chinese. *Hum.Brain Mapp.* 18: 149-157.
- Giraud, A.L., Kell, C., Thierfelder, C., Sterzer, P., Russ, M.O., Preibisch, C., Kleinschmidt, A. 2004. Contributions of sensory input, auditory search and verbal comprehension to cortical activity during speech processing. *Cereb.Cortex.* 14: 247-255.
- Grodzinsky, Y., Santi, A. 2008. The battle for Broca's region. *Trends Cogn Sci.* 12: 474-480.
- Grossberg, S. 2000. How hallucinations may arise from brain mechanisms of learning, attention, and volition. *J.Int.Neuropsychol.Soc.* 6: 583-592.
- Hugdahl, K. 2009. "Hearing voices": auditory hallucinations as failure of top-down control of bottom-up perceptual processes. *Scand.J.Psychol.* 50: 553-560.

- Myers, E.B., Blumstein, S.E., Walsh, E., Eliassen, J. 2009. Inferior frontal regions underlie the perception of phonetic category invariance. *Psychol.Sci.* 20: 895-903.
- Novick, J.M., Trueswell, J.C., Thompson-Schill, S.L. 2005. Cognitive control and parsing: reexamining the role of Broca's area in sentence comprehension. *Cogn Affect.Behav.Neurosci.* 5: 263-281.
- Price, C.J. 2010. The anatomy of language: a review of 100 fMRI studies published in 2009. *Ann.N.Y.Acad.Sci.* 1191: 62-88.
- Rota, G., Sitaram, R., Veit, R., Erb, M., Weiskopf, N., Dogil, G., Birbaumer, N. 2009. Self-regulation of regional cortical activity using real-time fMRI: the right inferior frontal gyrus and linguistic processing. *Hum.Brain Mapp.* 30: 1605-1614.
- Schilbach, L., Bzdok, D., Timmermans, B., Fox, P.T., Laird, A.R., Vogeley, K., Eickhoff, S.B. 2012. Introspective minds: using ALE meta-analyses to study commonalities in the neural correlates of emotional processing, social & unconstrained cognition. *PLoS.One.* 7: e30920.
- Seal, M.L., Aleman, A., McGuire, P.K. 2004. Compelling imagery, unanticipated speech and deceptive memory: neurocognitive models of auditory verbal hallucinations in schizophrenia. *Cogn Neuropsychiatry.* 9: 43-72.
- Seghier, M.L., Fagan, E., Price, C.J. 2010. Functional subdivisions in the left angular gyrus where the semantic system meets and diverges from the default network. *J.Neurosci.* 30: 16809-16817.
- Wildgruber, D., Riecker, A., Hertrich, I., Erb, M., Grodd, W., Ethofer, T., Ackermann, H. 2005. Identification of emotional intonation evaluated by fMRI. *Neuroimage.* 24: 1233-1241.

ACKNOWLEDGMENTS

Any scientific project always involves more than one person and requires input from many different minds. Accordingly, I need to thank several persons who contributed to this dissertation project.

First of all, I am deeply indebted to my supervisor Simon Eickhoff without whom the dissertation in the current form would not have been possible. Simon, you were always a great source of inspiration and support! Thank you for providing a never-ending stream of scripts, ideas, new methods and good humor!

Next, I would like to thank Tobias Kalenscher for his willingness to co-supervise and assess my dissertation as well as assisting with the administrative requirements of the dissertation procedure.

Furthermore, I would like to thank all co-authors and collaborators who contributed to the six studies reported in this dissertation. In particular, Robert Langner helped a lot in preparing and analyzing the fMRI study on degraded speech. Martin Meyer did not only provide the stimulus material for the same study but furthermore shared his expertise in the language domain which made me feel much more comfortable with the pitfalls of linguistic details. Iris Sommer and Kelly Diederer made the resting state studies possible by collecting and sharing the resting state data. Acquiring so many data sets, especially of the psychotic patients, was certainly a great effort that I highly appreciated. I would also like to thank Professor Karl Zilles and Professor Katrin Amunts who as the respective INM-2 and INM-1 institute heads at the Research Centre in Jülich provided the necessary equipment and infrastructure for conducting the experiments and analyzing the experimental data. Additionally, they gave valuable advice and their focus and insistence on neuroanatomy

taught me a great deal about the importance of anatomic principles that I surely will keep in mind.

Moreover, the relaxed atmosphere in our young team was awesome and an important motivational factor, therefore I want to thank every team member for their support, curiosity, helpfulness and creativity. It was a great time with you in and outside the office!

Last but not least, I would like to thank my family and Markus for supporting me from afar but always in touch. My four housemates in Aachen were a great company for living during my doctoral time and provided friendly reminders to relax more whenever necessary.